

ASYMMETRIC INDUCTION AND REACTION SELECTIVITY
IN SOLID STATE ORGANIC PHOTOCHEMISTRY

by

MATTHEW RUSSELL NETHERTON

B.Sc.(Hons.), The University of Western Ontario, 1995

A THESIS SUBMITTED IN PARTIAL FULFILMENT OF
THE REQUIREMENTS FOR THE DEGREE OF
DOCTOR OF PHILOSOPHY

in

THE FACULTY OF GRADUATE STUDIES
(DEPARTMENT OF CHEMISTRY)

We accept this thesis as conforming
to the required standard

THE UNIVERSITY OF BRITISH COLUMBIA

NOVEMBER 2000

©Matthew R. Netherton, 2000

In presenting this thesis in partial fulfilment of the requirements for an advanced degree at the University of British Columbia, I agree that the Library shall make it freely available for reference and study. I further agree that permission for extensive copying of this thesis for scholarly purposes may be granted by the head of my department or by his or her representatives. It is understood that copying or publication of this thesis for financial gain shall not be allowed without my written permission.

Department of Chemistry

The University of British Columbia
Vancouver, Canada

Date Dec 20, 2000

Abstract

A number of aromatic ketones were synthesized, and their type II photochemistry studied in solution and in the solid state. The purpose of these investigations was to elucidate the geometric parameters responsible for partitioning of the intermediate 1,4-hydroxybiradicals among the possible cleavage, cyclization, and reverse hydrogen transfer pathways. The four ketones studied proved to be very sensitive to changes in the disposition of the carbonyl chromophore, the position of which dictates the anticipated geometry of the biradical intermediate. In particular, it was found that cleavage was only efficient when reasonable overlap between the radical centres and the σ -bond undergoing scission was present. Parameters governing the efficiency of the Yang photocyclization were also established. In addition, γ -hydrogen/deuterium exchange was observed on photolysis of an unreactive aromatic ketone using *tert*-butanol as solvent. This reaction is unprecedented in ketones that undergo γ -hydrogen abstraction, and is indicative of the high efficiency of reverse hydrogen transfer relative to other reaction pathways in this system.

The *ionic chiral auxiliary* method of asymmetric induction was investigated in the solid state photochemistry of a series of macrocyclic aminoketones. Salts were formed between the achiral aminoketones (ring sizes of twelve, fourteen, and sixteen) and optically pure acids. The resulting chiral crystals were irradiated in the solid state, and the photoproducts analyzed for enantiomeric purity. Enantioselectivities ranging from poor to excellent were obtained, and X-ray crystallographic data from a number of these compounds provide insight on the origin of the observed stereoselectivities.

The same technique for asymmetric induction was also studied in a benzocyclohexadienone system which undergoes photochemical rearrangement to form a chiral benzobicyclo[3.1.0]hexanone derivative. The planarity of this system was expected to limit conformational bias in product enantiodetermination, and thus allow the anisotropic directing effects of the chiral cavity to be studied. The enantioselectivities observed for these salts was generally low, although one derivative displayed possible synthetic utility (ee ca. 80%). Two reactant crystal structures were obtained, one of which contained a unique arrangement in which two photoreactive benzocyclohexadienone moieties were present in the optically active crystal as conformational enantiomers. The net result of the analysis is that the enantioselectivity observed on photolysis of this substrate is independent of conformational bias. Further computational studies are required to garner a complete understanding of this reaction.

Table of Contents

Abstract	ii
Table of Contents	iv
List of Figures	viii
List of Tables	xii
List of Symbols and Abbreviations.....	xiii
Acknowledgements.....	xvi
Dedication	xvii

Introduction	1
--------------------	---

Chapter 1 – Introduction	1
--------------------------------	---

1.1 Preamble	1
1.2 Crystal Engineering	2
1.3 Factors Influencing Solid State Reactivity	5
1.4 Type II Photochemistry of Ketones	9
1.5 Geometric Requirements for Hydrogen Abstraction	12
1.6 Photochemistry of Linearly Conjugated Cyclohexadienones.....	15
1.7 Asymmetric Induction and the Ionic Chiral Auxiliary Concept.....	18
1.8 Research Objectives.....	22

Results and Discussion.....	25
-----------------------------	----

Chapter 2 – Competition between Cyclization, Cleavage and Reverse Hydrogen Transfer in the Solid State Norrish/Yang Type II Photochemistry of a Homologous Series of Spiroadamantyl Ketones.....	25
--	----

2.1 Synthesis of the Spiroadamantyl Ketones.....	25
2.1.1 Retrosynthetic Analysis	25
2.1.2 Preparation of Spiroketones 5 and 6 by Intramolecular Acylation.....	27
2.1.3 Synthesis of Spiroketones 7 and 8 by Ring-Closing Metathesis	29
2.1.4 Synthesis of the Unsaturated Spiroketone 70	31
2.2 Solution and Solid State Photolysis of Spiroketones 5-8	33
2.2.1 Photochemistry of Spiroketone 5	33
2.2.2 Photochemistry of Spiroketone 6	37

2.2.3 Photochemistry of Spiroketone 7	43
2.2.4 Photochemistry of Spiroketone 8	45
2.3 Solid State Structure-Reactivity Correlations.....	48
2.3.1 Hydrogen Abstraction Parameters and Biradical Geometries	49
2.3.2 Geometric Requirements for Cleavage.....	52
2.3.3 Geometric Requirements for Cyclization	55
2.3.4 Summary of Biradical Reactivity.....	57
2.4 Photochemistry of the Unsaturated Adamantyl Spiroketones 68 and 70	58
2.4.1 Photochemistry of Unsaturated Ketone 68	58
2.4.2 Photochemistry of Unsaturated Ketone 70	59
2.5 Summary	63

Chapter 3 – Asymmetric Induction in the Solid State Photochemistry of Macrocyclic Aminoketone Salts..... 64

3.1 Synthesis of the Aminoketones.....	64
3.1.1 Synthesis of the Twelve-membered Aminoketone 12	64
3.1.2 Synthesis of the Fourteen- and Sixteen-membered Aminoketones 14 and 16	65
3.2 Solution State Photochemistry of the Macrocyclic Aminoketones	68
3.2.1 Solution State Photochemistry of Cycloalkanones	68
3.2.2 Aminoketone Photochemistry.....	70
3.2.3 Quantum Yield Studies of Compound 14	74
3.3 Identification of the Photoproducts.....	77
3.3.1 Independent Synthesis of Reduced Product 119	77
3.3.2 Synthesis of the Type II Cleavage Products 123 and 126	79
3.3.3 Preparation of the Secondary Photoproduct 129	80
3.3.4 Stereochemical Assignment of the Cyclobutanol Photoproducts.....	81
3.4 Preparation of Optically Active Salts of the Macrocyclic Aminoketones.....	83
3.5 Photochemistry of the Optically Active Salts.....	88
3.5.1 Solution State Photolyses of the Optically Active Salts	89

3.5.2 Solid State Photolyses of the Optically Active Salts	90
3.6 Solid State Structure-Reactivity Correlations	94
3.6.1 Solid State Structure of Salt 147	95
3.6.2 Solid State Structure of Salt 128	97
3.6.3 Structure-Reactivity Relationships for Salts of the Fourteen-Membered Aminoketone	98
3.7 Summary	102

Chapter 4 – Asymmetric Induction in the Solid State Photochemistry of Linearly Conjugated Benzocyclohexadienone Salts

4.1 Synthesis of the Photochemical Substrate 52	103
4.2 Photochemistry of Compounds 52 and 166	104
4.3 Resolution of Ketoacid Photoproduct 53	107
4.4 Preparation of Optically Active Salts of Acid 52	109
4.5 Solution State Photochemistry of the Optically Active Salts	112
4.6 Solid State Photochemistry of the Optically Active Salts	112
4.7 Solid State Structure-Reactivity Analysis	115
4.8 Summary	117

Experimental

Chapter 5 – Preparation of Substrates

5.1 General Considerations	119
5.2 Synthesis of Adamantyl Spiroketones 5 , 6 , 7 , 8 , and 70	123
5.2.1 Preparation of the Five-Membered Adamantyl Spiroketone 5	123
5.2.2 Preparation of the Six-Membered Adamantyl Spiroketones 6 and 70	129
5.2.3 Preparation of the Seven-Membered Adamantyl Spiroketone 7	134
5.2.4 Preparation of the Eight-Membered Adamantyl Spiroketone 8	144

5.3 Synthesis of the Macrocyclic Aminoketones 12 , 14 , and 16 and Their Salts	151
5.3.1 Preparation of the Twelve-Membered Aminoketone 12	151
5.3.2 Preparation of the Twelve-Membered Aminoketone Salts.....	154
5.3.3 Preparation of the Fourteen-Membered Aminoketone 14	160
5.3.4 Preparation of the Fourteen-Membered Aminoketone Salts	165
5.3.5 Preparation of the Sixteen-Membered Aminoketone 16	178
5.3.6 Preparation of the Sixteen-Membered Aminoketone Salts.....	184
5.4 Synthesis of the Linearly Conjugated Benzocyclohexadienone 52 and its Salts	189
5.4.1 Preparation of the Benzocyclohexadienone Carboxylic Acid 52	189
5.4.2 Preparation of the Benzocyclohexadienone Salts	195
 Chapter 6 – Photochemical Studies	209
6.1 General Considerations.....	209
6.2 Photolysis of Adamantyl Spiroketones 5 , 6 , 7 and 8	211
6.3 Photolysis of Macrocyclic Aminoketones and Their Salts	222
6.3.1 Preparative Photolysis of Compound 12 in Solution.....	222
6.3.2 Independent Preparation of Alcohol Photoproduct 119	224
6.3.3 Solution Photolysis of Hydrochloride Salt 127	225
6.3.4 Independent Synthesis of Fourteen-Membered Cleavage Photoproduct	227
6.3.5 Preparative Photolysis of Aminoketone 16	233
6.3.6 Independent Synthesis of Sixteen-Membered Cleavage Photoproduct 126	235
6.4 Photolysis of Benzocyclohexadienone Derivatives	240
6.5 Resolution of Acid 53 with Brucine	243
6.6 Quantum Yield Determinations	245
 References	246

List of Figures

Figure	Caption	Page
1.1	Crystal engineering in directed solid state synthesis	3
1.2	(a) Ideal geometry for triacetylene 1,6-polymerization; (b) Monomer alignment in an engineered crystal	4
1.3	Template directed solid state dimerization	5
1.4	A thermal crystalline state reaction.....	6
1.5	Solid state bimolecular reaction of a mixed crystal	7
1.6	Illustration of the 'reaction cavity' concept	8
1.7	Solid state synthesis of α -cuparenone (21).....	8
1.8	Type II photochemistry of ketones	10
1.9	Dependence of reaction pathway on biradical conformation	11
1.10	Geometric parameters for γ -hydrogen atom abstraction.....	12
1.11	Two models of the ketone excited state	13
1.12	Although the C=O...H distance is favourable, a Δ value of 90° betrays a lack of orbital overlap	15
1.13	Photochemical pathways of linearly conjugated cyclohexadienones	16
1.14	Synthesis of crocetin dimethyl ester (40) using dienone-ketene photochemistry.....	17
1.15	Crystalline state absolute asymmetric syntheses	19
1.16	The photoreaction of β -ketoester 45 is highly diastereoselective in the crystalline state, but gives poor results in solution	20
1.17	An example of the ionic chiral auxiliary concept in the solid state Yang photocyclization of salt 48	21
1.18	Schematic representation of the ionic chiral auxiliary approach to asymmetric solid state synthesis: reaction <i>via</i> diastereomeric transition states.....	21
1.19	General scheme for the solid state photochemistry of macrocyclic aminoketone salts.....	23
1.20	Photorearrangement of benzocyclohexadienone 52	24
2.1	Retrosynthetic analysis for spiroketones 5-8	25
2.2	Preparation of ester 62	26

Figure	Caption	Page
2.3	Synthesis of spiroketones 5 and 6	27
2.4	ORTEP representations of (a) 5 ; (b) 6	28
2.5	Synthesis of ketones 7 and 8	29
2.6	ORTEP representations of (a) 68 ; (b) 7 ; (c) 8	30
2.7	Synthesis of compound 70	31
2.8	ORTEP representation of ketone 70	32
2.9	Photochemistry of ketone 5	33
2.10	Competing secondary photolysis reaction of 72	34
2.11	¹ H NMR vinylic region (δ 5-6 ppm) after photolysis of 5 showing signals due to enol tautomer 71 (E) and keto epimers 72 (K).....	35
2.12	Formation of silyl enol ether 76	36
2.13	Solvent-biradical hydrogen-bonding decreases the rate of reverse hydrogen transfer relative to product formation.....	37
2.14	Deuteration of 6 through H-D exchange in the biradical.....	38
2.15	(a) ¹ H NMR of 6 ; (b) ² H{ ¹ H} NMR of deuterated 6	39
2.16	Photochemistry of spiroketone 6 as an aqueous suspension.....	41
2.17	ORTEP representation of photoproduct 78	42
2.18	Photolysis of spiroketone 7	43
2.19	Partial ¹³ C NMR of crude solid state reaction mixture of 7	44
2.20	ORTEP representation of photoproduct 81	45
2.21	Solution and solid state photochemistry of spiroketone 8	46
2.22	ORTEP representation of cyclobutanol 82	46
2.23	Partial ¹³ C NMR spectrum of the crude 8 solid state photosylate.....	47
2.24	Kinetic scheme for type II ketone photochemistry.....	49
2.25	Comparison of carbonyl group orientations in spiroketones 5-8	50
2.26	Hydrogen abstraction parameters for type II photochemistry.....	51
2.27	Solid state biradical geometry.....	53
2.28	Geometric parameters for cyclization.....	55

Figure	Caption	Page
2.29	Photochemistry of unsaturated ketone 87	59
2.30	Photochemistry of unsaturated spiroketone 70	62
2.31	Mechanism for photorearrangement of 93 to 94	62
3.1	Synthesis of aminoketone 12	65
3.2	Synthetic scheme for macrocycles 14 and 16	66
3.3	Synthesis of bromoester 106	67
3.4	General scheme for type II photochemistry of cycloalkanones.....	68
3.5	Solution state photochemistry of aminoketone 12	70
3.6	Solution state photochemistry of aminoketones 14 and 16	71
3.7	Secondary photolysis of cleavage product 123	72
3.8	A portion of the ^{13}C NMR spectrum (C_6D_6) of the crude reaction mixture after exhaustive photolysis of 120 in MeCN.....	73
3.9	Excited state reactivity of aliphatic ketones (a) in the absence and (b) in the presence of a triplet quencher.....	75
3.10	Preparation of aminoalcohol 119	77
3.11	400 MHz ^1H NMR spectra (C_6D_6) of (a) <i>trans</i> -cyclobutanol 125 , and (b) <i>cis</i> -cyclobutanol 124	78
3.12	Independent preparation of cleavage products 123 and 126	79
3.13	Synthetic scheme for amine 129	80
3.14	Chiral GC trace showing the separation of starting material (14) and products	89
3.15	Ideal and crystallographically derived average H_γ -abstraction geometries.....	94
3.16	ORTEP representation of the macrocyclic cation in salt 147	96
3.17	ORTEP representation of the macrocyclic cation in salt 128	97
3.18	ORTEP representation of the macrocycle in salt 149	99
3.19	ORTEP representations of the macrocycle in salt 148	101
4.1	Synthetic scheme for the preparation of ketoacid 52	103
4.2	Solution state photolysis of compounds 52 and 166	104
4.3	ORTEP representation of photoproduct 53	105

Figure	Caption	Page
4.4	Absorption spectra for benzocyclohexadienones 70 and 166 in acetonitrile	105
4.5	Relative ordering of excited states in compounds 70 and 166	106
4.6	Solvent-induced reordering of excited states leads to different photochemical reactions for compound 169	107
4.7	ORTEP representation of salt 171	108
4.8	Chiral GC chromatogram showing the configuration of each enantiomer of ester 167	109
4.9	ORTEP representation of the benzocyclohexadienone moieties in salt 183	115
4.10	ORTEP representation of the asymmetric unit for salt 183 showing the pseudo-inversion center	118
4.11	Root-mean-square overlays of the anions: (a) native conformations in 183 . (b) Chirality-matched conformations in 183	118

List of Tables

Table	Caption	Page
1.1	Ideal and crystallographically derived H _γ -abstraction geometries.....	14
2.1	Photochemistry of ketone 5 in various media.....	34
2.2	Comprehensive NMR assignment data for ketone 6 in 1:1 CD ₃ OD / C ₆ D ₆	40
2.3	Values of α for ketones 5-8	50
2.4	Hydrogen abstraction parameters for the solid state spiroketones.....	51
2.5	Geometric parameters for biradicals derived from 5-8	54
2.6	Cyclization parameters for the 1,4-hydroxybiadicals	56
2.7	Photoproduct yields from 70 under various photolysis conditions.....	60
3.1	Product distributions in solution state cycloalkanone photochemistry.....	69
3.2	Product distributions for solution state photolyses of the macrocyclic aminoketones and their hydrochloride salts.....	72
3.3	Isolated yields from preparative scale photolyses of the macrocycles	74
3.4	Quantum yield determinations for aminoketone 14	75
3.5	¹³ C NMR chemical shifts (C ₆ D ₆) for the methine carbon in cyclobutanols 144	82
3.6	¹³ C NMR chemical shifts (C ₆ D ₆) for the methine carbons in aminocyclobutanols produced on photolysis of the aminoketones of ring size N.....	82
3.7	Optically active salts prepared from aminoketone 12	84
3.8	Optically active salts prepared from aminoketone 14	84
3.9	Optically active salts prepared from aminoketone 16	86
3.10	Additional salts prepared from the macrocyclic aminoketones	87
3.11	Solution state photolyses of some optically active aminoketone salts	90
3.12	Solid state photolysis of optically active salts of aminoketone 14	92
3.13	Solid state photolysis of optically active salts of aminoketone 12	93
3.14	Solid state photolysis of optically active salts of aminoketone 16	93
4.1	Optically active salts prepared from acid 52	110
4.2	Diastereotopic splitting of the <i>gem</i> -dimethyl groups in salts of acid 52	112
4.3	Solid state photolysis of optically active salts of benzocyclohexadienone 52	113

List of Symbols and Abbreviations

Å	angstrom
Δ	heat to reflux
δ	chemical shift (ppm)
Φ	quantum yield
anal.	analysis
APT	attached proton test
aq.	aqueous
bp	boiling point
br	broad
Bu	butyl
^t BuOH	<i>tertiary</i> -butyl alcohol
C ₆ D ₆	benzene- <i>d</i> ₆
calcd	calculated
CAS	Chemical Abstracts Service
cat.	catalytic
Cbz	carbobenzyloxy
CDCl ₃	chloroform- <i>d</i>
CD ₃ OD	methanol- <i>d</i> ₄
CI	chemical ionization
COSY	¹ H- ¹ H correlation spectroscopy
Cy	cyclohexyl
d	doublet
DBU	1,8-diazabicyclo[5.4.0]undec-7-ene
DBP	dibenzoyl peroxide
DCM	dichloromethane
de	diastereomeric excess
DEPT	distortionless enhancement by polarization transfer
DHQD ₂ PYR	hydroquinidine 2,5-diphenyl-4,6-pyrimidinediyl diether
DIPA	diisopropylamine

DIPEA	<i>N,N</i> -diisopropylethylamine
DMF	dimethylformamide
DMPU	<i>N,N'</i> -dimethylpropyleneurea
ee	enantiomeric excess
EI	electron impact
Et ₂ O	diethyl ether
EtOAc	ethyl acetate
EtOH	ethanol
GC	gas chromatography
Grubbs catalyst	bis(tricyclohexylphosphine)benzylideneruthenium (IV) dichloride
h	hour(s)
HOAc	acetic acid
hν	light
HMBC	heteronuclear multiple bond connectivity
HMQC	heteronuclear multiple quantum coherence
HPLC	high performance liquid chromatography
HRMS	high resolution mass spectrometry
IR	infrared
IUPAC	International Union of Pure and Applied Chemistry
<i>J</i>	coupling constant (Hz)
LAH	lithium aluminum hydride
LDA	lithium diisopropylamide
LRMS	low resolution mass spectrometry
M	molarity
Me	methyl
MeOH	methanol
MeCN	acetonitrile
Mosher's acid	α-methoxy-α-(trifluoromethyl)phenylacetic acid
mp	melting point
NBS	<i>N</i> -bromosuccinimide
NMR	nuclear magnetic resonance

NOE	nuclear Overhauser effect
OAc	acetate
ORTEP	Oak Ridge Thermal Ellipsoid Program
PCC	pyridinium chlorochromate
ppm	parts per million
Ph	phenyl
ⁱ Pr	isopropyl
q	quartet
quint	quintet
RCM	ring-closing metathesis
s	singlet
SDS	sodim dodecylsulfonate
t	triplet
Tf	triflate (trifluoromethanesulfonate)
TFA	trifluoroacetic acid
THF	tetrahydrofuran
TIPS	triisopropylsilyl
TMS	trimethylsilyl
Ts	tosyl (4-toluenesulfonyl)
TsOH	4-toluenesulphonic acid
UV / VIS	ultraviolet / visible

Acknowledgements

I would like to express my gratitude to Dr. John Scheffer for his guidance, encouragement, and support over the last five years. I can only hope that some of his patience, wisdom, and analytical ability has rubbed onto me.

None of the work presented in this thesis could have been carried out without the enormous effort of Dr. Eugene Cheung in the UBC structural chemistry laboratory. Eugene's ever-friendly manner and crystallographic genius have made our collaboration a very enjoyable one. Special thanks goes to Carl Scott for proofreading this manuscript.

Lastly, I would like to thank the current and past members of the third floor research groups for providing a stimulating and genial working atmosphere.

For my parents, with love

Chapter 1 - Introduction

1.1 Preamble

The study of organic chemistry relies on the development and interpretation of conceptual models in order to characterize patterns of observed reactivity, and perhaps more importantly, to predict and design reactivity with new synthetic targets in mind.¹ In constructing these models, information from theoretical, mechanistic, methodological, and synthetic studies are brought together to provide a set of rules, which attempt to reconcile both the underlying theory and experimental observations. As more experimental data are collected, and methods to quantify the fundamental physical forces involved in these chemical transformations become more sophisticated, the model evolves to become a more complete and useful predictive tool.

Because compounds in solution are relatively unencumbered by the surrounding solvent molecules, dynamic processes such as conformational exchange and intermolecular collision occur freely. With the geometry of the reactant in a constant state of flux, it is often difficult to amap the most probable trajectory for the reaction under study. In addition, several reaction pathways, each possibly giving rise to different products (e.g. stereoisomers, adducts) may be in competition, thus complicating interpretation with respect to a given model of reactivity. Such conformational flexibility requires additional measures to enforce a uniform mode of reactivity and improve reaction selectivity. In solution these constraints are often achieved through the use of tailored reagents and catalysts that interact with the reactive substrate in a specific manner. Examples of this strategy include the use of a sterically congested base to remove selectively the least hindered proton from a ketone during the formation of a kinetic enolate, and the asymmetric hydrogenation of an olefin mediated by an optically active catalyst.

An alternative to the approaches outlined above involves replacing the conventional isotropic solution medium with a more organized and constrained environment. By confining reactants in an anisotropic reaction cavity, conformational flexibility and diffusion are reduced such that molecular geometry and intermolecular

interactions are limited and thus more uniform than in solution. As a result, chemical reactions performed in such media tend to be more selective than their solution state counterparts as reaction trajectories that were attainable in solution become inaccessible. Access to 'latent' modes of chemical reactivity, those processes that do not proceed in solution but are favoured in the solid state, provides new synthetic avenues that are unavailable *via* conventional methodology.² Examples of organized and constrained media include polymer films, liquid crystals, zeolites, glasses, clays, and crystals.³

Reactions in the crystalline phase, in particular, have been extensively studied. In general, since the crystal lattice is constructed from a single structural element (i.e. the unit cell) which is repeated *ad infinitum* in three dimensions, all reactant molecules exist in the same conformation and are subject to the same anisotropic forces from neighbouring molecules. In addition to the increased selectivity imparted by geometric uniformity, studies of reactivity in the crystalline state provide valuable mechanistic insight. The exact structure of the crystal may be determined through single crystal X-ray diffraction, providing structural information which is not available for the corresponding solution state reactions. When this information is compared to the observed outcome of a solid state reaction, powerful insight into the reaction's geometric and steric requirements is gained. Indeed, this *solid state structure-reactivity correlation method*, because it is based on reactions involving identically oriented reactants for which quantitative information is available (e.g. interatomic distances and angles), has proven to be a valuable tool in defining and refining models of chemical reactivity.

1.2 Crystal Engineering

Although the crystal structure-reactivity approach is able to predict and explain the manner in which solid state reactions proceed, it gives no control over how molecules are arranged within a crystal. The term *crystal engineering*⁴ refers to the study of the chemical and physical properties of crystalline solids with the goal of understanding and directing the crystallization process.^{5,6} When employed in tandem, structure-reactivity analysis and crystal engineering allow retrosynthetic analysis from a desired product to a crystalline starting material, and from these reactant crystals to their individual chemical

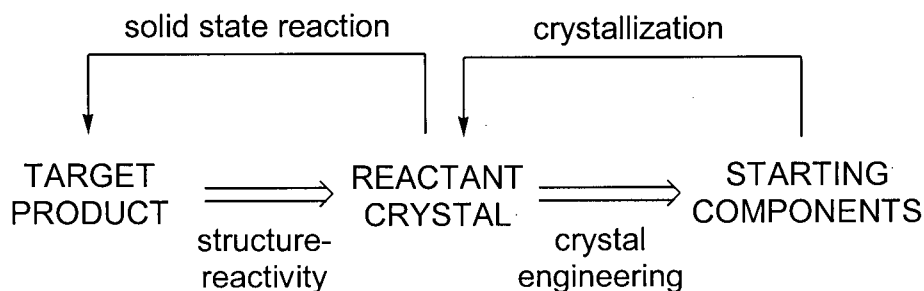


Figure 1.1 Crystal engineering in directed solid state synthesis

components. In this way, the design of highly selective solid state syntheses is, in theory, made possible from first principles (Figure 1.1).⁷

Even though the current understanding of the intra- and intermolecular interactions leading to an observed crystal packing is incomplete, and attempts to engineer crystals have largely been a process of trial and error, significant inroads have been made. An elegant solid state study by Lauher *et al.*⁸ describes the 1,6-polymerization of a triacetylene, a long-standing synthetic problem of considerable interest and a transformation unknown in solution (Figure 1.2). From previous theoretical studies,⁹ and experimental data from structure-reactivity correlations,¹⁰ the geometrical relationships required for successful reaction have been defined (Figure 1.2.a). The ideal crystal would see the monomers tilted 28°, with a distance of 3.5 Å between neighbouring chains and a repeat distance of 7.4 Å. After analyzing two model systems, a two-component crystal composed of vinylogous amide **1** and triacetylene **2** was prepared (Figure 1.2.b). X-ray crystallography confirmed that a suitable arrangement had been engineered (tilt 29.2°; intermolecular distance 3.49 Å; repeat distance 7.14 Å), and γ -irradiation of the crystalline solid indeed led to the desired polymer.

In another system investigated by MacGillivray *et al.*,¹¹ resorcinol (**3**) was employed as a template to organize two molecules of diene **4** such that their double bonds were in a geometry suitable for efficient [2 + 2] photocycloaddition to occur in the solid state. The yield of a single photoproduct, cyclobutane **9**, was quantitative, in stark contrast to the solution state reaction which produces a number of cyclobutane stereoisomers (Figure 1.3).

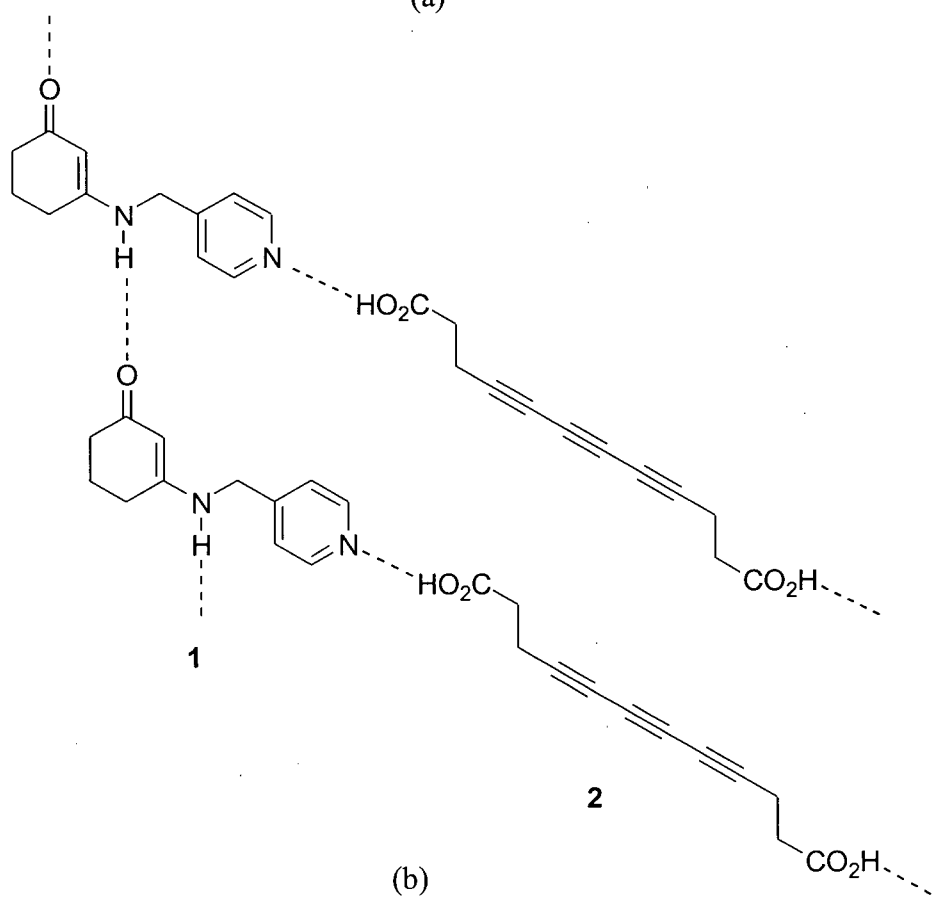
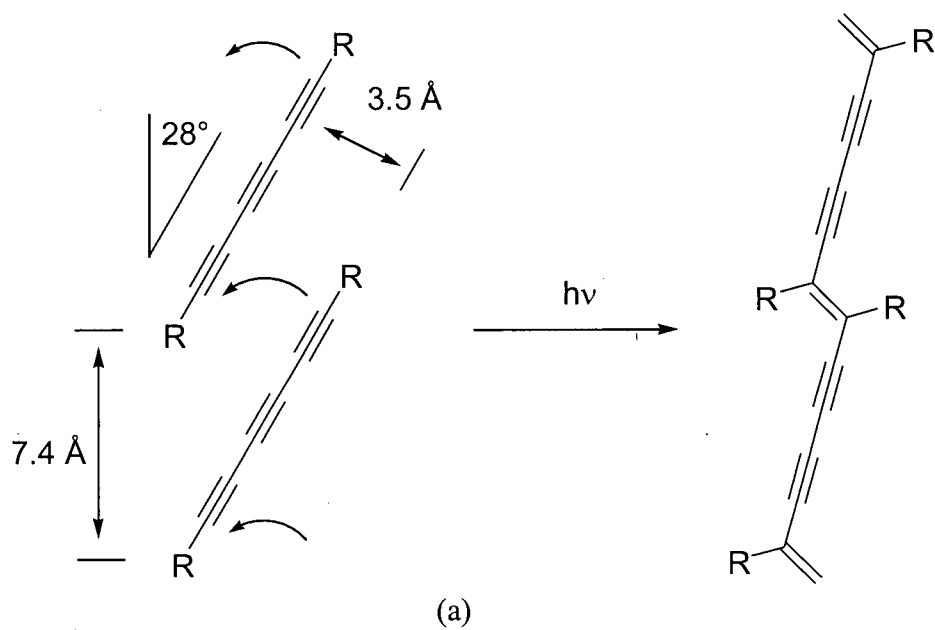


Figure 1.2 (a) Ideal geometry for triacetylene 1,6-polymerization; (b) Monomer alignment in an engineered crystal.

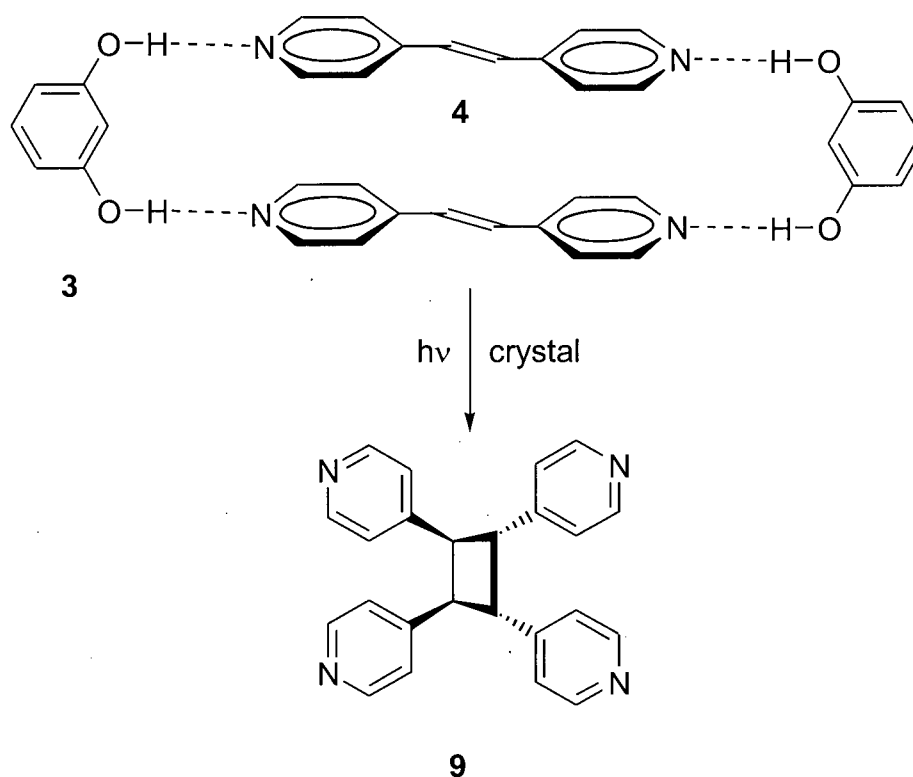


Figure 1.3 Template directed solid state dimerization.

1.3 Factors Influencing Solid State Reactivity

Photochemical reactions are often chosen for study in the solid state for a number of reasons. Light, which may be viewed as a 'reagent' in these transformations, is easily introduced into the crystal without disrupting the lattice. The wavelength of radiation may be tailored to the absorption characteristics of the photochemical substrate, and reactions may be carried out at ambient or reduced temperature. Thermal reactions, although not precluded from crystalline state chemistry, suffer the disadvantage that the thermal energy required to promote reactivity also increases the likelihood of crystal melting and concomitant loss of crystal lattice rigidity and regularity. An interesting example of a thermal solid state reaction comes from the research of Toda *et al.*¹² and is illustrated in Figure 1.4. When crystals of the thermally labile diallene **10** are heated to 150 °C, a

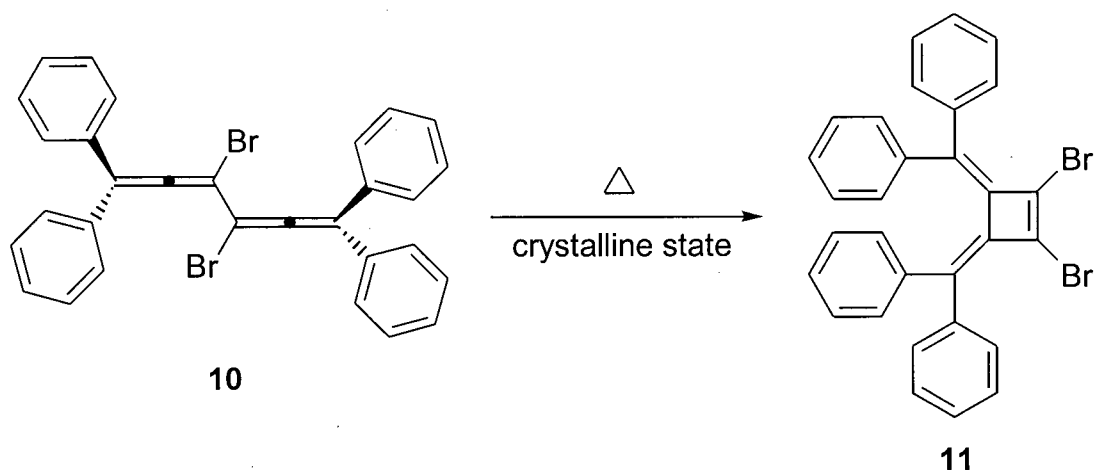


Figure 1.4 A thermal crystalline state reaction.

spontaneous electrocyclic rearrangement takes place in which dimethylenecyclobutene **11** is formed.

With the current limitations of crystal engineering in the design of multiple-component systems, solid state studies have focussed primarily on unimolecular reactions (e.g., rearrangements) and dimerizations. An effective strategy for performing *heterobimolecular* solid state reactions comes from the growth of mixed crystals formed by co-crystallization of two structurally similar molecules. Compounds with similar structural features, such as acrylamide (**13**) and cinnamamide (**15**) will often crystallize together in a regular array (Figure 1.5).¹³ Subsequent reaction (irradiation in this case) selectively produces the mixed dimer **17** as well as the *anti* head-to-tail homodimer **18** with excellent regio- and stereocontrol.

With the advent of modern X-ray crystallographic techniques in the 1960's, seminal work by Schmidt and co-workers provided a set of guidelines, the *topochemical rules*, to which solid state reactions should adhere.^{14,4} Chief among these is the principle of *least motion*, which supposes that, since crystalline state reactions proceed in a constrained environment, they do so with a minimum of atomic and molecular motion. Thus, when two or more reaction pathways are chemically available to a reacting species, the reaction course involving the least atomic displacement should be favoured. Schmidt was also able to define a set of geometric parameters describing the relative geometry

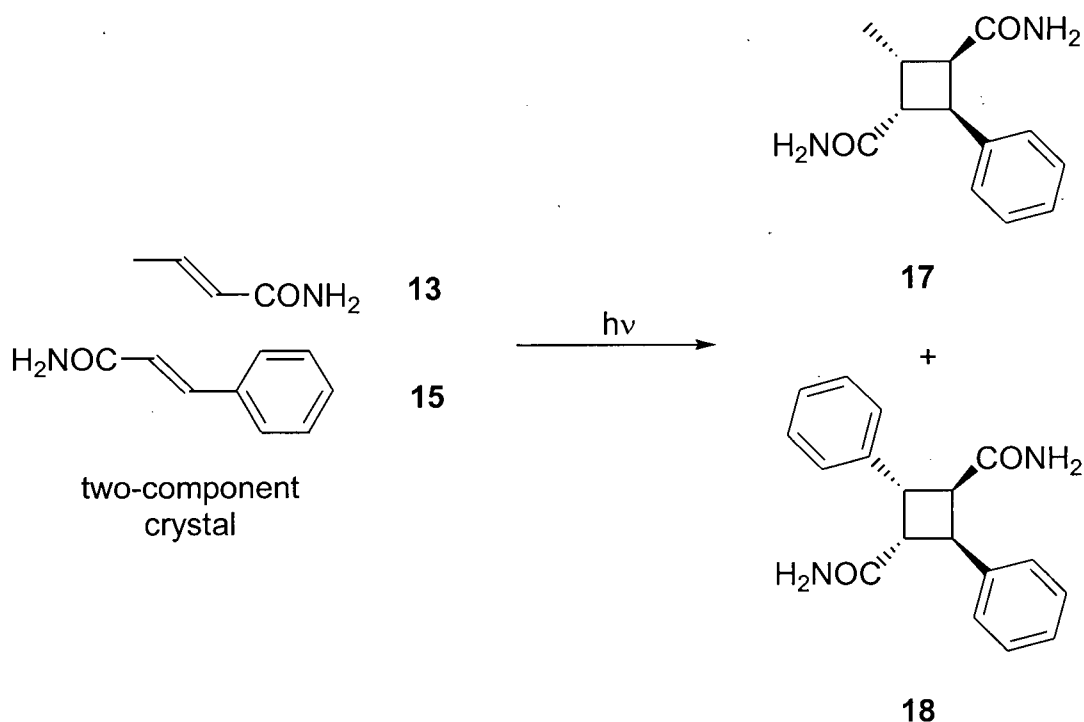


Figure 1.5 Solid state bimolecular reaction of a mixed crystal.

(e.g. distances, and angles) necessary for the [2 + 2] photocycloaddition of substituted cinnamic acids to proceed successfully.

Solid state reaction theory was furthered by Cohen and co-workers with the development of the *reaction cavity concept*.^{15,16} In this paradigm, the reacting molecule is considered to exist in a cavity bounded by its nearest neighbours. As the shape of the molecule changes along a reaction pathway through transition state to product, steric interactions between the cavity and any intermediate structure will favour transition state geometries that least interfere with the cavity walls (Figure 1.6). An elegant illustration of reaction cavity and topochemical control comes from the work of Garcia-Garibay *et al.* on the total synthesis of α -cuparenone (**21**, Figure 1.7).¹⁷ On photolysis of ketone precursor **19**, expunction of carbon monoxide leads to formation of 1,5-biradical **20**. Constrained by the reaction cavity, the biradical cyclizes to **21** with retention of stereochemistry at the benzylic position. It should be noted, however, that not all solid state reactions can be understood from simple inspection of the crystal structure. The

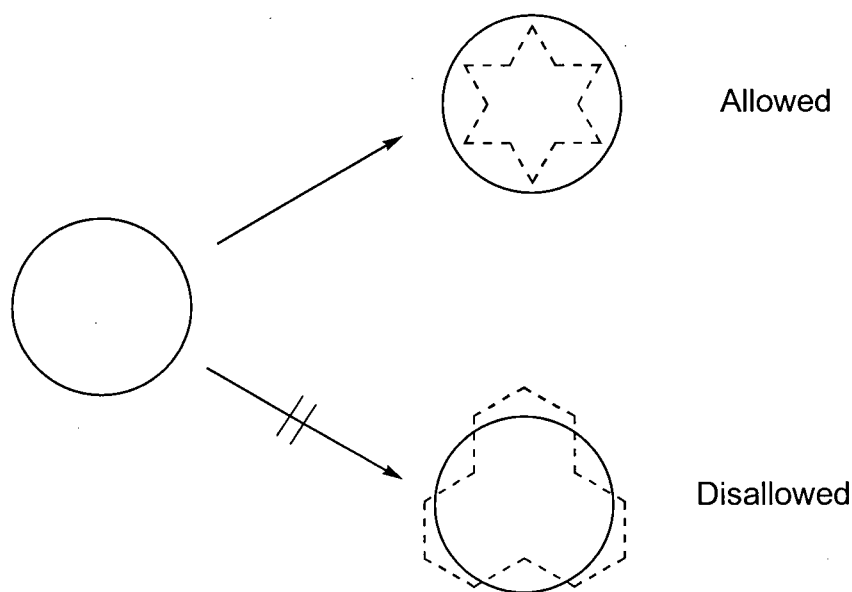


Figure 1.6 Illustration of the 'reaction cavity' concept. Processes are allowed only if the transition state (dashed line) fits within the cavity (solid line).

reaction depicted in Figure 1.4 is decidedly non-topochemical, with a large motion of compound **10** required, from the *s-trans* to the reactive *s-cis* conformation, before the reaction can proceed. The role of crystal surface reactions, lattice defects and phase transitions¹² have been invoked to help explain such results.

More quantitative approaches to the analysis of solid state reactivity have also been put forward.¹⁸ In general, these involve constructing a computer model of a section

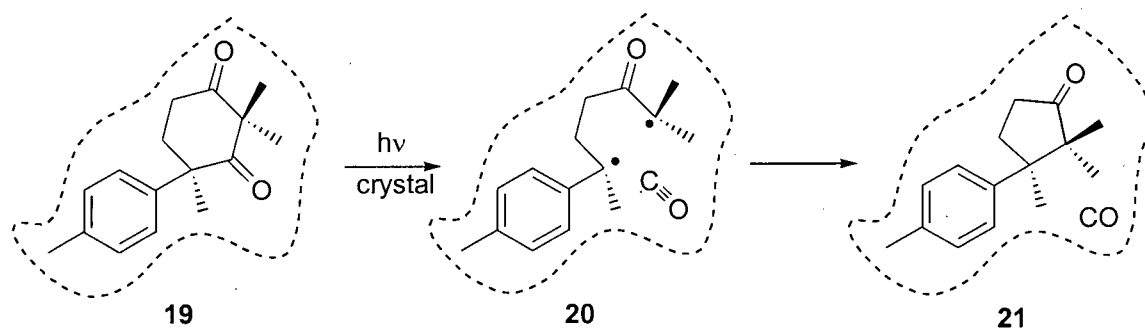
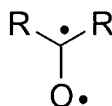


Figure 1.7 Solid state synthesis of α -cuparenone (**21**). Confinement in the reaction cavity promotes stereoselective cyclization.

of the reactant crystal based on X-ray crystallographic data. A chemical reaction is simulated by replacing a molecule in the centre of the mini crystal lattice with a species representing the transition state of a proposed reaction pathway. Computer modelling then allows the cumulative effect of this replacement on the surrounding molecules to be calculated. In this manner the energetic requirements for a number of reaction pathways may be compared, and a prediction made on the outcome of a solid state reaction for which qualitative assessment of the crystal structure provides no obvious answers.

1.4 Type II Photochemistry of Ketones¹⁹

Both aliphatic and aromatic ketones absorb ultraviolet (UV) light in the 290-330 nm region.²⁰ Photons of this energy promote an electron from one of the non-bonding orbitals on oxygen, to the anti-bonding π^* orbital of the carbonyl chromophore in what is referred to as an $n \rightarrow \pi^*$ transition. After this electron promotion, the resulting excited state species possesses an unpaired electron localized on each of the oxygen and carbon atoms, and the reactivity of this moiety may in some ways be likened to that of a 1,2-biradical (22).²¹ In the type II reaction, an intramolecular hydrogen atom abstraction occurs by the oxygen atom of the excited state ketone, and the result is a hydroxybiradical (Figure 1.8). Abstraction of a γ -hydrogen atom to form a 1,4-biradical (23) is favoured as it proceeds *via* a six-membered transition state; however, β - and δ -hydrogen abstraction may also be observed, especially when no γ -hydrogen atoms are available for reaction.



22

Three reaction pathways are available to the intermediate 1,4-hydroxybiradical: (1) disproportionation *via* reverse-hydrogen transfer, thus reforming the starting ketone in a degenerate reaction; (2) scission of the α - β C-C σ -bond (the Norrish Type II reaction),

the result of this cleavage being an enol (**24**) and an alkene (**25**), which subsequently tautomerizes to the corresponding ketone; (3) cyclization of the biradical (Yang photocyclization) to form a cyclobutanol (**26**). Partitioning among these three pathways is believed to be controlled by the conformation and spin multiplicity of the intermediate biradical.^{19a} In particular, overlap between the two half-filled p-orbitals and the breaking σ -bond is a stereoelectronic requirement for cleavage. The transoid, gauche, and cisoid conformations shown in Figure 1.9 all potentially allow such requirements to be met. Cyclization, on the other hand, requires that the two radical centres overlap efficiently.²² For this to occur, the directionality of the p-orbitals and their separation must be taken into account, and the transoid geometry is clearly not acceptable.

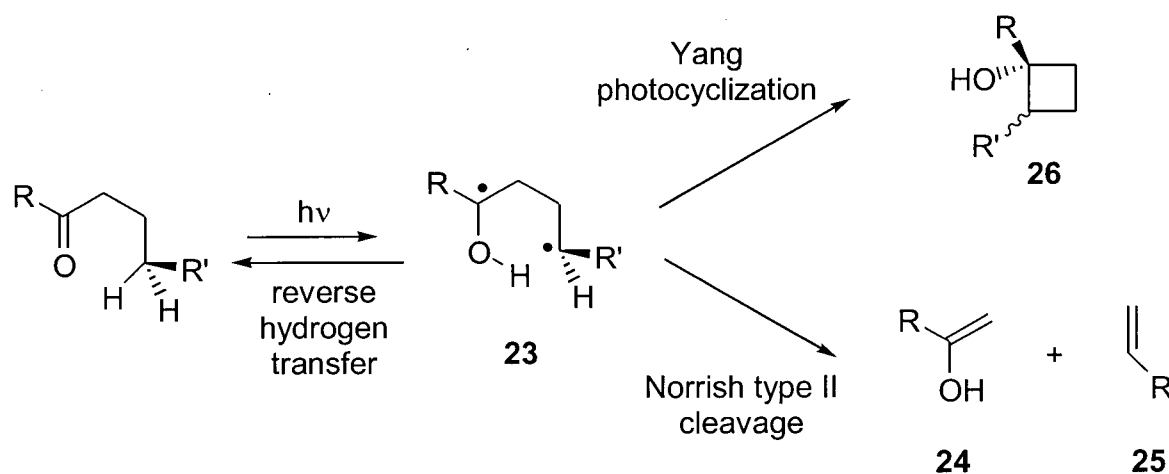


Figure 1.8 Type II photochemistry of ketones.

In addition to these geometric requirements, there is an additional electronic aspect to consider. For any of the three pathways to proceed, the biradical must exist in the singlet state, i.e. with unpaired electrons of opposite spin. In general, aromatic ketones undergo type II hydrogen abstraction from the triplet excited state, while, for aliphatic ketones, both the singlet and triplet species may have lifetimes sufficiently long for type II abstraction to occur.²³ In solution, any triplet 1,4-hydroxybiradicals, since they cannot undergo intramolecular reaction, are long enough lived to experience conformational interchange. Thus, the products derived from these intermediates will be

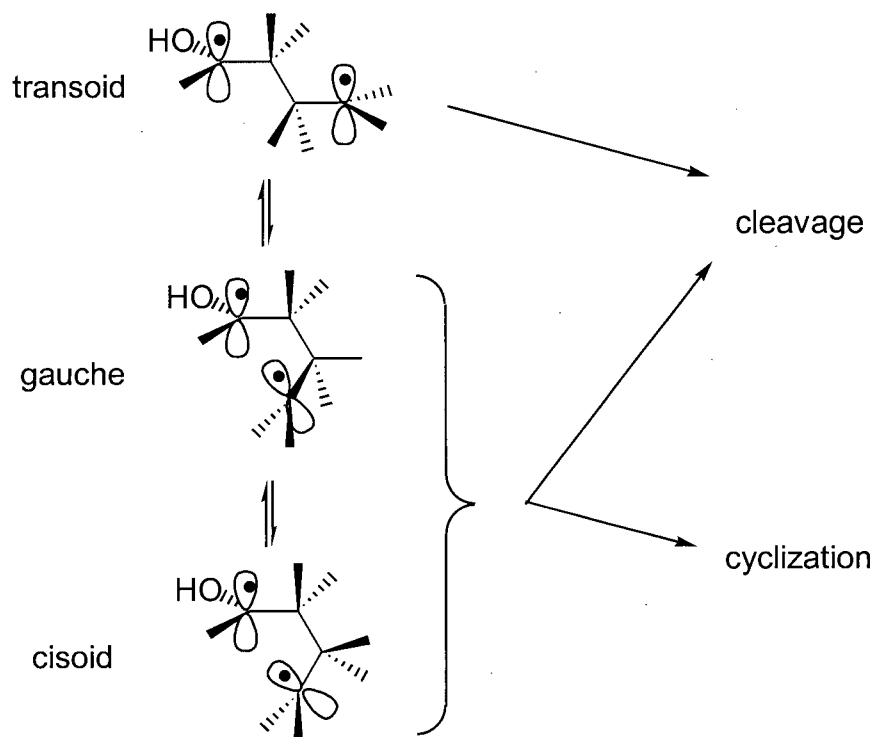


Figure 1.9 Dependence of reaction pathway on biradical conformation.

strongly influenced by the geometry at which triplet→singlet intersystem crossing occurs, and may not necessarily correlate with the geometry of the initially formed biradical, or its lowest energy conformer(s).²⁴ Conducting these reactions in the solid state circumvents this thorny issue, as the biradical is trapped in the crystal lattice and has limited conformational flexibility. In addition, since biradical formation involves only the motion of a hydrogen atom over a relatively short distance, the geometry of the biradical should resemble that of the starting ketone. Correlation of crystalline ground state ketone structures with observed reactivity, therefore, should provide quantitative data not available from solution state studies.

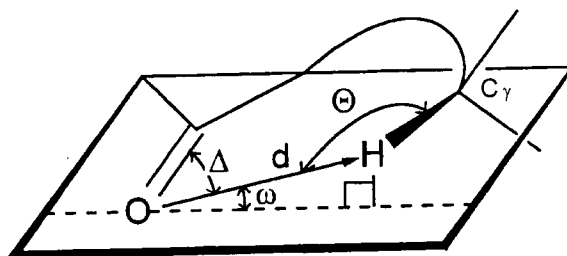


Figure 1.10 Geometric parameters for γ -hydrogen atom abstraction.

1.5 Geometric Requirements for Hydrogen Abstraction

Extensive crystalline state studies by Scheffer and co-workers on type II hydrogen abstraction has provided a detailed model that quantifies the geometric requirements for this process.²⁵ Four parameters uniquely define the disposition of a hydrogen atom with respect to the reactive n-orbital on the oxygen atom of the electronically excited carbonyl group. These are illustrated in Figure 1.10: d , the O \cdots H interatomic distance; Δ , the C=O \cdots H angle; θ , the O \cdots H-C angle; and ω , the dihedral angle that the O-H vector makes with respect to the nodal plane of the π -system. Correlation of (n,π^*) excited state reactivity with the geometry of the ground state ketone is valid because the excitation is known to be highly localized in the carbonyl group such that geometric changes in the rest of the molecule are negligible.²⁶

From a theoretical standpoint, ideal values for the four parameters have been deduced. The sum of the van der Waals radii for a hydrogen and an oxygen atom is 2.72 Å,²⁷ and this value has been put forward as the optimum value of d , as it ensures that orbitals from the oxygen and hydrogen atoms are in close contact. The angle ω measures the deviation of the hydrogen atom under consideration with the plane that contains the half-filled oxygen n-orbital. Overlap is maximized when ω is 0°, and approaches zero as an orthogonal geometry is approached ($\omega = 90^\circ$). On the basis of mathematical and experimental kinetic studies, Wagner has proposed that the abstraction rate is proportional to $\cos^2\omega$.²⁸ *Ab initio* calculations by Houk have likewise shown that the enthalpy of activation increases significantly as θ deviates from 180°, suggesting that a

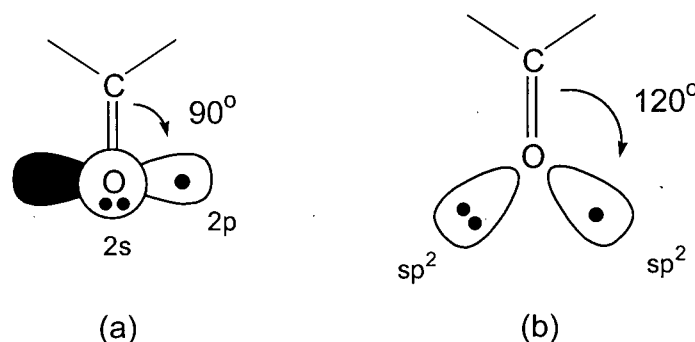
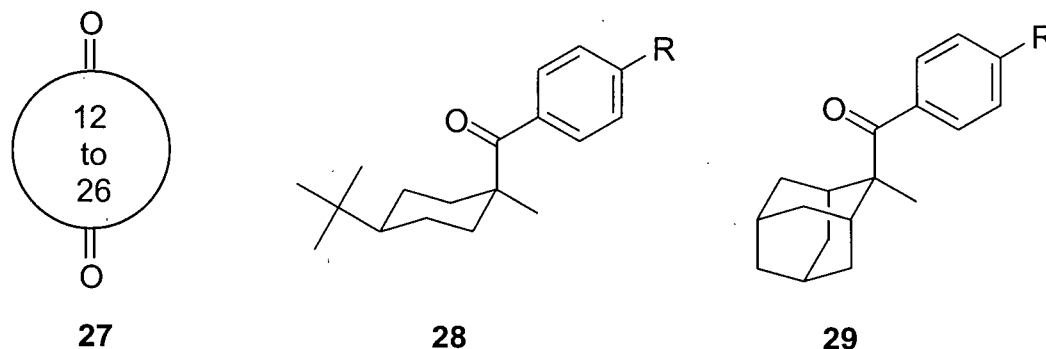


Figure 1.11 Two models of the ketone excited state: (a) Kasha's proposal –oxygen unhybridized; (b) sp^2 -hybridized 'rabbit ear' model.

linear O···H-C arrangement is preferred.²⁹ Pinpointing an ideal value for the Δ parameter is complicated by the fact that two models of the (n,π^*) excited state ketone exist (Figure 1.11). In the so-called 'rabbit ear' conception, the atomic orbitals on oxygen are hybridized, and the two non-bonding sp^2 hybrids are degenerate, each forming a 120° angle with the carbonyl C=O bond. In the model proposed by Kasha,³⁰ the oxygen atom is not hybridized, resulting in non-degenerate non-bonding orbitals, one largely of 2s character, and the other 2p-like. The latter, which forms an angle of 90° with respect to the C=O bond, contains the unpaired electron in the excited state. In general, therefore, the ideal Δ angle is thought to lie in the 90-120° range.

Inspection of the above data reveals that it is geometrically impossible for all of the atoms to be ideally aligned in a six-membered transition state; some of the parameters must deviate significantly from their optimum value. The solid state study of two series of compounds by Scheffer *et al.*²⁵ has provided average values for γ -hydrogen abstraction parameters in the homologous macrocyclic aliphatic ketones **27**,³¹ and for the aromatic ketones³² **28** and **29** (Table 1.1). A number of important points are revealed in these numbers. The fact that both the aliphatic and aromatic ketones possess such similar geometries in the solid state provides strong support for this idea that such orientation is a general predictor of successful γ -hydrogen atom abstraction. Considerable deviation of the ω (up to 62°) and θ (as low as 113°) angles from ideal values clearly does not prevent the abstraction process. The fact that Δ lies closer to 90° than 120° fits more closely with the Kasha model, but by no means excludes the possibility of the 'rabbit ear' orbital



configuration. The interatomic distance d is arguably the most useful predictor of type II reactivity. In cases where more than one hydrogen atom is properly aligned for abstraction, only abstraction of the closer atom is observed. To date, the largest reported value³³ of d for successful γ -hydrogen atom abstraction is 3.10 Å (*vide infra*), demonstrating that the upper limit for $\text{C}=\text{O}\cdots\text{H}$ contact extends beyond the van der Waals limit. It must be emphasized, however, that a favourable value of d alone does not ensure that abstraction will take place. Figure 1.12 illustrates a transformation proposed by Prinzbach *et al.*³⁴ in which two consecutive photocyclizations were envisaged. Although the calculated abstraction distance of 2.34 Å was indeed favourable, failure of the photochemical transformation of diketone **30** to product **31** may reasonably be attributed to its ω angle of $\sim 90^\circ$, rigidly constrained by the cage structure.³⁵

Table 1.1 Ideal and crystallographically derived H_γ -abstraction geometries.

	d (Å)	ω (°)	θ (°)	Δ (°)
Ideal	< 2.72	0	180	90-120
27	2.73 ± 0.03	52 ± 5	115 ± 2	83 ± 4
28 / 29	2.63 ± 0.06	58 ± 3	114 ± 1	81 ± 4

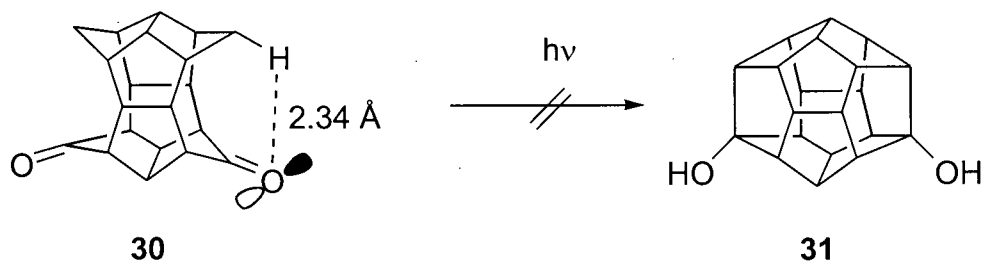


Figure 1.12 Although the $\text{C}=\text{O}\cdots\text{H}$ distance is favourable, a Δ value of 90° betrays a lack of orbital overlap.

1.6 Photochemistry of Linearly Conjugated Cyclohexadienones³⁶

Conjugation of the carbonyl chromophore with aliphatic double bonds dramatically changes its excited state chemistry compared to that of aliphatic and aromatic ketones. In particular, the photochemistry of linearly conjugated cyclohexadienones (and benzocyclohexadienones) **32** has been a subject of much research, as their reactions tend to proceed cleanly and efficiently while providing products of greater structural complexity. In addition to their synthetic potential, mechanistic studies on the photochemistry of these compounds have provided an interesting and detailed picture of the reaction pathways. Most notable among these discoveries is the dependence of the mode of reactivity on the nature of the excited state (i.e. (n,π^*) or (π,π^*)).^{36b}

The general mechanistic scheme is outlined in Figure 1.13. Reaction *via* the $^1(n,\pi^*)$ surface results in α -cleavage, a type I photochemical process which gives rise to the twisted singlet biradical **33**. Simple bond rotations bring the isolated radical centres into conjugation with the π -system of the diene, thus forming ketene **34**. The formation of the ketene intermediates has been unambiguously confirmed by low temperature IR studies in frozen matrices. In the presence of a suitable nucleophile, the ketene may also be trapped to form compounds of general structure **35**. In the absence of such trapping agents, the unsaturated ketene may either undergo an electrocyclozation to re-form the starting cyclohexadienone **32**, or proceed to bicyclo[3.1.0]hexane **36** by way of an internal crossed $[4 + 2]$ cycloaddition. The same bicyclic product is formed when the reaction proceeds by way of the $^1(\pi,\pi^*)$ manifold, a fact which greatly complicates the

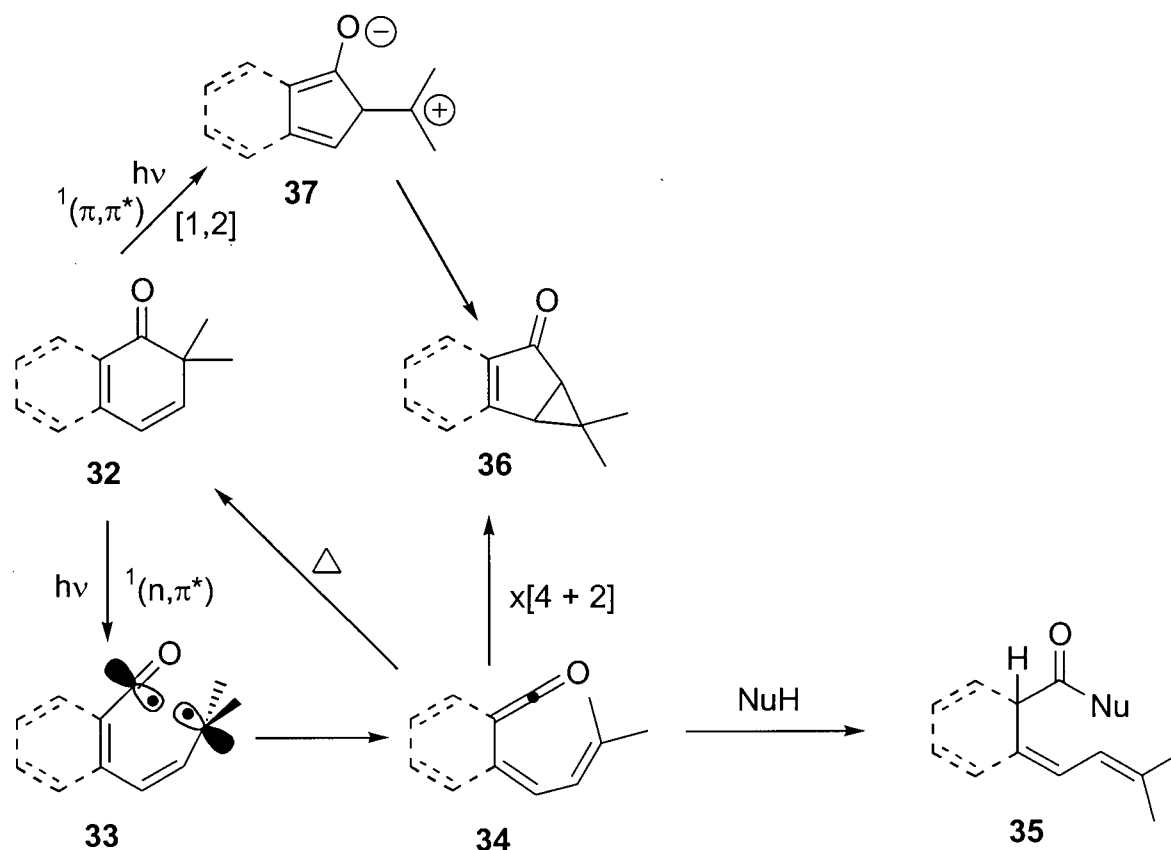


Figure 1.13 Photochemical pathways of linearly conjugated cyclohexadienones.

study of this reaction. In this process, however, no ketene intermediate is involved. While Quinkert *et al.* have suggested that a concerted $[\pi_2^a + \sigma_2^a]$ rearrangement may be in operation,^{36a} others have proposed that the [1,2] shift involves a zwitterionic (37) or biradical intermediate.^{36b}

Regardless of the excited state involved, triplet quenching studies have established that both pathways proceed exclusively from singlet excited states. Through manipulation of experimental conditions (e.g. solvent, additives) and substrate functionalization, it has been possible to alter the relative energies of the $^1(n, \pi^*)$ and $^1(\pi, \pi^*)$ excited states and thus exercise a measure of control over reactivity. Ultraviolet spectroscopy has also proven useful in determining which of the two excited states is of lower energy, and hence responsible for the observed reactivity.

A synthetic application of this reaction is shown in Figure 1.14.³⁷ Dienone **38** is readily synthesized from 2,6-dimethylphenol and (*E*)-1,4-dibromobut-2-ene in two steps. Photolysis of this compound in methanol gives rise to diester **39** *via* an intermediate diketene. Further oxidation leads to crocetin dimethyl ester (**40**), providing an efficient route to this natural polyene.

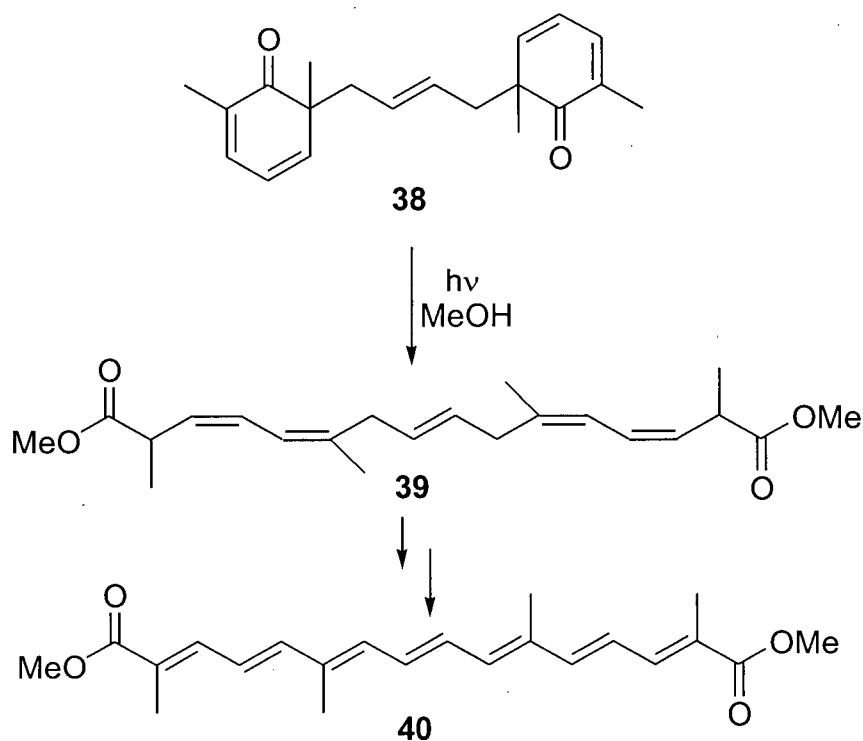


Figure 1.14 Synthesis of crocetin dimethyl ester (**40**) using dienone-ketene photochemistry.

1.7 Asymmetric Induction and the Ionic Chiral Auxiliary Concept

The demand for optically pure, rather than racemic synthetic molecules, has increased dramatically over the last decade. This pressure stems largely from the pharmaceutical and biotechnology industries, and has fuelled research interest such that asymmetric synthesis has become the rule rather than the exception. At the heart of the matter is the desire to selectively alter an achiral molecule in such a way that more of one product enantiomer is formed than the other. In solution, excellent results have been achieved using optically active reagents, catalysts, and auxiliaries.

Crystalline state chemistry has also proven effective at asymmetric induction, through the action of crystal to molecular chirality transfer. Of the 230 space groups in which a molecule may crystallize, 65 are chiral. This means that, since no inversion or reflection symmetry elements are present in these crystals, all molecules in the lattice are influenced by the same chiral anisotropic forces. Achiral molecules that crystallize in this manner are hence expected to react such that one product enantiomer is favoured over another. This process is termed *absolute asymmetric synthesis*,³⁸ since no external source of optical activity (e.g. a chiral auxiliary) is influencing the reaction. In this manner, the chirality of the crystal lattice is manifested in the absolute configuration of the optically active product. Figure 1.15 illustrates two such photochemical transformations. In the first example, single crystals of dibenzobarrelene **41**, which crystallizes in the chiral space group $P2_12_12_1$, are transformed into dibenzosemibullvalene **42** in greater than 95% enantiomeric excess.³⁹ The second reaction, taken from the work of Toda *et al.*, concerns the Yang photocyclization of α -oxoamide **43**, which also crystallizes in $P2_12_12_1$. Crystalline state photolysis of single crystals of compound **43** affords the chiral β -lactam **44** in 93% enantiomeric excess.⁴⁰

While the crystallization of achiral molecules in chiral space groups is by no means an uncommon occurrence, it is neither a general nor a predictable phenomenon. This severely limits the utility of absolute asymmetric reactions in synthesis. A more general approach to solid state asymmetric induction is to use the conventional concept of a chiral auxiliary. By covalently attaching an optically active moiety to the reactive substrate, one is assured of obtaining optically active crystals, as enantiomerically pure compounds are required to crystallize in chiral space groups. An example of this

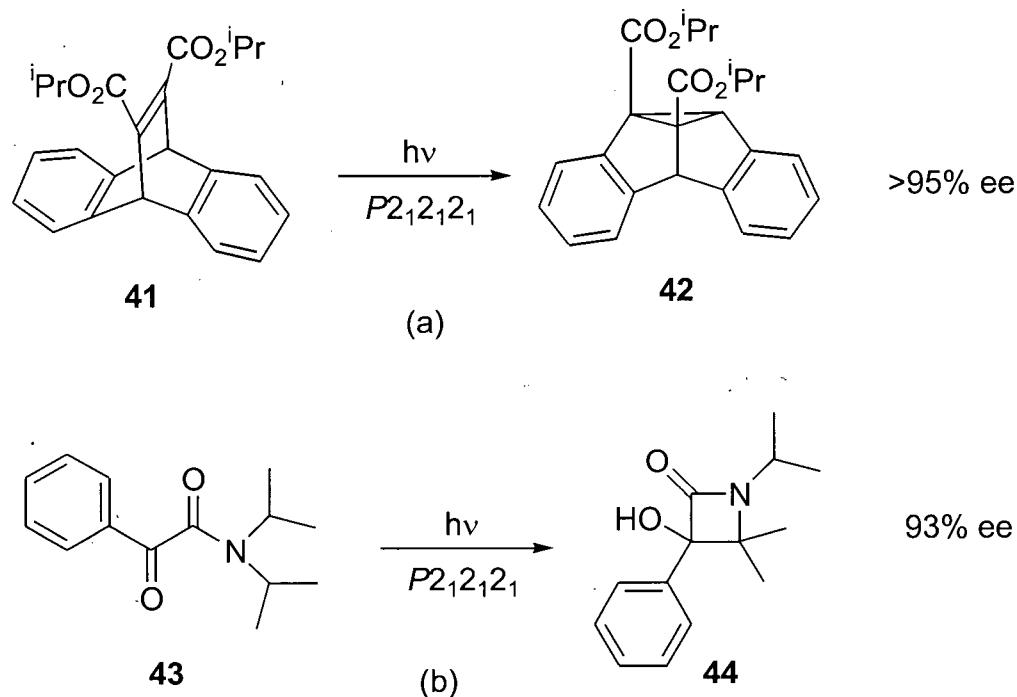


Figure 1.15 Crystalline state absolute asymmetric syntheses: (a) A di- π -methane rearrangement; (b) A Yang photocyclization.

approach is illustrated in Figure 1.16. While solution state photolysis of β -ketoester **45** gives rise to diastereomers **46** and **47** with low stereoselectivity (14% de), the corresponding crystalline state reaction is far more selective, with a measured de of 96%.⁴¹ Not only does this example illustrate the selectivity afforded by conducting the reaction in the solid state, but also emphasizes a critical difference between the mechanism of action of chiral auxiliaries in the solution and solid states. In solution, the chiral auxiliary is generally required to alter the steric environment at the reaction site, by either blocking or facilitating access in a stereoselective manner. Attachment of the auxiliary in close proximity to the reaction locale is not, however, a requirement in the solid state. The mere presence of a stereogenic element conveys chirality throughout the entire crystal lattice, and this influence is manifested in the conformation of the reactant and the shape of the reaction cavity, the ultimate determinants of the reaction's steric course.

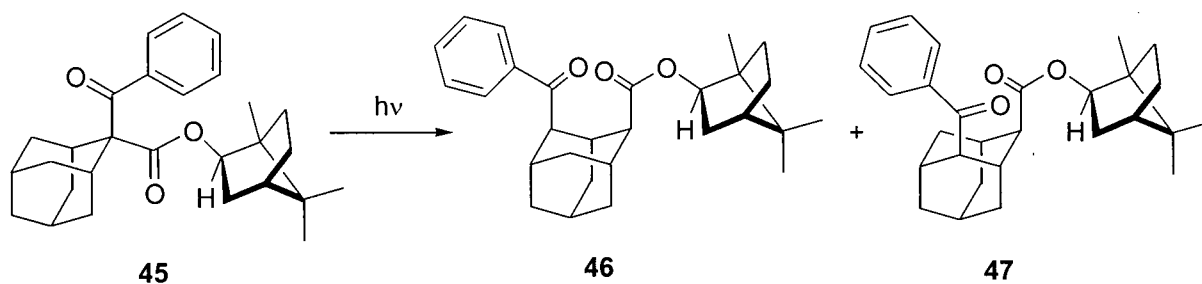


Figure 1.16 The photoreaction of β -ketoester **45** is highly diastereoselective in the crystalline state, but gives poor results in solution.

The fact that the optically active moiety does not need to be tightly bound to the reactive substrate provides a great degree of flexibility in the design of asymmetric solid state reactions, and this has been exploited by Scheffer and co-workers. Through the use of *ionic* chiral auxiliaries,⁴² salts are formed between an achiral, photoreactive carboxylic acid (or amine) and an optically pure amine (acid). Figure 1.18 demonstrates the general concept. Since the crystalline environment is chiral, reaction of the photolabile ion can proceed *via* either of two diastereomeric transition states of differing energy. The pathway with the lowest kinetic barrier proceeds at a greater rate, and the product of this reaction will predominate.⁴³ Subsequent removal of the ionic auxiliary with simple acid-base extraction provides the optically active photoproduct. An example of this concept put into practice is shown in Figure 1.17. Optically active salt **48** provides cyclobutanol **49** after crystalline state photolysis and subsequent diazomethane workup.⁴⁴

Since salts are generally higher melting than molecular solids, they tend to better retain their crystallinity and resist melting during photolysis. The ease with which the ionic chiral auxiliary can be 'attached' or changed rivals typical solution state chemistry, and in all reports on this method to date an effective (>80% ee) ionic auxiliary has been found. Although crystals suitable for X-ray crystallographic analysis are not required for successful asymmetric induction, solid state structure-reactivity correlations resulting from these studies have helped lend further detail to existing reaction models.

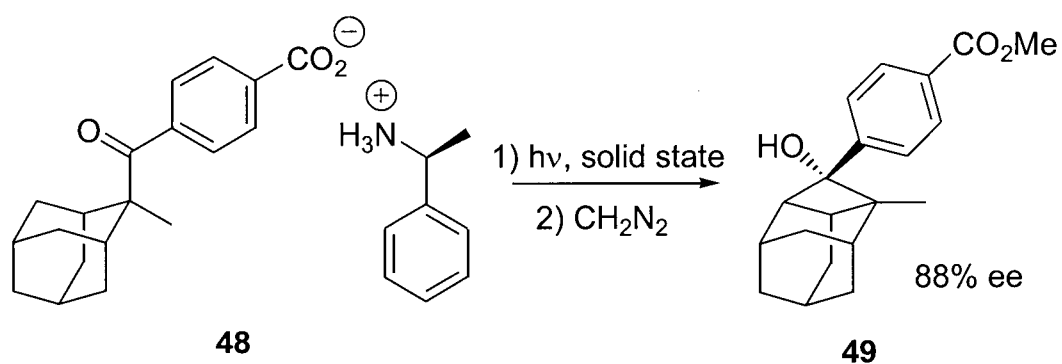


Figure 1.17 An example of the ionic chiral auxiliary concept in the solid state Yang photocyclization of salt **48**.

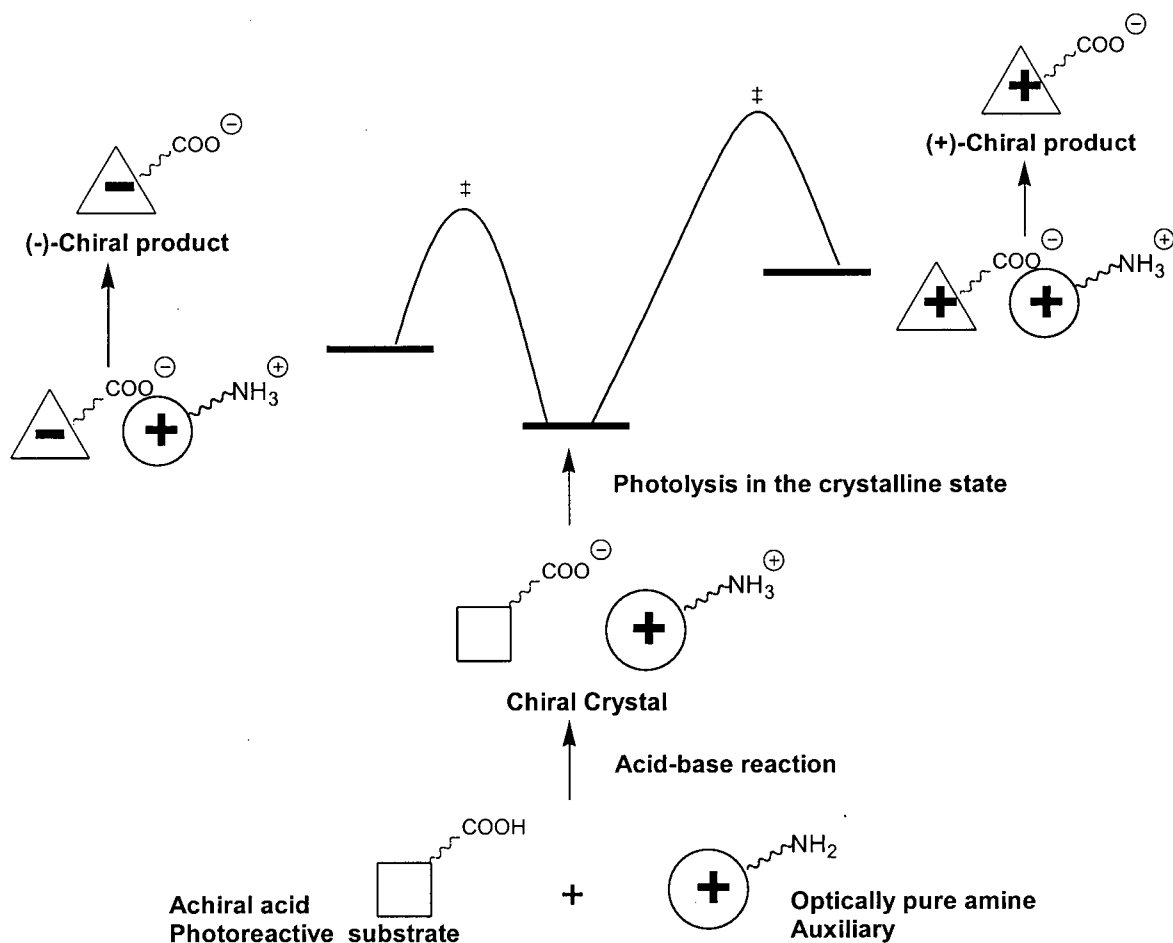
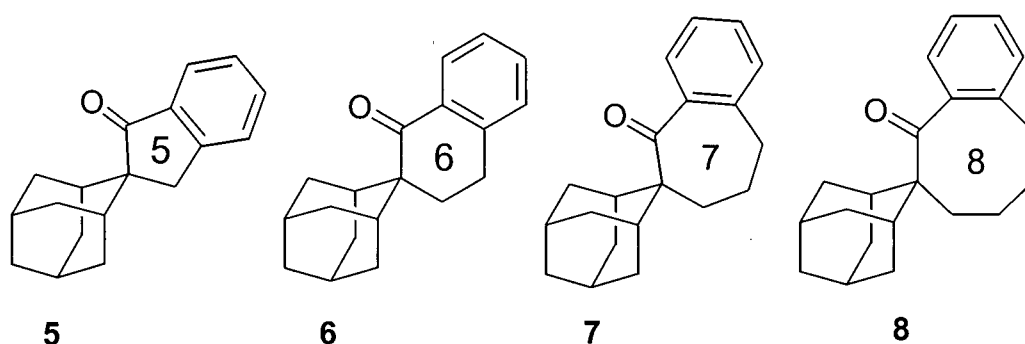


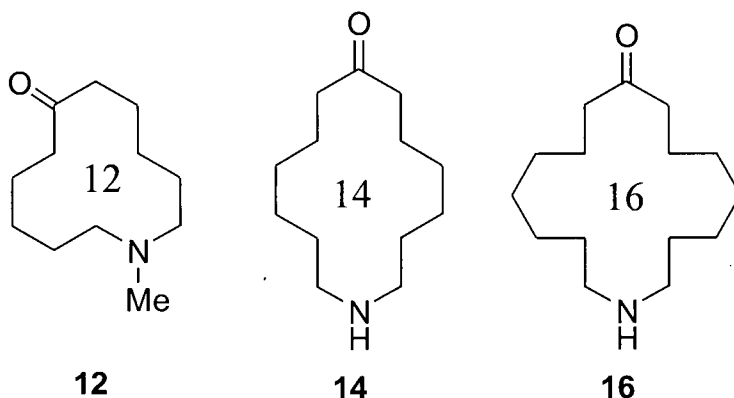
Figure 1.18 Schematic representation of the ionic chiral auxiliary approach to asymmetric solid state synthesis: reaction *via* diastereomeric transition states.

1.8 Research Objectives

This thesis reports on three separate studies, each designed to explore a different aspect of crystalline state chemistry through solid state structure-reactivity correlation. The first project stems from earlier studies in our laboratory on the solid state Norrish/Yang Type II photochemistry of phenyladamantylketones **29** (Table 1.1).³² X-ray crystallography has revealed that, regardless of the substituent on the phenyl ring, all of these ketones adopt solid state conformations in which the mean plane of the carbonyl group is roughly orthogonal to the plane bisecting the adamantyl skeleton. Since all the compounds possessed similar solid state geometries, it was not surprising that they reacted in the same manner, producing only the *endo*-aryl cyclobutanols (see Figure 1.17). In order to probe the effect of carbonyl geometry on the reaction outcome, and to model the reaction for a number of different ketone geometries, our interest lay in studying a series of benzoyladamantyl ketones in which the disposition of the photoreactive carbonyl group could be altered systematically. Our strategy was to synthesize spiroadamantyl ketones **5-8**, compounds in which a methylene chain of varying length constrains the orientation of the carbonyl group through the introduction of five- to eight-membered rings. Previous experience with adamantane-derived compounds in our laboratory suggested that the substrates chosen would have a reasonable chance of forming crystals suitable for X-ray crystallographic analysis.



Since a great deal of our studies on the ionic chiral auxiliary approach to asymmetric synthesis have employed optically active *cations* as the chiral influence, we sought to extend this methodology by studying salts in which the *anion* introduces chirality to the crystal lattice. The macrocyclic amino ketones **12**, **14**, and **16** seemed



to be logical choices for the photolabile achiral component of the salts for a number of reasons. The synthesis of compound **12** has been reported in the literature⁴⁵ and is straightforward, thus allowing a number of different salts to be synthesized and in quantity. Cyclic ketones, in contrast to their acyclic analogues, are known to give rise to a greater proportion of cyclization versus cleavage products in their type II photochemistry. This is advantageous because it is the chiral cyclobutanol products **50** and **51** that are of interest; cleavage products are achiral and thus give no information on solid state asymmetric induction (Figure 1.19). The possibility of selectivity in the formation of either the *cis*- or *trans*-fused cyclobutanols adds another element that may be analyzed in terms of the solid state geometry. Being a type II photoreaction, these systems will contribute further to the reactivity model we have formulated for these processes.

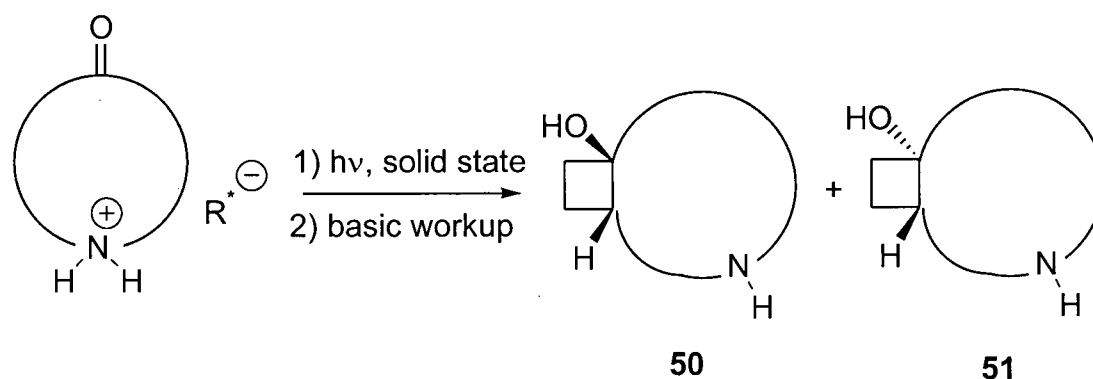


Figure 1.19 General scheme for the solid state photochemistry of macrocyclic aminoketone salts.

In the third study, exploration of solid state asymmetric induction was again the main objective. The object of this undertaking was to provide information on how solid state reactivity is influenced by the anisotropic cavity in which the reactive substrate lies. In the previous Type II photoreactivity studies, conformational bias alone was able to explain the observed reactivity, as typically only one of two enantiotopic hydrogen atoms is capable of reacting. The substrate in this instance was chosen based on its limited conformational lability. The anion in optically active salts of carboxylic acid **52** is hypothesized to be nearly planar, with only small conformational variations expected among its different solid state structures. Removing the conformational bias would thus allow the influence of the cavity to be evaluated on its own, as the rearrangement to ketone **53** proceeds (Figure 1.20).

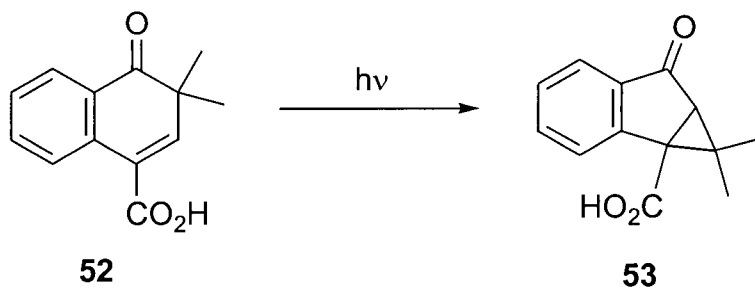


Figure 1.20 Photorearrangement of benzocyclohexadienone **52**.

Results and Discussion

Chapter 2 – Competition between Cyclization, Cleavage and Reverse Hydrogen Transfer in the Solid State Norrish/Yang Type II Photochemistry of a Homologous Series of Spiroadamantyl Ketones

2.1 Synthesis of the Spiroadamantyl Ketones

2.1.1 Retrosynthetic Analysis

Two different strategies were employed in the synthesis of ketones **5-8** (Figure 2.1). Retrosynthetic analysis of the key spirocyclization step led to the disconnection of bond **a** as a logical first choice. Formation of the five- and six-membered compounds **5** and **6** *via* an intramolecular Friedel-Crafts acylation from the corresponding acyclic precursors **54** and **55** was indeed successful. Attempts to form the seven-membered substrate **7** by this method from its corresponding acyl derivative ($n = 3$, $X = \text{Cl}$) resulted solely in acyclic products lacking a carbonyl moiety, presumably due to the slow rate of cyclization of the intermediate acylium ion relative to decarbonylation. Ring-closing metathesis (RCM),⁴⁶ which has emerged as a powerful tool in the synthesis of medium-sized rings,⁴⁷ proved an efficient route to the seven- and eight-membered spiroketones **7** and **8**. Bond disconnection **b** illustrates this strategy, with dienes **56** and **57** as the cyclization precursors.

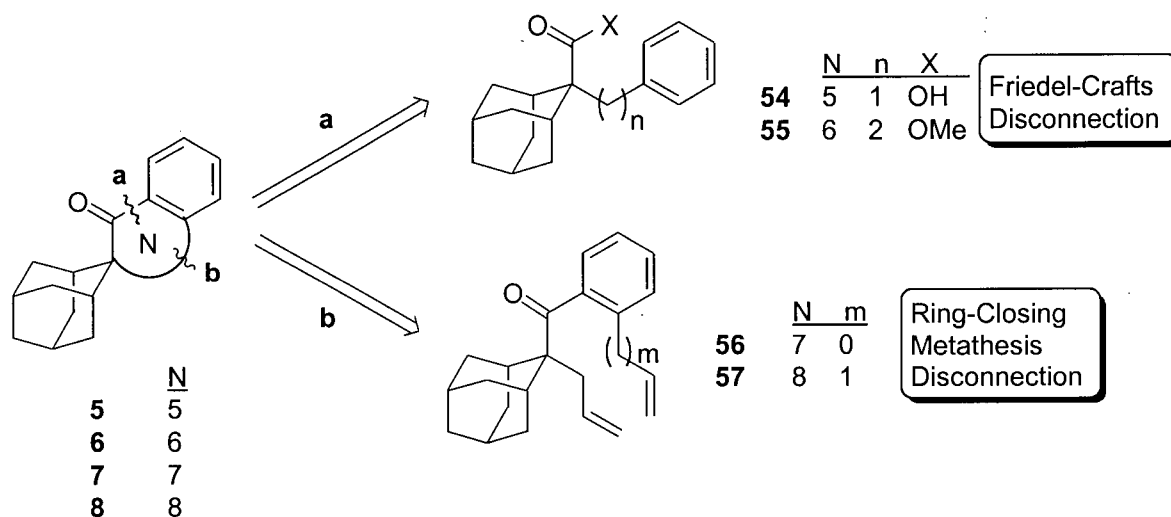


Figure 2.1 Retrosynthetic analysis for spiroketones **5-8**.

The source of the adamantane-2-carbonyl* skeleton for all of the spiroketones reported here was adamantane-2-carboxylic acid (**58**), which was prepared by the method of Alberts *et al.*⁴⁸ from the commercially available 2-adamantanone (**59**) (Figure 2.2). Wittig olefination of this ketone with the ylide formed from methoxymethyltriphenylphosphonium bromide provided enol ether **60**. This compound was subsequently hydrolyzed to aldehyde **61**, which was oxidized to the desired acid **58**. The overall yield for this one-pot process was 64%. Preparation of the known methyl ester **62** was achieved by reaction of **58** with oxalyl chloride followed by *in situ* quenching of the resultant acid chloride with methanol. It is interesting to note that the traditional Fisher esterification protocol (acid **58**, methanol, cat. H_2SO_4 , Δ) led to the decomposition of **58**.

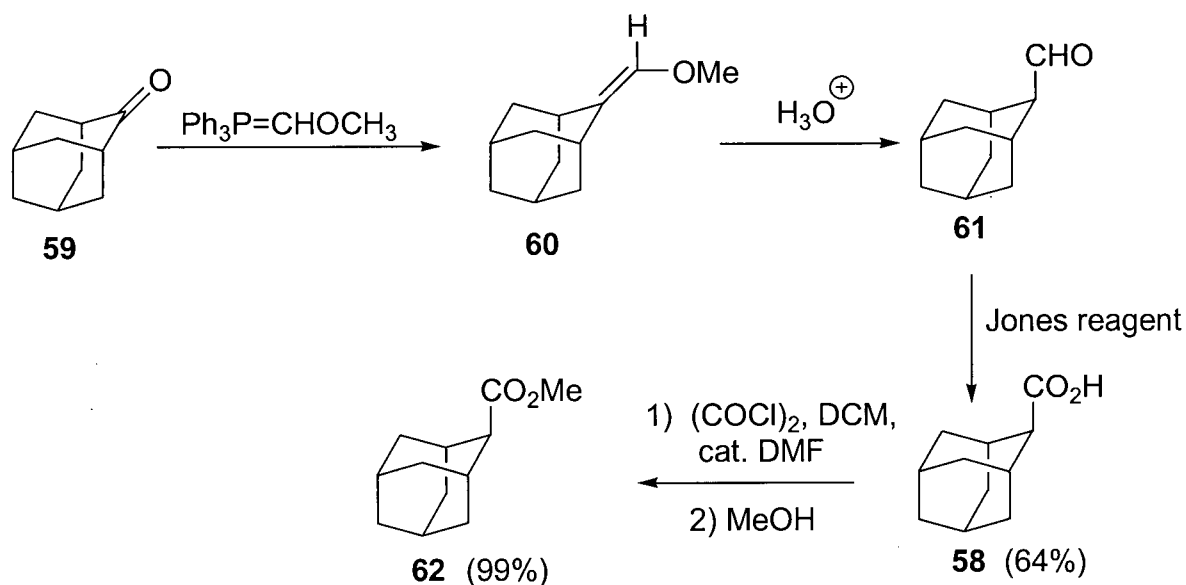


Figure 2.2 Preparation of ester **62**.

* The IUPAC name for the parent hydrocarbon adamantane is tricyclo[3.3.1.1^{2,7}]decane.

2.1.2 Preparation of Spiroketones **5** and **6** by Intramolecular Acylation

The synthesis of compounds **5** and **6**, starting from ester **62**, is outlined in Figure 2.3. Alkylation of the lithium enolate of ester **62** with either benzyl bromide or 2-phenethyl bromide afforded the esters **185** and **55** respectively. During the reaction, an equivalent of butyllithium was added to the enolate to re-form LDA from DIPA. The sterically congested ester products were inert to conventional hydrolysis conditions (e.g. LiOH, methanol-water, Δ ; NaCN, DMSO, Δ), but **185** yielded, albeit sluggishly, to the "in situ iodotrimethylsilane" reagent of Olah *et al.*⁴⁹ giving carboxylic acid **54** in good yield. In a one-pot procedure this acid was subsequently transformed into the corresponding acid chloride, which was treated with aluminum chloride to effect the intramolecular acylation. The overall yield of spiroketone **5** from ester **62** was 58%.

Hydrolysis of ester intermediate **55** proved to be more difficult than that of its shorter chain homologue. Failure of the Olah procedure in cleaving this ester group prompted the search for alternative reaction conditions, especially those known to be effective in the hydrolysis of sterically hindered systems. One such literature procedure,⁵⁰ which employed boron trichloride as the cleaving reagent, was attempted. Instead of ester hydrolysis, however, it was found that treatment of **55** with boron trichloride effected the Friedel-Crafts reaction directly, without the need to proceed by way of the acid chloride as in the case of ketone **5**. Spiroketone **6** was synthesized in 86% overall yield from **62**.

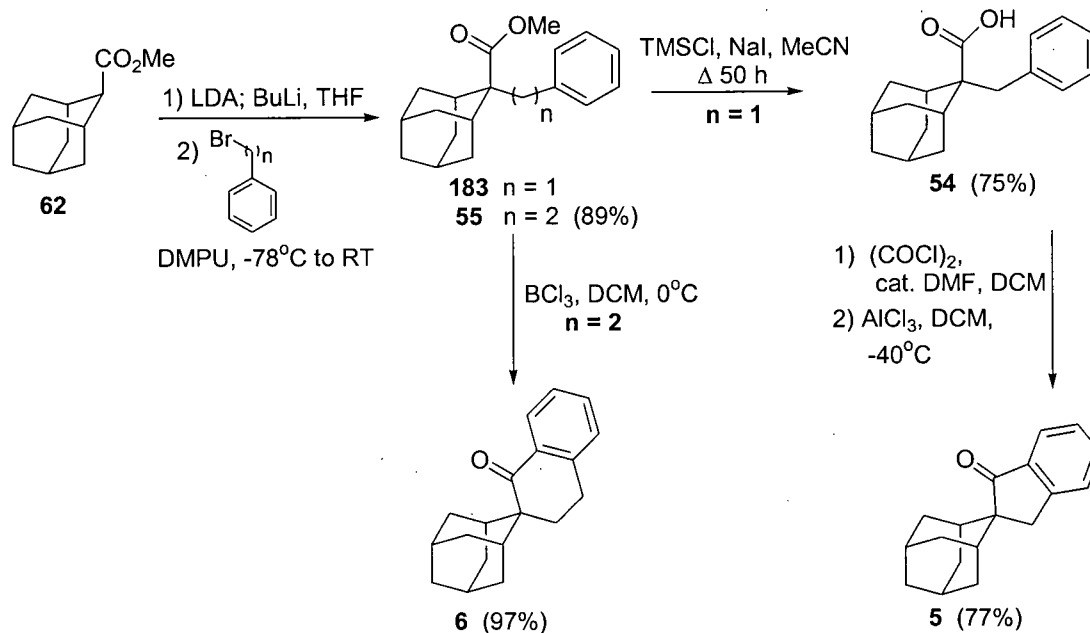


Figure 2.3 Synthesis of spiroketones **5** and **6**.

Spectral data for compounds **5** and **6** were in full accord with the assigned structures. In addition, X-ray crystal structures for these compounds were obtained and are presented in Figure 2.4.

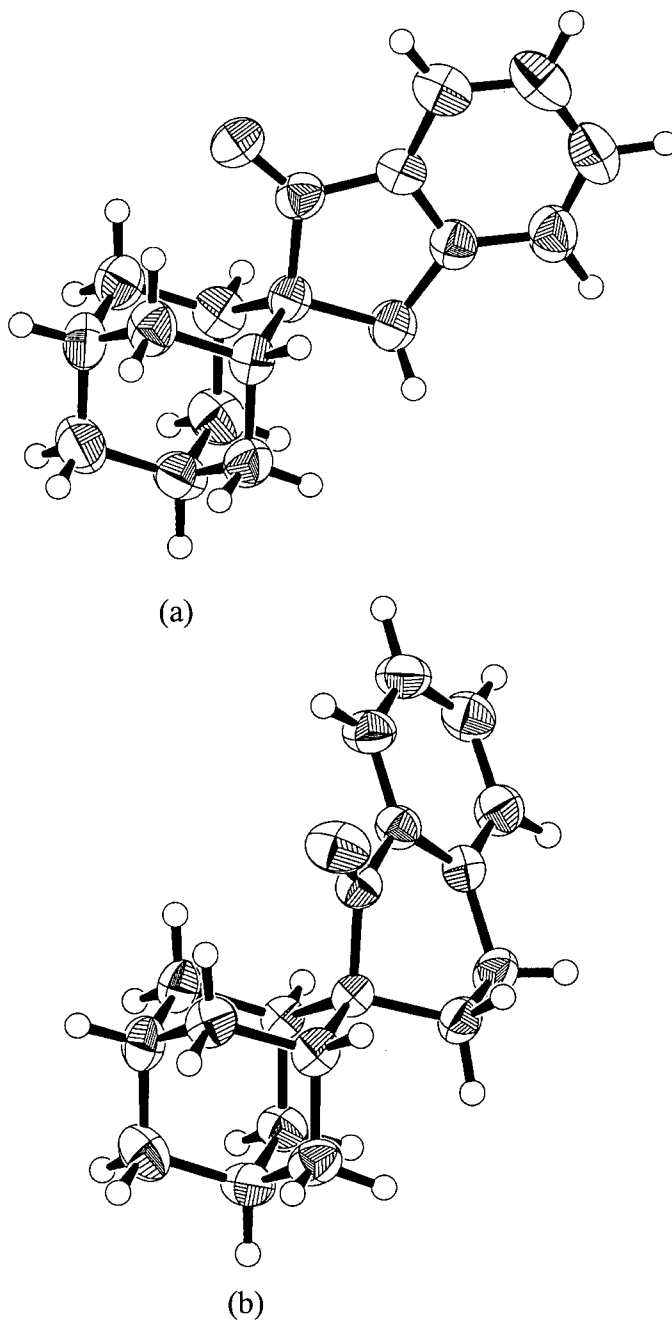


Figure 2.4 ORTEP representations of (a) **5**; (b) **6**.

2.1.3 Synthesis of Spiroketones 7 and 8 by Ring-Closing Metathesis

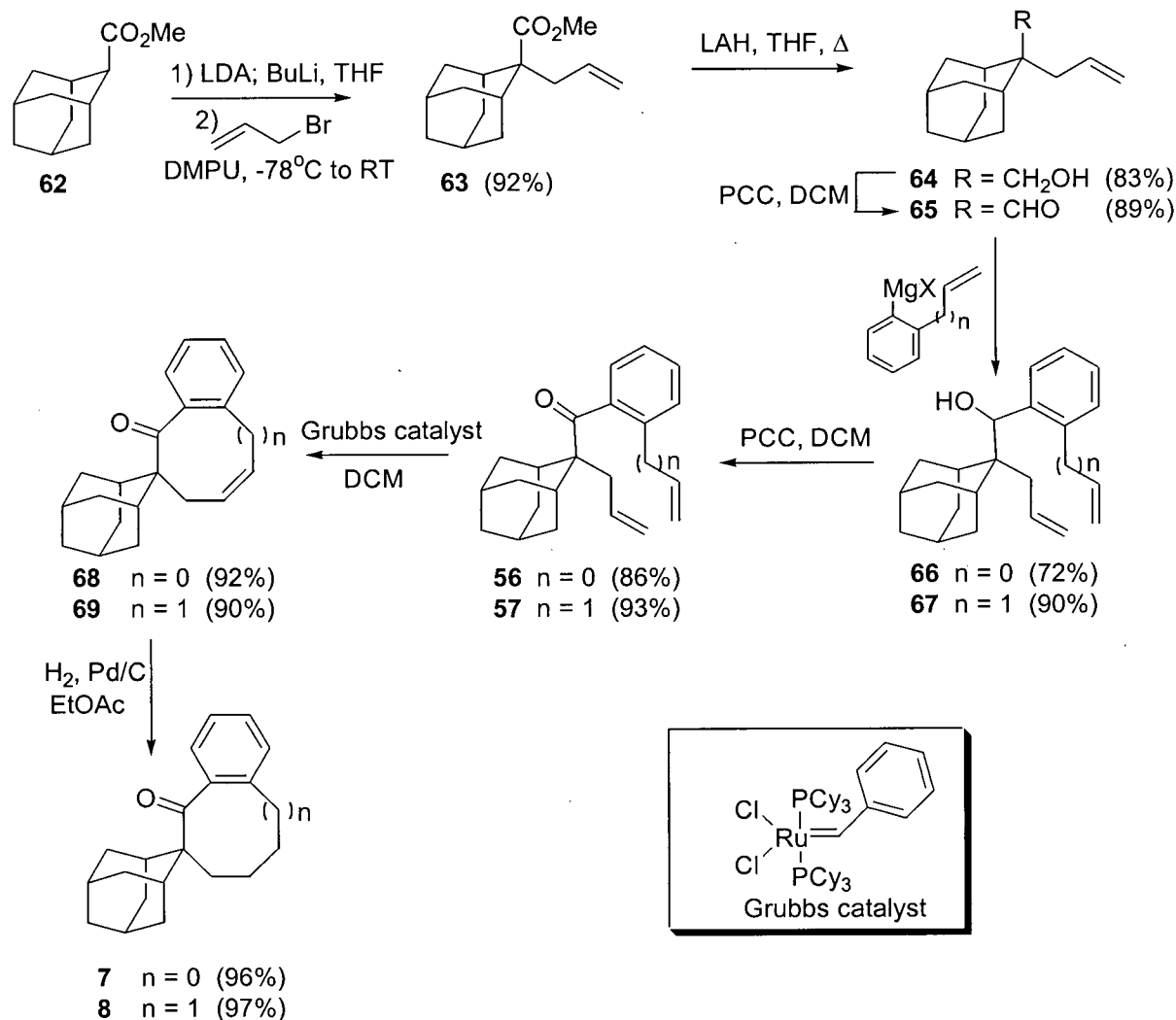


Figure 2.5 Synthesis of ketones 7 and 8.

Both the seven- and eight-membered spiroketones (7 and 8) were synthesized from a common aldehyde precursor, 65 (Figure 2.5). This compound was prepared by alkylation of ester 62 with allyl bromide to first form ester 63, followed by reduction to alcohol 64, and subsequent PCC oxidation.⁵¹ The syntheses diverged at this point, where a Grignard reagent, possessing either a vinyl or an allyl substituent in the *ortho* position, was reacted with 14. The products of these reactions, the homologous alcohols 66 and 67, are the ultimate precursors to 7 and 8, respectively. Although

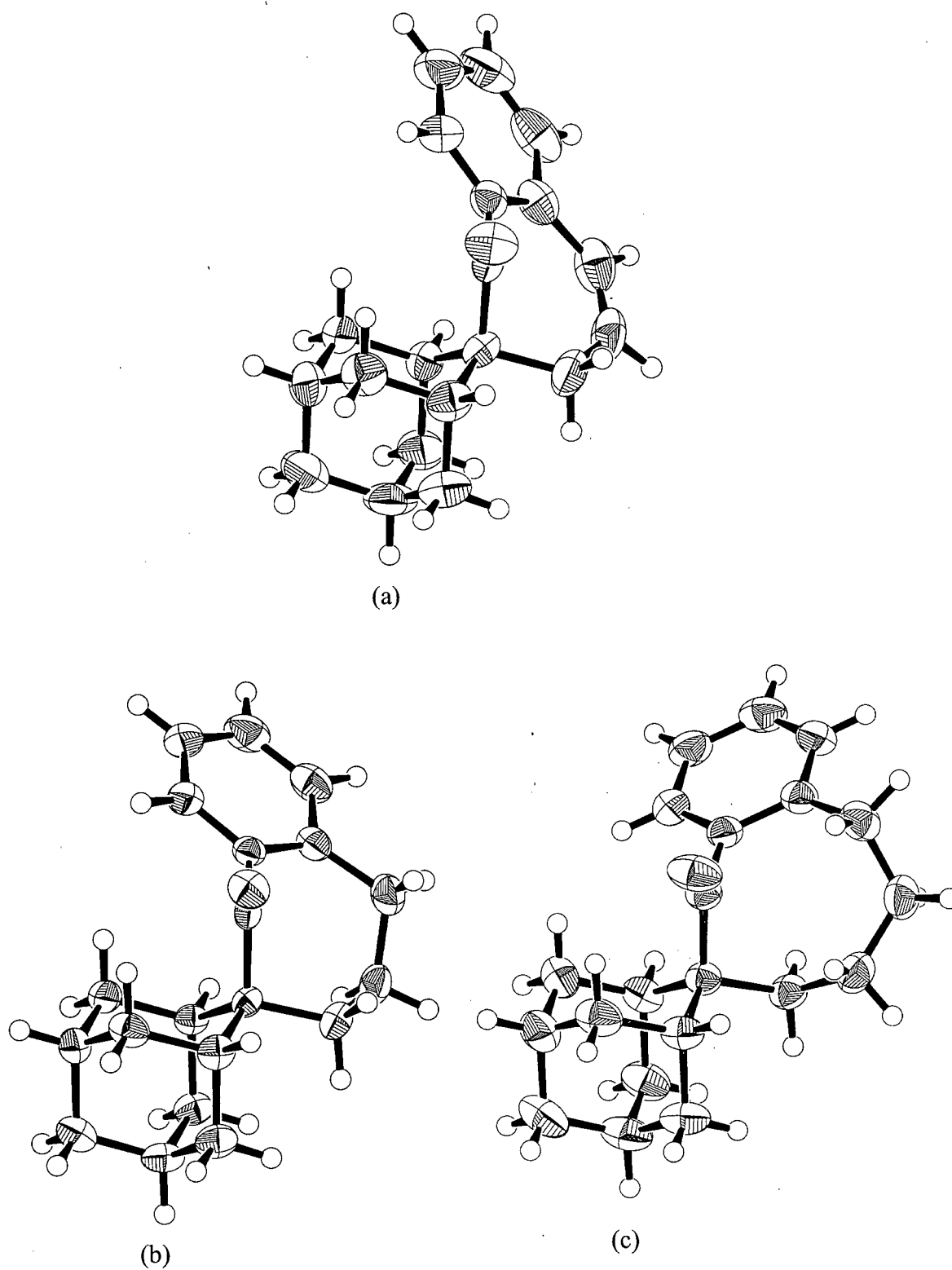


Figure 2.6 ORTEP representations of (a) **68**; (b) **7**; (c) **8**.

ring-closing metathesis was attempted on these alcohol substrates, no detectable reaction took place. After oxidation to the corresponding ketones **56** and **57**, however, treatment with the Grubbs catalyst⁵² in dichloromethane led smoothly to the desired unsaturated spiroketones **68** and **69** in excellent yields. The structure of compound **68** was confirmed by X-ray crystallography (Figure 2.6.a). Catalytic hydrogenation of the unsaturated carbocycles led cleanly to the desired ketones **7** and **8**. The overall yields, starting from ester **62**, were 37% (**7**) and 50% (**8**). The spectroscopic and X-ray crystallographic data (Figure 2.6) for these compounds are in accord with the assigned structures.

2.1.4 Synthesis of the Unsaturated Spiroketone **70**

Preparation of the unsaturated six-membered spiroketone **70** was achieved in a one-pot procedure starting from the corresponding saturated compound. Benzylic bromination of compound **6** with NBS was followed immediately by dehydrobromination of the intermediate bromide with DBU in THF. This sequence afforded ketone **70** in 48% yield (Figure 2.7). The X-ray crystal structure is presented in Figure 2.8.



Figure 2.7 Synthesis of compound **70**.

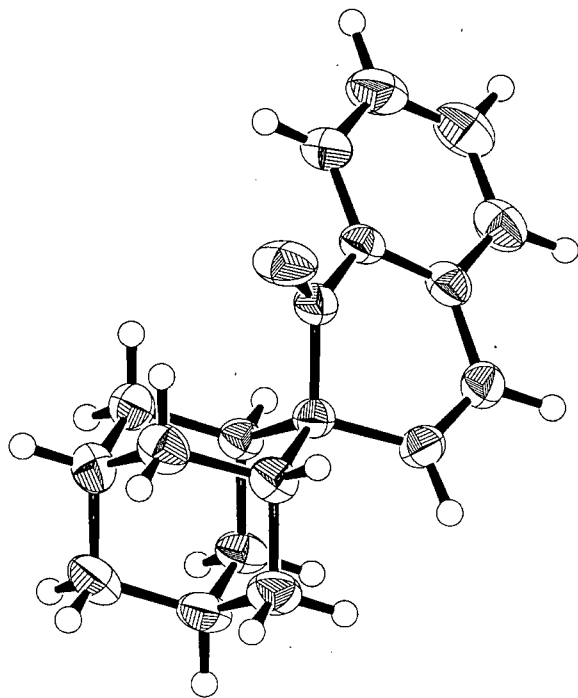


Figure 2.8 ORTEP representation of ketone 70.

2.2 Solution and Solid State Photolysis of Spiroketones 5-8

Before structure-reactivity correlations were undertaken, the photochemistry of the spiroketones was explored in both solution and the crystalline state. Preparative solution photolyses readily provided the reaction products for structural determination, while analytical scale solid state reactions were undertaken to determine the mode of reactivity in that medium.

2.2.1 Photochemistry of Spiroketone 5

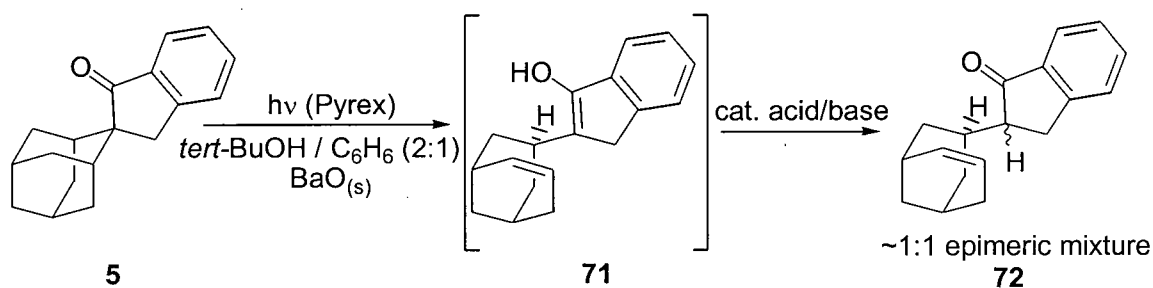


Figure 2.9 Photochemistry of ketone **5**.

Pyrex-filtered irradiation of ketone **5** in both the solid state and in solution proceeded exclusively *via* Norrish Type II cleavage (Figure 2.9). In solution, photolyses were conducted in the presence of solid barium oxide in order to scavenge any acidic impurities that might promote the tautomerization of intermediate enol **71** to ketone epimers **72**. Upon prolonged irradiation, or in the presence of catalytic acid or base, secondary photolysis (Norrish Type II cleavage) of **72** competed with the primary photoreaction such that only trace amounts of the initial product were observed. 1-Indanone (**73**) was the only product isolated under these conditions, while peaks with the correct mass for dienes **74** (formed from reaction at carbon X) and **75** (formed from reaction at carbon Y) were observed by GC-MS of the reaction mixture (Figure 2.10). Compound **72** was the only product observed when **5** was photolysed to low conversion

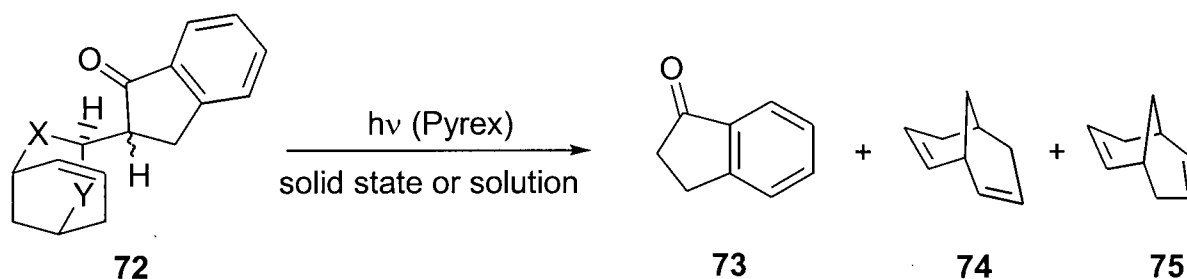


Figure 2.10 Competing secondary photolysis reaction of **72**.

in the solid state. Above 2% conversion, compounds **73**, **74**, and **75** are also observed, presumably through the competitive enol-keto tautomerization and secondary photolysis seen in solution. Table 2.1 summarizes the photochemistry of **5**.

Table 2.1 Photochemistry of ketone **5** in various media.

Photolysis Conditions ^a		Duration	% Conversion ^b	72 (% yield) ^b	73 (% yield) ^b
2:1 <i>tert</i> -butanol / C ₆ H ₆ , BaO		1.5 h	40	38	trace
		2.3 h	72	54	12
MeCN, BaO, -20 °C		3.0 h	42	29	6
2:1 <i>tert</i> -butanol / C ₆ H ₆ , 1% HOAc		2.0 h	86	16	64
2:1 <i>tert</i> -butanol / C ₆ H ₆ , 1% NH ₃		1.5 h	81	8	62
Solid state	RT	0.2 h	2	2	0
		0.7 h	4	2.5	1.5
		6.0 h	10	7	3
	0 °C	6.0 h	7	5	2
		11.0 h	16	7	8

^aPyrex filtered light, 450W Hanovia medium pressure mercury lamp. ^bGC analysis.

The intermediacy of enol **71** was established by ¹H NMR spectroscopy. Photolysis of **5** at 0 °C in 2:1 *tert*-butanol-*d*₁₀ / benzene-*d*₆ to 40% conversion revealed two new resonances in the vinylic region (δ 5.42 ppm and δ 5.79 ppm) corresponding to the newly formed 1,2-disubstituted double-bond (Figure 2.11). A second spectrum, taken immediately after the addition of a trace amount of trifluoroacetic acid (TFA), contains

vinyl signals for the enol as well as four new resonances (δ 5.34 ppm, δ 5.38 ppm, δ 5.60 ppm, δ 5.72 ppm) arising from the two newly formed ketone epimers **72**. Another spectrum acquired five minutes later contained no enol signals, indicating that complete conversion to the keto tautomers had occurred. Since the solvent system employed for this experiment contained exchangeable deuterium atoms, the enolic O-H resonance was not observed. A signal for these relatively acidic alcohol protons was observed as a singlet at δ 6.32 ppm, however, when the solvent was acetonitrile- d_3 ; the OH signal for propen-2-ol has previously been observed at δ 8.40 ppm in tetramethylsilane.⁵³ In acetonitrile- d_3 , the vinyl resonances appeared at δ 5.50 ppm and δ 5.87 ppm. The Norrish Type II reaction has provided ready access to numerous enols,⁵⁴ and extensive kinetic and thermodynamic characterization of the closely related 1-indanone enol-keto system has been reported by Kresge *et al.*⁵⁵

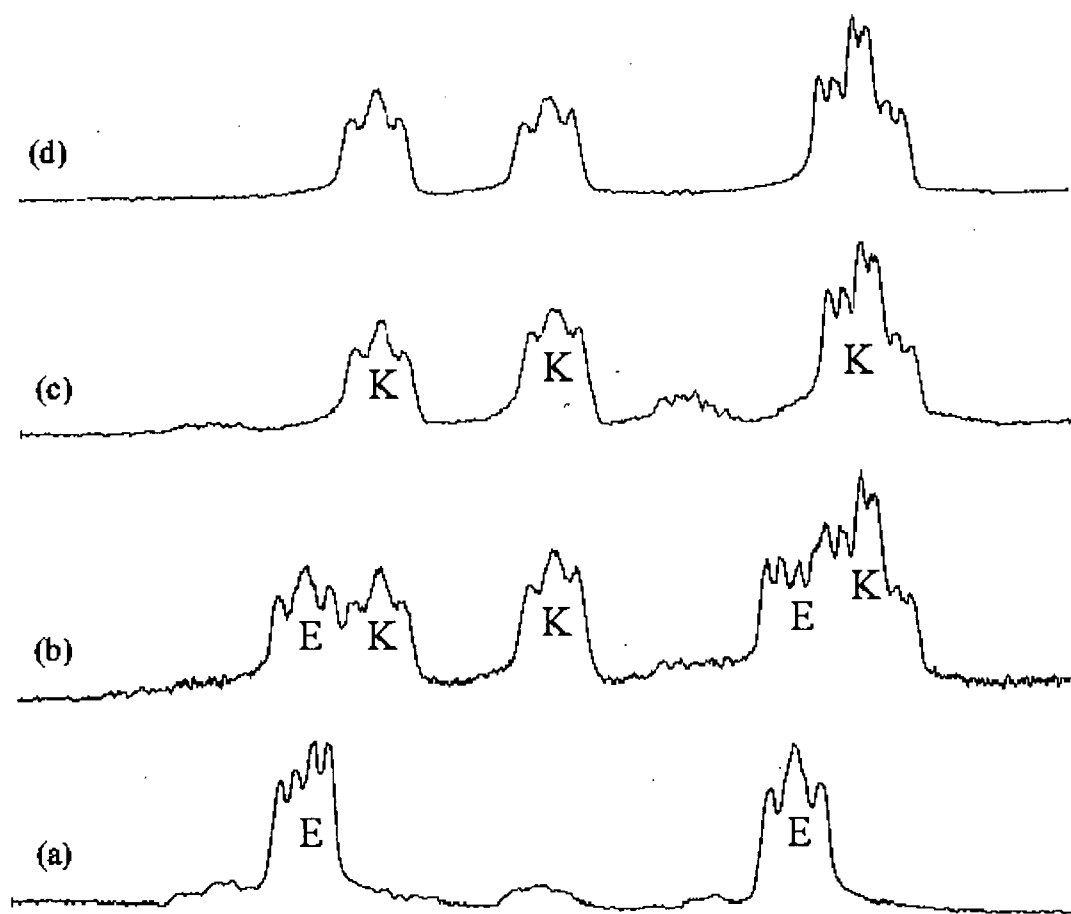


Figure 2.11 ^1H NMR vinyl region (δ 5-6 ppm) after photolysis of **5** showing signals due to enol tautomer **71** (E) and keto epimers **72** (K): (a) after photolysis; (b) immediately following addition of catalytic TFA; (c) five minutes post addition; (d) purified sample of **72**.

The diastereomeric ketone products **72** were isolated as a single chromatographic band. Integration of the ^1H NMR signals revealed that the two epimers were present in equal amounts, indicating that protonation of the intermediate enol proceeded without any stereoselectivity under the reaction conditions. Treatment of ketone mixture **72** with triisopropyl triflate and triethylamine produced one product, silyl enol ether **76**, in 87% yield (Figure 2.12). This result provides conclusive evidence that the two diastereomers are epimeric α to the carbonyl group, and that both arise from enol ether **71**.

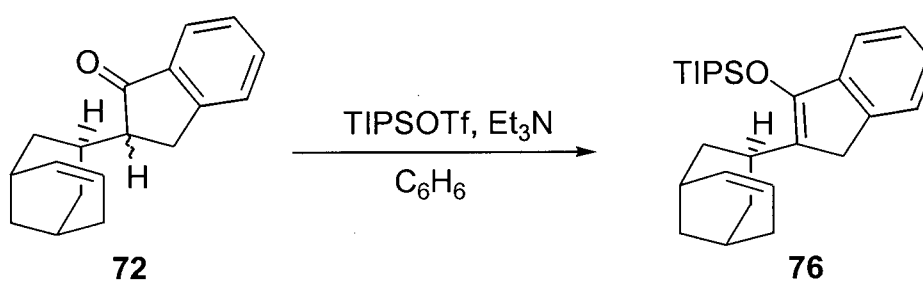


Figure 2.12 Formation of silyl enol ether **76**.

2.2.2 Photochemistry of Spiroketone 6

In sharp contrast to its smaller-ring homologue, the six-membered spiroketone **6** proved to be remarkably photostable. Although the starting material was eventually consumed (recovery was 50% after irradiation for 29 h in 2:1 *tert*-butanol / benzene), no major photoproducts were isolated. This suggests that both the cyclization and cleavage pathways are kinetically much slower than the degenerate reverse hydrogen transfer from 1,4-hydroxybiradical **77** back to starting material. The use of Lewis base solvents that are capable of hydrogen-bonding with the 1,4-hydroxybiradical, such as *tert*-butanol, is well-documented⁵⁶ in attenuating the rate of reverse-hydrogen transfer relative to the cyclization and cleavage pathways (Figure 2.13). The photostability of **6** under these conditions is rather unusual, and therefore warranted further investigation.

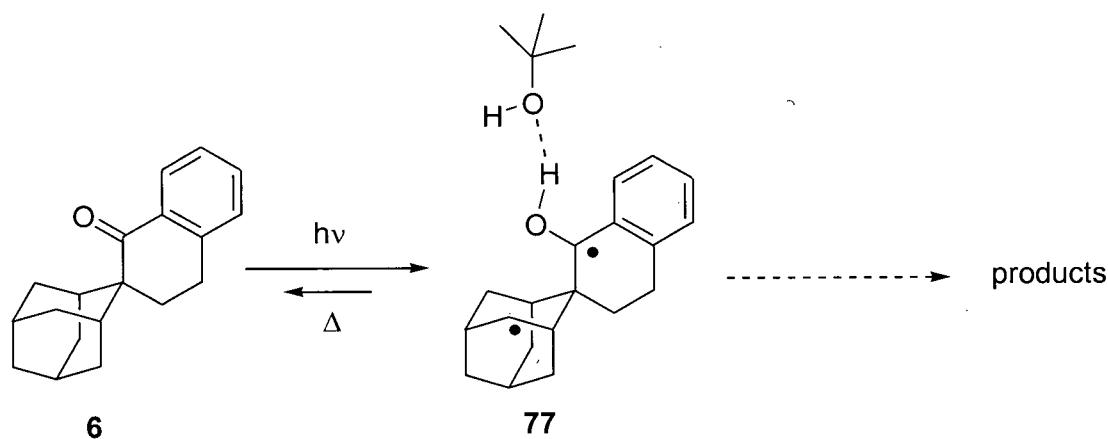


Figure 2.13 Solvent-biradical hydrogen-bonding decreases the rate of reverse hydrogen transfer relative to product formation. In the case of **77**, however, this failed to promote product formation.

To confirm that biradical **77** was indeed being produced, photolysis was conducted in *tert*-butanol-OD. Irradiation for 29 h afforded recovered starting material **6** (50% after chromatography) into which deuterium had been incorporated stereospecifically at the axial positions of either or both of the γ -carbons (Figure 2.14). The intermediate biradical **77** is able to exchange its alcohol protium atom for a deuterium donated by the solvent. The biradical then undergoes reverse-transfer back to the starting material **6-d₁**. In this process, up to two deuterium atoms may be

incorporated. Mass spectrographic analysis of starting material recovered from the above experiment determined the overall deuteration at the γ -carbon to be 31%, corresponding to abundances for **6-d**₀, **6-d**₁, and **6-d**₂ of 48%, 42%, and 10% respectively. Deuteration could also be achieved using 7% D₂O in MeCN as the solvent. In this case 12% deuteration was achieved in 24 h, with abundances for **6-d**₀, **6-d**₁, and **6-d**₂ of 78%, 20%, and 2% respectively.

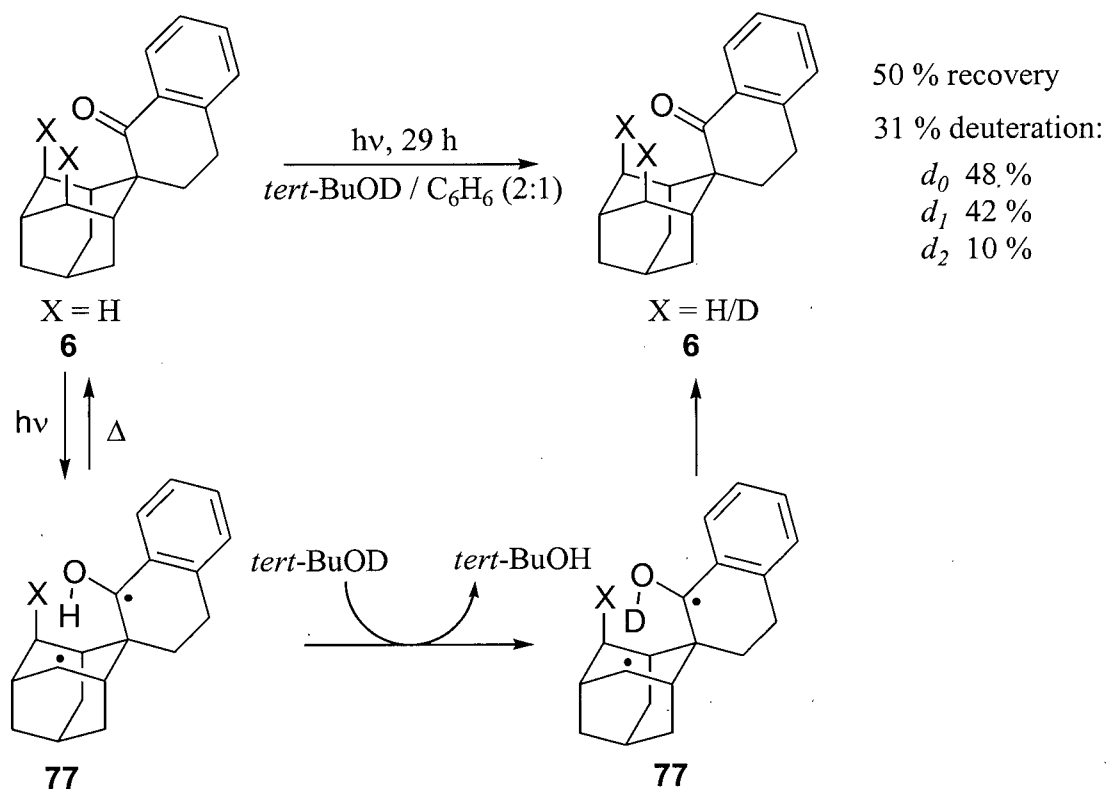


Figure 2.14 Deuteration of **6** through H-D exchange in the biradical.

Evidence for the stereospecificity of deuterium incorporation comes from $^2\text{H}\{^1\text{H}\}$ NMR studies. Figure 2.15 shows the proton NMR spectrum for the aliphatic region of **6** (solvent 1:1 CD₃OD / C₆D₆), and the corresponding deuterium spectrum of the deuterated product. The presence of a deuterium resonance at the axial hydrogen's frequency (H_{ax} , δ 2.24 ppm), and the absence of any signal corresponding to its geminal partner (H_{eq} , δ 1.51 ppm) strongly supports the mode of reactivity presented. Intermolecular abstraction of deuterium by **77** is precluded, as this would give rise to product deuterated at both the

axial and equatorial positions. Complete assignment of the ^1H and ^{13}C NMR data are presented in Table 2.2. Because H_{ax} lies squarely in the deshielding region of the carbonyl group, its chemical shift is influenced by the magnetic anisotropic effect and is downfield from that of H_{eq} .⁵⁷

Deuteration *via* the mechanism described here is not a general phenomenon. Similar experiments conducted by Wagner *et al.*⁵⁸ on $\gamma,\gamma\text{-d}_2$ -nonaphenone failed to produce products where deuterium was replaced by protium from the solvent. Indeed, trapping of 1,4-hydroxybiradicals is often achieved intermolecularly, through the addition of efficient radical scavengers such as thiols,⁵⁹ stannanes,⁵⁹ molecular oxygen,⁶⁰ hydrogen selenide,⁶¹ hydrogen bromide,⁶² and selenoketones⁶³. A recent report by Neckers *et al.*⁶⁴ proposed that H/D exchange in a 1,5-hydroxybiradical proceeded as outlined here, but the researchers have not quantified the extent of deuteration nor provided experimental details for this work.

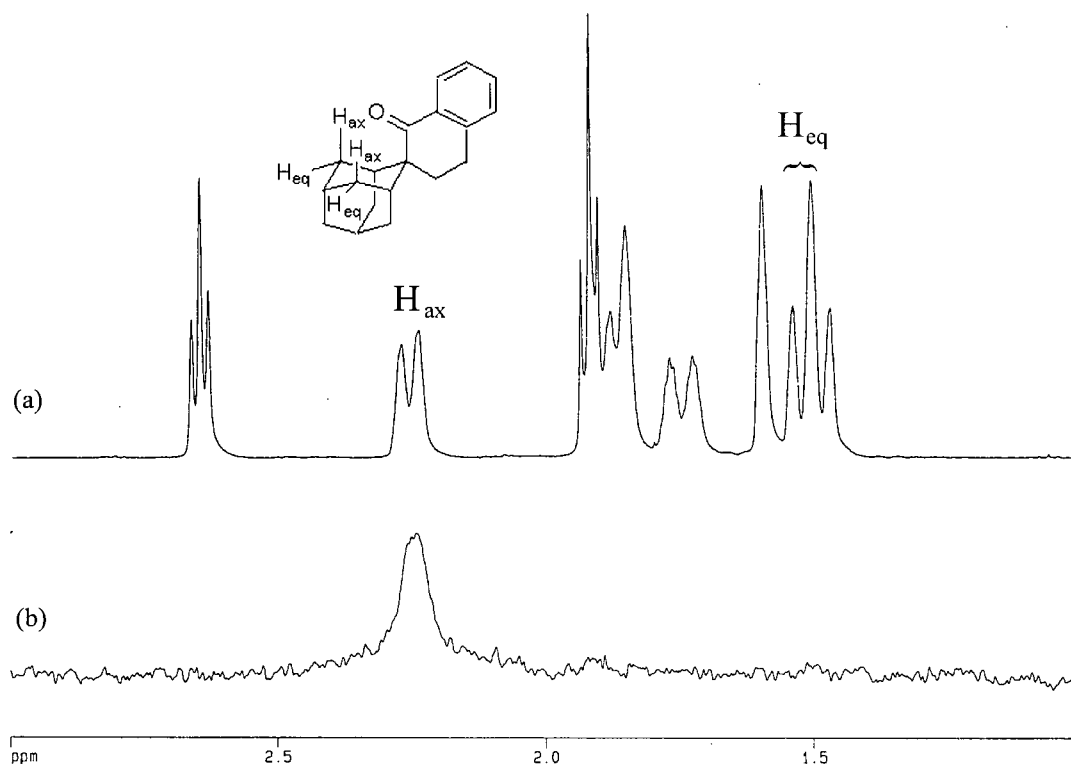
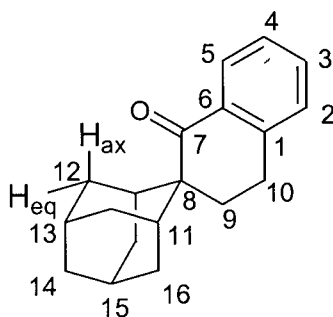


Figure 2.15 (a) ^1H NMR of **6**; (b) $^2\text{H}\{^1\text{H}\}$ NMR of deuterated **6**.



Carbon #	^{13}C δ (ppm)	^1H δ (ppm) (correlations from HMQC)	^1H - ^1H COSY correlations	HMBC (long-range) ^{13}C - ^1H correlations
1	143.05	—	—	H3, H5, H9, H10
2	128.96	7.00 d, $J = 7.5$ Hz, 1H	H3	H4, H10
3	133.05	7.28 m, 1H	H2, H4	H5, H10
4	127.23	7.13 t, $J = 7.5$ Hz, 1H	H3, H5	H2, H10,
5	128.14	7.83 d, $J = 7.7$ Hz, 1H	H4	H3
6	135.08	—	—	H2, H4, H9, H10
7	207.42	—	—	H2, H5, H9, H10
8	50.42	—	—	H9, H10, H12 _{eq} , H16"
9	31.83	1.92 t, $J = 6.3$ Hz, 2H	H10	H10
10	24.78	2.64 t, $J = 6.3$ Hz, 2H	H9	H2, H9
11	32.45	1.86 br s, 2H	H12 _{ax} , H12 _{eq} , H16', H16"	H9
12	34.91	H _{ax} 2.24 d, $J = 12.9$ Hz, 2H	H12 _{eq} , H13, H11	H14, H16"
		H _{eq} 1.51 d, $J = 12.9$ Hz, 2H	H12 _{ax} , H13, H11	
13	28.93	1.77 m, 1H	H12 _{ax} , H12 _{eq} , H14,	H14, H16"
14	39.27	1.60 br s, 2H	H13, H15	H11
15	28.63	1.73 m, 1H	H16', H16", H14	H12 _{eq} , H14, H16'
16	33.64	H' 1.90 obscured m, 2H	H11, H15, H16"	H12 _{eq} , H14
		H'' 1.49 d, $J = 14.1$ Hz, 2H	H11, H15, H16'	

Table 2.2 Comprehensive NMR assignment data for ketone **6** in 1:1 CD₃OD / C₆D₆.

Although ketone **6** proved to be photostable under conventional reaction conditions, reactivity was observed when the ketone was irradiated as a suspension in water to which a small amount of surfactant (sodium dodecylsulfonate, SDS) had been added. Ordinarily, irradiation of suspensions provides a convenient method for the scale-up of solid state reactions, and gives rise to the same products as observed in the 'dry' analytical runs. In this case, however, alcohol **78**, which is not produced under any other conditions, was isolated in 21% yield (51% based on recovered starting material). A mechanism, proceeding through the expected cyclobutanol **79** with subsequent rearrangement to the stabilized cyclopropylcarbinyl cation **80**, can be envisaged for this transformation (Figure 2.16). During the reaction, the product was observed to slough off the reactant crystals, forming a second, fluffy, solid phase. This observation, and the fact that the reaction proceeds only in the presence of water, suggests that this process likely involves interactions between water and the ketone molecules on the solid surface, and is not a uniform process occurring in the bulk solid. The structure of alcohol **78** was determined by X-ray crystallography (Figure 2.17).

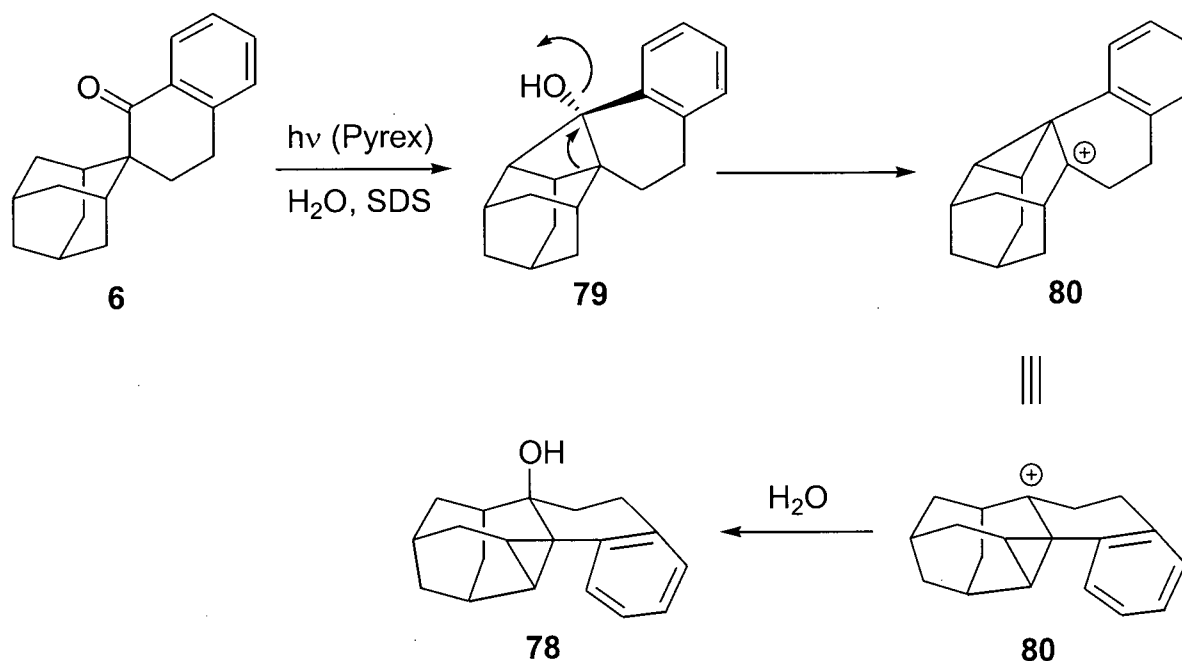


Figure 2.16 Photochemistry of spiroketone **6** as an aqueous suspension.

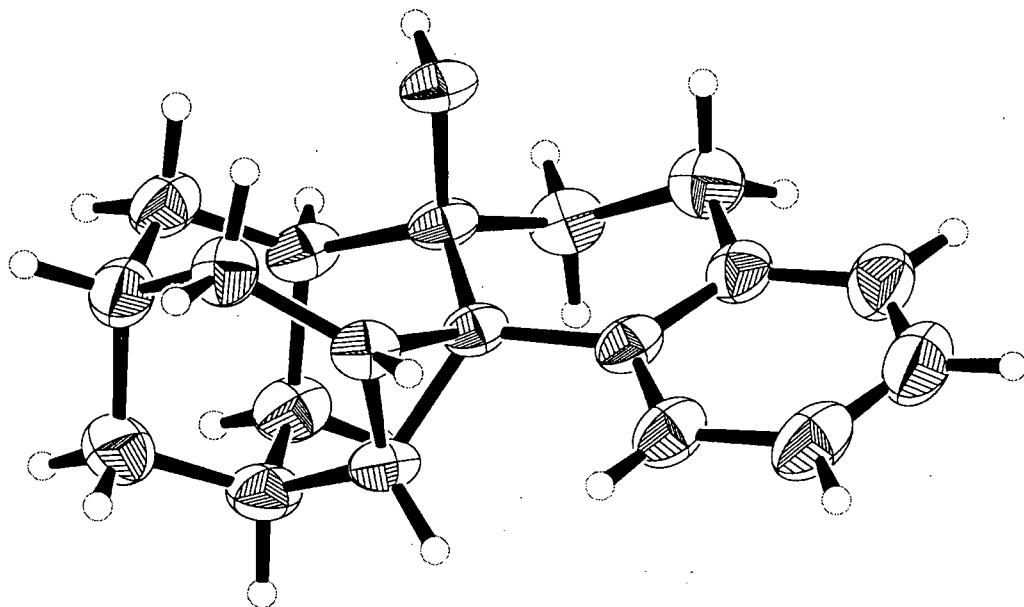


Figure 2.17 ORTEP representation of photoproduct **78**.

2.2.3 Photochemistry of Spiroketone **7**

While the five-membered ketone followed the Norrish Type II cleavage pathway and the six-membered spiroketone underwent only reverse hydrogen transfer from its 1,4-hydroxybiradical, the next homologue in the series, compound **7**, reacted *via* the Yang photocyclization to afford cyclobutanol **81** in both the crystalline state and in solution (Figure 2.18). Preparative photolysis in 2:1 *tert*-butanol / benzene provided photoproduct **81** in 57% yield (76% based on recovered starting material).

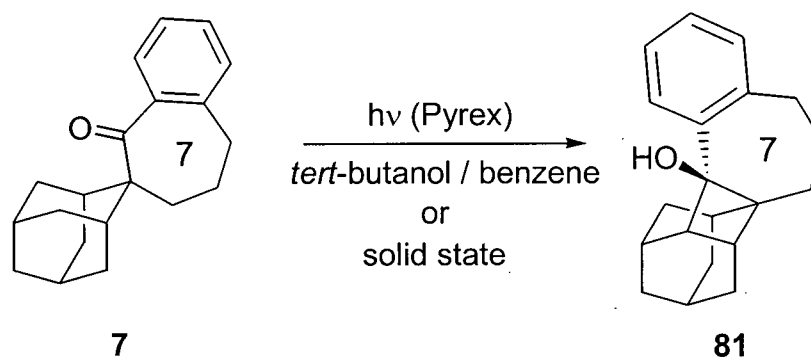


Figure 2.18 Photolysis of spiroketone **7**.

The same reaction also proceeded cleanly in the solid state. Figure 2.19 shows a portion of a ^{13}C NMR spectrum of the crude reaction mixture after solid state irradiation (20 h, Pyrex filter). Only signals from the starting material (o) and product (x) are seen, attesting to the selectivity of the reaction. Product analysis by GC was not possible due to the thermal instability of the cyclobutanol photoproduct. The structure of photoproduct **81** was confirmed by X-ray crystallography (Figure 2.20).

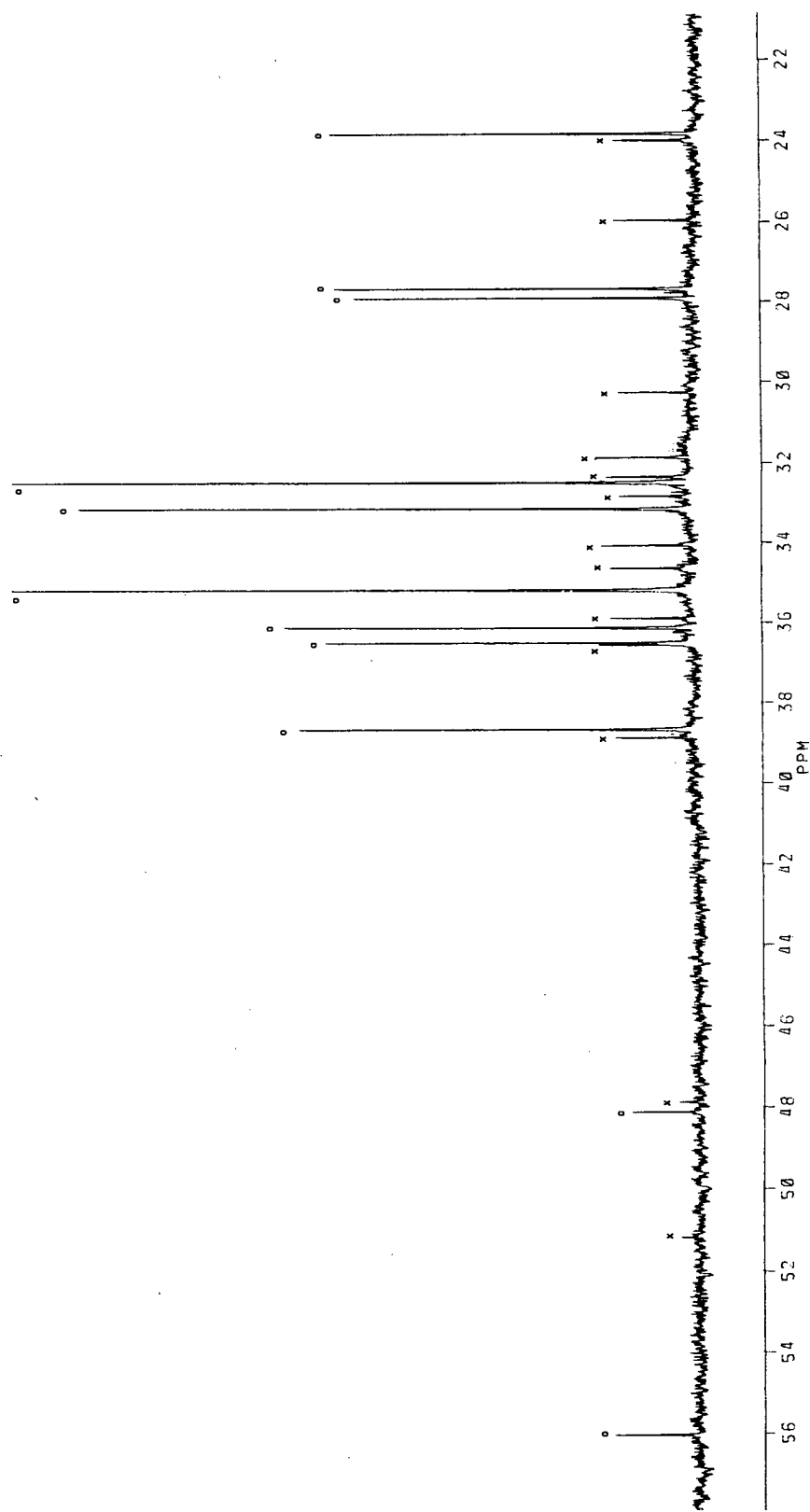


Figure 2.19 Partial ^{13}C NMR of crude solid state reaction mixture of **7**. (o = **7**; x = **81**).

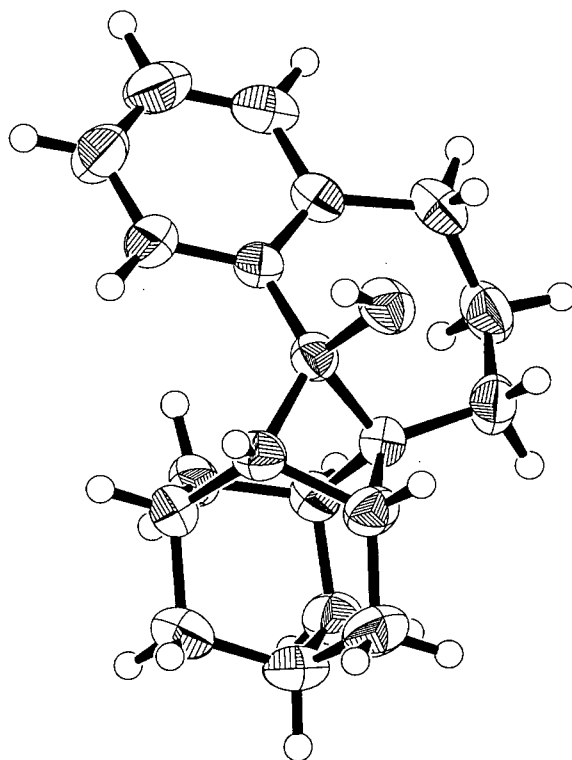


Figure 2.20 ORTEP representation of photoproduct **81**.

2.2.4 Photochemistry of Spiroketone **8**

The photochemistry of the eight-membered spiroketone **8** mirrored that of the seven-membered ring, with cyclization as the sole reaction pathway. Qualitatively, this reaction proceeded faster than that of **7**, with complete conversion to product after 10 h of irradiation (Pyrex filter, *tert*-butanol / benzene 2:1, 72% isolated yield) (Figure 2.21). The structure of the cyclobutanol photoproduct **82** was confirmed by X-ray crystallography (Figure 2.22), and possessed the same relative stereochemistry as compound **81** at the carbinol centre, with the aryl group *endo* to the adamantyl skeleton. Solid state photolysis proceeded cleanly, affording only **82**. GC analyses were again hampered by the thermal lability of the photoproduct. However, ^{13}C NMR analysis (Figure 2.23) of the crude solid

state photosylate showed only signals due to starting material **8** (labeled o) and photoproduct **82** (labeled x).

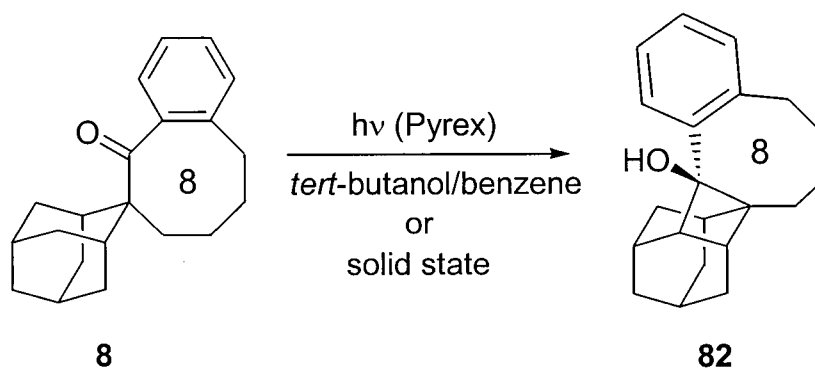


Figure 2.21 Solution and solid state photochemistry of spiroketone **8**.

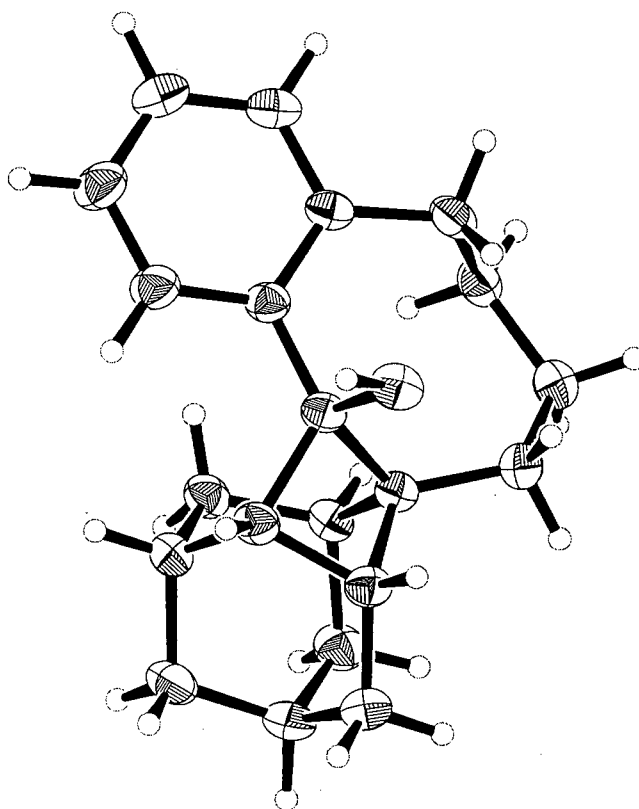


Figure 2.22 ORTEP representation of cyclobutanol **82**.

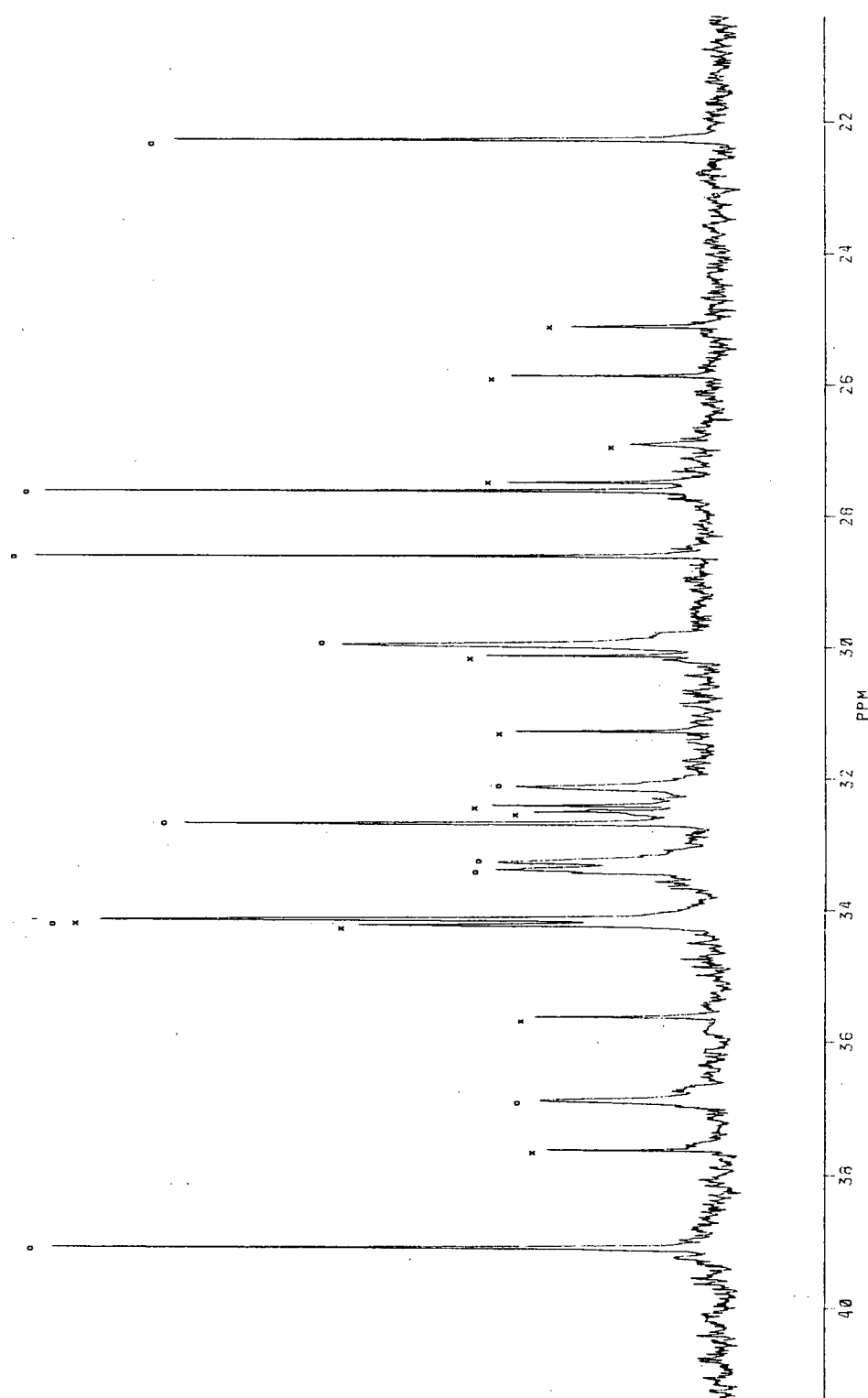


Figure 2.23 Partial ^{13}C NMR spectrum of the crude **8** solid state photosylate ($o = 8$; $x = 82$).

2.3 Solid State Structure-Reactivity Correlations

The five- through eight-membered spiroketones display the full range of type II photochemistry. In addition to cyclobutanols, which were the only products observed in the previous study of acyclic adamantyl aryl ketones,⁶⁵ a cleavage product was observed in the current study. The remarkable solution and solid state photostability of the six-membered ketone **6**, as well as the unique reactivity it displays under irradiation as a suspension in water, provides an additional and unexpected mode of reactivity in type II photochemistry. Fortuitously, each of the four ketones followed only one of the three pathways (cleavage, cyclization, reverse-hydrogen transfer), thus simplifying the following analysis.

From a kinetic standpoint, three unimolecular rate constants control the partitioning of the 1,4-hydroxybiradical intermediate (**83**) among the possible reaction pathways (Figure 2.24). These are k_H , the rate of reverse hydrogen transfer, k_{cy} the rate of cyclization, and k_{cl} , the rate of σ -bond cleavage. The hydrogen abstraction efficiency and the rate of reverse H transfer (k_H), although determining factors in the overall rate of product formation, do not contribute to the observed product ratios. Cleavage will predominate if $k_{cl} > k_{cy}$, and will account for greater than 99% of observed products when $k_{cl}/k_{cy} > 100$. Exclusive formation of the cyclization product likewise indicates that k_{cy} is likely at least two orders of magnitude larger than k_{cl} . Where no reaction is observed it can be concluded that both k_{cl} and k_{cy} are much smaller than k_H , and are essentially unable to compete with the pathway back to the starting ketone. Analysis of the solid state geometries of the intermediate 1,4-biradicals in light of their differing reactivities will serve to reconcile the predicted mechanism with experimental observations.

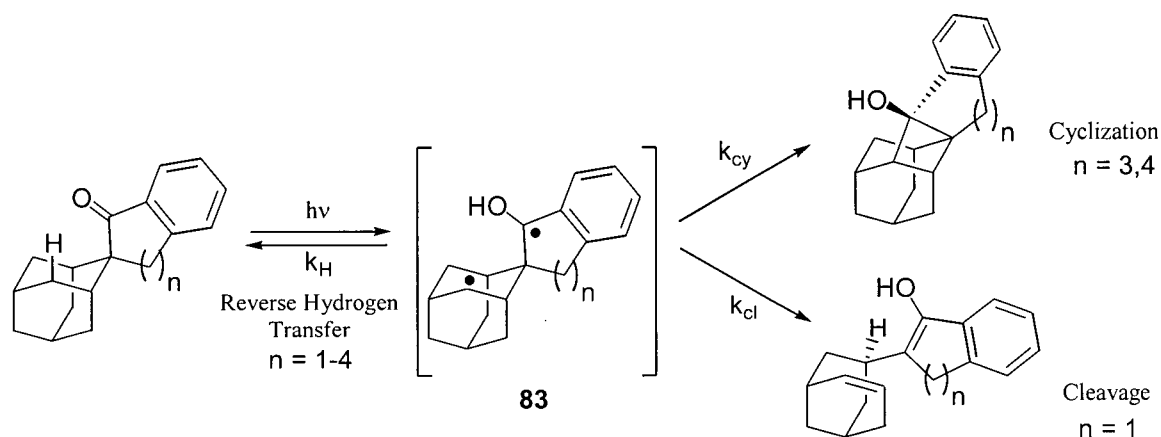


Figure 2.24 Kinetic scheme for type II ketone photochemistry.

2.3.1 Hydrogen Abstraction Parameters and Biradical Geometries

Superposition of the X-ray structures of the crystalline ketones provides an illustration of how the orientation of the carbonyl moiety varies with ring size (Figure 2.25). Because the adamantyl skeleton is rigid and possesses the same conformation in each of the four ketones studied, the primary factor in differentiating reactivity among the ketones is the relative position of the carbonyl group with respect to the adamantane system. The angle α , defined as the deviation of the carbonyl group from the plane bisecting the adamantane ring through carbons A, B, and C, allows a quantitative comparison to be made between the structures. In compound **5**, α is 9° , and the carbonyl group projects out over the adamantyl framework (Table 2.3). The C=O bond in the six- and eight-membered ketones share nearly identical geometries that eclipse one of the C-C bonds in the adamantane moiety. The seven-membered ketone **7** most closely resembles the acyclic systems studied previously, where the carbonyl group, and the aryl group *anti* to it, prefer an alignment nearly perpendicular to the adamantyl anchor. Compound **84**, for example, has an α value of 86° .

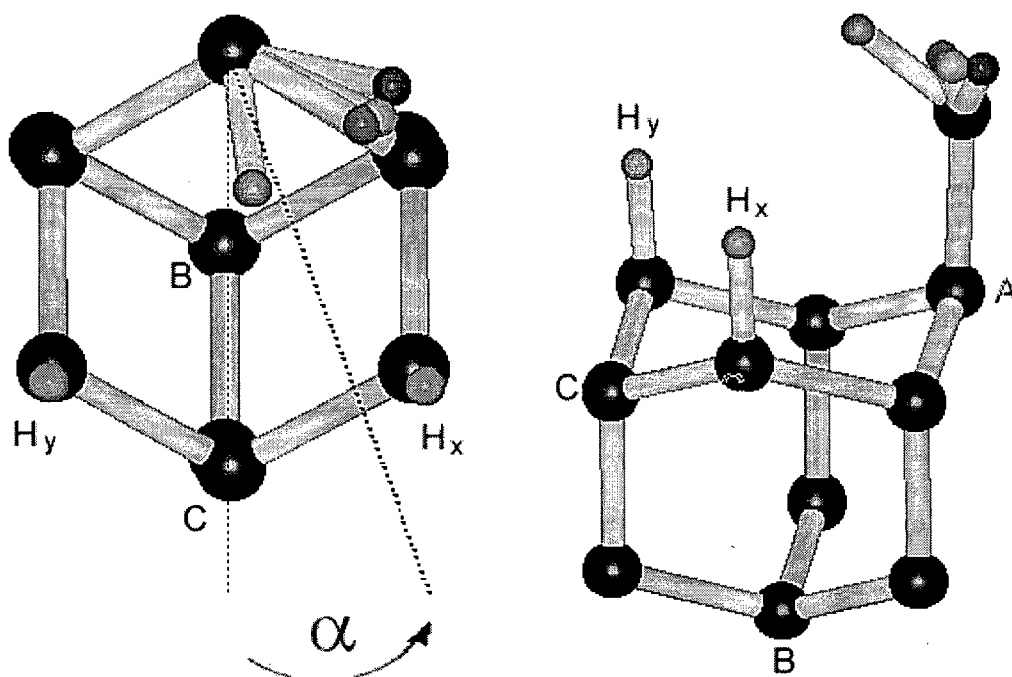


Figure 2.25 Comparison of carbonyl group orientations in spiroketones 5-8.

Compound	Ring Size	α ($^{\circ}$)	Oxygen Atom Colour	Solid State Reactivity
5	5	9	green	cleavage
6	6	59	red	NR ^a
7	7	80	blue	cyclization
8	8	61	yellow	cyclization
84	—	86	—	cyclization

^aNo reaction observed in the anhydrous solid state

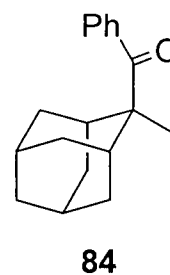


Table 2.3 Values of α for ketones 5-8.

In the previous chapter, the parameters used in predicting the feasibility of hydrogen atom abstraction in the type II photochemistry of ketones were presented. Figure 2.26 and Table 2.4 describe these values for the ketones under current study, as well as average values from the X-ray data of compounds **85**.⁶⁵ For compounds **6-8**, one of the two γ -hydrogen atoms (denoted H_x for the atom toward which the carbonyl is directed, and H_y for its conformationally diastereotopic partner) is in close proximity to the carbonyl oxygen (H_x , $d < 2.72$ Å), while the other is too far removed to participate ($d \geq 3.10$ Å). For ketone **5**, whose carbonyl group lies almost directly between H_x and H_y , it is impossible to predict which γ -hydrogen is preferentially abstracted, if either. Two modes of reactivity are possible, and therefore both possible 1,4-hydroxybiradicals must be considered.

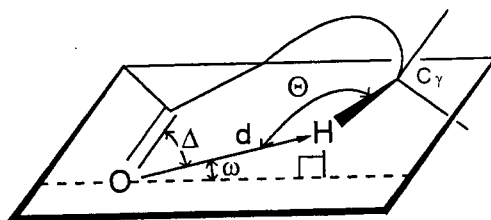
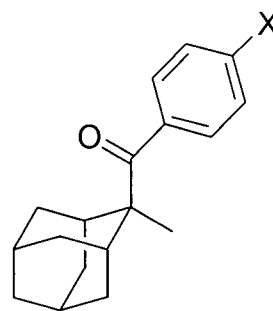


Figure 2.26 Hydrogen abstraction parameters for type II photochemistry.

		d (Å)	ω (°)	θ (°)	Δ (°)
Ideal ⁶⁶		< 2.72	0	180	90-120
5	H_x	2.35	66	120	98
	H_y	2.37	50	123	91
6	H_x	2.39	33	119	96
	H_y	3.10	58	111	60
7	H_x	2.48	55	119	85
	H_y	3.33	46	112	45
8	H_x	2.34	41	121	94
	H_y	3.13	55	114	56
Average (85)		2.63 ± 0.03	58 ± 3	114 ± 1	81 ± 4



85

X = F, CO₂Me,
and others

Table 2.4 Hydrogen abstraction parameters for the solid state spiroketones.

In constructing the biradical model, a number of assumptions are made. Since the abstraction process involves only the transfer of a single hydrogen atom over a distance of ~ 2.5 Å, the positions of the heavy atoms in the solid state 1,4-hydroxybiradical should correlate well to those in the ground state ketone. The resulting unpaired electrons are placed in p-type orbitals whose directionalities are orthogonal to the calculated mean plane of the sp^2 -hybridized carbon radical centres. Combining the positional data from X-ray crystallography with the guidelines for hydrogen atom abstraction geometry and biradical formation listed above allows a picture such as Figure 2.27 to be constructed for each biradical intermediate. Subsequent analysis of these models allows the efficiency of the cyclization and cleavage reactions to be examined in terms of biradical structure.

2.3.2 Geometric Requirements for Cleavage

The geometry of the biradicals may be characterized by three torsion angles as defined with reference to structure **86** (Figure 2.27, Table 2.5). Angle φ_1 is defined as the dihedral angle between the C_2 - C_3 σ bond and the p-orbital lobe on C_1 with which it most nearly overlaps; φ_4 is likewise defined as the analogous angle involving the C_2 - C_3 σ bond and the most favourably oriented p-orbital lobe on C_4 . The third angle is given the symbol φ and refers to the C_1 - C_2 - C_3 - C_4 torsion angle. In the present instance, this angle is fixed at $63 \pm 1^\circ$ (gauche) owing to the rigid adamantane carbon skeleton. The same conformational rigidity fixes the φ_4 angle at a value of $30 \pm 1^\circ$ for the compounds studied. This greatly simplifies the analysis, as only one parameter, φ_1 , is responsible for the variance in geometry, and hence the reactivity among the four biradicals.

For the cleavage process to occur, overlap between the σ -bond undergoing scission (C_2 - C_3) and both p-orbitals (C_1 and C_4) must be efficient.⁶⁷ Maximum overlap (100%) will occur when the p/ σ orbitals are eclipsed, i.e. φ_1 and φ_4 are 0° . Similarly, when the orbitals are orthogonal (φ_1 or φ_4 is 90°) no overlap occurs, and cleavage is prevented. Since the overlap of a p_z orbital and an adjacent σ -type orbital is proportional to the cosine of their dihedral angle,⁶⁸ the functions $\cos \varphi_1$ and $\cos \varphi_4$ are direct measures of the extent of p/ σ overlap, and as such, may be used to predict the efficiency of the cleavage reaction.

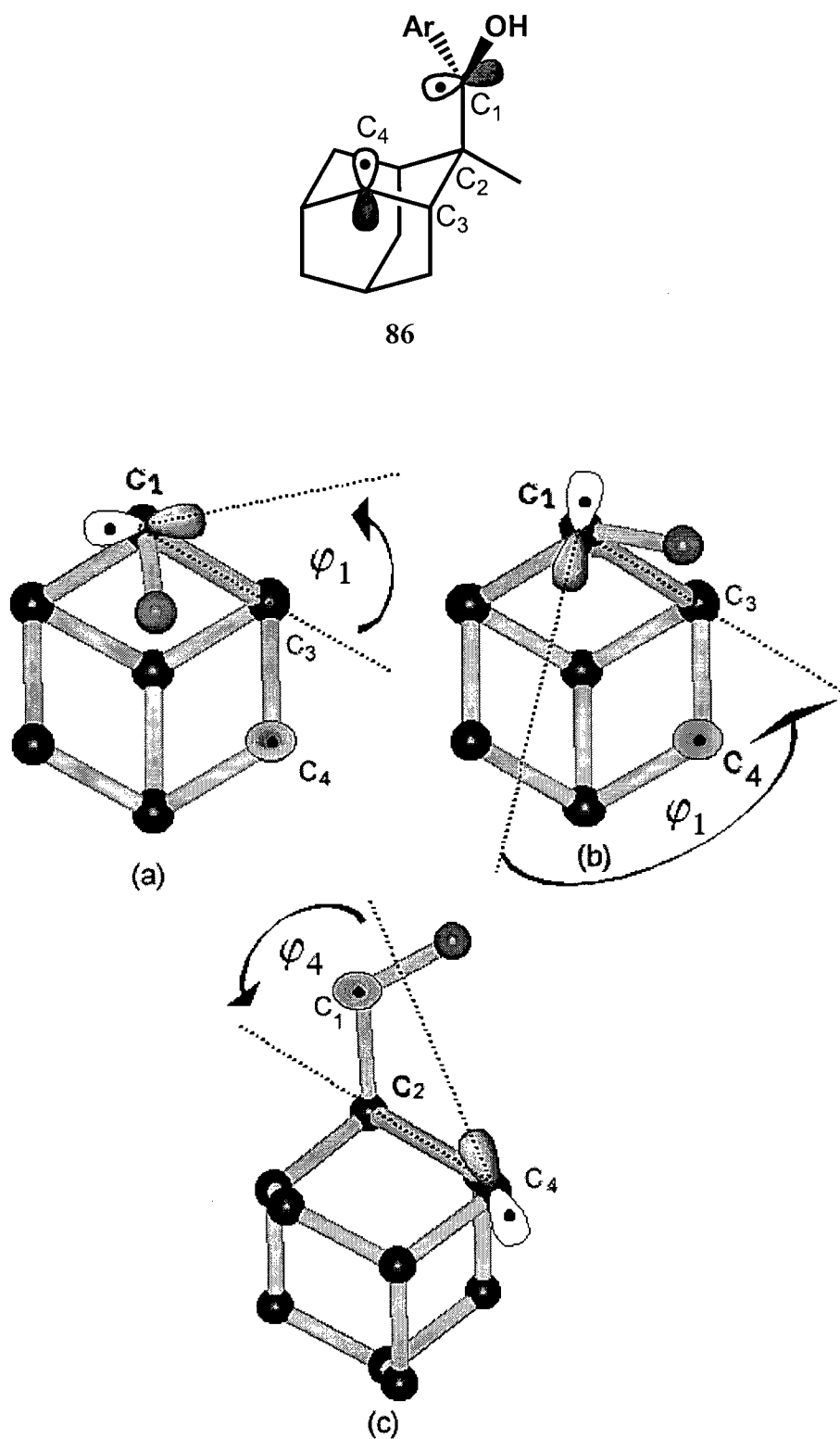


Figure 2.27 Solid state biradical geometry: (a) Representation of ϕ_1 in **5**. (b) Representation of ϕ_1 in **7**. (c) Representation of ϕ_4 for all spiroketones.

Biradical		ϕ_1 (°)	$\cos \phi_1$	ϕ_4 (°)	$\cos \phi_4$	ϕ (°)
5	H _x	-21	0.93	29	0.87	-64
	H _y	40	0.77	-30	0.87	62
6		-87	0.05	31	0.86	-63
7		70	0.34	30	0.87	-62
8		-85	0.09	31	0.86	-62
84		66	0.41	30	0.87	-63

Table 2.5 Geometric parameters for biradicals derived from **5-8**.

Figure 2.27.c clearly shows the 'fixed' ϕ_4 angle, and it is easy to see that significant overlap (86-87% of the maximum) exists between the C₂-C₃ σ -bond (shown in green) and the C₄ p orbital. For the biradicals derived from compound **5** (H_x abstraction pictured in Figure 2.27.a), $\cos \phi_1$ is at least 0.77, and this considerable overlap is readily apparent in the figure. Thus, the good overlap of both radical orbitals with the C₂-C₃ σ -bond in the **5** system is consistent with its type II cleavage photochemistry. In sharp contrast to this, the C₁ p-orbitals in the biradicals derived from **6** and **8** lie nearly perpendicular to the C₂-C₃ bond. Low calculated overlaps of 5% and 9% respectively predict that cleavage in these cases should be very inefficient. Indeed, the remarkable stability of the biradical derived from **6** with respect to both cleavage and cyclization attests to the fact that cleavage from this geometry is extremely disfavoured. Compound **7** (Figure 2.27.b), for which cyclization is the only observable mode of reactivity, is also poorly aligned for cleavage at the C₁ centre, with a predicted overlap of only 34%. This is similar to the acyclic compounds of which **84** is representative (41% calculated overlap), and for which no cleavage is observed. Overall, therefore, while perfect orbital overlap is not required for cleavage, it should at least be very good and should involve both p-orbitals. The data clearly indicate that excellent overlap on one side and poor overlap on the other does not lead to cleavage.

2.3.3 Geometric Requirements for Cyclization

Having dealt with the features that favour 1,4-hydroxybiradical cleavage, it is equally important to focus on the geometric factors that facilitate cyclization. Intuitively, it makes sense that Yang photocyclization will proceed efficiently when the radical-containing carbon atoms C_1 and C_4 are close to one another, most likely $< 3.40 \text{ \AA}$, which is the sum of the van der Waals radii⁶⁹ for two carbon atoms. The C_1 - C_4 distances calculated here are given the symbol D , and are well within the van der Waals limit for each of the ketones investigated (Table 2.6). A second important consideration is the *directionality* of the orbitals in question, i.e. how well the orbitals on these radical centres overlap. Interaction is maximized when the C_1 orbital is parallel to the C_2 - C_4 vector, this angle being represented by the parameter β (Figure 2.28, Table 2.6). Likewise, interaction between the two radical centres diminishes as β approaches 90° .

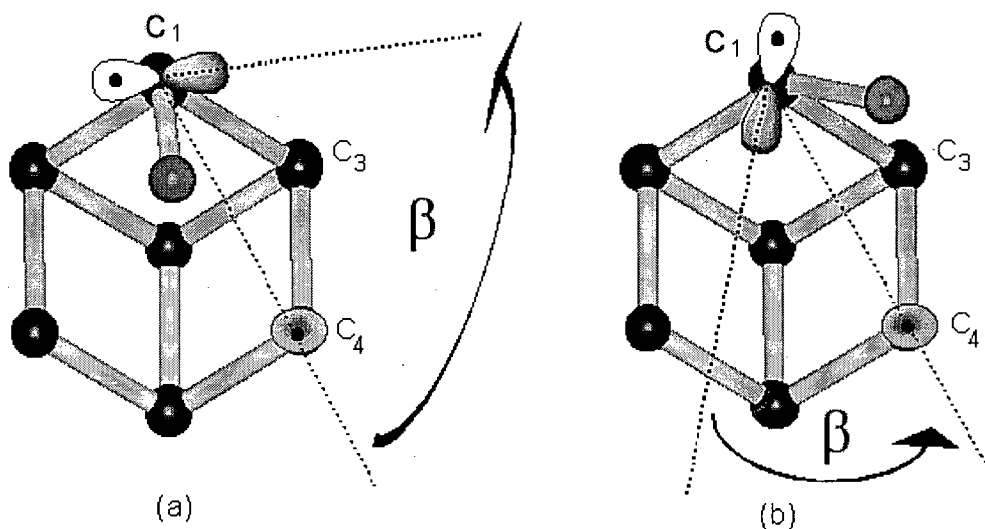
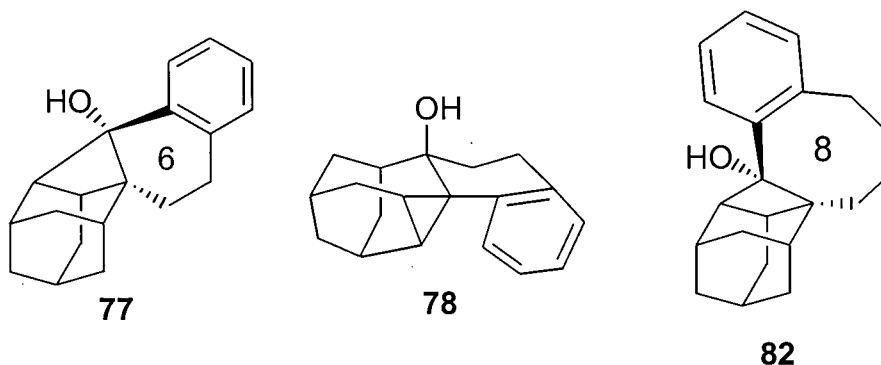


Figure 2.28 Geometric parameters for cyclization: (a) biradical derived from **5** (H_x); (b) biradical derived from **7**.

Parent Ketone		β (°)	D (Å)
5	H _x	52	3.03
	H _y	69	3.08
6		59	3.07
7		39	3.02
8		61	3.05
84		32	3.02

Table 2.6 Cyclization parameters for the 1,4-hydroxybiadicals.

The biradical derived from the seven-membered spiroketone, **7**, (Figure 2.28.b) possesses the most favourable geometry for cyclization, again similar to that of the acyclic compound **84**. In the six- and eight-membered compounds, also similar in geometry, β lies around 60°. The five-membered ketone, **5**, which arguably adopts the least favourable cyclization geometry, might also be hindered along this pathway by the kinetic barrier required to produce a strained cyclobutanol. This situation is readily illustrated in the case of compounds **6** and **8**. While the disposition of the carbonyl groups (α) in these two compounds differs only by 2°, the eight-membered ring cyclizes, while its six-membered homologue is remarkably unreactive. The formation of a 6,4-*trans* ring fusion in the cyclization to cyclobutanol **79** must be very inefficient, so much so that it can not compete with reverse-hydrogen transfer. Steric interactions between the biradical and the crystal lattice can be ruled out as causative factors, as **6** undergoes reverse hydrogen transfer in solution as well as in the solid state. In the special case where **6** is photolysed as an aqueous suspension, water is thought to aid in the formation of **79**, though how this is achieved is not understood. Subsequent cyclobutanol rearrangement to the observed product **78** proceeds under unusually mild conditions, most likely driven by the high strain energy associated with the cyclobutanol intermediate. The corresponding 8,4-*trans* fused cyclobutanol **82** readily forms upon irradiation of **8** and is stable in water.

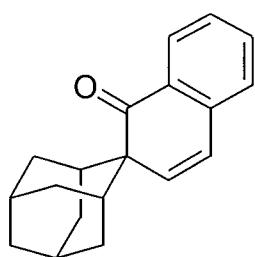
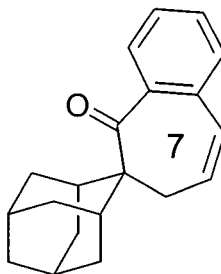
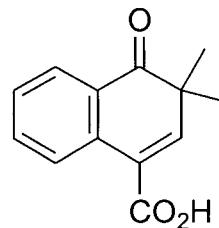


2.3.4 Summary of Biradical Reactivity

The photochemical reactivity displayed by the benzoyladamantane system is exquisitely sensitive to the geometry of the intermediate 1,4-hydroxybiradicals. Recalling the kinetic scheme for biradical reactivity introduced in Figure 2.23, a physical basis can now be ascribed to the efficiencies of the cleavage and cyclization processes. Compound **5** exists in a conformation for which cleavage is favourable and cyclization improbable ($k_{cl} \gg k_{cy}$), and this prediction is borne out by experiment. For ketones **7** and **8**, biradical geometry disfavors the cleavage reaction, but orbital alignment for σ -bond formation is acceptable ($k_{cy} \gg k_{cl}$), and cyclization is indeed the observed outcome. Compound **6**, although similar in geometry to **8**, is not able to cyclize in the anhydrous solid state, most likely owing to the kinetic barrier associated with the production of a strained cyclobutanol (**79**). In this instance, only reverse hydrogen transfer occurs, and no new compounds are formed ($k_H \gg k_{cl}, k_{cy}$).

2.4 Photochemistry of the Unsaturated Adamantyl Spiroketones **68** and **70**

In the course of preparing the saturated adamantyl spiroketones, two solid unsaturated analogues, **70** and **68**, were synthesized and subsequently characterized by X-ray crystallography (**70**: Figure 2.8; **68**: Figure 2.24.a). Their photochemistry was investigated in both the solid state and in solution.

**70****68****52**

2.4.1 Photochemistry of Unsaturated Ketone **68**

The crystal structure of compound **68** revealed that this achiral molecule crystallizes in space group $P2_12_12_1$, one of the 65 chiral space groups. Thus the possibility that an 'absolute' asymmetric reaction, one in which the asymmetry is presented spontaneously (through crystallization) and is not provided by an external source of optical activity,³⁸ might be possible on irradiation of a single crystal of the ketone. Unfortunately, however, **68** proved to be photochemically unreactive in the solid state. Although a γ -hydrogen is suitably positioned for abstraction to occur in a type II fashion ($d = 2.47 \text{ \AA}$), photochemical reactions in conjugated systems of this type, such as **87**, are known to proceed only through reaction at the site of the double bond (Figure 2.29).⁷⁰ The resulting products are either dimers (**88**) produced *via* [2+2] photocycloaddition reactions, or other adducts (**89**, **90**, and **91**) resulting from the highly reactive *E*-cycloheptene intermediate (**92**). Solution photolysis of **68** produced a complex mixture of compounds that lacked vinylic ^1H NMR signals, and were not volatile enough to be observed by GC, characteristics consistent with product dimers. Study of this system was not pursued further.

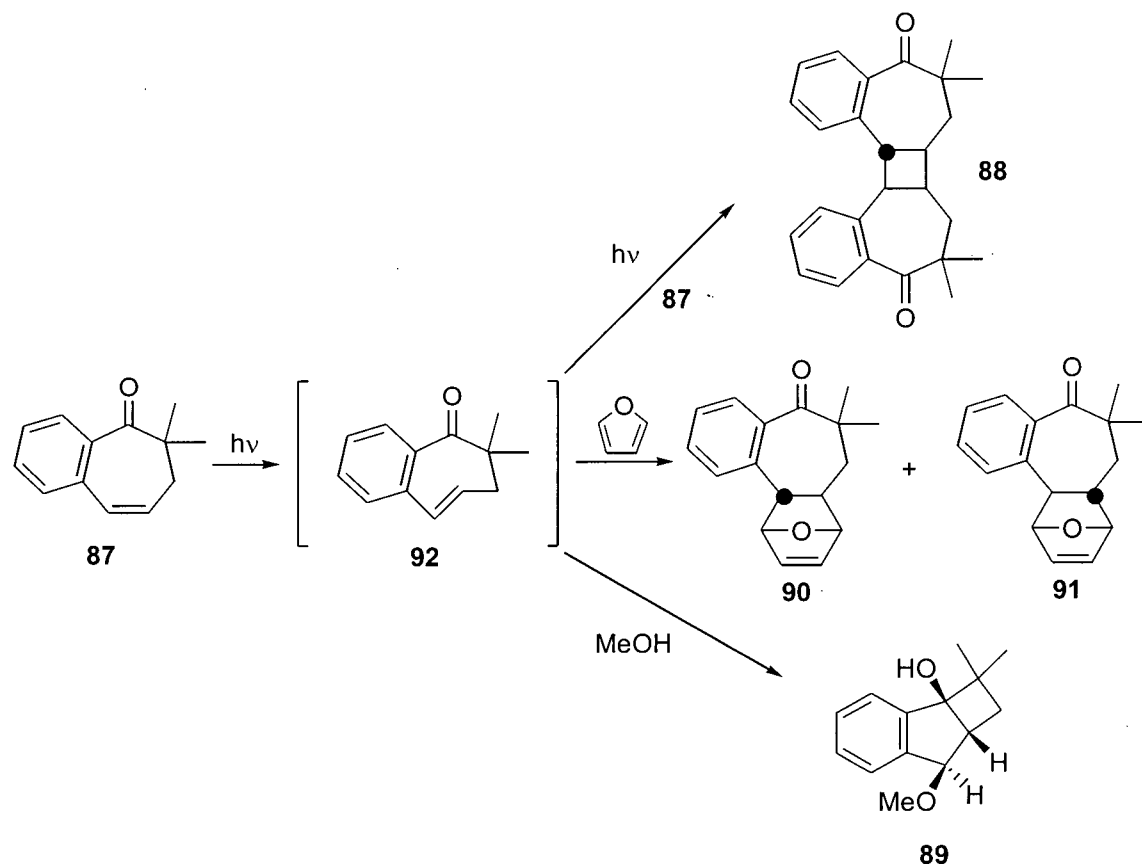


Figure 2.29 Photochemistry of unsaturated ketone **87**.

2.4.2 Photochemistry of Unsaturated Ketone **70**

Enone **70** contains the 1-(2*H*)-naphthalenone chromophore, the photochemistry of which is investigated further in Chapter 4 through the study of compound **52** and its derivatives. An overview of the photochemistry of the broader class of linearly conjugated cyclohexadienones is given in Chapter 1, and the photoreactivity of **70** will be presented in the context of this introduction.

Irradiation (Pyrex or Uranium filter) of **70** in both the solid state and solution proceeded efficiently with cyclopropane **93** as the sole primary photoproduct (Figure 2.30). This compound is itself photochemically labile and rearranges to α -naphthol derivative **94**. This secondary photolysis is competitive with the consumption of **70** when Pyrex-filtered light is used ($\lambda > 290$ nm) such that the concentration of **93** is low throughout the reaction. When light of longer wavelength is employed ($\lambda > 330$ nm), the efficiency of the secondary photolysis relative to that of the first is decreased, and **93** may

be obtained in moderate yield (Table 2.7). This phenomenon is easily explained by the decreased absorbance of **93** ($\lambda_{\max} = 301$ nm, $\epsilon = 310$) versus **70** ($\lambda_{\max} (\pi, \pi^*) = 318$ nm, $\epsilon = 1350$; $\lambda_{\max} (n, \pi^*) = 356$ nm, $\epsilon = 740$) at longer wavelengths.

Filter ^a	Solvent	Irradiation Time (min)	Conversion ^b (%)	93 (%) ^b	94 (%) ^b
Pyrex	MeCN	60	88	2	83
		15	85	12	67
	EtOH	30	96	2	86
		20	40	22	14
		60	77	24	48
		150	97	2	93
Uranium	MeCN	10	20	18	trace
		40	55	44	1
		90	85	69	13
	Solid State	30	30	21	9
		105	59	29	30

^a450W Hanovia medium pressure mercury lamp. ^bGC analysis.

Table 2.7 Photoproduct yields from **70** under various photolysis conditions.

The mechanism of this reaction was clearly established as proceeding by way of ketene intermediate **95**, which is known in analogous systems to arise from the $^1(n, \pi^*)$ excited state.⁷¹ Irradiation of **70** in MeCN containing dimethylamine gave rise to amide **96** in 82% yield, with no trace of compounds **93** or **94** (Figure 2.30). Formation of **93**, therefore, occurs only *via* the thermal crossed [2+4] internal cycloaddition of ketene **95**, and does not proceed from **70** by the concerted $[\pi_2^a + \sigma_2^a]$ ^{71a} or step-wise mechanisms⁷² proposed for cyclohexadienones that react from the $^1(\pi, \pi^*)$ excited state. The position of the double bond in compound **96** was confirmed by the presence of an olefinic quaternary centre in the ¹³C NMR spectrum. The benzylic methylene doublet (δ 3.30 ppm) in the ¹H NMR spectrum also confirms that the double bond is not in conjugation with the phenyl

ring. The structure of photoproduct **93** is completely in accord with the observed spectral data and reaction mechanism. The geminal methine protons on the cyclopropane ring give rise to a diagnostic pair of doublets (δ 2.28, 2.87 ppm, $J = 4.6$ Hz) which form an isolated spin system (verified by a COSY experiment). In addition, the carbonyl stretching frequency of 1695 cm^{-1} is consistent with the presence of a more highly strained indanone rather than tetralone ring system,⁷³ and correlates well to the ketone stretching frequency in **5** which is 1694 cm^{-1} . The carbonyl IR bands for the larger six-through eight-membered rings **6-8** occur at 1686 , 1683 , and 1681 cm^{-1} , respectively.

The mechanism for the transformation of **93** to **94** also has literature precedent.⁷² Photoinduced cleavage of the internal cyclopropane bond leads to zwitterionic intermediate **97**. Subsequent [1,2]-alkyl migration produces ketone **98** which readily aromatizes to its stable enol tautomer, photoproduct **94**. Spectral data for compound **94** were in accord with the assigned structure, most notably the reduction in number of ^{13}C and ^1H NMR signals resulting from the introduction of a molecular plane of symmetry. In addition, NOE difference experiments confirm the substitution pattern of the naphthalene system as shown in Figure 2.31.

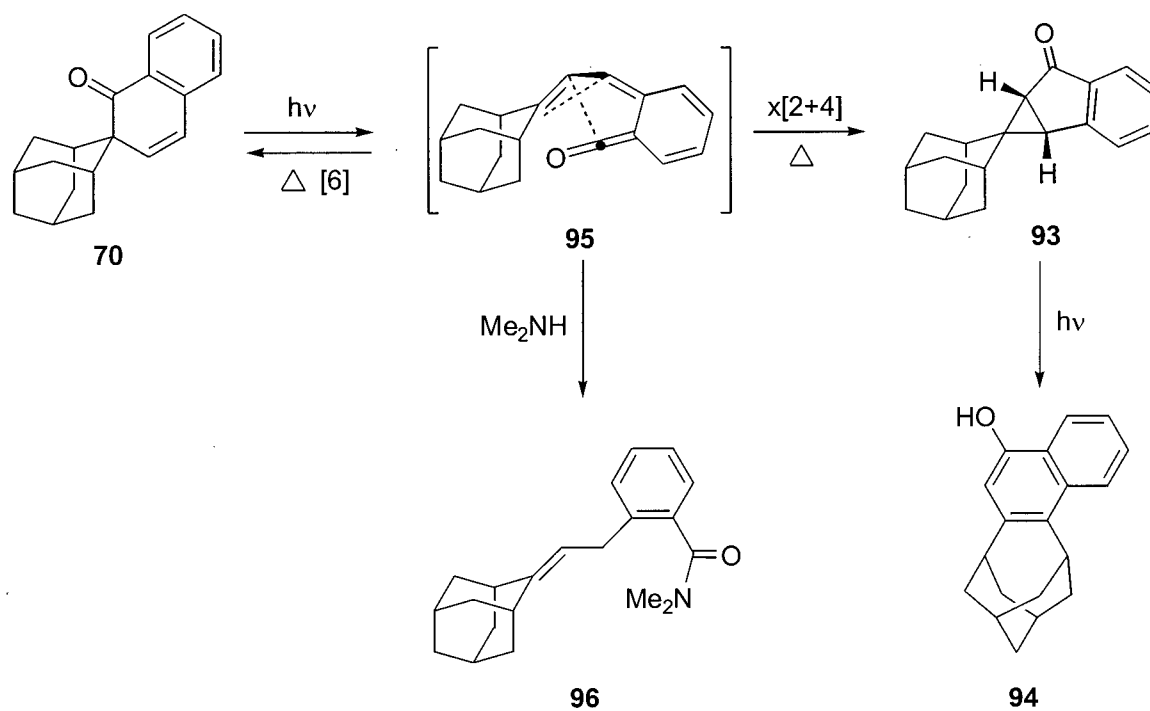


Figure 2.30 Photochemistry of unsaturated spiroketone **70**.

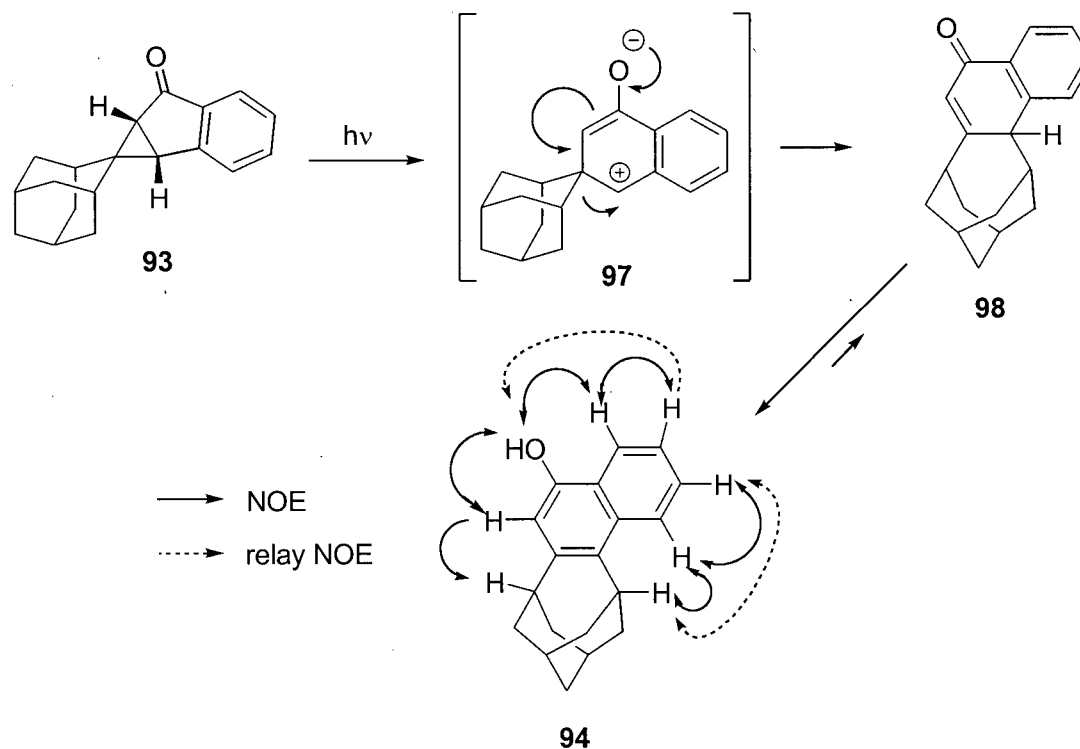


Figure 2.31 Mechanism for photorearrangement of **93** to **94**.

2.5 Summary

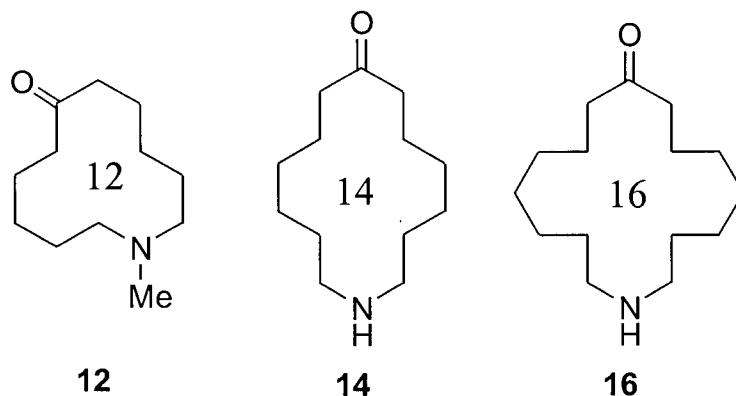
Constraining the carbonyl group in the benzoyladamantane system by introducing spiro-fused rings of varying sizes has proven an effective strategy in obtaining biradical geometries that are inaccessible in the acyclic series. The structural similarity of the four saturated homologues has simplified the correlation of structure and reactivity, as only a few key parameters differ among the biradical intermediates. Analysis of the data has provided a quantitative assessment of the extent of orbital overlap required for the cleavage and cyclization reactions to occur. The remarkable photostability of the biradical in the six-membered ring system, in which one p-orbital is orthogonal to the σ -bond and hence can not participate in a cleavage reaction, not only supports the accepted model for this type of reactivity, but also highlights the predictive value of solid state structure analysis. The results are also significant as they present numerical structural data, in terms of angles and distances, that may be used to engineer molecules, crystals, and other assemblies with selective, 'designer' reactivities.

Although the unsaturated spiroketone **70** did not show any difference in reactivity between the solid and solution states, it demonstrated that the linearly conjugated benzocyclohexadienone system reacts cleanly and efficiently in the solid state. This compound served as a model for a series of compounds based on the 1-(2*H*)-naphthalenone chromophore. The photochemistry of these compounds is concerned with solid state asymmetric synthesis and is described in chapter 4 of this thesis.

Chapter 3 – Asymmetric Induction in the Solid State Photochemistry of Macrocyclic Aminoketone Salts

3.1 Synthesis of the Aminoketones

The macrocyclic aminoketones **12**, **14**, and **16** were synthesized *via* a straightforward Dieckmann condensation – decarboxylation approach under high dilution conditions. The twelve-membered compound (**12**) was first synthesized by Spanka *et al.*,⁷⁴ and the same general approach was employed in the preparation of the previously unknown fourteen- and sixteen-membered aminoketones **14** and **16**.



3.1.1 Synthesis of the Twelve-membered Aminoketone 12

Figure 3.1 shows the synthetic scheme for macrocycle **12**. Cyclization precursor **99** was prepared from methylammonium chloride and the commercially available (Aldrich) ethyl 6-bromohexanoate (**100**) according to a procedure modified from that which Leonard *et al.*⁷⁵ used to prepare similar compounds. Addition of aminodiester **99** to a refluxing suspension of potassium *tert*-butoxide in anhydrous xylenes over forty hours was achieved using a syringe pump in order to maintain low starting material concentration, and thus minimize dimerization. The material isolated following acid-catalyzed ester hydrolysis and decarboxylation consisted of a mixture of the desired twelve-membered aminoketone (**12**) and the twenty-four-membered dimer **101**. The dimer was isolated by fractional crystallization from diethyl ether, and the remaining monomer purified by vacuum sublimation. Although not observed in the literature

procedure, dimers similar to compound **101** have been reported for Diekmann condensations of shorter-chain aminodiester.⁷⁶ In the literature procedure,⁷⁴ a specially designed high-dilution apparatus was used for the macrocyclization, and a yield of 68% was obtained. Without such equipment, the effective diester concentration was higher than that previously reported, resulting in a lower yield of ketone **99** (31%) and concomitant dimer formation.

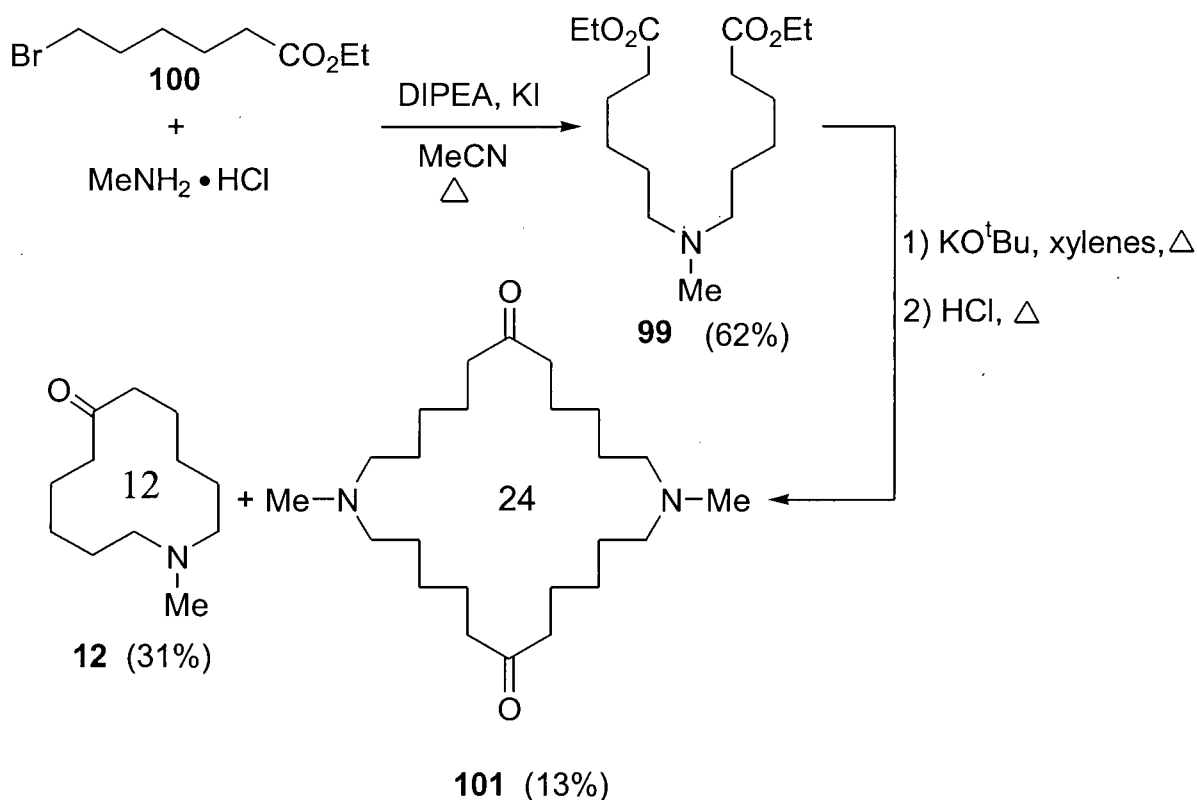


Figure 3.1 Synthesis of aminoketone **12**.

3.1.2 Synthesis of the Fourteen- and Sixteen-membered Aminoketones **14** and **16**

Two modifications to the above procedure were employed in the synthesis of the fourteen- and sixteen-membered aminoketones. The macrocycles were prepared as their *N*-benzyl derivatives, with the nitrogen protecting groups removed in the final step to liberate the desired secondary amines **14** and **16**. The *seco* aminodiester **102** and **103**

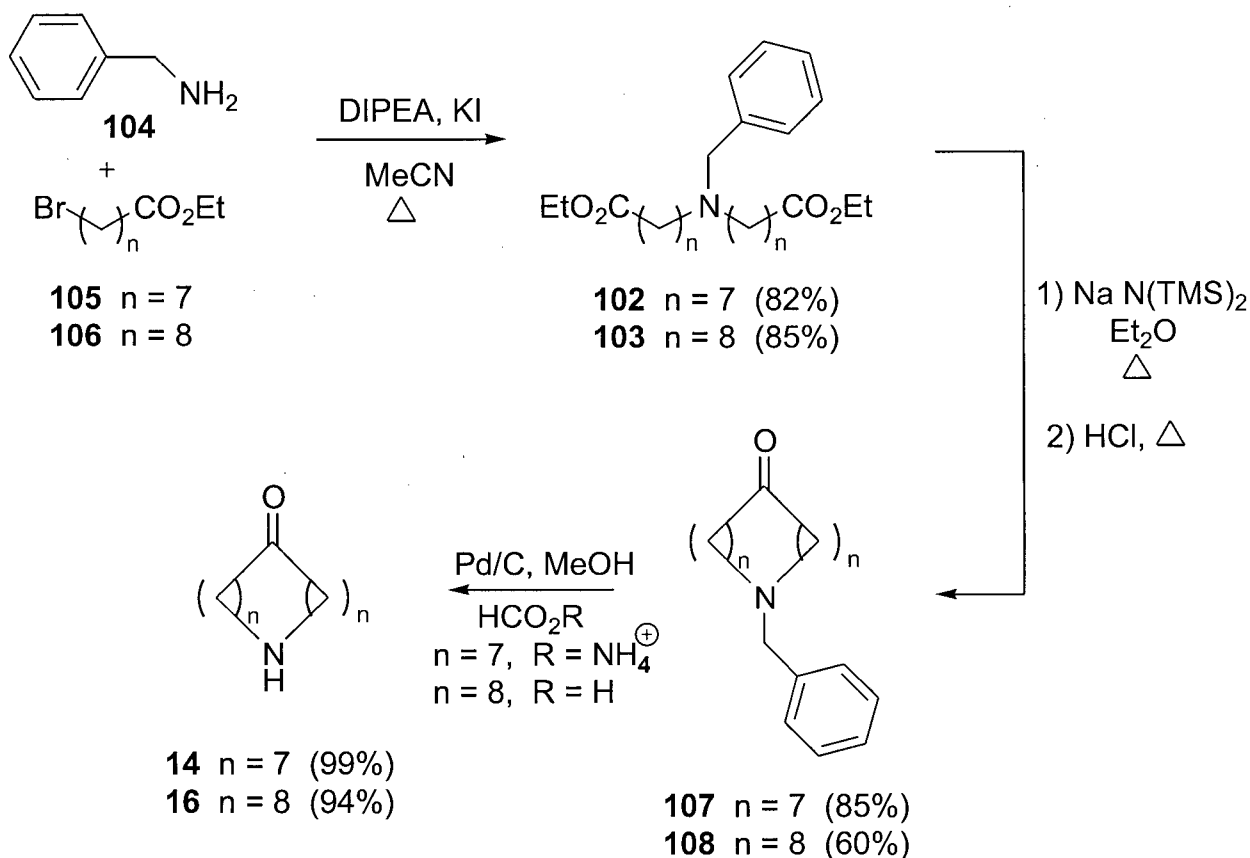


Figure 3.2 Synthetic scheme for macrocycles **14** and **16**.

were prepared in good yield *via* dialkylation of benzylamine (**104**) with ethyl 7-bromoheptanoate (**105**) and ethyl 8-bromooctanoate (**106**) respectively (Figure 3.2). The Dieckmann condensations were effected using sodium hexamethyldisilazide in refluxing diethyl ether, a protocol employed by Hurd *et al.* in the synthesis of the natural macrocyclic ketone zearalanone.⁷⁷ As in the case of the twelve-membered ring, high-dilution conditions were maintained, with addition of the diesters proceeding over a period of 40 hours. The *N*-benzyl macrocycles **107** and **108** were isolated in good yield following acid catalyzed ester hydrolysis and decarboxylation. Palladium catalyzed hydrogenolysis of **107** proceeded smoothly with ammonium formate in refluxing methanol,⁷⁸ while debenzylation of **108** was optimal at room temperature with formic acid as the hydrogen donor. Aminoketones **14** and **16** were isolated as low-melting

amorphous solids (33-34 °C and 50-51 °C respectively), which gave spectra and elemental analyses consistent with their assigned structures. X-ray crystallographic analysis of salts of these two amines (*vide infra*) confirmed the identity of the macrocyclic aminoketones.

While compound **105** was commercially available (Aldrich), bromoester **106** was synthesized in three steps from 1,8-octanediol (**109**) (Figure 3.3). Monobromination of diol **109** was achieved according to the procedure of Kang *et al.*⁷⁹ and was followed directly by Jones oxidation to give 8-bromooctanoic acid (**110**). Fisher esterification completed the preparation of the eight carbon alkylating agent **106**.

Although the reaction conditions employed for the above macrocyclizations were not identical, the product yields follow the general trend reported by Leonard *et al.*⁸⁰ for the preparation of cycloalkanones with rings sizes of eleven to fifteen. In this study, the yield of cyclic monomer was observed to increase with ring size, with a corresponding decrease in dimer formation (< 3% for cyclotetradecanone). Steric repulsion between the alkylene chains in the Dieckmann cyclization of straight-chain diesters is cited⁸⁰ as the main kinetic barrier in the formation of medium-sized rings (nine- to twelve-membered); such strain is avoided in larger rings, where cyclization is more efficient.

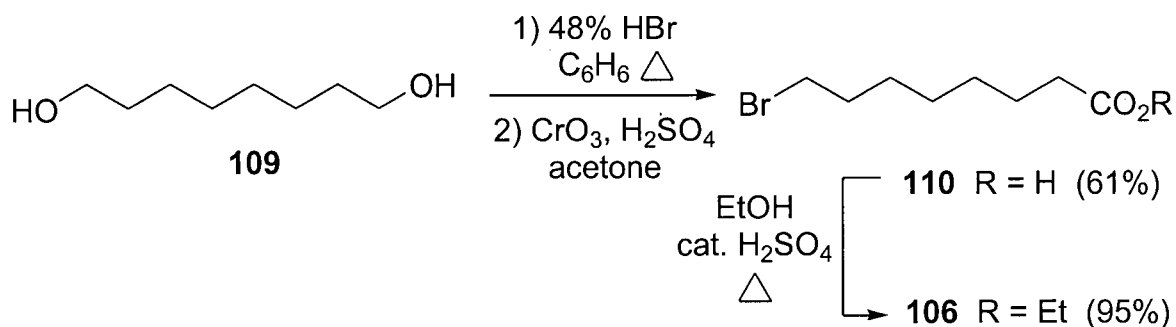


Figure 3.3 Synthesis of bromoester **106**.

3.2 Solution State Photochemistry of the Macrocyclic Aminoketones

The three macrocyclic aminoketones under study were first photolyzed in solution in order to determine their photoreactivity and to isolate and characterize their photoproducts. In all three cases, the expected Norrish/Yang Type II photochemistry proceeded cleanly and efficiently.

3.2.1 Solution State Photochemistry of Cycloalkanones

In looking at the photochemistry of the cyclic aminoketones, it is useful to review the photochemical behaviour of the medium-sized and macrocyclic alkanones **111**, which have been studied previously in solution.⁸¹ Figure 3.4 depicts the reactivity of these compounds, which display typical Type II photochemistry in producing both *cis*- and *trans*-cyclobutanols (**112** and **113** respectively) as well as cleavage product **114**. In the smaller rings (eleven- to thirteen-membered), cycloalkanols **115** are produced in low yield *via* photoreduction of the excited state ketone by solvent.^{81d} Table 3.1 presents the data from these studies, as well as the ratio of *cis*- and *trans*- cyclobutanols (**112**:**113**) and the ratio of products derived from cyclization to those from cleavage (**112**+**113**:**114**).

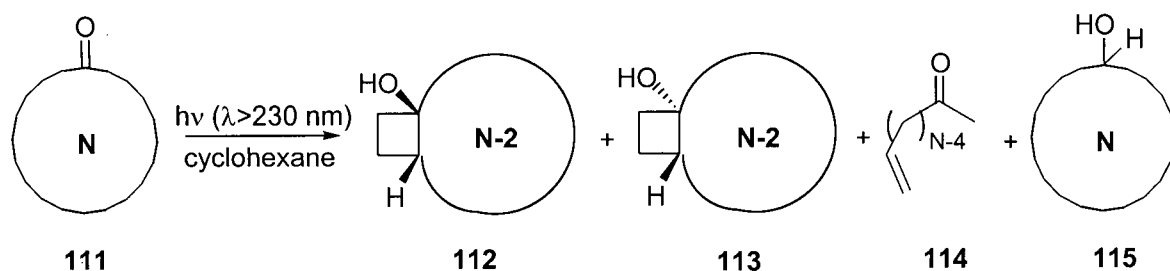


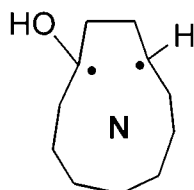
Figure 3.4 General scheme for type II photochemistry of cycloalkanones.

Table 3.1 Product distributions^{81a} in solution state cycloalkanone photochemistry.

N (111)	% 112	% 113	% 114	% 115	% other ^a	<i>cis/trans</i> Ratio	Cyclization/ cleavage Ratio
11	40	14	8	12	26	2.9	6.8
12	64	11	8	7	10	5.8	9.4
13	45	23	18	5	9	2.0	3.8
14	39	12	30	<1	20	3.3	1.7
15	17	11	52	<1	14	1.5	0.5
16	13	9	58	<1	20	1.4	0.4

^a Unknown products, polymers, etc.

A number of trends come to light when looking at these results. Intermolecular hydrogen abstraction leading to the photoreduced product **115** decreases as ring size increases, and becomes negligible at ring sizes of fourteen and above. This phenomenon can be attributed to conformational restrictions to closure and cleavage of the intermediate cyclic 1,4-biradical **116**, such that intermolecular processes are able to compete.⁸² In addition, both the ratio of *cis*- to *trans*-cyclobutanol and the ratio of cyclization to cleavage products decrease as N increases. These trends are consistent with the greater conformational flexibility and reduced transannular interactions experienced by the intermediate 1,4-biradicals in the larger rings.^{81d} Indeed, these ratios approach those observed for acyclic ketones; photolysis of valerophenone⁸³ gives a *cis/trans* ratio of 0.3 and a cyclization/cleavage ratio of 0.3. It should be noted, however, that except for conformationally rigid systems such as those described in Chapter 2 of this thesis, conformational analysis is of limited utility in predicting product ratios in solution state type II photochemistry.⁸⁴ Since the 1,4-biradical intermediate may revert to the starting

**116**

ketone as well as proceeding on to product, the reaction outcome does not necessarily correlate with reactant conformer populations, and can be determined largely by non-minimum energy geometries.⁸⁵

3.2.2 Aminoketone Photochemistry

The photochemistry of the macrocyclic aminoketones proceeded in a fashion analogous to that of the cycloalkanones discussed in the previous section. Figure 3.5 outlines the reactivity of the twelve-membered species **12**, and Figure 3.6 depicts the photochemistry of the fourteen- and sixteen-membered homologues **14** and **16**. The product ratios for the solution reactivity of these compounds are summarized in Table 3.2.

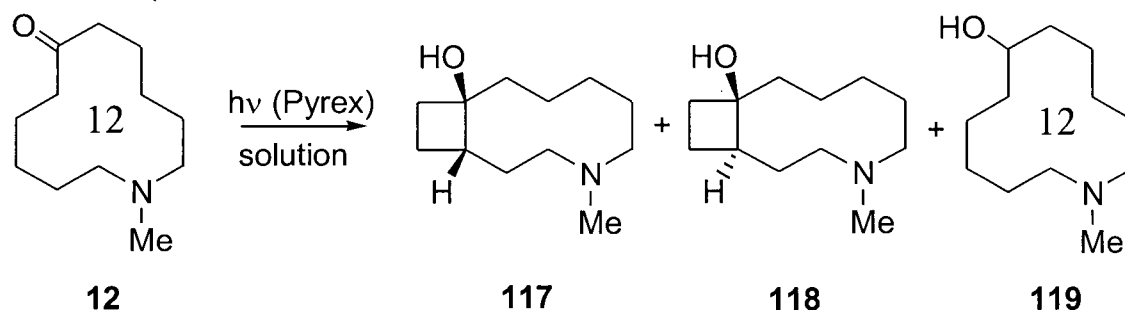


Figure 3.5 Solution state photochemistry of aminoketone **12**.

The two larger macrocycles (**14** and **16**) yielded both *cis*- and *trans*-cyclobutanols from the Yang photocyclization, as well as the Norrish type II cleavage product. Since the latter is itself photolabile, the product ratios for **14** and **16** are reported at low conversion. For the twelve-membered compound, only cyclization (**117** and **118**) and photoreduction (**119**) products were obtained. This differs from the studies of cyclododecanone photochemistry⁸¹ (Table 3.1) where a small amount (8%) of cleavage was reported. Additionally, it was discovered that the intermolecular photoreduction pathway could be suppressed if the hydrochloride salt **120** was photolyzed in place of the free base **12**. Hydrogen atoms on carbons α - to an amine nitrogen are known to be susceptible to radical abstraction.⁸⁶ There is no lone electron pair on the protonated ammonium nitrogen to stabilize an α -carbon radical, however, and intermolecular

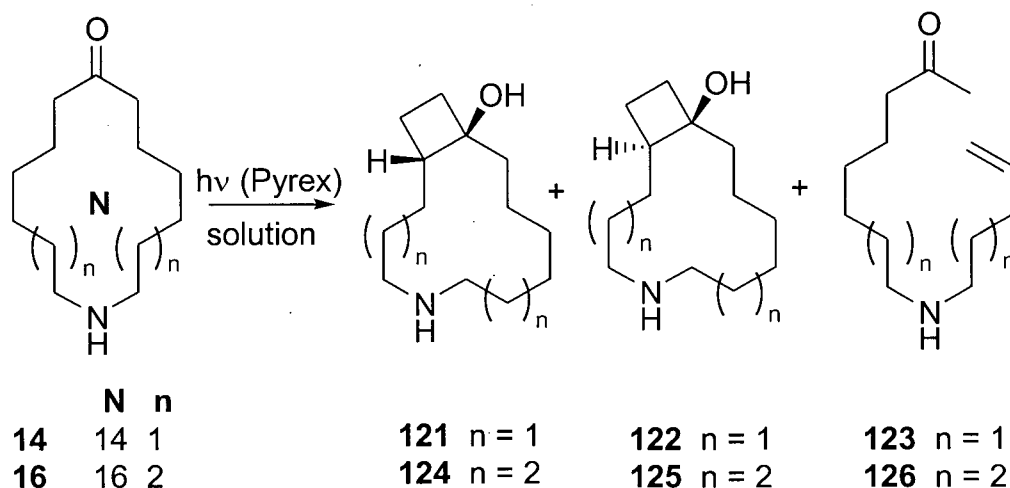
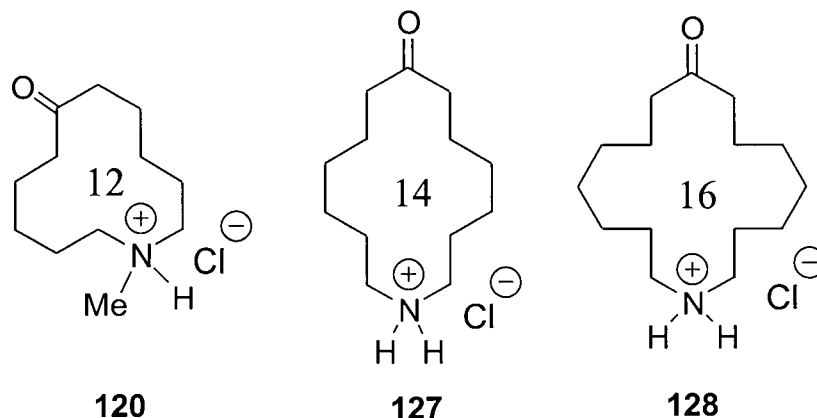


Figure 3.6 Solution state photochemistry of aminoketones **14** and **16**.

photoreduction *via* radical abstraction at this site is energetically less favourable. Preparative scale photolyses of the three macrocycles, conducted in order to isolate and characterize their photoproducts, were thus performed on their hydrochloride salts (**120**, **127**, and **128**) in acetonitrile.



The isolated yields for the preparative photolyses are presented in Table 3.3. The low yields reported do not reflect poor reaction selectivity and are easily explained by practical considerations. The *cis*- and *trans*-cyclobutanols are not readily separable by chromatographic methods, and thus the yield of pure samples of these compounds was low. The cleavage products **123** and **126** are themselves photolabile, and their isolated yields do not reflect the portion that was consumed during irradiation. Figure 3.7 illustrates the secondary photolysis of **123** to **129** that was observed qualitatively by ^{13}C

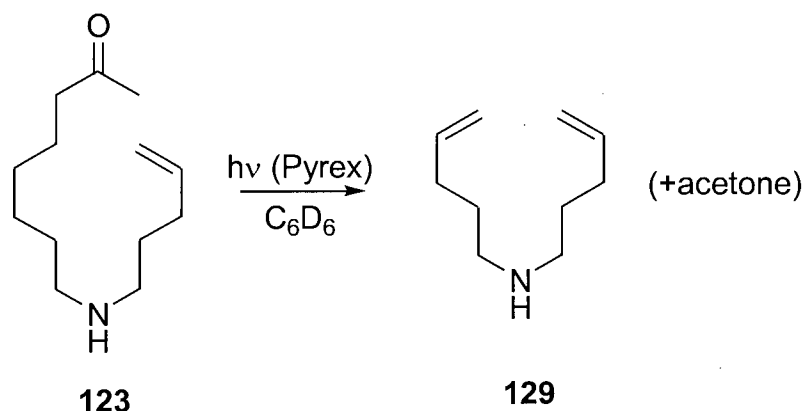


Figure 3.7 Secondary photolysis of cleavage product **123**.

NMR spectroscopy of the crude reaction mixture. Diene **129** was too volatile for practical isolation; its spectroscopic data were determined from an authentic sample (*vide infra*). To further illustrate the clean nature of these reactions, a sample of **120** was irradiated in acetonitrile until no starting material remained. The crude reaction mixture was analyzed by ^{13}C NMR following basic workup. The spectrum is remarkably clean, displaying only peaks for cyclobutanols **117** and **118**. A portion of this spectrum is reproduced as Figure 3.8.

Table 3.2 Product distributions for solution state photolyses^a of the macrocyclic aminoketones and their hydrochloride salts.

Substrate	Solvent	% Cyclobutanol		% Cleavage	% 119	<i>cis/trans</i> Ratio	Cyclization/ Cleavage Ratio
		<i>cis</i>	<i>trans</i>				
12	C ₆ H ₆	65	18	0	17	3.6	—
120	MeCN	68	32	0	0	2.2	—
14	C ₆ H ₆	50	23	27	—	2.2	2.7
	^t BuOH	50	28	22	—	1.8	3.5
127	MeCN	49	29	22	—	1.7	3.4
16	C ₆ H ₆	40	16	44	—	2.5	1.3
	MeCN	39	11	50	—	3.5	1.0
	^t BuOH	29	16	55	—	1.8	0.8
128	MeCN	30	30	40	—	1.0	1.5

^aPyrex-filtered light ($\lambda > 290$ nm). Product ratios determined by GC at low conversion (< 10%).

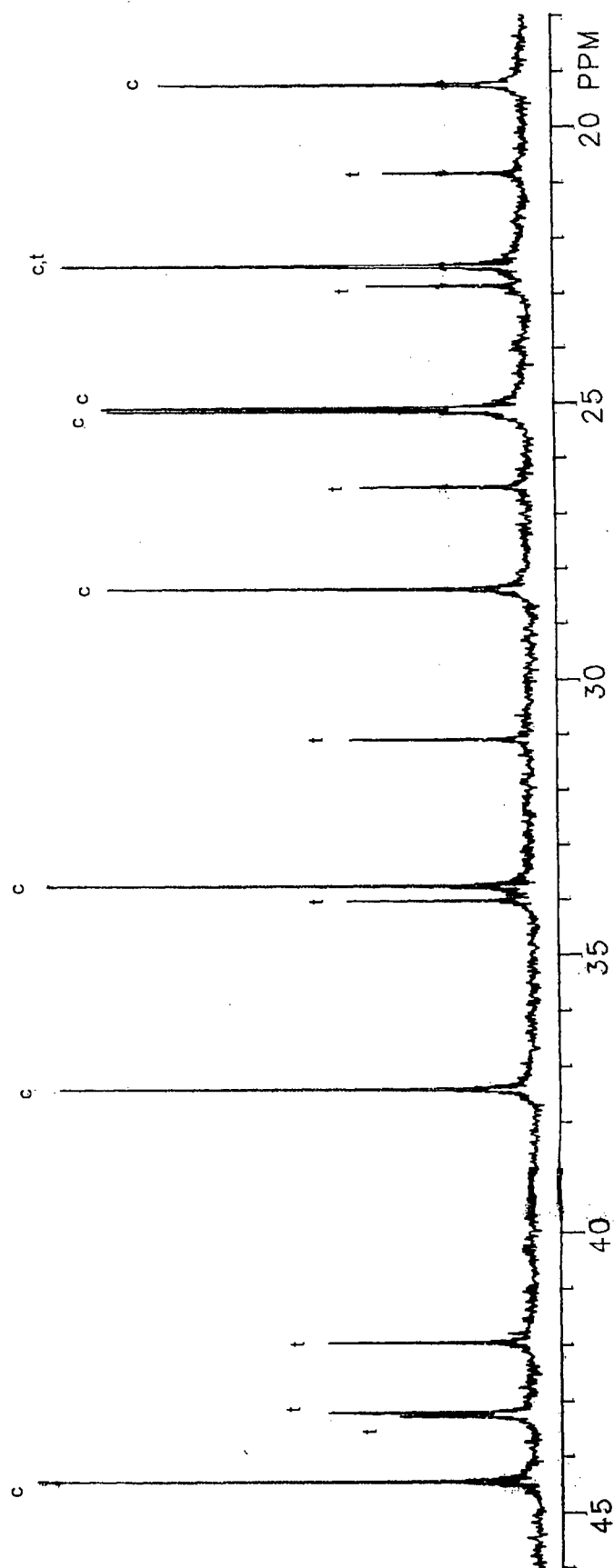


Figure 3.8 A portion of the ^{13}C NMR spectrum (C_6D_6) of the crude reaction mixture after exhaustive photolysis of **120** in MeCN. The *cis*- (**117**, labelled c) and *trans*- (**118**, labelled t) cyclobutanols are the sole photoproducts.

Table 3.3 Isolated yields from preparative scale photolyses of the macrocycles.

Ring Size ^a	Cyclobutanol		Cleavage	Photoreduced
	<i>cis</i>	<i>trans</i>		
12	117 (16%)	118 (11%)	—	119 (30%) ^b
14	121 (35%)	122 (24%)	123 (8%)	—
16 ^c	124 (17%)	125 (8%)	126 (32%)	—

^aPhotolysis (Pyrex filter) of aminoketone hydrochloride salts in acetonitrile solution unless otherwise noted.

^bPhotoreduction product isolated from photolysis of the free amine. Compound **119** is not formed on photolysis of the hydrochloride salt. ^cData represent photolysis of the free amine.

3.2.3 Quantum Yield Studies of Compound 14

In order to provide a more quantitative analysis of the solution state photochemistry described above, quantum yields (Φ) for product formation from the fourteen-membered aminoketone **14** were measured. at 313 nm. The quantum yield of a photochemical process reflects the probability that a particular event will take place once a photon has been absorbed by the molecule under study. In other words, the quantum yield measures the efficiency of a pathway available to the excited state species. For the photochemical process $A \rightarrow [A^*] \rightarrow B$, the mathematical expression for Φ_B (quantum yield for the formation of B) is presented here:

$$\Phi_B = \frac{\text{Number of molecules B formed per unit time per unit volume}}{\text{Quanta of light absorbed by A per unit time per unit volume}}$$

The quantum yields for ketone **14** were determined both in benzene and in 2:1 *tert*-butanol / benzene. As mentioned in Chapter 2 (Section 2.2.2, Figure 2.13), the addition of Lewis bases such as *tert*-butanol stabilize the 1,4-hydroxybiradical type II intermediate against disproportionation back to the starting ketone, thus increasing the proportion that go on to product (cyclization or cleavage). As can be seen in Table 3.4, the quantum yields for product formation roughly double on addition of the alcohol. The total quantum yield for product formation from cyclotetradecanone in cyclohexane solution is 0.29 as reported by Schulte-Elte *et al.*,^{81a} and agrees favourably with our result. Quantum yields for cycloalkanones with ring sizes from eleven sixteen were in the range of 0.10 to 0.38.

Information on the multiplicity of the photochemical reaction, that is whether it occurs from a singlet or triplet excited state, may be garnered through quenching experiments. Figure 3.9 illustrates this concept. In part (a), irradiation promoted the

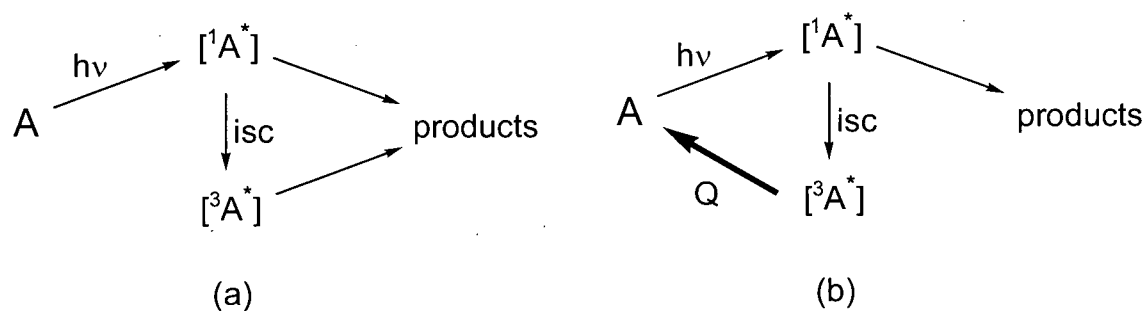


Figure 3.9 Excited state reactivity of aliphatic ketones (a) in the absence and (b) in the presence of a triplet quencher.

ground state molecule A to its singlet excited state. Ignoring decay process which return $^1A^*$ back to the ground state, this species may react to give products, or undergo intersystem crossing (isc) to the lower energy triplet excited state ($^3A^*$). Reaction to product can proceed *via* this species also. Certain chemical species, dubbed quenchers, are able to deactivate triplet excited species through energy transfer. For this to occur, the quencher's triplet energy must be lower than that of the species being quenched (i.e, the energy transfer must be exothermic). If the concentration of quencher is sufficient, reaction from the triplet excited state is completely suppressed, and quantum yields determined under these conditions will reflect reactivity along the singlet manifold only (Figure 3.9.b).

Table 3.4 Quantum yield^a determinations for aminoketone **14**.

Solvent	Cyclobutanols		Φ_{cleavage}	Φ_{total}
	Φ_{cis}	Φ_{trans}		
benzene	0.105 ± 0.009	0.048 ± 0.003	0.057 ± 0.004	0.210 ± 0.016
<i>tert</i> -butanol	0.218 ± 0.003	0.120 ± 0.003	0.097 ± 0.003	0.435 ± 0.009
Φ_{singlet}	0.0241 ± 0.014	0.0046 ± 0.010	0.0143 ± 0.007	0.043 ± 0.012

^aReported \pm the estimated standard deviation.

For aryl ketones, such as those described in Chapter 2 of this thesis, inter-system crossing is an efficient process and type II photochemistry proceeds exclusively through triplet excited states. For aliphatic ketones, however, isc is much less efficient, and both singlet and triplet pathways contribute to product formation. Quenching studies were undertaken with aminoketone **14** in benzene, using 2,5-dimethyl-2,4-hexadiene as the triplet energy acceptor (quencher). The results of these experiments are summarized under the heading Φ_{singlet} in Table 3.4. Comparing this number to Φ_{benzene} , which represents both singlet and triplet contributions to the quantum yield, 20% of products arise from the singlet excited state. Direct participation of the singlet excited state in type II product formation is known to be a minor process;⁸⁷ for cyclododecanone it accounts for only 5% of product formation in cyclohexane.^{81d}

3.3 Identification of the Photoproducts

Because the photochemical reactions of the aminoketones involve rearrangements that produce mixtures of structural isomers and diastereomers (i.e., the *cis*- and *trans*-cyclobutanols), not only did isolation of the pure compounds prove challenging, but also assignment of their correct structure and stereochemistry. The presence of many unfunctionalized methylene carbons and relative lack of heteroatoms and elements of unsaturation unfortunately meant that most of the ^1H NMR signals appeared as overlapping multiplets in the aliphatic region (δ 1.0 – 2.5 ppm), and hence were not of much use in structure elucidation. Figure 3.11 depicts the ^1H NMR spectra of cyclobutanols **124** (*cis*) and **125** (*trans*), photoproducts of the sixteen-membered aminoketone **16**. Secondary photolysis of the cleavage products **123** and **126** also hampered its isolation and characterization. Although all spectra and analyses of the isolated products were completely in accord with the assigned structures, they could not unambiguously confirm the atomic connectivity. To help resolve this issue the cleavage and reduction products were independently synthesized, while the cyclobutanol physical and spectral information was compared to data from analogous compounds.

3.3.1 Independent Synthesis of Reduced Product **119**

The structure of photoproduct **119** was readily confirmed by borohydride reduction of aminoketone **12** in ethanol (Figure 3.10).

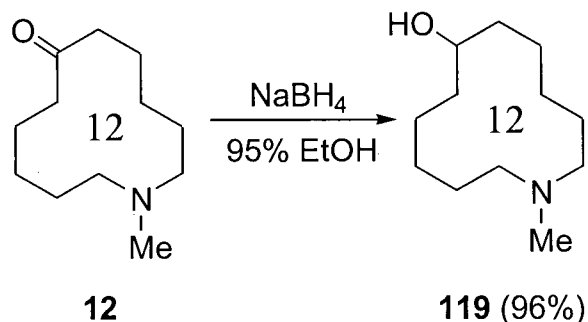


Figure 3.10 Preparation of aminoalcohol **119**.

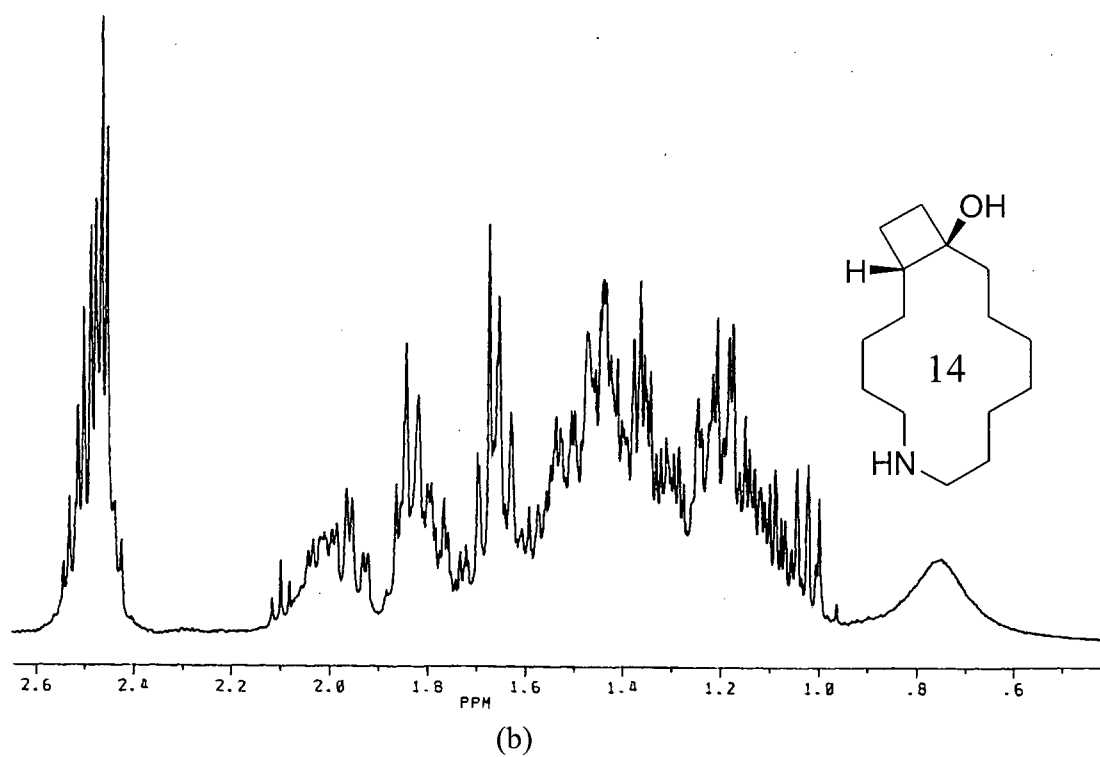
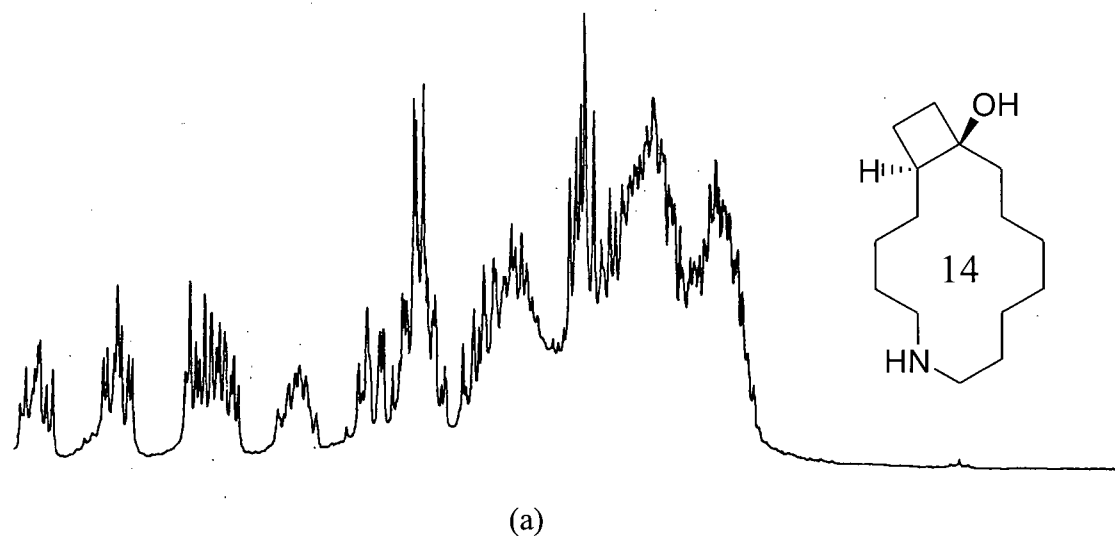


Figure 3.11 400 MHz ^1H NMR spectra (C_6D_6) of (a) *trans*-cyclobutanol **125**, and (b) *cis*-cyclobutanol **124**.

3.3.2 Synthesis of the Type II Cleavage Products 123 and 126

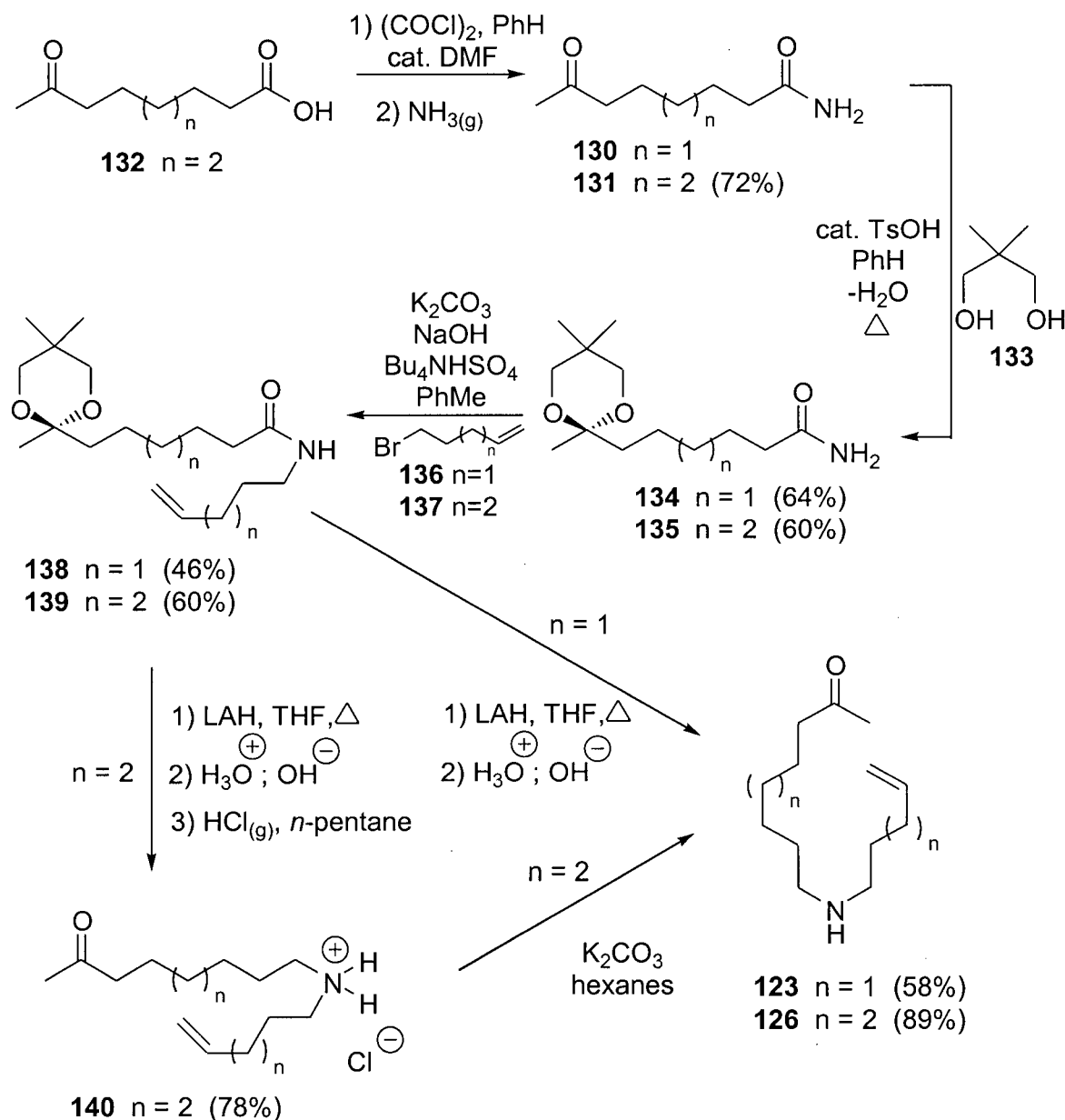


Figure 3.12 Independent preparation of cleavage products 123 and 126.

Figure 3.12 outlines the synthetic scheme employed for the preparation of the aminoketone cleavage products **123** (produced from the fourteen-membered ring) and **126** (from photolysis of the sixteen-membered ring). While oxoamide **130** was commercially available (Aldrich), the nine carbon homologue **131** was synthesized from

the corresponding acid **132** via its acid chloride. The carbonyl groups were protected by reaction with neopentyl glycol (**133**) to give the corresponding cyclic ketals (**134** or **135**). Alkylation of the amide nitrogen atoms was effected using a solid-liquid phase-transfer protocol developed by Gajda and Zwierzak⁸⁸ using either 5-bromo-1-pentene (**136**) or 6-bromo-1-hexene (**137**) as the alkylating agent. The secondary amide products (**138** or **139**) were subsequently reduced to their corresponding secondary amines with lithium aluminum hydride. An acidic workup was employed in order to remove the ketal protecting group. In the case of compound **123**, the amine was extracted from the reaction mixture after addition of alkali. The longer-chain homologue **126** was isolated and characterized first as its hydrochloride salt **140**; the free amine was subsequently liberated by reaction with potassium carbonate and characterized.

3.3.3 Preparation of the Secondary Photoproduct **129**

Since diene **129** was too volatile to be isolated from photolysis reaction mixtures of **14** or **123** (see Figure 3.7 above), it was synthesized independently (Figure 3.13) and its presence confirmed by identification of its ¹³C NMR signals in the crude photosylate

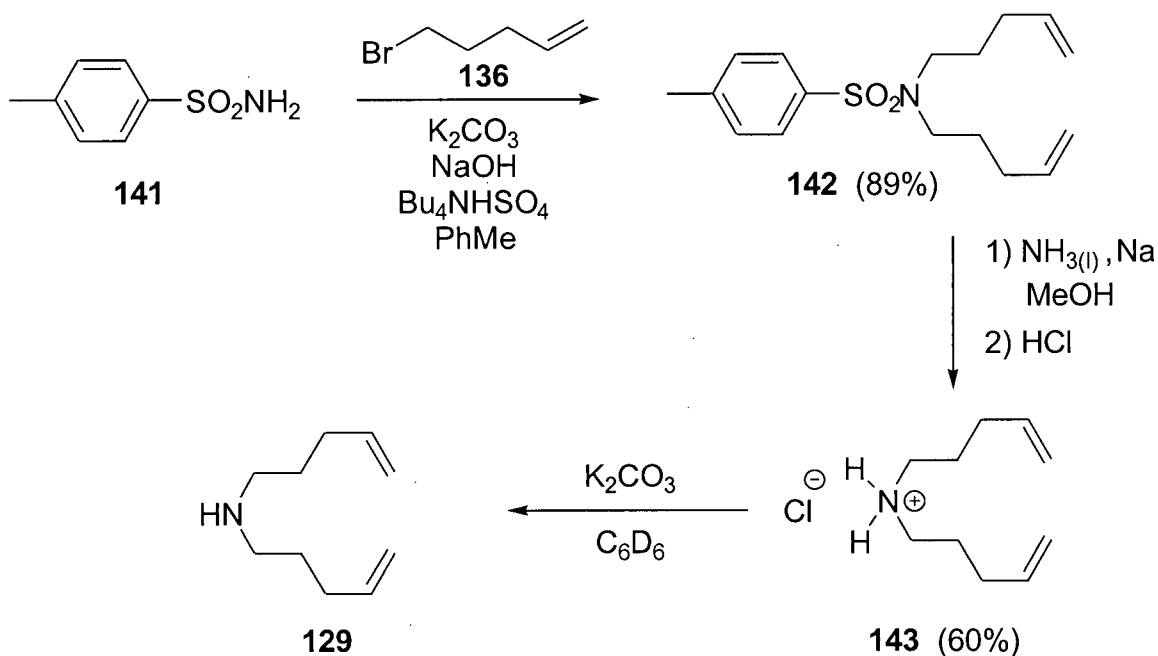


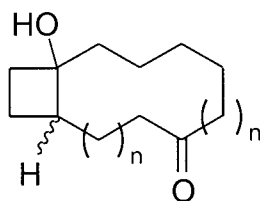
Figure 3.13 Synthetic scheme for amine **129**.

mixtures. Dialkylation of 4-toluenesulfonamide (**141**) with 5-bromo-1-pentene (**136**) gave the tertiary sulfonamide **142**. Reductive cleavage of the sulfonyl group with sodium in liquid ammonia, followed by reaction with hydrogen chloride, afforded ammonium salt **143**. The free amine, **129**, was liberated *in situ* by reaction with a suspension of potassium carbonate in benzene-*d*₆. NMR analysis was then performed.

3.3.4 Stereochemical Assignment of the Cyclobutanol Photoproducts

Assignment of the relative stereochemistry of the *cis/trans* cyclobutanol pairs was based on a number of observations. By analogy with the known reactivity of medium-sized and large-ring cycloalkanones (ring sizes 11 to 16, see Table 3.1) for which the cyclobutanols with a *cis* ring fusion were formed preferentially, the predominant cyclobutanol in the solution state aminoketone photolyses was designated as the *cis* diastereomer (see Table 3.2). Additional support for this assignment comes from the empirical observation, reported independently in three different studies,^{81d,89,90} that among *cis/trans* cyclobutanol pairs, the *trans* isomer is eluted first during gas chromatography on a poly(siloxane) column (26 pairs in total). The behaviour of the cyclobutanols studied herein are consistent with this observation.

More compelling evidence for the stereochemical assignments presented here comes from analysis of the cyclobutanol ¹³C NMR spectra in benzene-*d*₆. Specifically, in the series of compounds **144** studied by Scheffer and Lewis,^{90,91} the chemical shifts of the bridgehead methine carbons were consistently found to occur ca. 6-9 ppm further downfield in the *cis*-fused systems (Table 3.5). Additionally, the chemical shift ranges for the *cis*- (48.6 to 50.1 ppm) and *trans*- (40.4 to 43.7 ppm) diastereomers are relatively small and do not overlap. The spectroscopic data from the aminocyclobutanols studied here fit well with this model (Table 3.6). A tentative explanation based on conformationally-dependent anisotropic shielding has been put forward to explain this phenomenon.⁹⁰

**144****Table 3.5** ^{13}C NMR chemical shifts (C_6D_6) for the methine carbon in cyclobutanols **144**.

n	<i>cis</i> - 144 δ (ppm)	<i>trans</i> - 144 δ (ppm)	$\Delta\delta$ (ppm)
1	48.6 ^a	—	—
2	49.2	40.4	8.8
3	49.8	41.6 ^a	8.2
4	—	42.2	—
5	50.1	43.1	7.0
6	49.5	43.4	6.1
7	50.1	43.5	6.6
8	50.1	43.7	6.4

^aStructures confirmed by X-ray crystallography.**Table 3.6** ^{13}C NMR chemical shifts (C_6D_6) for the methine^a carbons in aminocyclobutanols produced on photolysis of the aminoketones of ring size N.

N	<i>cis</i> δ (ppm)	<i>trans</i> δ (ppm)	$\Delta\delta$ (ppm)
12	51.2	43.3	7.9
14	50.1	43.1	7.0
16	50.0	43.7	6.3

^aSignal assignments confirmed with either the DEPT or APT pulse programs.

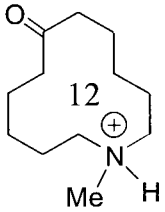

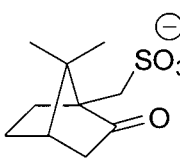
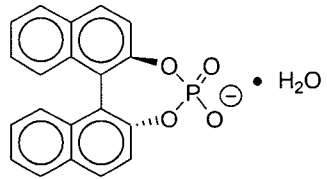
3.4 Preparation of Optically Active Salts of the Macrocyclic Aminoketones

Optically active salts of the macrocyclic aminoketones were generally prepared by reacting equimolar amounts of the amine, as a solution in ether, and the commercially obtained optically active acid dissolved in an appropriate solvent. In cases where the salt precipitated on mixing, the solids were filtered, dried, and subsequently recrystallized. When no spontaneous crystallization occurred, the solvent was removed *in vacuo*, and the residual solid or oil recrystallized. The most effective recrystallization method for these salts was found to be vapour diffusion of petroleum ether or *n*-pentane into a chloroform solution of the salt. This was generally achieved by placing a vial with the chloroform solution in a sealed Erlenmeyer flask containing a reservoir of the hydrocarbon solvent. Crystallization was achieved over a period of days to weeks. The composition and stoichiometry of the organic salts were unambiguously determined by ^1H NMR spectroscopy and elemental analysis. Solvent or water of crystallization, where present, could also be detected through these procedures.

Although salt formation *via* reaction of the aminoketones with a large number of optically active acids (**12**: 18; **14**: 22; **16**: 25) was conducted, the fraction of attempts that produced crystalline salts was low. In many of the failed attempts, the salt would 'oil out' of solution during recrystallization (common), or crystallization of the free acid would occur, leaving the amine in solution (rare). The frequency of these failures suggests that the problem is intrinsic to the macrocycles; however, the origin of this phenomenon (e.g. hygroscopicity, effective solvent entrainment, effects due to conformational lability, etc.) is not understood. The fact that the fourteen-membered macrocycle exhibited the greatest success in salt formation is also puzzling, and rules out simple explanations for this behaviour based on melting point or substitution at nitrogen (i.e. secondary versus tertiary amines) for the free amines.

The identity and melting points of the optically active salts are detailed in Tables 3.7 (**12**), 3.8 (**14**), and 3.9 (**16**). Some achiral salts prepared from the aminoketones are described in Table 3.10. Salt crystals suitable for X-ray crystallographic analysis were obtained for four compounds, including one derived from each of the twelve-, fourteen-, and sixteen-membered macrocycles.

Table 3.7 Optically active salts prepared from aminoketone **12**.

 12			
Salt	Anion	Recrystallization Solvent	mp (°C)
145		CHCl ₃ / pet. ether	78-80
146		CHCl ₃ / pet. ether	78-80
147^a		MeOH / water	154-157

^aX-ray crystal structure obtained.**Table 3.8** Optically active salts prepared from aminoketone **14**.

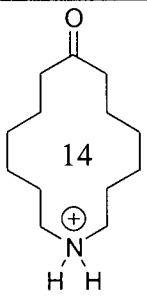
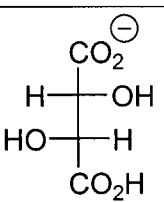
 14			
Salt	Anion	Recrystallization Solvent	mp (°C)
148^a		CHCl ₃ / pet. ether	139-140

Table 3.8 continued

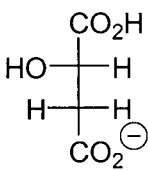
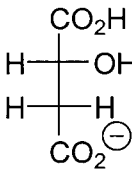
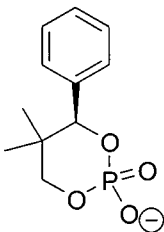
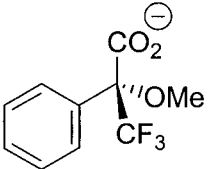
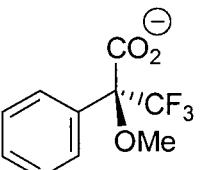
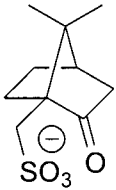
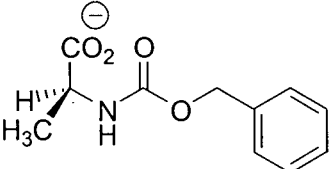
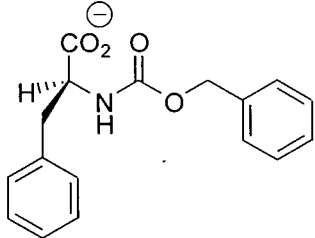
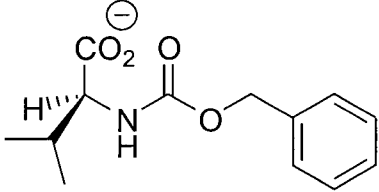
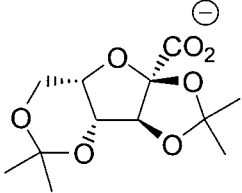
Salt	Anion	Recrystallization Solvent	mp (°C)
149 ^a		CHCl ₃ / pet. ether	117-120
150		CHCl ₃ / pet. ether	117-120
151		MeOH	207-210
152 ^b		CHCl ₃ / pet. ether	132
153		CHCl ₃ / pet. ether	132
154		CHCl ₃ / pet. ether	166-167
155		CHCl ₃ / pet. ether	103-104

Table 3.8 continued

Salt	Anion	Recrystallization Solvent	mp (°C)
156		CHCl ₃ / pet. ether	142-143
157		CHCl ₃ / pet. ether	130-131
158		CHCl ₃ / pet. ether	189-191 (dec.)

^aX-ray crystal structure obtained. ^bPartial crystallographic analysis performed (*vide infra*).

Table 3.9 Optically active salts prepared from aminoketone 16.

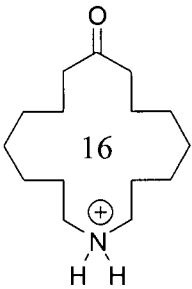
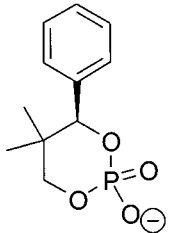
			
Salt	Anion	Recrystallization Solvent	mp (°C)
159		CHCl ₃ / <i>n</i> -pentane	235-240 (dec.)

Table 3.9 continued

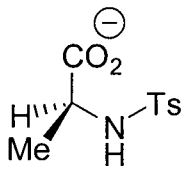
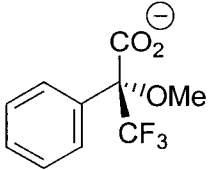
Salt	Anion	Recrystallization Solvent	mp (°C)
160		CHCl ₃ / <i>n</i> -pentane	154-155
161		CHCl ₃ / <i>n</i> -pentane	155-156

Table 3.10 Additional salts prepared from the macocyclic aminoketones.

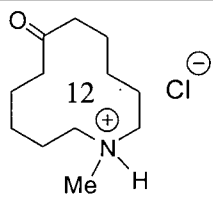
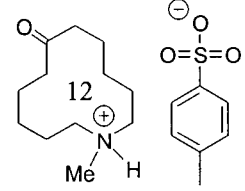
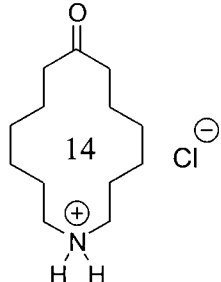
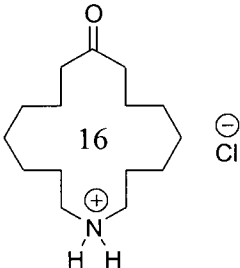
Salt	Structure	Recrystallization Solvent	mp (°C)
120		Et ₂ O / MeOH	182-183
162		EtOH / Et ₂ O	112-113
127		Et ₂ O / MeOH	179-180

Table 3.10 continued

Salt	Structure	Recrystallization Solvent	mp (°C)
128^a	 <p>Chemical structure of compound 16, a 16-membered ring containing a ketone group and a secondary ammonium group, shown as a salt with a chloride counterion.</p>	MeCN	200-202 (dec.)

^aX-ray crystal structure obtained.

3.5 Photochemistry of the Optically Active Salts

Because the products derived from Type II cleavage are achiral, they are of no value in assessing the extent of asymmetric induction in the photoreactions of the optically active salts. The cyclobutanol photoproducts, however, are chiral, and measurement of their enantiomeric excess was used to gauge the efficiency of asymmetric induction. Enantiomeric excesses were measured by chiral GC following photolysis of the salt and basic workup to remove the chiral auxiliary and liberate the photoproducts as free amines. Resolution of the cyclobutanol enantiomers could be achieved for all but compounds **118** and **125**, the *trans*-cyclobutanol photoproducts of the twelve- and sixteen-membered aminoketones. A typical chromatogram for a chiral GC run is depicted in Figure 3.14. The starting material (**14**), cleavage product (**123**), and both enantiomers of the *cis*- and *trans*-cyclobutanols (**121** and **122** respectively) are cleanly resolved. In the case of compound **121**, enough enantiomerically enriched compound was isolated to allow the sign of optical rotation to be determined; the peaks for **121** in Figure 3.14 are labelled to reflect these results. For all other ee determinations, the predominant enantiomer is designated as either the first or second enantiomer eluted from the GC.

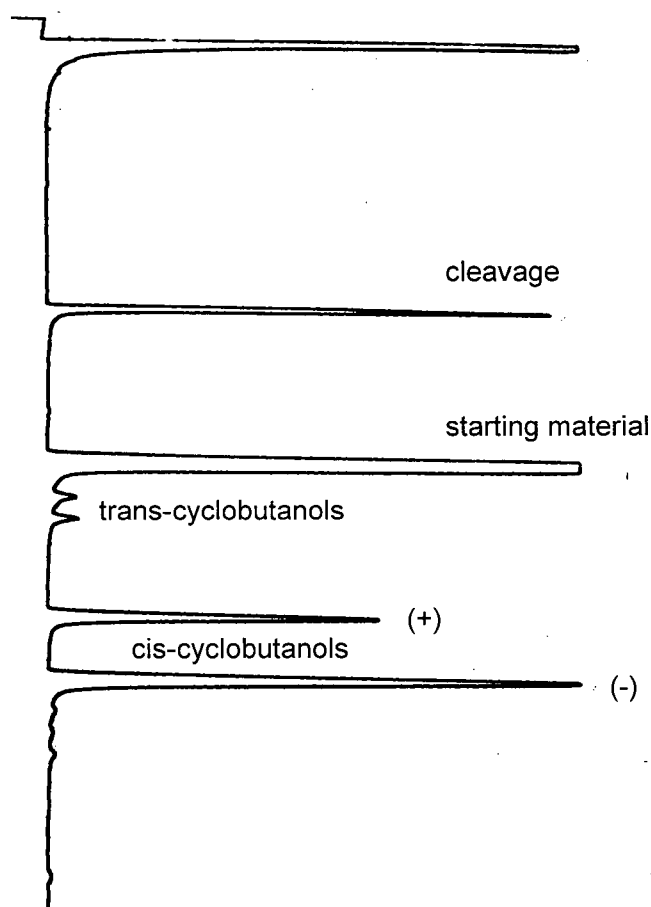


Figure 3.14 Chiral GC trace showing the separation of starting material (**14**) and products.

3.5.1 Solution State Photolyses of the Optically Active Salts

In previous studies using ionic chiral auxiliaries, asymmetric induction was observed only in the solid state photolyses. In the solution state, the optically active ions had no effect in directing the steric course of the photoreaction. The same holds true in the present instance. A number of the optically active salts were photolysed in acetonitrile solution and their photoproducts subsequently analyzed by chiral GC. All chiral products were produced as racemic mixtures. The product ratios are also essentially anion-independent, a further indication that, in solution, the anisotropy of the chiral ion has no effect on reaction selectivity. The results of these experiments are presented in Table 3.11. Refer to Table 3.2 for solution state photolysis data for the free amines and their hydrochloride salts.

Table 3.11 Solution state photolyses of some optically active aminoketone salts.

Salt ^d	Cyclobutanol ^f (%)		Cleavage (%)
	<i>cis</i>	<i>trans</i>	
145 ^a	65	35 ^g	—
148 ^b	51	25	24
141 ^b	43	29	29
151 ^{b,c}	45	31	24
161 ^c	32	25 ^g	43
159 ^c	26	28 ^g	44

^aTwelve-membered macrocycle. ^bFourteen-membered macrocycle. ^cSixteen-membered macrocycle.

^dPhotolyses conducted in MeCN with Pyrex-filtered light. Conversions kept below 10% to minimize secondary reactions. ^eWater added to effect salt dissolution. ^fMeasured enantiomeric excesses were nil within error limits. ^gEe determination not available for this compound (see text).

3.5.2 Solid State Photolyses of the Optically Active Salts

Irradiation of the salts in the solid state leads to the expected asymmetric induction and enhanced photoproduct selectivity. The most striking results are those involving the fourteen-membered macrocycle (Table 3.12). On examination of the data a general trend is immediately apparent: while solution state irradiation leads to a *cis:trans* cyclobutanol ratio of approximately 2:1, little or none of the *trans*-isomer is produced when the salts are photolyzed in the crystalline state. Enantiomeric excesses for the *cis*-cyclobutanol in the solid state range from excellent (**148**, **141**, **150**) to negligible (**156**). Particularly impressive is the formation of *cis*-cyclobutanol **121** in 81.9% ee from salt **151** at 69% conversion. As expected, irradiation of enantiomeric salts (e.g., **141** and **150**, **152** and **153**) gives rise to enantiomeric cyclobutanols of similar ee. This result demonstrates that the reacting systems are well-behaved, and can provide access to either product enantiomer with a simple substitution of the ionic chiral auxiliary. The dramatic change in reactivity exhibited on switching from *solution* to *solid state* photolysis highlights the importance of conformational rigidity in controlling the course of the reaction.

The crystalline state photochemistry of the enantiomeric salts **145** and **146**, derived from the twelve-membered macrocycle, display a marked improvement in

cis:trans selectivity in the solid state versus solution (Table 3.13). The enantioselectivity of *cis*-cyclobutanol formation is, however, mediocre, and decreases rapidly with increasing conversion. This progressive decline in enantioselectivity is thought to result from the breakdown of the ordered crystal lattice as photoproducts replace starting material. The rate of this decline varies widely among the salts studied and is an important factor, along with ee, that must be considered when evaluating the synthetic utility of these reactions.

The crystalline state photochemistry of salts **161**, **160**, and **159**, all derived from the sixteen-membered aminoketone, show poor reaction selectivity in the solid state (Table 3.14). All three photoproducts are produced in significant quantities, while the observed ees for the *cis*-cyclobutanol are low.

Although, as indicated in Chapter 1, the ability to predict crystals structures and hence design solid state asymmetric reactions *a priori* is not currently available, the ionic auxiliary method for asymmetric induction seems well-suited to a combinatorial approach to chiral auxiliary selection. Since only a small quantity of salt is required to test the efficacy of a particular ionic auxiliary, and synthesis of the salts is, in principle, a trivial matter, rapid screening should be possible. In addition, photolysis of the test samples in parallel, with subsequent chiral GC (or HPLC) analysis, would allow identification of promising candidate auxiliaries with minimal consumption of starting material. Although X-ray quality crystals are required in order to analyze the steric course of the reaction, they are *not* necessary for synthetic purposes. Salt **151** (Table 3.12) exemplifies this fact: although it crystallizes as fine needles which are too small to mount for X-ray crystallographic analysis, it produces product with high enantioselectivity in the solid state.

Table 3.12 Solid state photolysis of optically active salts of aminoketone 14.

Salt	Acid	% Conversion	% Yield ^a			% ee ^b	α^c
			121	122	123		
148	(2 <i>R</i> , 3 <i>R</i>)-tartaric acid	3	3	0	0	41.4	-
		5	5	0	0	42.9	
		7	7	0	0	44.6	
		13	13	0	0	44.3	
		24	24	0	0	43.8	
149	(S)-malic acid	10	5	0	4	> 98	-
		20	9	0	11	95.3	
		31	13	0	18	92.9	
		50	20	1	29	85.5	
		60	24	2	32	81.3	
150	(<i>R</i>)-malic acid	11	6	0	5	> 98	+
151	(<i>R</i>)-2-hydroxy-5,5-dimethyl-4-phenyl-1,3,2-dioxaphosphorinane-2-oxide	6	6	0	trace	> 98	-
		21	17	0	4	> 98	
		30	23	0	7	96.0	
		53	35	0	18	88.7	
		69	45	0	24	81.9	
152	(<i>R</i>)-Mosher's acid	5	5	0	0	20.9	+
		9	9	0	trace	18.7	
153	(S)-Mosher's acid	11	9	trace	2	17.8	-
		25	20	1	4	11.4	
154	(1 <i>S</i>)-10-camphorsulphonic acid	4	4	0	trace	52.8	-
		12	10	0	2	44.7	
		24	18	1	5	35.1	
155	<i>N</i> -Cbz-L-alanine	6	6	0	trace	41.3	-
		15	12	1	2	37.8	
156	<i>N</i> -Cbz-L-phenylalanine	6	4	0	2	6.4	-
		22	13	1	8	2.4	
157	<i>N</i> -Cbz-L-valine	7	6	trace	1	32.6	+
		15	10	2	3	30.2	
158	2,3:4,6-di- <i>O</i> -isopropylidene-2-keto-L-gulonic acid	5	4	1	0	26.3	+
		28	16	5	7	5.5	

^aIrradiations conducted at -20°C on 5-10 mg samples of crushed crystals sandwiched between two Pyrex plates. Yields were determined by GC following basic workup. ^bEnantiomeric excesses reported for compound 121. ^cIndicates the sign of rotation of the predominant enantiomer of 121 at the sodium D-line.

Table 3.13 Solid state photolysis of optically active salts of aminoketone **12**.

Salt	Acid	% Conversion	% Yield ^a		% ee ^b	α^c
			117	118		
145	(1 <i>S</i>)-10-camphorsulphonic acid	15	11	3	24.7	1
		21	17	3	19.2	
146	(1 <i>R</i>)-10-camphorsulphonic acid	4	4	trace	47.0	2
		7	7	trace	36.8	
		12	10	2	29.4	
		25	21	4	15.0	
		27	20	4	15.2	

^aIrradiations (Corning glass #9720 filter employed) conducted at -20°C on 5-10 mg samples of crushed crystals sandwiched between two quartz plates. Yields were determined by GC following basic workup.

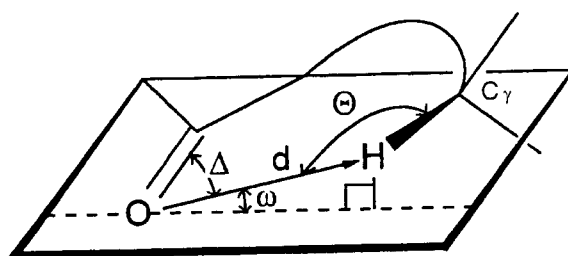
^bEnantiomeric excesses reported for compound **117**. ^cIndicates the order of elution of the predominant enantiomer of **117** from the chiral GC column.

Table 3.14 Solid state photolysis of optically active salts of aminoketone **16**.

Salt	Acid	% Conversion	% Yield ^a			% ee ^b	α^c
			124	125	126		
161	(R)-Mosher's acid	8	4	2	2	40.6	2
		27	18	9	5	41.3	
		47	24	10	13	39.0	
160	<i>N</i> -tosyl-L-alanine	10	3	3	4	16.3	2
		23	6	5	12	15.5	
		41	9	4	28	6.4	
159	(R)-2-hydroxy-5,5-dimethyl-4-phenyl-1,3,2-dioxaphosphorinane-2-oxide	8	5	2	1	27.9	1
		22	9	7	6	24.9	
		29	7	6	16	25.2	

^aIrradiations conducted at -20°C on 5-10 mg samples of crushed crystals sandwiched between two Pyrex plates. Yields were determined by GC following basic workup. ^bEnantiomeric excesses reported for compound **124**. ^cIndicates the order of elution of the predominant enantiomer of **124** from the chiral GC column.

3.6 Solid State Structure-Reactivity Correlations

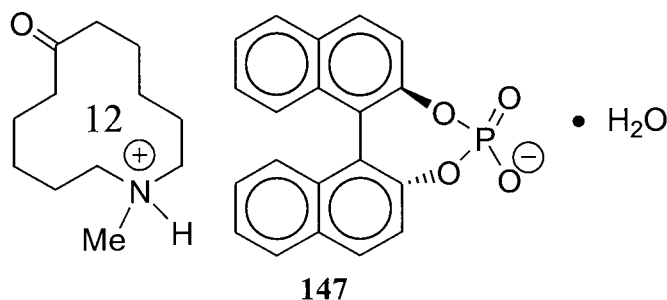


	d (Å)	ω (°)	θ (°)	Δ (°)
Ideal	< 2.72	0	180	90-120
Average	2.73 ± 0.03	52 ± 5	115 ± 2	83 ± 4

Figure 3.15 Ideal and crystallographically derived average (based on a series of aliphatic ketones)⁹¹ H_γ -abstraction geometries.

The four crystal structures that were obtained for various salts (**147**, **148**, **149**, and **128**) of the macrocyclic aminoketones were analyzed in light of their observed photoreactivity. The geometric parameters pertaining to γ -hydrogen abstraction are reviewed in Figure 3.15. It is important to keep in mind that, while the ground state geometry is useful as a model in predicting excited state reactivity, the distance and angular geometric parameters obtained from crystallographic studies do not necessarily reflect the geometry of the excited state species. For aliphatic ketones in particular, significant pyramidalization of the carbonyl carbon (22 - 45°) upon electronic excitation has been predicted by *ab initio* studies.⁹² While this effect is thought to play a minimal role in type II reactions of aromatic ketones,⁹³ such as those dealt with in Chapter 2 of this thesis, the ketones with which we are concerned here are aliphatic, and thus the notion of 'ideal' parameter values may be more relaxed. Since the theoretical studies were based on the situation in the solution state, it is unknown what effect the crowded crystalline environment may have in limiting pyramidalization.⁹⁴

3.6.1 Solid State Structure of Salt 147



Binaphthylphosphoric acid, a commercially available and widely applied resolving agent,⁹⁵ was one of only three optically active acids that formed a crystalline salt with aminoketone **12**. The X-ray crystal structure of the cation from this compound is shown in Figure 3.16. The abstraction parameters for the two inside γ -hydrogens (H_a : $d = 3.06 \text{ \AA}$, $\omega = 56^\circ$, $\Delta = 62^\circ$, $\theta = 121^\circ$; H_b : $d = 2.93 \text{ \AA}$, $\omega = 56^\circ$, $\Delta = 72^\circ$, $\theta = 110^\circ$), reveal that, although the d values are larger than usual, abstraction of H_b may be stereoelectronically possible. This salt did not react on irradiation in the solid state. This lack of observed reactivity may also be due to quenching of the ketone excited state by the naphthalene rings *via* energy transfer. Naphthalene is known to quench the triplet excited state of benzophenone efficiently,⁹⁶ and would thus be able to quench the higher-energy excited state of an aliphatic ketone.

In order to coerce the salt into reacting in the solid state, it was exposed to γ -radiation from a ^{60}Co source at total doses up to 30 Mrad.⁹⁷ This attempt failed, however, and the starting material was recovered unchanged. Although no conclusive structure-reactivity correlations can be drawn from this example, it does provide unequivocal proof of the structure of the twelve-membered macrocycle.

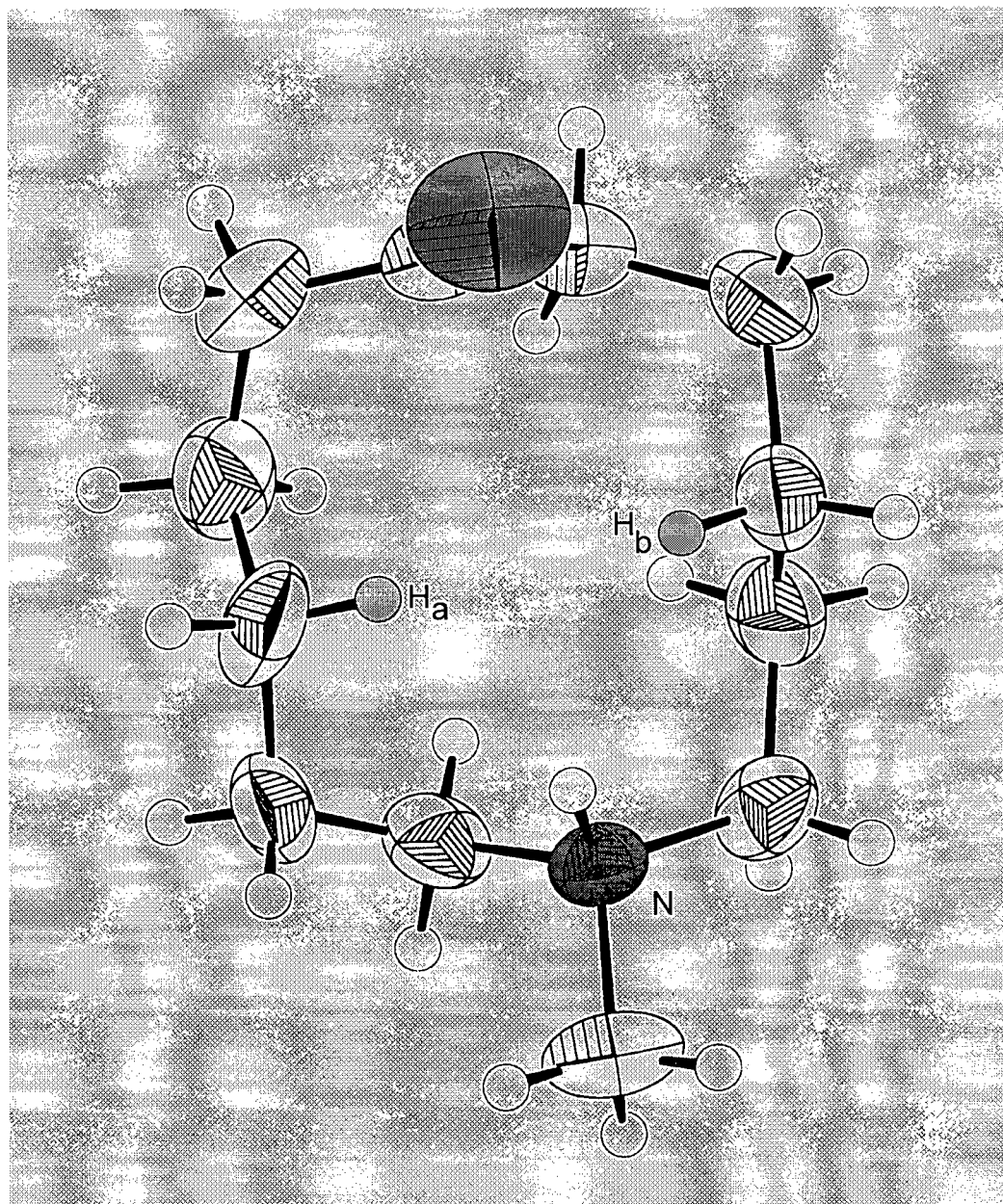


Figure 3.16 ORTEP representation of the macrocyclic cation in salt 147.

3.6.2 Solid State Structure of Salt 128

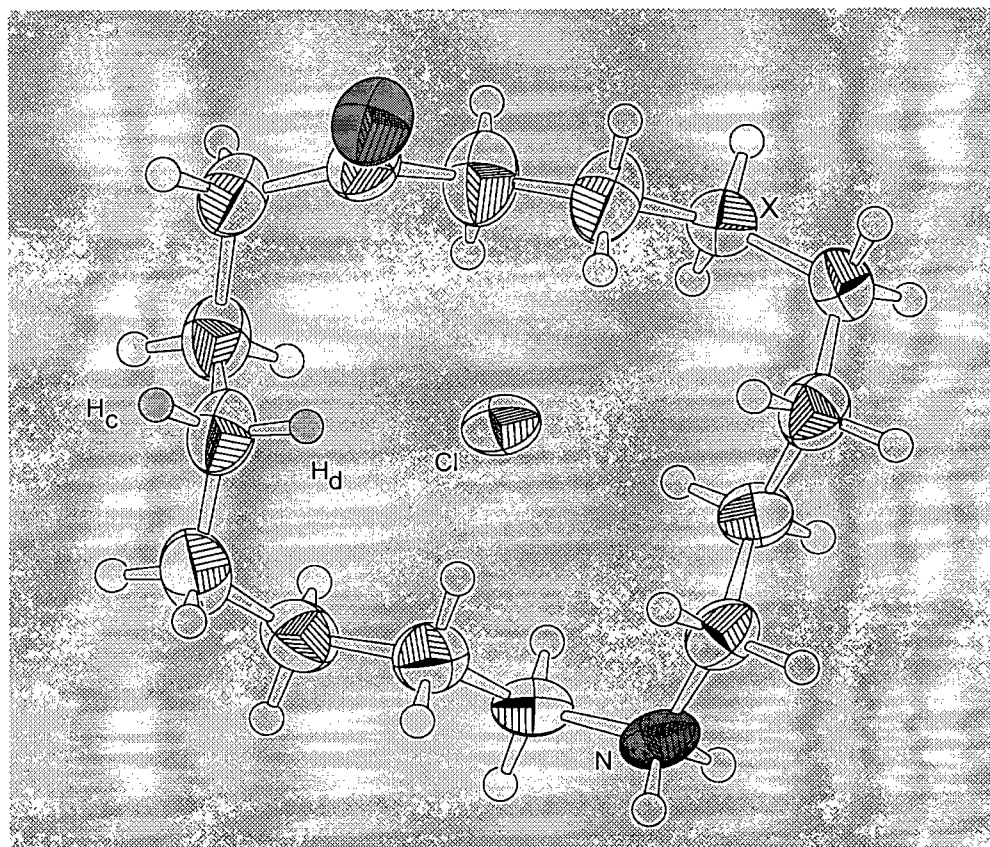


Figure 3.17 ORTEP representation of the macrocyclic cation in salt **128**.

The only salt of the sixteen-membered macrocycle that provided crystals suitable for X-ray analysis was the achiral hydrochloride salt **128**. Although it too failed to react in the solid state, analysis of the abstraction geometries for the closest two γ -hydrogen atoms shed light on its photostability. Figure 3.17 shows the macrocycle, as well as the chloride counterion. The two γ -hydrogen atoms located on the same side of the ring as the carbonyl group lie on the same carbon and possess the following abstraction parameters: H_c ($d = 3.59 \text{ \AA}$, $\omega = 41^\circ$, $\Delta = 67^\circ$, $\theta = 87^\circ$); H_d ($d = 3.26 \text{ \AA}$, $\omega = 55^\circ$, $\Delta = 58^\circ$, $\theta = 111^\circ$). The hydrogen atoms on the γ -carbon labelled X are both $>4 \text{ \AA}$ away from the carbonyl oxygen, and lie on the opposite side of the macrocycle. Both H_c and H_d lie well beyond the average d ($2.73 \pm 0.03 \text{ \AA}$) reported in Figure 3.15, and this would seem the most

likely explanation for the lack of observed solid state reactivity. The angular parameters for H_c abstraction also deviate significantly from previously determined values.

3.6.3 Structure-Reactivity Relationships for Salts of the Fourteen-Membered Aminoketone

Three salts of aminoketone **14** provided crystals that were suitable for X-ray crystallographic analysis. In the case of salt **152** (derived from **14** and (*R*)-Mosher's acid), the space group and unit cell data could be determined (*P*1; $a = 11.273(1)$ Å, $b = 12.758(2)$ Å, $c = 9.4415(8)$ Å; $\alpha = 93.14(1)^\circ$, $\beta = 102.28(1)^\circ$, $\gamma = 65.50(1)^\circ$; $Z = 2$), however the macrocycles were found to be extremely disordered and could not be refined satisfactorily. This disorder is reflected in low ee (ca. 20%, see Table 3.12) observed after solid state photolysis of this salt, even to low conversions. This example raises an interesting point concerning the application of structure-reactivity analysis in conjunction with the ionic chiral auxiliary method: in previous studies, X-ray quality crystals could be grown almost exclusively for salts which demonstrated high enantioselectivities. Those salts which showed poor asymmetric induction generally do not form crystals suitable for crystallographic structure determination. As a result, the reactivity of highly selective solid state processes has been well studied, while structural and mechanistic information relating to crystals that display poor enantioselectivity is scarce. With crystal structures of both the (*S*)-malate salt **149**, which gives rise to very high product ee, and the (2*R*, 2*R*)-tartrate salt **148**, for which only moderate (ca. 44% ee) enantioselectivity results, we are able to contrast and compare cases in which both high and low selectivities in the photochemistry of aminoketone **14** arise.

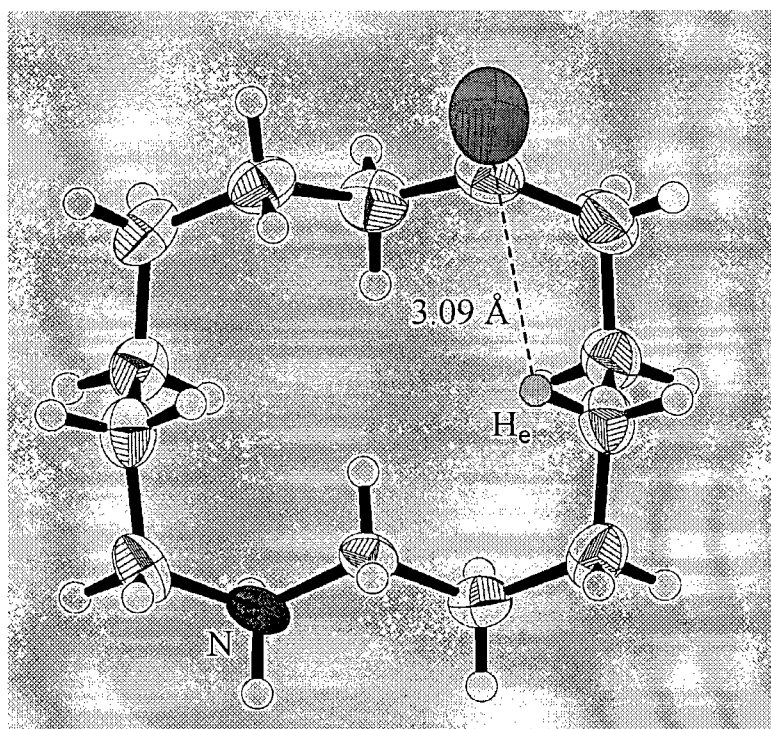


Figure 3.18 ORTEP representation of the macrocycle in salt **149**.

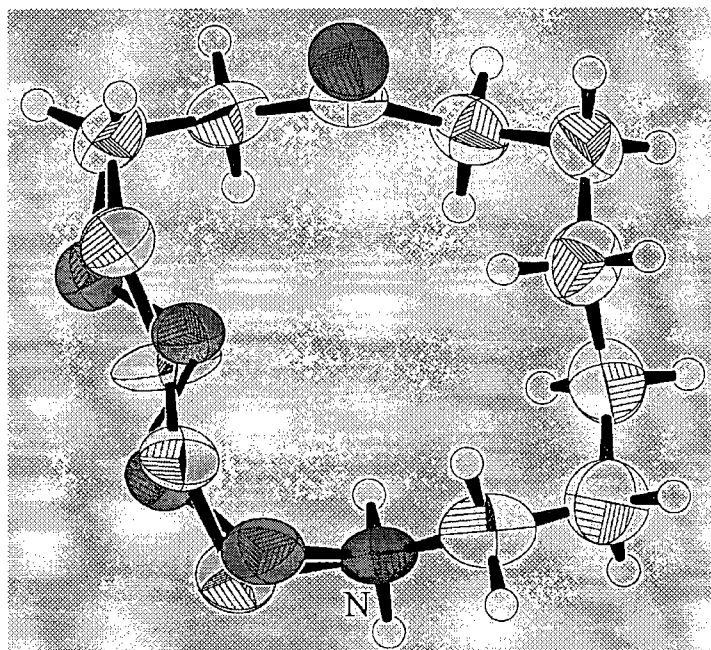
Figure 3.18 shows the solid state conformation of the macrocycle in salt **149**. Since the absolute configuration of the counterion is known, the absolute configuration of the reacting macrocycle can be assigned unequivocally. The X-ray structure clearly shows the carbonyl group poised to abstract only *one* γ -hydrogen (H_e), the others being too far away ($> 4 \text{ \AA}$) and/or unfavourably oriented. At 3.09 \AA , the $C=O \cdots H_e$ distance is the longest measured to date for an aliphatic ketone.⁹⁴ The angular parameters for H_e are: $\omega = 56^\circ$, $\Delta = 60^\circ$, $\theta = 117^\circ$; ω and θ are within the range of average values reported in Figure 3.15, while Δ is 23° lower than the average value of 83° . The fact that d and Δ deviate significantly from typical values may suggest that some change in geometry is occurring on ketone excitation.

The biradical formed on abstraction of H_e has a pre-*cis* geometry (C-OH and C_γ -H bonds in a *syn* relationship), such that topochemically controlled, least motion cyclization leads to (-)-*cis*-cyclobutanol **121**. The configuration of the intermediate biradical is such that the (-)-*cis*-cyclobutanol **121** should possess the (1*S*, 12*S*) stereochemistry. Thus, the

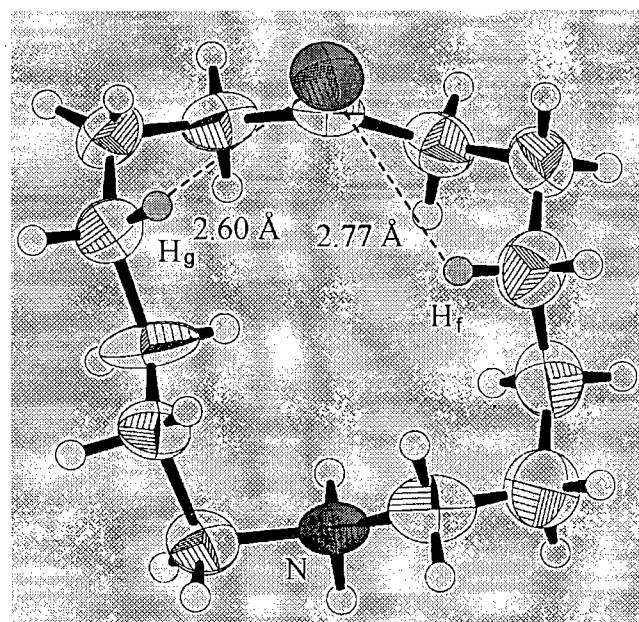
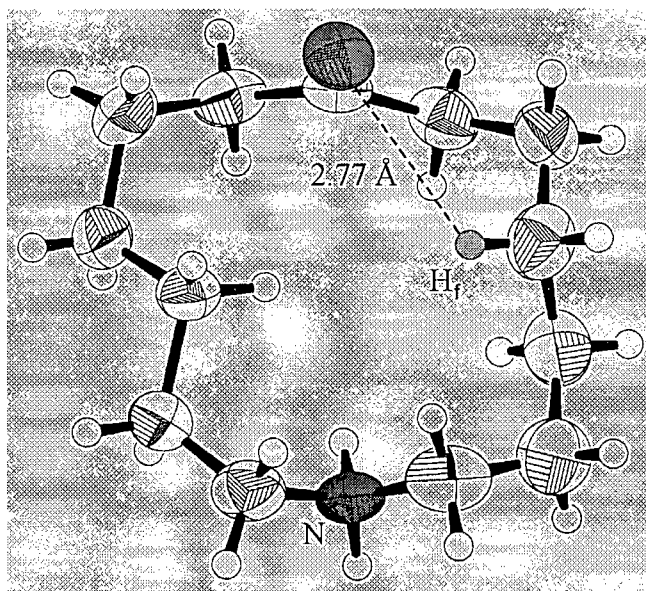
high enantioselectivity of the reaction is governed by the abstraction of only one of two enantiotopic γ -hydrogens, while the product *cis/trans* diastereoselectivity arises from the fixed conformation of the intermediate biradical.

In the solid state photochemistry of salt **148**, the moderate ee of cyclobutanol **121** (ca. 44% in favour of the (-)-enantiomer) must be rationalized. Analysis of the X-ray data revealed disorder in the macrocycle. Two conformations were found (occupancy ratio 72:28), which differ only in the placement of four methylene groups. Figure 3.19.a shows the superposition of the two conformers. The atoms coloured purple belong to the major conformer, while those in yellow are part of the minor conformer. The major conformer contains only one abstractable γ -hydrogen (Figure 3.19.b; H_f : $d = 2.77 \text{ \AA}$, $\omega = 49^\circ$, $\Delta = 82^\circ$, $\theta = 114^\circ$), and the absolute configuration of the ring is similar to that of **149**, such that formation of the (-)-enantiomer of cyclobutanol **121** is expected from reaction at this site. For the minor solid state conformer (Figure 3.19.c), however, the stereoelectronically favoured γ -hydrogen is H_g ($d = 2.60 \text{ \AA}$, $\omega = 47^\circ$, $\Delta = 95^\circ$, $\theta = 113^\circ$), which predicts formation of the (+)-enantiomer of cyclobutanol **121**. It is tempting, therefore, to equate the 44% enantiomeric excess favouring (-)-**121** with the $72\% - 28\% = 44\%$ difference in conformer population, and this seems to be the most straightforward explanation of the reduced stereochemistry in this case. Complete discrimination in the type II abstraction of the nearer of two γ -hydrogen atoms whose d values differ by 0.27 \AA has previously been observed.⁹¹

The explanation put forward above requires that the two conformers react with equal quantum efficiencies, and that the minor conformer reacts exclusively by abstraction of H_g . An alternative scenario is one in which the 44% ee is the accidental result of the minor conformer reacting more efficiently (more favourable abstraction parameters) than the major one, but with less than 100% enantioselectivity. Regardless of the details, it is clear that competing reactions from independent conformers are responsible for the low ee.



(a)



(c)

Figure 3.19 ORTEP representations of the macrocycle in salt **148**: (a) major (purple) and minor (yellow) conformers superimposed; (b) major conformer; (c) minor conformer.

3.7 Summary

Application of the *ionic chiral auxiliary* approach to asymmetric synthesis has been extended to include enantioselective photochemical reactions of amines, employing acids as the chiral auxiliaries. High enantioselectivities were achieved for a number of the optically active salts on photolysis in the solid state. In addition, solid state structure-reactivity correlations have revealed the origin of both high and moderate stereoselectivities, data for the latter of which have been hard to come by. These studies have also hinted that disorder of the molecules in the crystalline state may play a large role in instances where low selectivities are observed. In terms of the geometric requirements for hydrogen abstraction in the solid state, the long d value of 3.09 Å observed in salt **149**, along with the shortest abstraction distance possible in the unreactive sixteen-membered salt **128** (3.26 Å), would seem to define an upper limit for d values in the Type II abstraction of aliphatic ketones.

Chapter 4 – Asymmetric Induction in the Solid State Photochemistry of Linearly Conjugated Benzocyclohexadienone Salts

4.1 Synthesis of the Photochemical Substrate 52

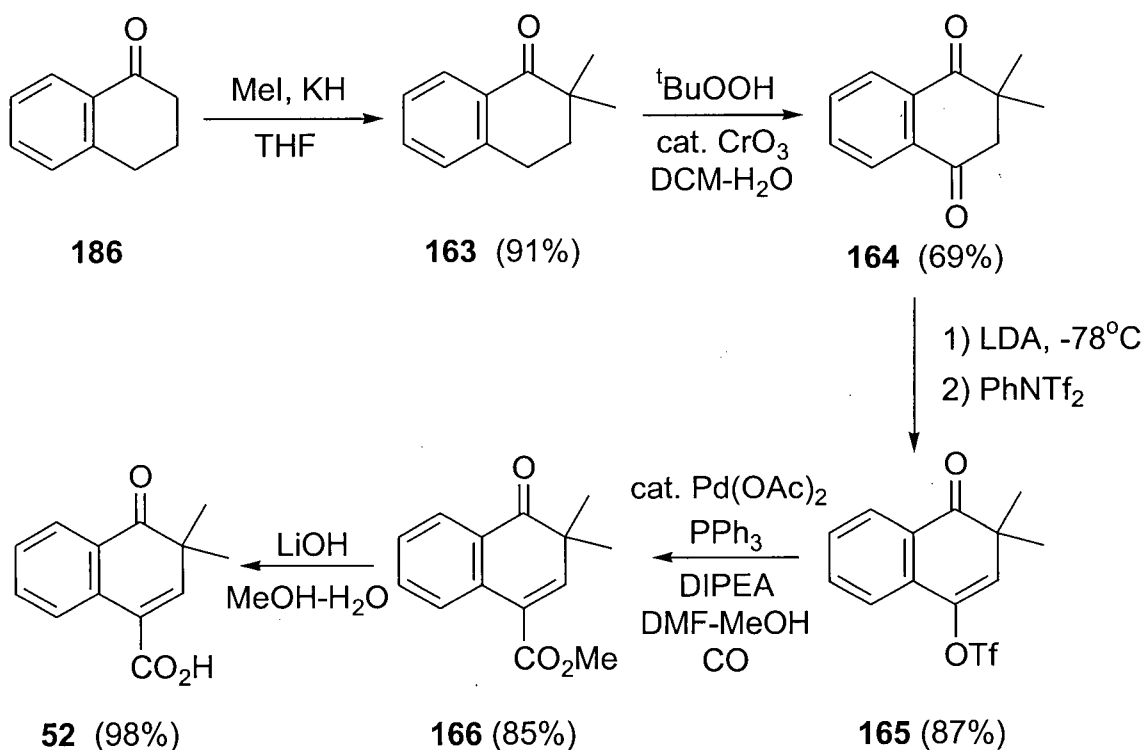


Figure 4.1 Synthetic scheme for the preparation of ketoacid **52**.

The previously unknown ketoacid **52** was prepared in five steps from 1-tetralone (**186**) in an overall yield of 45% (Figure 4.1). Dimethylation of ketone **186** with methyl iodide and potassium hydride furnished the substituted tetralone **163**. Employing a general procedure reported for the oxidation of benzylic methylene groups to the corresponding aromatic ketones,⁹⁸ compound **163** was oxidized with *tert*-butylhydroperoxide and catalytic chromium trioxide to dione **164**. Enolate formation followed by *O*-alkylation with *N*-phenyltrifluoromethanesulfonimide led smoothly to vinyl triflate **165**. Palladium(0)-catalyzed methoxycarbonylation⁹⁹ of this substrate

4.2 Photochemistry of Compounds 52 and 166

52 R = H
166 R = Me

53 R = H (87%)
167 R = Me (82%)

While this reaction is formally equivalent to the conversion of benzocyclohexadienone **70** to benzobicyclo[3.1.0]hexane **93** (discussed in section 2.4.2, Figure 2.30), it does not proceed *via* the $^1(n,\pi^*)$ excited state and thus does not involve a ketene intermediate (see section 1.6 for a detailed description of this reaction). Irradiation of **166** in the presence of a large excess of dimethylamine failed to produce any amide from the trapping of a transient ketene; only product **167** was isolated. This is consistent with reaction from the $^1(\pi,\pi^*)$ manifold, which most likely proceeds by way of the dipolar or diradical intermediate **168**.¹⁰⁰ Further evidence in support of the $^1(\pi,\pi^*)$ pathway comes from a comparison of the UV absorption spectra of compounds **70** and **166** (Figure 4.4). While the lowest energy absorption band for compound **70** corresponds to an (n,π^*) transition,¹⁰¹ in compound **166** this band is shifted to higher energy (shorter

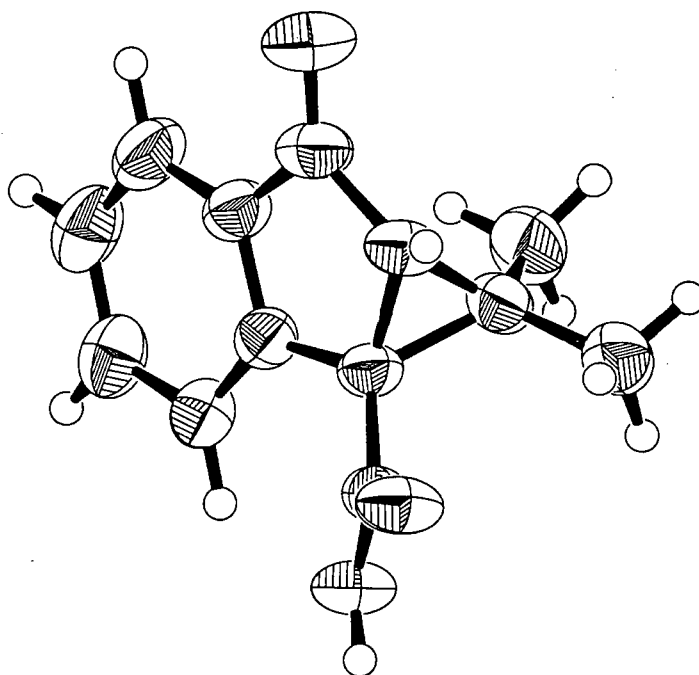


Figure 4.3 ORTEP representation of photoproduct 53.

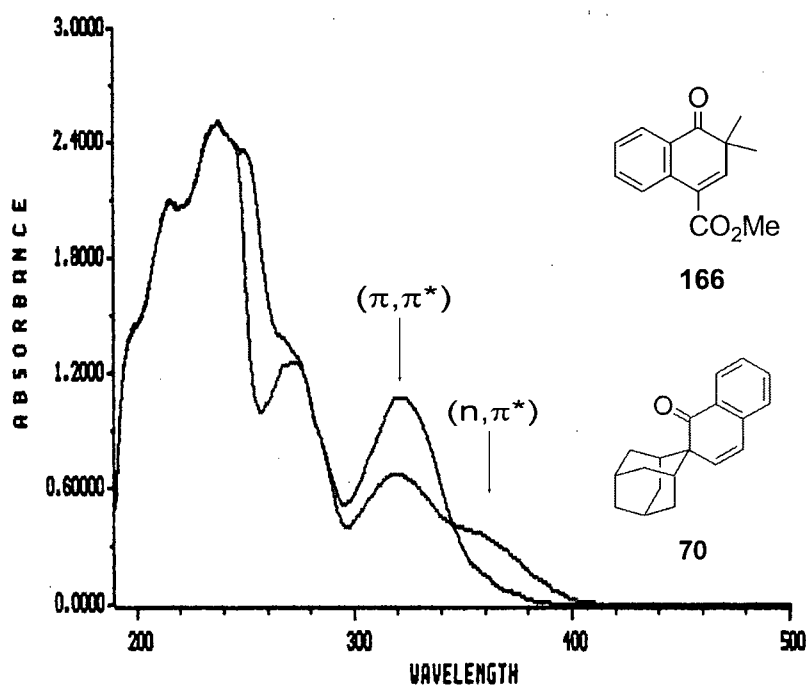
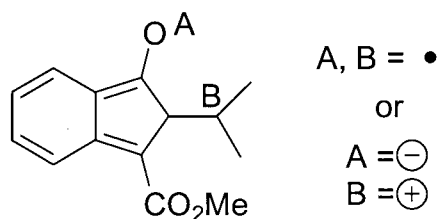


Figure 4.4 Absorption spectra for benzocyclohexadienones 70 and 166 in acetonitrile (5.0×10^{-4} M).

**168**

wavelength). Figure 4.5 illustrates the relative energies of the $^1(n,\pi^*)$ and $^1(\pi,\pi^*)$ excited states for the compounds in question, and indicates the difference in the nature of the reactive (lowest energy) excited state for each. An analogous reordering of excited states has been observed in the photochemistry of compound **169** (Figure 4.6).¹⁰⁰ In methylcyclohexane, the absorption spectrum of ketone **169** resembles that of ketone **70** (Figure 4.4, red line), and products derived from ketene intermediates are observed. When the solvent is 2,2,2-trifluoroethanol, the absorption spectrum of dienone **169** is similar to that of compound **166** (Figure 4.4, blue line). Photolysis in this medium results in compound **170**, and no ketene transient could be trapped or observed spectroscopically.¹⁰⁰ As has been noted for previously investigated cyclohexadienones,¹⁰² photolysis of **166** proceeded in the presence of the triplet quencher piperylene (2 M concentration), suggesting that reactions of this type occur from a singlet excited state.

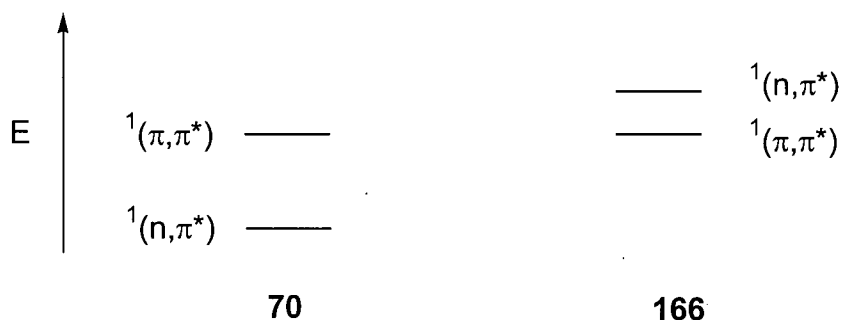


Figure 4.5 Relative ordering of excited states in compounds **70** and **166**.

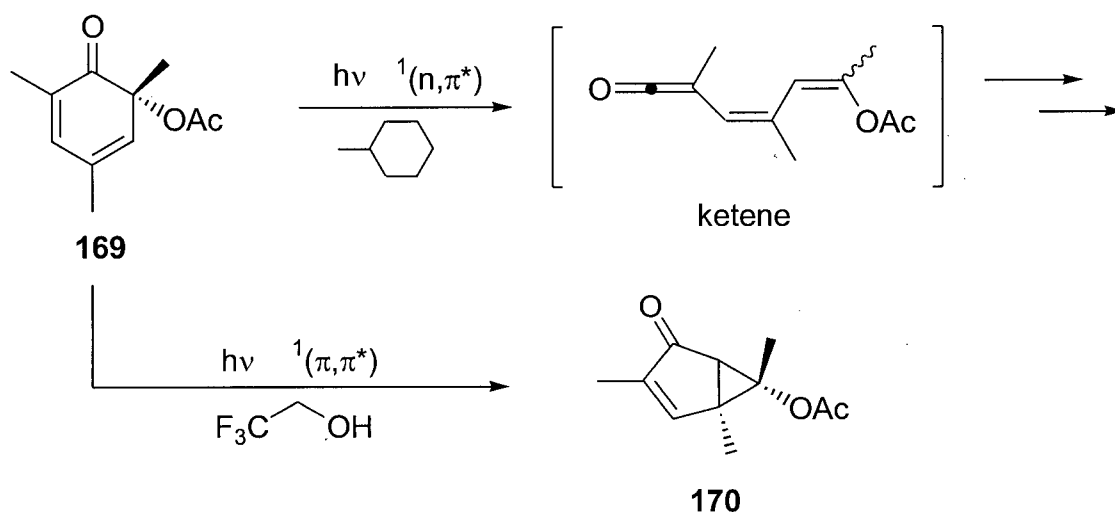


Figure 4.6 Solvent-induced reordering of excited states leads to different photochemical reactions for compound **169**.¹⁰⁰

4.3 Resolution of Ketoacid Photoproduct **53**

In order to map the absolute steric course of solid state reactions, it is necessary to know the absolute stereochemistry of both the crystalline starting material (salts of acid **52** in this case) and the resulting product (ketoacid **53**). Since the ionic chiral auxiliaries employed in these studies are of known absolute configuration, it remains only to assign the configuration of the stereogenic centres in the optically active photoproduct, i.e., to determine which enantiomer of **53** is produced in excess. To achieve this goal, a classical Pasteur resolution¹⁰³ of racemic carboxylic acid **53** was carried out, employing brucine as the resolving agent. A crop of the optically pure salt **171** was recovered in 30% yield, and subsequently recrystallized. X-ray crystallographic analysis of salt **171** revealed that the anion possessed the (1*aS*, 6*aR*)[¶] absolute configuration (Figure 4.7). Treatment of this optically pure salt with diazomethane provided the corresponding methyl ester, (1*aS*, 6*aR*)-**167**. Chiral GC analysis of this product then allowed the absolute configuration

[¶] The numbering scheme for compound **53** is based on its CAS name: 6,6a-dihydro-1,1-dimethyl-6-oxo-cycloprop[*a*]indene-1*a*(1*H*)-carboxylic acid.

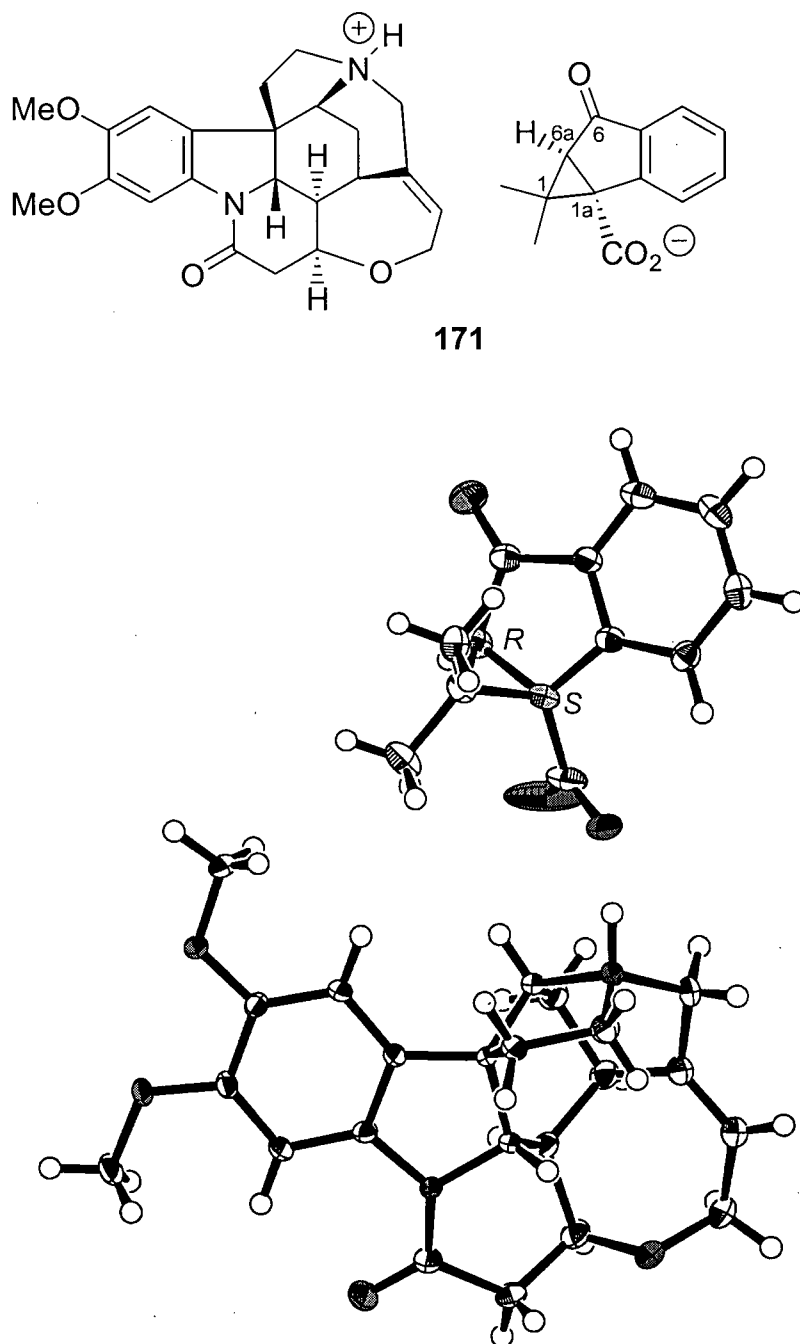


Figure 4.7 ORTEP representation of salt 171. Stereocentres of interest are shown in green.

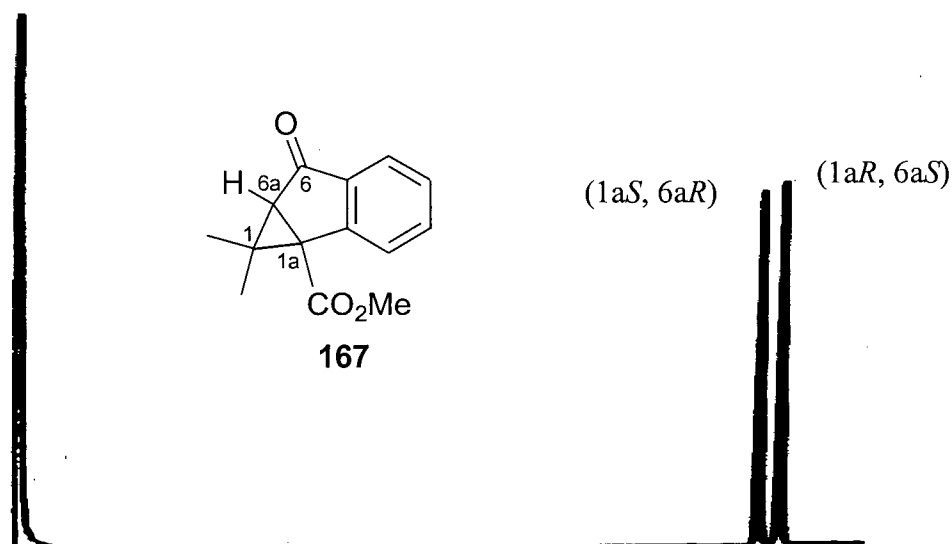


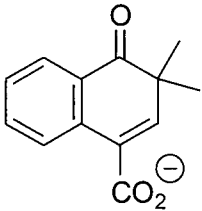
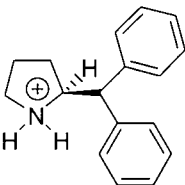
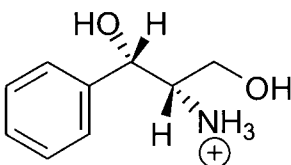
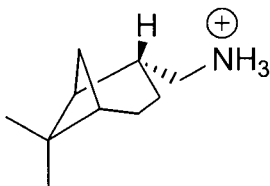
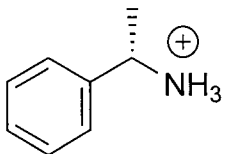
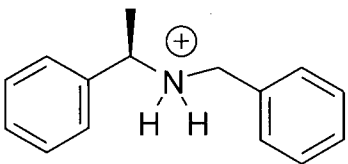
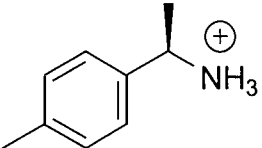
Figure 4.8 Chiral GC chromatogram showing the configuration of each enantiomer of ester **167**.

of the enantiomers of ester **167** to be identified on the GC trace. Figure 4.8 depicts a chiral GC chromatogram of racemic **167** with the absolute configuration assignments labelled for each peak.

4.4 Preparation of Optically Active Salts of Acid **52**

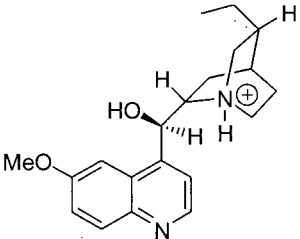
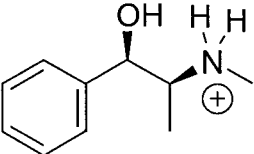
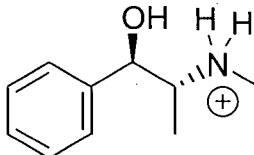
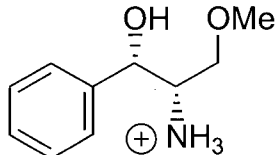
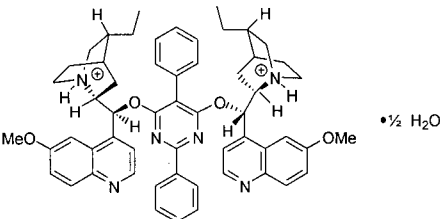
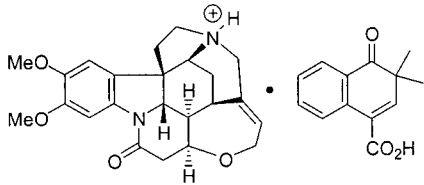
Salts of carboxylic acid **52** were formed with twelve optically pure amines of known absolute configuration. The identity, melting points, and solvent of recrystallization for these compounds are reported in Table 4.1. The spectral data and elemental analysis results provided the stoichiometry for each of the salts synthesized. The presence of water or solvent of crystallization could also be detected from these analyses.

Table 4.1 Optically active salts prepared from acid **52**.

			
Salt	Cation	Recrystallization Solvent	mp (°C)
172^a		EtOAc	182-184
173		MeCN / <i>n</i> -pentane	84-88
174		Et ₂ O	134 (sharp)
175		Et ₂ O / <i>n</i> -pentane	96-104
176		MeOH / Et ₂ O	107-109
177		Et ₂ O	129-138 (dec.)

^aX-ray crystal structure obtained.

Table 4.1 continued

Salt	Cation	Recrystallization Solvent	mp (°C)
178		MeOH / Et ₂ O	143-148
179		EtOAc	148-149
180		MeCN / hexanes	144-145
181		Et ₂ O	101-103
182 ^b	 • ½ H ₂ O	MeOH / Et ₂ O	187-189
183 ^{a,c}		MeOH / Et ₂ O	187-190 (dec.)

^aX-ray crystal structure obtained. ^bForms a 2:1 salt. ^cSalt is complexed with one equivalent of free acid.

4.5 Solution State Photochemistry of the Optically Active Salts

For four of the chiral salts, the ^{13}C NMR signal for the *gem*-dimethyl carbons in the carboxylate moiety was split into two peaks. Close contact between the chiral cation and achiral anion in the solvated ion pair places the two methyl groups in a diastereotopic relationship. This phenomenon has been exploited for the determination of enantiomeric purity of compounds by NMR spectroscopy, in which case the optically pure ion is known as a *chiral solvating agent*.¹⁰⁴ Table 4.2 lists the chemical shift difference for the two methyl groups measured in chloroform-*d* at 75 MHz. Despite the chiral anisotropy displayed by these salts in solution, asymmetric induction in the photoproduct was not observed after irradiation of these compounds in chloroform. Diastereotopic splitting was not observed in the ^1H NMR spectra of any of the salts of acid **52**.

Table 4.2 Diastereotopic splitting of the *gem*-dimethyl groups in salts of acid **52**.

Salt	^{13}C $\Delta\delta$ (ppm)
177	0.04
181	0.05
180	0.08
173	0.04

4.6 Solid State Photochemistry of the Optically Active Salts

The previous chapter of this thesis described the application of the ionic chiral auxiliary method of asymmetric synthesis in the Norrish/Yang type II photochemistry of macrocyclic aminoketones. In those systems, a large degree of conformational flexibility was present in the reactant, thus allowing it to crystallize in a chiral conformation that favoured formation of one enantiomer of the product over the other. With planar molecules such as compound **52**, however, such biases are expected to be small. The origin of asymmetric induction in this case may have less to do with the conformation of the reactant and may be more influenced by the availability of free space in the crystal lattice. Molecular modelling (HyperChem MM+) of the methyl ester **166** predicts a planar ring system, with the molecule possessing overall C_s symmetry. It was expected, therefore, that the benzocyclohexadienone moiety in the optically active salts formed from acid **52** should also be planar.

As can be seen from the data in Table 4.3, only one chiral auxiliary, 1-phenylethylamine (salt **175**), gave a respectable enantiomeric excess (ca. 80%). The others gave ees ranging from 5-65%. Performing the photolyses at low temperatures had little effect on the product ee, except in the case of salt **182**, where an increase of ca. 17% was realized when the reaction temperature was lowered from ambient to $-78\text{ }^{\circ}\text{C}$. Although the majority of the salts do not provide product with synthetically useful optical purity, the result obtained for salt **175** (71% ee at 80% conversion) offers promise that further trials of ionic chiral auxiliaries can better this result.

Table 4.3 Solid state photolysis of optically active salts of benzocyclohexadienone **52**.

Salt	Amine	Temperature	% Conversion	% ee	Abs. Config. 53 ^a
172	(2 <i>S</i>)-diphenylmethylpyrrolidine	ambient	7	55.0	(1 <i>aS</i> , 6 <i>aR</i>)
			17	32.4	
			37	18.2	
173	(1 <i>S</i> , 2 <i>S</i>)-2-amino-1,3-dihydroxypropylbenzene	ambient	17	5.4	(1 <i>aS</i> , 6 <i>aR</i>)
			38	3.2	
		$-78\text{ }^{\circ}\text{C}$	18	4.9	
174	(1 <i>S</i> , 2 <i>R</i> , 5 <i>S</i>)- <i>cis</i> -myrtanylamine	ambient	19	8.1	(1 <i>aR</i> , 6 <i>aS</i>)
			33	5.9	
			54	1.6	
			64	1.2	
175	(5 <i>S</i>)-1-phenylethylamine	ambient	25	81.0	(1 <i>aR</i> , 6 <i>aS</i>)
			39	75.6	
			80	70.6	
		$-78\text{ }^{\circ}\text{C}$	30	86.5	
176	(1 <i>R</i>)- <i>N</i> -benzyl-1-phenylethylamine	ambient	12	12.6	(1 <i>aS</i> , 6 <i>aR</i>)
			26	8.4	
177	(1 <i>R</i>)-1-(4-methylphenyl)ethylamine	ambient	2	65.0	(1 <i>aS</i> , 6 <i>aR</i>)
			9	50.1	
			12	48.1	
			28	27.8	
			33	31.8	
		$-78\text{ }^{\circ}\text{C}$	15	47.6	

^aAbsolute configuration of the predominant enantiomer of photoproduct **53** as measured by chiral GC analysis of the corresponding methyl ester **167**.

Table 4.3 continued

Salt	Amine	Temperature	% Conversion	% ee	Abs. Config. 53 ^a
178	hydroquinidine	ambient	18	12.9	(1aR, 6aS)
			39	12.6	
			50	10.7	
			78	7.7	
179	(1R, 2S)-ephedrine	ambient	17	30.6	(1aS, 6aR)
			36	32.3	
			61	30.5	
			78	24.2	
		-78 °C	68	32.7	
180	(1R, 2R)-pseudoephedrine	ambient	11	38.1	(1aS, 6aR)
			35	36.2	
			57	31.8	
			67	29.1	
181	(1S, 2S)-2-amino-3-methoxy-1-phenyl-1-propanol	ambient	7	23.7	(1aS, 6aR)
			12	21.9	
			40	15.8	
182	hydroquinidine 2,5-diphenyl-4,6-pyrimidinediyl diether (DHQD ₂ PYR)	ambient	36	35.6	(1aR, 6aS)
			56	35.1	
			69	36.7	
		-78 °C	53	52.5	
183	brucine	ambient	15	20.2	(1aR, 6aS)
			49	21.9	
			76	25.2	

^a Absolute configuration of the predominant enantiomer of photoproduct **53** as measured by chiral GC analysis of the corresponding methyl ester **167**.

4.7 Solid State Structure-Reactivity Analysis

Two of the optically active salts provided crystals suitable for X-ray crystallographic analysis: **183**, for which brucine was the ionic chiral auxiliary, and **172**, the (2*S*)-diphenylmethylpyrrolidine salt of acid **52**. The brucine salt is actually a complex formed between a brucinium cation, the carboxylate anion of acid **52**, and a molecule of the free acid. Thus, the photoreactive benzocyclohexadienone unit is present in two forms that are chemically and crystallographically independent, and reside in different chiral environments. Figure 4.9 shows the anion and free acid as found in the crystal; the carboxyl hydrogen atom is highlighted in green.

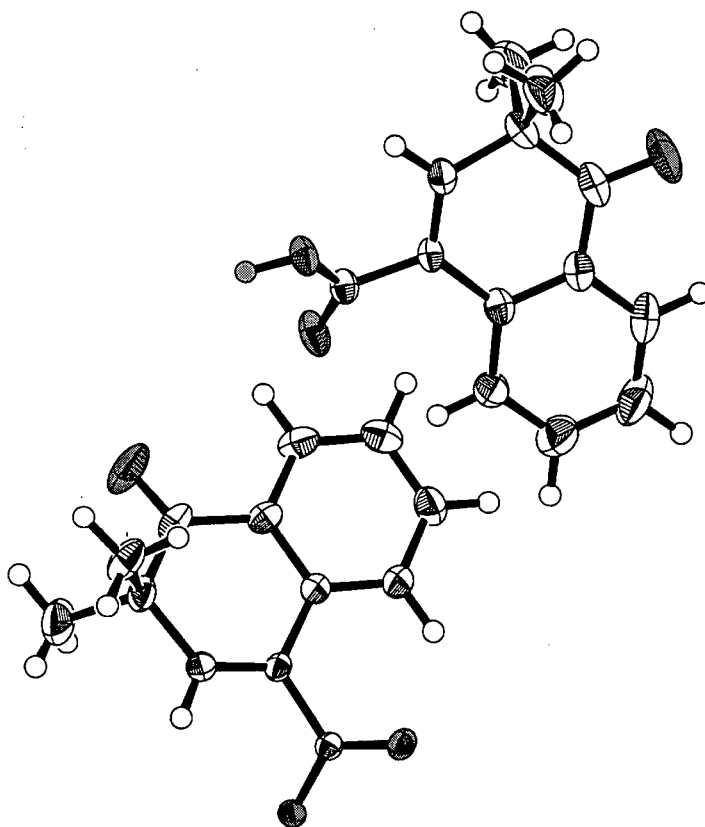


Figure 4.9 ORTEP representation of the benzocyclohexadienone moieties in salt **183**.

It seems likely that the presence of two independent photoreactive forms of the acid is responsible for the low enantioselectivity (ca. 20%) observed on solid state photolysis of this salt. In order to achieve high ees, each of the two components would need to produce the same photoproduct enantiomer, and do so with good selectivity.

Although salt **172** consists of an optically active cation and the photoreactive anion in a 1:1 ratio, X-ray crystallographic analysis reveals that the solid state structure has a greater degree of complexity than anticipated. The crystal asymmetric unit, i.e. the minimum set of atoms required to describe the crystal structure before any elements of symmetry are introduced,¹⁰⁵ contains two sets of anion-cation pairs. For crystals of organic compounds, the asymmetric unit typically contains one formula unit (e.g., molecule or anion-cation pair), but this need not be the case.¹⁰⁵ At first glance, the situation encountered with this salt seems similar to that described above for salt **183**, namely the presence of two independent photoreactive moieties reacting from different conformations and in differing chiral cavities. Closer examination of the asymmetric unit reveals, however, that a pseudo-centre of inversion is present, and the two independent anions are *near-perfect conformational enantiomers*. The ammonium counterions are not related by any elements of symmetry. Figure 4.10 shows the asymmetric unit for salt **183**. The green atoms highlighted in the anion are related by inversion through the pseudo-centre. The benzylic atoms of the cation (shown in yellow) both point out of the page and are therefore not related by inversion.

The superposition of the two anion conformations is shown in Figure 4.11.a, and reveals that the ring systems are nearly coplanar. The pendant carboxyl groups, however, are related to the ring system with torsional angles of opposite sign (36.0° and -36.9°). The root-mean-square error (RMSE) calculated for the overlap of the two species is 0.47 Å. Stereochemical inversion of one anion with subsequent superposition onto the other confirms that the anions are conformational enantiomers (Figure 4.11.b). The RMSE value for overlap in this case is negligible at 0.03 Å.

One would expect that, all other factors being equal, irradiation of crystals containing equal amounts of conformational enantiomers should result in a racemic photoproduct. The observed ee at 7% conversion is an astonishing 55%. This ee, then, is a direct measure of the anisotropic influence of the chiral crystalline environment, and is

independent of the reactant's own conformational asymmetry. Since the overall enantioselectivity is the cumulative result of a large number of small interactions, prediction of the steric course of the reaction is not straightforward, and detailed computational analysis is required.¹⁰⁶ Such calculations are planned in collaboration with experts in this field.

4.8 Summary

The planar photosubstrate was expected to show little conformational bias in the solid state, thus relying on the chiral reaction cavity to exert the most influence on the stereoselectivity of the photoreaction. The generally low ees observed in the solid state photolyses are consistent with conformations where the ring system deviates little from an achiral geometry.

The X-ray studies have provided some insight on the low ees by revealing two instances where more than one reactant geometry is present in the crystal. In these cases, two independent asymmetric reactions are essentially taking place simultaneously, with the overall selectivity expressed in the measured ees. For salt **172**, the serendipitous discovery that the two anion conformers were conformational enantiomers means that the enantioselectivity expressed on photolysis is not conformationally derived. Future studies will help to model the solid state chemical processes at work and discover what features of the crystal are responsible for steering this reaction.

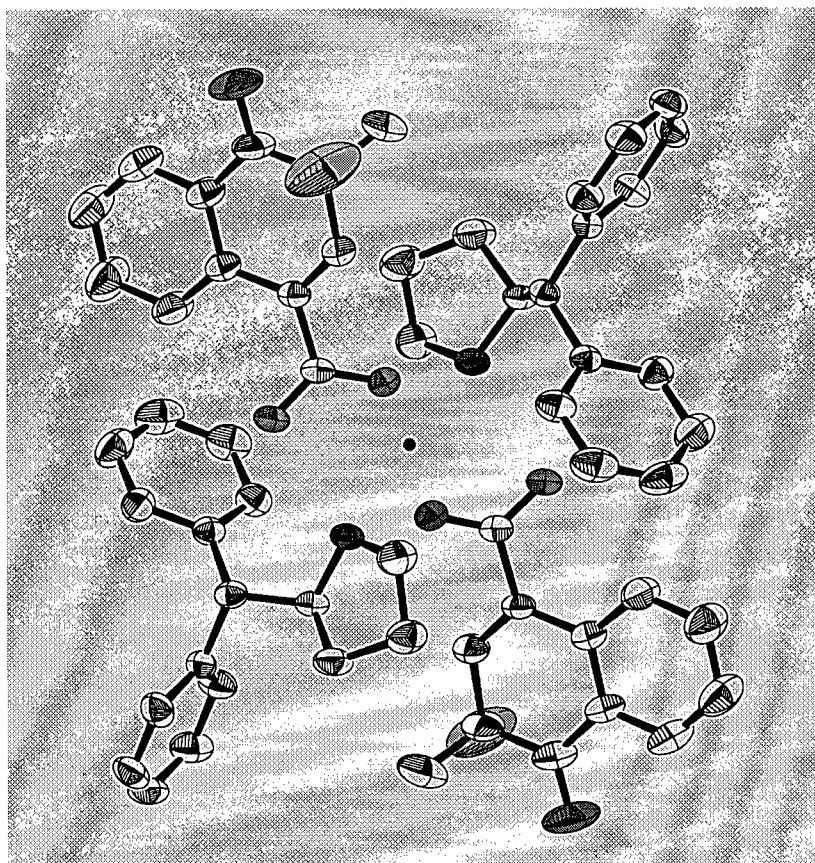


Figure 4.10 ORTEP representation of the asymmetric unit for salt **183** showing the pseudo-inversion center (•).

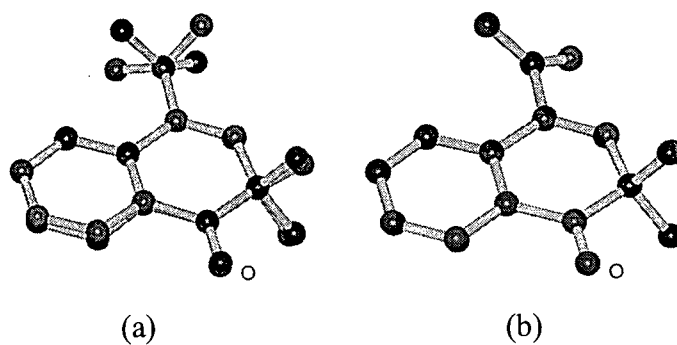


Figure 4.11 Root-mean-square overlays of the anions: (a) native conformations in **183**. (b) Chirality-matched conformations in **183**.

Experimental

Chapter 5 – Preparation of Substrates

5.1 General Considerations

Infrared Spectra (IR)

Infrared spectra were recorded on a Perkin-Elmer model 1710 Fourier transform spectrometer. Liquid samples were analyzed neat as thin films between two sodium chloride plates. Solid samples (2-5 mg) were ground with IR grade KBr (100-200 mg) in an agate mortar and pelleted in an evacuated die (Perkin-Elmer 186-0002) with a laboratory press (Carver, model B) at 17,000 psi. The positions of selected absorption maxima (ν_{max}) are reported in units of cm^{-1} .

Melting Points (mp)

Melting points were determined on a Fisher-Johns hot stage apparatus and are uncorrected. When recrystallized samples were analyzed, the solvent of recrystallization is given in parentheses.

Nuclear Magnetic Resonance (NMR) Spectra

Proton nuclear magnetic resonance (^1H NMR) spectra were recorded in deuterated solvents as noted. Data were collected on the following instruments: Bruker AC-200 (200 MHz), Varian XL-300 (300 MHz), Bruker WH-400 (400 MHz), Bruker AM-400 (400 MHz), and Bruker AMX-500 (500 MHz). Chemical shifts (δ) are reported in parts per million (ppm) of the spectrometer base frequency, and are referenced to the shift of the residual ^1H solvent signals, with tetramethylsilane (δ 0.00) as an external standard: chloroform (7.24 ppm), benzene (7.15 ppm), acetonitrile (1.93 ppm), methanol (3.30 ppm), and dimethylsulfoxide (2.49 ppm). The signal multiplicity, coupling constants, number of hydrogen atoms, and assignments are given in parentheses following the signal position. Multiplicities are abbreviated as follows: multiplet (m), singlet (s), doublet (d), triplet (t), quartet (q), quintet (quint), and broad (br). Nuclear Overhauser Effect

Difference (**NOE**) spectra were acquired on the Bruker WH-400 instrument. ^1H - ^1H correlation spectroscopy (**COSY**) was conducted on the Bruker WH-400 or Bruker AMX-500 spectrometers.

Carbon nuclear magnetic resonance (^{13}C NMR) spectra were recorded on the following instruments: Bruker AC-200 (50.3 MHz), Varian XL-300 (75.4 MHz), Bruker AM-400 (100.5 MHz), and Bruker AMX-500 (125.6 MHz). All experiments were conducted using broadband ^1H decoupling. Chemical shifts (δ) are reported in ppm and are referenced to the centre of the solvent multiplet, with tetramethylsilane (δ 0.0) as an external reference: chloroform (77.0 ppm), benzene (128.0 ppm), acetonitrile (29.8 ppm), methanol (49.0 ppm), and dimethylsulfoxide (39.5 ppm). Some spectra are supported by data from the Attached Proton Test (APT). Where these are given, (-ve) denotes a negative APT peak corresponding to a methine (CH) or methyl (CH_3) moiety; while no assignment signifies a quaternary or methylene (CH_2) centre.

Two-dimensional ^{13}C - ^1H correlation spectra were obtained on the Bruker AMX-500 spectrometer using the Heteronuclear Multiple Quantum Coherence (**HMQC**) experiment for one-bond correlations and the Heteronuclear Multiple Bond Connectivity (**HMBC**) experiment for long-range connectivities.

Mass Spectra

Low and high resolution mass spectra (**LRMS** and **HRMS**) were recorded on a Kratos MS 50 instrument using electron impact (EI) ionization at 70 eV, or chemical ionization (CI) with the ionizing gas noted. Analyses were performed by in-house technicians under the supervision of Dr. G. Eigendorf.

Ultraviolet-Visible Spectra (UV / VIS)

Electronic absorption spectra were recorded on a Perkin-Elmer Lambda-4B UV / VIS spectrometer in the solvents and concentrations indicated using spectral grade solvents. Absorption maxima (λ_{max}) are reported in nanometers (nm), with molar extinction coefficients (ϵ) reported in parentheses in units of $\text{M}^{-1}\text{cm}^{-1}$.

Microanalysis (Anal.)

Elemental analyses were obtained for most new compounds. These were performed by Mr. P. Borda on a Carlo Erba CHN Model 1106 analyzer.

Crystallography

Single crystal X-ray analysis was performed on either a Rigaku AFC6S four-circle diffractometer (Cu-K α or Mo-K α radiation) or a Rigaku AFC7 four-circle diffractometer equipped with a DSC Quantum CCD detector (Mo-K α radiation). Structures were determined by Eugene Cheung and Dr. Brian Patrick under the supervision of Dr. James Trotter. Structures are represented as ORTEP drawings at the 50% probability level.

Optical Rotations

Optical rotation data were recorded on a Jasco-J710/ORD-M instrument at room temperature at the sodium D-line (589.3 nm).

Gas Chromatography (GC)

Gas chromatographic analyses in a helium carrier gas were performed on a Hewlett-Packard 5890A or a 5890 Series II Plus gas chromatograph, each equipped with a flame ionization detector. The following fused silica capillary columns (Supelco) were used: DB-5 (30 m \times 0.25 mm ID), Chiral Select 1000 (30 m \times 0.25 mm ID), and a Custom Chiral Column (50% 6-TBDMS-2,3-dimethyl- β -cyclodextrin dissolved in OV-1701, 20 m \times 0.25 mm ID). Analyses were run with a split injection port (split ratios between 25:1 and 100:1) with column head pressures of 100 kPa (DB-5) or 250 kPa (chiral columns).

High Pressure Liquid Chromatography (HPLC)

HPLC analyses were performed on a Waters 600E system coupled to a tunable UV absorbance detector (Waters 486) using an 88:12 isopropyl alcohol–hexane eluent. The Chiralcel AS column (250 mm \times 4.6 mm ID) employed was obtained from Chiral Technologies Incorporated.

Silica Gel Chromatography

Analytical thin layer chromatography (TLC) was performed on commercial pre-coated (silica gel on aluminum) plates (E. Merck, type 5554). Preparative chromatography was performed using either the flash column method with Merck 9385 silica gel (particle size 230-400 mesh) or radial elution chromatography on a Chromatotron (Harrison Research).

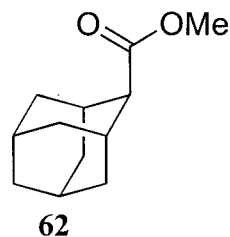
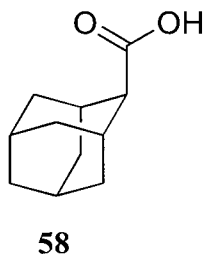
Solvents and Reagents

THF and Et₂O were refluxed over the sodium ketyl of benzophenone under an atmosphere of argon and distilled prior to use. Anhydrous dichloromethane, benzene, xylenes, and MeCN were obtained by refluxing the commercial solvent (Fisher Scientific) over calcium hydride and distilling prior to use. Unless otherwise noted, all reactions were conducted under an atmosphere of dry argon in oven-dried glassware.

5.2 Synthesis of Adamantyl Spiroketones 5, 6, 7, 8, and 70

5.2.1 Preparation of the Five-Membered Adamantyl Spiroketone 5

2-Tricyclo[3.3.1.1^{3,7}]decanecarboxylic Acid (58) and its Methyl Ester (62)



A procedure modified from that of Alberts *et al.* was employed:¹⁰⁷ To a cooled (5° C), stirred suspension of methoxytriphenylphosphonium chloride (20.0 g, 58.3 mmol) in Et₂O (200 mL) was added *n*-butyllithium (41.6 mL of a 1.6 M solution in hexanes, 66.6 mmol) over five minutes. The mixture was warmed to room temperature and stirred for 1.5 h when it took on a rust colour. A solution of 2-adamantanone (7.5 g, 50.0 mmol) in Et₂O (100 mL) was added dropwise to the ylide solution, and the reaction mixture stirred overnight at room temperature. Anhydrous ZnCl₂ (10 g) was added to precipitate the suspended triphenylphosphine oxide and the pale yellow solution was decanted. To this was added perchloric acid (10 mL of a 35% aqueous solution) and the mixture was stirred vigorously for 2 h. The Et₂O solution was washed with water (3 × 100 mL), dried (MgSO₄), and the solvent removed *in vacuo* to give the crude adamantane-2-carboxaldehyde as a colourless oil (9.1 g).

The crude aldehyde was oxidized directly in acetone (200 mL) with dropwise addition of Jones' Reagent (prepared from 6.3 g chromium trioxide, 18 mL water and 5.4 mL conc. sulfuric acid), maintaining the reaction temperature at 10-15 °C. After stirring for 2 h, the solvent was removed *in vacuo*, and the dark residue was taken up in water (500 mL) and extracted with Et₂O (3 × 250 mL). The organic extracts were combined and extracted with 3 M KOH (5 × 100 mL). The combined basic extracts were washed with

Et₂O (2 × 100 mL) and carefully acidified to a pH 3 with conc. HCl. The precipitated carboxylic acid was extracted into Et₂O (4 × 150 mL), and the combined ethereal extracts were dried (MgSO₄), followed by the removal of solvent *in vacuo*. Recrystallization from MeOH / water afforded adamantane-2-carboxylic acid (**58**) (6.2 g, 64% from 2-adamantanone) as a white powder (mp 139-141 °C, lit.¹⁰⁷ 141-143 °C).

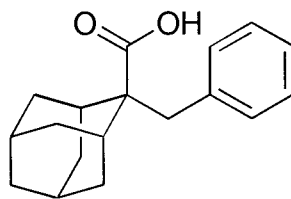
To a room temperature solution of acid **58** (8.2 g, 45.6 mmol) in anhydrous dichloromethane (150 mL) was added oxalyl chloride (8 mL, 92 mmol) and DMF (20 μL). Evolution of CO and CO₂ ceased after 1.5 h of stirring and the solvent was removed *in vacuo*. The residue was placed under high vacuum (<1 Torr) to remove the last traces of oxalyl chloride, then taken up in dichloromethane (100 mL). Anhydrous MeOH (10 mL) was added and the reaction stirred at room temperature for 45 minutes, followed by removal of the solvent *in vacuo*. The pale yellow residue was taken up in Et₂O (200 mL) and washed successively with 5% aqueous sodium bicarbonate (30 mL), water (2 × 50 mL), and brine (50 mL). The organic layer was dried (MgSO₄) and the solvent removed *in vacuo* to yield methyl adamantane-2-carboxylate (**62**) (8.8 g, 99%) as a pale yellow oil which solidified upon standing. The product thus obtained gave spectra in agreement with those reported previously,¹⁰⁸ and was of sufficient purity to be used in subsequent reactions.

mp: 131-133 °C

¹H NMR (400 MHz, CDCl₃): δ 1.59 (br s, 1H), 1.62 (br s, 1H), 1.7-1.8 (br m, 4H), 1.8-1.9 (br m, 6H), 2.31 (br s, 2H), 2.59 (br s, 1H, CHCO₂Me), 3.72 (s, 3H, CH₃).

¹³C NMR (100 MHz, CDCl₃): δ 27.42, 27.47, 29.55, 33.57, 37.39, 38.12, 49.57, 51.30, 175.11.

IR (neat): 1734, 1453, 1344, 1266, 1201, 1174, 1100, 1051 cm⁻¹.

2-Benzyltricyclo[3.3.1.1^{3,7}]decane-2-carboxylic Acid (**54**)**54**

To a cold (-78 °C) solution of LDA (prepared from 8.7 mmol DIPA and 8.04 mmol *n*-butyllithium) in THF (50 mL) was added ester **62** (1.20 g, 6.19 mmol) in THF (8 mL) over 15 minutes. After stirring in the cold for 1.5 h, an additional portion of *n*-butyllithium (4.3 mL of a 1.6 M solution in *n*-hexane, 6.81 mmol) was added dropwise. The reaction was stirred for 30 minutes, followed by the addition of DMPU (2.25 mL, 18.6 mmol). Benzyl bromide (5.3 g, 31 mmol) was added and the reaction stirred in the cold for 3 h before warming slowly to room temperature and stirring overnight. The reaction was quenched with water (65 mL) and extracted with Et₂O (3 × 50 mL). The combined ethereal extracts were washed with brine (2 × 30 mL), dried (MgSO₄), and the solvent removed *in vacuo*. The residue was taken up in anhydrous MeCN (50 mL). To this solution was added sodium iodide (15 g, 100 mmol) and chlorotrimethylsilane (12.7 mL, 100 mmol). The reaction was refluxed under an atmosphere of dry argon for 26 h followed by careful quenching with water (50 mL). Extraction with Et₂O (3 × 75 mL) was followed by successive washing with 25% aqueous sodium thiosulfate (50 mL) and water (2 × 30 mL). The acid was extracted into 10% aqueous KOH (4 × 70 mL) and the combined basic extracts washed with Et₂O (3 × 50 mL). The aqueous layer was carefully acidified with conc. HCl to a pH of 3 after which the precipitated carboxylic acid was extracted into Et₂O (3 × 75 mL), and the combined organic extracts dried (MgSO₄). Removal of the solvent *in vacuo* provided carboxylic acid **54** (1.26 g, 75%) as a white solid. The compound did not require further purification.

mp: 89-91 °C (*n*-pentane)

¹H NMR (400 MHz, CDCl₃): δ 1.7-1.8 (br m, 6H), 1.8-2.0 (br m, 4H), 2.12 (br s, 2H), 2.24 (br s, 1H), 2.27 (br s, 1H), 3.06 (s, 2H, CH₂Ph), 7.10 (m, 2H), 7.22 (m, 3H), CO₂H not observed.

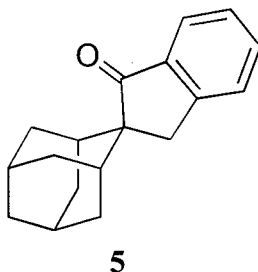
¹³C NMR (100 MHz, CDCl₃): δ 27.22, 27.30, 31.95, 32.45, 35.53, 38.44, 41.51, 54.24, 126.55, 127.96, 129.48, 137.39, 182.04.

IR (KBr pellet): 3400-2500 (br), 1697, 1274, 1206, 738, 700 cm⁻¹.

HRMS (EI) calcd for C₁₈H₂₂O₂ 270.1620, found 270.1622.

Anal. Calcd: C, 79.96; H, 8.20. Found: C, 80.01; H, 8.16.

Spiro[2*H*-indene-2,2'-tricyclo[3.3.1.1^{3,7}]decan]-1(3*H*)-one (**5**)



To a solution of acid **54** (317 mg, 1.17 mmol) in anhydrous dichloromethane (15 mL) was added oxalyl chloride (2.35 mL of a 2.0 M solution in dichloromethane, 4.7 mmol) and DMF (3 μL). The reaction was stirred at room temperature for 2 h, when the evolution of CO and CO₂ ceased. The solvent was removed *in vacuo* and the residue placed under high vacuum (<1 Torr) to remove the last traces of oxalyl chloride. The crude acid chloride was taken up in dichloromethane (8 mL) and this solution was added

to a cooled (-23 °C) suspension of aluminum trichloride (700 mg, 5.2 mmol) in dichloromethane (10 mL) over ten minutes. The reaction was stirred in the cold for 3 h and allowed to warm to room temperature and stir overnight. After dilution with dichloromethane (50 mL) and quenching with water (20 mL), the organic layer was washed successively with saturated aqueous sodium carbonate (15 mL), water (15 mL), and brine (15 mL), followed by drying (MgSO₄) and removal of the solvent *in vacuo*. Silica gel chromatography (Chromatotron, 2% Et₂O in petroleum ether) afforded the ketone **5** (269 mg, 77%) as a white solid.

mp: 89-90 °C (EtOAc)

¹H NMR (400 MHz, CDCl₃): δ 1.53 (br s, 1H), 1.56 (br s, 1H), 1.66-1.83 (br m, 4H), 1.85-2.04 (br m, 6H), 2.80 (m, 2H), 3.18 (s, 2H, CH₂Ph), 7.30 (dt, *J* = 0.7, 7.3 Hz, 1H), 7.38 (d, *J* = 7.6 Hz, 1H), 7.52 (dt, *J* = 1.1, 7.6 Hz, 1H), 7.68 (d, *J* = 7.6 Hz, 1H).

¹³C NMR (100 MHz, CDCl₃): δ 26.86 (-ve), 27.34 (-ve), 31.95, 33.97 (-ve), 35.67, 38.71, 40.60, 54.64, 124.02 (-ve), 125.94 (-ve), 127.11 (-ve), 134.23 (-ve), 136.86, 151.26, 209.63.

IR (KBr pellet): 1692, 1609, 1451, 952, 776, 728 cm⁻¹.

UV / VIS (6.90 × 10⁻⁴ M, MeCN): 294 (2480), 331 (70) nm (M⁻¹cm⁻¹).

HRMS (EI) calcd for C₁₈H₂₀O 252.1514, found 252.1516.

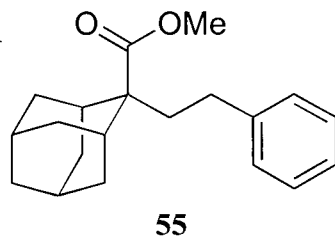
Anal. Calcd: C, 85.67; H, 7.99. Found: C, 85.39; H, 8.01.

This structure was confirmed by X-ray crystallographic analysis:

Habit	colourless plates
Space group	$P2_1/c$
a , Å	6.7952(6)
b , Å	6.7557(8)
c , Å	28.909(3)
α (°)	90
β (°)	92.94(1)
γ (°)	90
Z	4
R	0.053

5.2.2 Preparation of the Six-Membered Adamanyl Spiroketones 6 and 70

Methyl 2-(2-Phenylethyl)tricyclo[3.3.1.1^{3,7}]decane-2-carboxylate (55)



To a cold (-78 °C) solution of LDA (1.9 mmol; prepared from 2.1 mmol DIPA and 1.9 mmol *n*-butyllithium) in THF (30 mL) was added a solution of ester **62** (290 mg, 1.5 mmol) in THF (5 mL) over ten minutes. The reaction was stirred in the cold for 1.5 h, followed by the addition of DMPU (360 μ L, 3.0 mmol) and further stirring for ten minutes. 2-(Bromoethyl)benzene (450 μ L, 3.0 mmol) was added over two minutes and the reaction mixture stirred for 5 h in the cold before warming to room temperature and stirring overnight. The reaction was quenched with 5% HCl (25 mL) and taken up in Et₂O (150 mL). The mixture was extracted further with Et₂O (2 \times 50 mL) and the combined organic extracts washed successively with water (3 \times 25 mL) and brine (25 mL), then dried (MgSO₄), and concentration *in vacuo*. Silica gel chromatography (3% Et₂O in petroleum ether) gave **55** (415 mg, 89%) as a colourless oil.

¹H NMR (400 MHz, CDCl₃): δ 1.60 (br s, 1H), 1.63 (br s, 1H), 1.69 (br s, 3H), 1.73 (br s, 1H), 1.84 (br m, 4H), 1.99 (m, 4H), 2.18 (br s, 2H), 2.42 (m, 2H, CH₂Ph), 3.71 (s, 3H, CH₃), 7.14 (m, 3H), 7.26 (m, 2H).

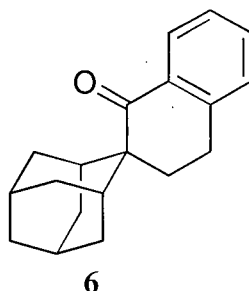
¹³C NMR (75 MHz, CDCl₃): δ 26.98 (-ve), 27.44 (-ve), 30.15, 32.07 (-ve), 32.15, 35.59, 37.87, 38.35, 51.22 (-ve), 52.21, 125.75 (-ve), 128.27 (-ve), 128.34 (-ve), 142.39, 177.21.

IR (neat): 1729, 1603, 1455, 1250, 1197, 1152, 1099, 700 cm^{-1} .

HRMS (DCI, $\text{NH}_3 + \text{CH}_4$) calcd for $\text{C}_{20}\text{H}_{27}\text{O}_2$ ($\text{M}+\text{H}$)⁺ 299.2011, found 299.2009.

Anal. Calcd for $\text{C}_{20}\text{H}_{26}\text{O}_2$: C, 80.50; H, 8.78. Found: C, 80.72; H, 8.82.

3,4-Dihydrospiro[naphthalene-2(1H), 2'-tricyclo[3.3.1.1^{3,7}]decan]-1-one (6)



To a cold ($-78\text{ }^{\circ}\text{C}$) solution of ester **55** (565 mg, 1.9 mmol) in anhydrous dichloromethane (5 mL) was added boron trichloride (9.5 mL of a 1.0 M solution in dichloromethane, 9.5 mmol) over five minutes. The reaction was warmed slowly to $0\text{ }^{\circ}\text{C}$ and stirred for 3 h after which it was poured onto crushed ice (10 g). Dichloromethane (125 mL) was added, and the organic layer washed successively with 5% aqueous sodium carbonate (25 mL), water (2 x 25 mL), and brine (50 mL), followed by drying of the organic layer (MgSO_4) and removal of the solvent *in vacuo*. Silica gel chromatography (5% Et_2O in petroleum ether) afforded the ketone **6** (491 mg, 97%) as a white solid.

mp: 99-100 $^{\circ}\text{C}$ (Et_2O / petroleum ether)

^1H NMR (400 MHz, CDCl_3): δ 1.58 (br s, 1H), 1.62 (br m, 2H), 1.67 (br m, 3H), 1.86 (br m, 2H), 1.97 (br s, 2H), 2.07 (br s, 1H), 2.10 (br s, 1H), 2.17 (br s, 1H), 2.21 (m,

3H), 2.95 (t, $J = 6.2$ Hz, 2H, CH₂Ph), 7.14 (d, $J = 7.6$ Hz, 1H), 7.24 (t, $J = 7.6$ Hz, 1H), 7.38 (t, $J = 7.6$ Hz, 1H), 7.77 (d, $J = 7.6$ Hz).

¹³C NMR (100 MHz, CDCl₃): δ 24.26, 27.75, 27.94, 31.14, 31.55, 33.10, 34.18, 38.62, 49.58, 126.41, 127.58, 127.93, 132.01, 134.32, 141.95, 205.91.

IR (KBr pellet): 1686, 1603, 1217, 938, 902, 757, 740 cm⁻¹.

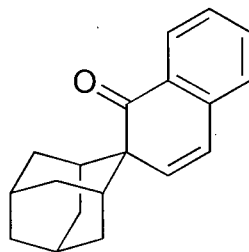
UV / VIS (MeCN, 1.16×10^{-3} M): 285 (1230), 331 (80) nm (M⁻¹cm⁻¹).

HRMS (EI) calcd for C₁₉H₂₂O 266.1671, found 266.1671.

Anal. Calcd: C, 85.67; H, 8.32. Found: C, 85.41; H, 8.39.

This structure was confirmed by X-ray crystallographic analysis:

Habit	colourless cubes
Space group	<i>C2/c</i>
<i>a</i> , Å	17.788(2)
<i>b</i> , Å	12.827(2)
<i>c</i> , Å	12.960(2)
α (°)	90
β (°)	104.178(7)
γ (°)	90
<i>Z</i>	8
<i>R</i>	0.050

Spiro[naphthalene-2(1*H*), 2'-tricyclo[3.3.1.1^{3,7}]decan]-1-one (70)**70**

To a solution of ketone **6** (1.32g, 5.0 mmol) in carbon tetrachloride (25 mL) was added N-bromosuccinimide (900 mg, 5.5 mmol) and dibenzoyl peroxide (15 mg). The suspension was refluxed for 1.5 h followed by dilution with chloroform (100 mL). The organic layer was washed successively with water (3 × 15 mL) and brine (25 mL) followed by drying (MgSO₄) and removal of the solvent *in vacuo*. The crude benzylic bromide was taken up in THF (40 mL). To this solution was added DBU (2.2 mL, 14.7 mmol) and the reaction was stirred for 40 h at room temperature. Water (30 mL) and Et₂O (150 mL) were introduced and the organic layer washed successively with 5% HCl (2 × 15 mL), water (3 × 40 mL) and brine (50 mL). Following drying (MgSO₄) and removal of the solvent *in vacuo*, the product was recrystallized from MeCN to yield enone **70** (632 mg, 48%) as a white powder.

mp: 148-150 °C (MeCN)

¹H NMR (400 MHz, CDCl₃): δ 1.58-1.73 (br m, 6H), 1.88 (br m, 2H), 2.07 (br s, 2H), 2.19 (br m, 2H), 2.37 (br m, 2H), 6.47 (d, *J* = 10.0 Hz, 1H), 6.69 (d, *J* = 10.0 Hz, 1H), 7.06 (d, *J* = 7.3 Hz, 1H), 7.23 (m, 1H), 7.42 (td, *J* = 1.3, 7.6 Hz, 1H), 7.62 (d, *J* = 7.0 Hz, 1H).

^{13}C NMR (100 MHz, CDCl_3): δ 27.06 (-ve), 27.65 (-ve), 34.02, 34.12, 34.28 (-ve), 38.61, 54.19, 124.56 (-ve), 125.50 (-ve), 126.29 (-ve), 127.74 (-ve), 132.59, 132.72 (-ve), 136.72, 138.48 (-ve), 208.83.

IR (KBr pellet): 1687, 1621, 1598, 1451, 1202, 766 cm^{-1} .

UV / VIS (1.20×10^{-3} M, MeCN): 318 (1350), 356 (740) nm ($\text{M}^{-1}\text{cm}^{-1}$).

HRMS (EI) calcd for $\text{C}_{19}\text{H}_{20}\text{O}$ 264.1514, found 264.1513.

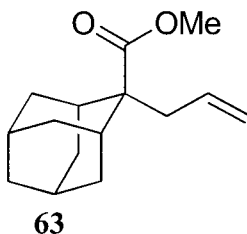
Anal. Calcd: C, 86.32; H, 7.63. Found: C, 86.12; H, 7.57.

This structure was confirmed by X-ray crystallographic analysis:

Habit	colourless prisms
Space group	$P2_1/n$
a , Å	6.7536(8)
b , Å	19.359(3)
c , Å	10.638(1)
α (°)	90
β (°)	98.47(1)
γ (°)	90
Z	4
R	0.048

5.2.3 Preparation of the Seven-Membered Adamantyl Spiroketone 7

Methyl 2-(2-Propenyl)tricyclo[3.3.1.1^{3,7}]decan-2-carboxylate (**63**)



To a cold (-78 °C) solution of LDA (7.4 mmol; prepared from 7.9 mmol DIPA and 7.4 mmol *n*-butyllithium) in THF (80 mL) was added ester **62** (1.1 g, 5.7 mmol) in THF (15 mL) over ten minutes. After stirring in the cold for 1.5 h, an additional portion of *n*-butyllithium (3.9 mL of a 1.6 M solution in hexanes, 6.2 mmol) was added over ten minutes, and the reaction kept cold for 1 h. DMPU (1.37 mL, 11.3 mmol) was introduced, and the solution stirred for ten minutes followed by the dropwise addition of allyl bromide (2.74 g, 22.7 mmol). The reaction was stirred for 5 h at -78 °C, then warmed slowly and allowed to stir overnight at room temperature. The reaction was quenched with 5% HCl (25 mL), taken up in Et₂O (200 mL) and washed successively with water (2 × 25mL) and brine (50 mL). The organic layer was dried (MgSO₄) and the solvent removed *in vacuo*. Silica gel chromatography (5% Et₂O in petroleum ether) afforded methyl 2-(2-propenyl)adamantane-2-carboxylate (**63**) (1.22 g, 92%) as a colourless oil.

¹H NMR (400 MHz, CDCl₃): δ 1.58 (br m, 1H), 1.61 (br m, 1H), 1.67 (br m, 4H), 1.80 (br m, 4H), 1.96 (br s, 1H), 1.99 (br s, 1H), 2.09 (br s, 2H), 2.43 (d, *J* = 7.4 Hz, 2H, CH₂CH=CH₂), 3.63 (s, 3H, CH₃), 4.98 (m, 2H, CH=CH₂), 5.64 (m, 1H, CH=CH₂).

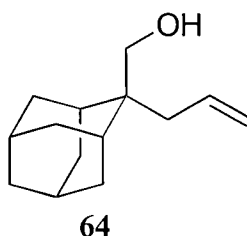
^{13}C NMR (100 MHz, CDCl_3): δ 27.08 (-ve), 27.40 (-ve), 31.98 (-ve), 32.14, 35.56, 38.43, 40.23, 50.97 (-ve), 52.81, 116.95, 133.65 (-ve), 176.66.

IR (neat): 1731, 1640, 1462, 1435, 1211, 1131, 1100, 994 cm^{-1} .

HRMS (EI) calcd for $\text{C}_{15}\text{H}_{22}\text{O}_2$ 234.1620, found 234.1621.

Anal. Calcd: C, 76.88; H, 9.46. Found: C, 76.65; H, 9.46.

2-(Hydroxymethyl)-2-(2-propenyl)tricyclo[3.3.1.1^{3,7}]decane (**64**)



To a solution of ester **63** (1.9 g, 8.0 mmol) in THF (100 mL) was added LAH (24 mL of a 1.0 M solution in THF, 24 mmol). The reaction was heated slowly, and allowed to reflux for 18 h. The reaction was cooled, quenched carefully with saturated aqueous sodium sulfate (5 mL) and saturated aqueous ammonium chloride (5 mL), dried (MgSO_4), and the solvent removed *in vacuo*. Silica gel chromatography (20% Et_2O in petroleum ether) provided the alcohol **64** (1.36 g, 83%) as a white powder.

mp: 49-50 $^{\circ}\text{C}$

^1H NMR (400 MHz, CDCl_3): δ 1.34 (s, 1H), 1.54 (br s, 2H), 1.56 (br s, 2H), 1.61 (br s, 2H), 1.68 (br s, 2H), 1.85 (m, 2H), 1.98 (br s, 1H), 2.01 (br s, 1H), 2.04 (br s, 1H),

2.08 (br s, 1H), 2.40 (d, $J = 7.5$ Hz, 2H, $\text{CH}_2\text{CH}=\text{CH}_2$), 3.75 (s, 2H, CH_2OH), 5.10 (m, 2H, $\text{CH}=\text{CH}_2$), 5.88 (m, 1H, $\text{CH}=\text{CH}_2$).

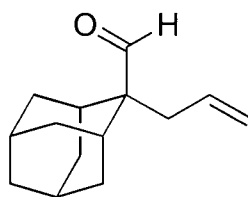
^{13}C NMR (75 MHz, CDCl_3): δ 27.88 (-ve), 28.13 (-ve), 31.16 (-ve), 32.64, 32.85, 37.14, 39.59, 42.30, 65.13, 116.84, 135.59 (-ve).

IR (KBr): 3256 (br), 1820, 1637, 1476, 1461, 1446, 1032, 988, 908 cm^{-1} .

HRMS (DCI, $\text{NH}_3 + \text{CH}_4$) calcd for $\text{C}_{14}\text{H}_{23}\text{O}$ ($\text{M}+\text{H}$) $^+$ 207.1749, found 207.1750.

Anal. Calcd for $\text{C}_{14}\text{H}_{22}\text{O}$: C, 81.50; H, 10.75. Found: C, 81.34; H, 10.85.

2-(2-Propenyl)tricyclo[3.3.1.1^{3,7}]decane-2-carboxaldehyde (65)



65

A mixture of Celite[®] 545 (6g) and PCC (5.16 g, 23.9 mmol) was ground in a mortar and pestle until homogeneous. This solid was suspended in a solution of alcohol **64** (3.18 g, 15.4 mmol) in anhydrous dichloromethane (100 mL) and stirred for 2.5 h at room temperature. Following the addition of anhydrous Et_2O (400 mL), the reaction mixture was filtered through a column of Celite[®] 545 on Florisil[®] and the remaining solids triturated well with anhydrous Et_2O . Solvent removal *in vacuo* was followed by silica gel chromatography (3% Et_2O in petroleum ether) to give the aldehyde **65** (2.81 g, 89%) as a pale yellow oil.

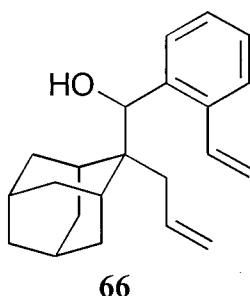
^1H NMR (400 MHz, CDCl_3): δ 1.57-1.78 (br m, 7H), 1.82 (br m, 1H), 1.87 (br m, 1H), 1.96-2.04 (br m, 3H), 2.36 (d, $J = 7.7$ Hz, 1H), 5.02 (m, 2H, $\text{CH}=\text{CH}_2$), 5.58 (m, 1H, $\text{CH}=\text{CH}_2$), 9.43 (s, 1H, CHO).

^{13}C NMR (100 MHz, CDCl_3): δ 27.58 (-ve), 27.59 (-ve), 30.60, 31.79, 34.57, 36.71, 38.06, 54.03, 118.03 (-ve), 132.02, 207.43 (-ve),

IR (neat): 2669, 2698, 1728, 1640, 1460, 994, 915, 859 cm^{-1} .

HRMS (EI) calcd for $\text{C}_{14}\text{H}_{20}\text{O}$ 204.1514, found 204.1512.

Dienol 66



To a suspension of Mg turnings (250 mg, 10.5 mmol) in THF (10 mL) was added iodine (30 mg) and 1,2-dibromoethane (50 μL). The mixture was gently heated until evolution of ethylene ceased and the solution became colourless. 2-Bromostyrene (915 mg, 5.0 mmol) was added slowly so as to maintain a gentle reflux, and the reaction stirred for 1 h. Aldehyde **65** (500 mg, 2.45 mmol) in THF (10 mL) was introduced dropwise and the reaction stirred for 2 h at room temperature. The reaction was diluted with Et_2O (75 mL) and 5% HCl (10 mL) and washed successively with water (3×15 mL) and brine (20 mL). The organic layer was dried (MgSO_4) and the solvent removed *in vacuo*. Silica gel chromatography (7% Et_2O in petroleum ether) provided alcohol **66** (541 mg, 72% from **65**) as a colourless oil.

^1H NMR (400 MHz, CDCl_3): δ 1.28 (br s, 1H), 1.43 (m, 1H), 1.57 (m, 2H), 1.70-1.85 (br m, 4H), 1.99 (br m, 2H), 2.10-2.27 (br m, 4H), 2.46 (d, $J = 12$ Hz, 1H), 2.60 (d, $J = 6.4$ Hz, 1H, $\text{CH}_2\text{CH}=\text{CH}_2$), 2.64 (d, $J = 6.4$ Hz, 1H, $\text{CH}_2\text{CH}=\text{CH}_2$), 4.95 (m, 2H), 5.25 (dd, $J = 1.3, 11.0$ Hz, 1H), 5.50 (dd, $J = 1.1, 17.3$ Hz, 1H), 5.71 (s, 1H, CHOH), 5.84 (m, 1H), 7.19 (dd, $J = 11, 17.3$ Hz, 1H), 7.25 (m, 2H), 7.38 (m, 1H), 7.66 (m, 1H).

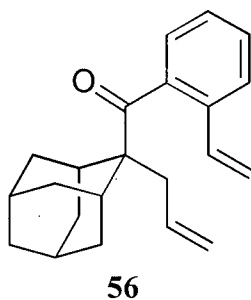
^{13}C NMR (75 MHz, CDCl_3): δ 27.24 (-ve), 27.88 (-ve), 30.63 (-ve), 31.60 (-ve), 32.83, 33.09, 33.14, 34.75, 35.16, 39.63, 45.95, 72.95 (-ve), 115.75, 115.81, 126.98 (-ve), 127.31 (-ve), 127.45 (-ve), 129.05 (-ve), 136.86 (-ve), 137.07 (-ve), 137.85, 140.31.

IR (neat): 3457 (br), 1826, 1631, 1567, 1480, 1463, 1013, 909, 761, 732 cm^{-1} .

HRMS (DCI, $\text{NH}_3 + \text{CH}_4$) calcd for $\text{C}_{22}\text{H}_{32}\text{NO}$ ($\text{M}+\text{NH}_4$) $^+$ 326.2484, found 326.2485.

Anal. Calcd for $\text{C}_{22}\text{H}_{28}\text{O}$: C, 85.66; H, 9.15. Found: C, 85.75; H, 9.23.

Dienone 56



A mixture of Celite[®] 545 (1 g) and PCC (740 mg, 2.9 mmol) was ground in a mortar and pestle until homogeneous. This solid was suspended in a solution of alcohol **66** (450 mg, 1.46 mmol) in anhydrous dichloromethane (75 mL) and stirred for 3 h at room temperature. Following the addition of anhydrous Et₂O (150 mL), the reaction mixture was filtered through a column of Celite[®] 545 on Florisil[®] and the remaining solids triturated well with anhydrous Et₂O. Solvent removal *in vacuo* was followed by silica gel chromatography (5% Et₂O in petroleum ether) to give the ketone **56** (386 mg, 86%) as a colourless oil.

¹H NMR (400 MHz, CDCl₃): δ 1.5-1.7 (m, 8H), 1.76 (br m, 1H), 1.83 (br m, 1H), 2.11 (d, *J* = 12.5 Hz, 2H), 2.33 (br s, 2H), 2.78 (d, *J* = 7.3 Hz, 2H, CH₂CH=CH₂), 5.0-5.1 (m, 2H), 5.28 (dd, *J* = 1.2, 9.0 Hz, 1H), 5.64 (dd, *J* = 1.3, 17.4 Hz, 1H), 5.73 (m, 1H), 7.04 (dd, *J* = 11.0, 17.4 Hz, 1H), 7.20 (dt, *J* = 1.1, 7.7, 1H), 7.37 (dt, *J* = 0.8, 7.1 Hz, 1H), 7.55 (dd, *J* = 1.0, 7.7 Hz, 1H), 7.62 (d, *J* = 7.6 Hz, 1H).

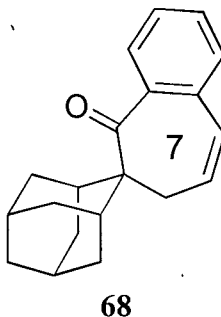
¹³C NMR (75 MHz, CDCl₃): δ 26.69 (-ve), 27.30 (-ve), 32.41, 32.58 (-ve), 34.95, 38.36, 39.79, 57.37, 116.38, 117.15, 125.16 (-ve), 126.22 (-ve), 127.40 (-ve), 129.92 (-ve), 133.58 (-ve), 135.12 (-ve), 137.65, 138.41, 209.96.

IR (neat): 1669, 1639, 1597, 1475, 1462, 1213, 1101, 995, 912, 771 cm⁻¹.

HRMS (EI) calcd for C₂₂H₂₆O 306.1983, found 306.1990.

Anal. Calcd: C, 86.23; H, 8.55. Found: C, 86.16; H, 8.57.

Spiro[6*H*-benzocycloheptene-6,2'-tricyclo[3.3.1.1^{3,7}]decan]-5(7*H*)-one (68)



To a solution of ketone **56** (250 mg, 0.82 mmol) under an atmosphere of argon in degassed, anhydrous dichloromethane (75 mL) was added a solution of Grubbs' catalyst (18 mg, 3 mol%) in degassed, anhydrous dichloromethane over ten minutes. A light orange colour replaced the initial purple colour, and the reaction was allowed to stir at room temperature for 12 h. Silica gel (1 g) and triethylamine (500 μ L) were added and the mixture stirred for 1 h. The suspension was filtered through Celite[®] 545 and the solvent removed *in vacuo*. Purification by silica gel chromatography (10% Et₂O in petroleum ether) afforded the enone **68** (210 mg, 92%) as a pale orange solid. Further purification by recrystallization from EtOAc provided a colourless product.

mp: 129-131 °C (EtOAc / petroleum ether)

¹H NMR (400 MHz, CDCl₃): δ 1.50-1.75 (br m, 10H), 1.82 (br m, 2H), 2.19 (br s, 2H), 2.63 (dd, J = 1.7, 5.2 Hz, 2H, CH₂CH=CH), 5.82 (dt, J = 5.2, 12.1 Hz, 1H, CH₂CH=CH), 6.37 (d, J = 12.1 Hz, 1H, CH₂CH=CH), 7.11 (d, J = 7.5 Hz, 1H), 7.26 (m, 1H), 7.38 (td, J = 1.4, 7.5 Hz, 1H), 7.53 (dd, J = 1.0, 7.6 Hz, 1H).

¹³C NMR (100 MHz, CDCl₃): δ 27.33, 27.74, 31.39, 32.71, 34.94, 35.47, 38.20, 52.17, 127.25, 127.46, 129.41, 130.07, 130.77 (2 acc. eq.), 133.08, 137.90, 209.62.

IR (KBr): 1671, 1596, 1460, 1421, 1269, 776, 765, 755 cm^{-1} .

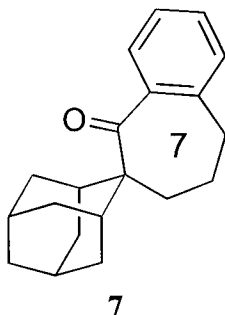
HRMS (EI) calcd for $\text{C}_{20}\text{H}_{22}\text{O}$ 278.1671, found 278.1671.

Anal. Calcd: C, 86.29; H, 7.97. Found: C, 86.00; H, 7.81.

This structure was confirmed by X-ray crystallographic analysis:

Habit	colourless prisms
Space group	$P2_12_12_1$
a , Å	12.320(4)
b , Å	16.226(6)
c , Å	7.352(3)
α (°)	90
β (°)	90
γ (°)	90
Z	4
R	0.044

8,9-Dihydrospiro[6*H*-benzocycloheptene-6,2'-tricyclo[3.3.1.1^{3,7}]decan]-5(7*H*)-one (7)



A suspension of 10% palladium on charcoal (15 mg) and ketone **68** (67 mg, 0.241 mmol) in EtOAc (5 mL) was placed under an atmosphere of H₂. The mixture was stirred for 1 h and filtered through Celite[®] 545. Removal of the solvent *in vacuo* provided analytically pure ketone **7** (65 mg, 96%) as a white solid.

mp: 143-144 °C (EtOAc)

¹H NMR (400 MHz, CDCl₃): δ 1.48-1.65 (br m, 6H), 1.76 (m, 4H), 1.89 (m, 2H), 1.94-2.08 (br m, 6H), 2.85 (d, *J* = 5.5 Hz, 2H, CH₂Ph), 7.08 (d, *J* = 7.2 Hz, 1H), 7.24 (m, 2H), 7.31 (dd, *J* = 1.5, 7.2 Hz, 1H).

¹³C NMR (100 MHz, CDCl₃): δ 23.63, 27.21 (-ve), 27.41 (-ve), 32.31, 32.80 (-ve), 34.92, 35.94, 36.43, 38.36, 56.04, 125.97 (-ve), 128.16 (-ve), 128.58 (-ve), 129.30 (-ve), 137.71, 141.46, 213.33.

IR (KBr pellet): 1683, 1597, 1462, 1444, 1431, 1257, 952, 742, 635 cm⁻¹.

UV / VIS (1.06 × 10⁻³ M, MeCN): 274 (600), 316 (160) nm (M⁻¹cm⁻¹).

HRMS (EI) calcd for C₂₀H₂₄O 280.1827, found 280.1833.

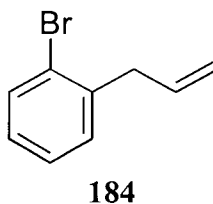
Anal. Calcd: C, 85.67; H, 8.63. Found: C, 85.51; H, 8.56.

This structure was confirmed by X-ray crystallographic analysis:

Habit	colourless cubes
Space group	$P\bar{1}$
a , Å	10.898(4)
b , Å	11.213(2)
c , Å	7.218(6)
α (°)	99.52(3)
β (°)	109.01(4)
γ (°)	62.27(2)
Z	2
R	0.048

5.2.4 Preparation of the Eight-Membered Adamantyl Spiroketone 8

2-Propenylbromobenzene (184)

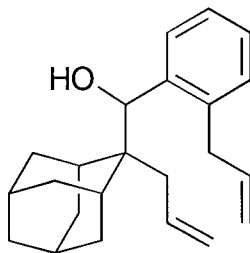


The procedure of Boymond *et al.* was followed:¹⁰⁹ To a cold (-25 °C) solution of 2-bromoiodobenzene (4.57 g, 16.1 mmol) in THF (75 mL) was added isopropylmagnesium chloride (8.9 mL of a 2.0 M solution in Et₂O, 17.8 mmol) over five minutes. Stirring was continued in the cold for 1 h after which time allyl bromide (1.6 mL, 17.8 mmol) was added. After 30 minutes the reaction was warmed to room temperature and stirred for 1 h. The reaction was quenched overnight with an aqueous solution (10 mL) containing 5% ammonium hydroxide and 5% ammonium chloride. Extraction with Et₂O (3 × 75 mL) was followed by successive washing of the combined organic extracts with 5% HCl (3 × 20 mL), 5% aqueous sodium bicarbonate (25 mL), water (2 × 25 mL), and brine (50 mL). After drying (MgSO₄), and removal of the solvent *in vacuo*, aryl bromide **184** (2.97 g, 93%) was isolated as a colourless liquid. The product was of sufficient purity to use in subsequent reactions.

¹H NMR (400 MHz, CDCl₃): δ 3.50 (dt, *J* = 1.3, 8.5 Hz, 2H), 5.10 (m, 3H), 5.97 (m, 1H), 7.06 (m, 1H), 7.23 (m, 2H), 7.54 (m, 1H).

¹³C NMR (75 MHz, CDCl₃): δ 40.17, 116.53, 124.54, 127.45, 127.79, 130.40, 132.72, 135.53, 139.39.

LRMS (EI) (*m/z*): 198 (M⁺ {⁷⁹Br}, 35), 196 (M⁺ {⁸¹Br}, 37), 117 (100).

Dienol 67**67**

To a suspension of Mg turnings (1.5 g, 62.5 mmol) in THF (20 mL) was added iodine (50 mg) and 1,2-dibromoethane (100 μ L). The mixture was gently heated until evolution of ethylene ceased and the solution became colourless. Aryl bromide **184** (2.0 g, 10.2 mmol) was added slowly so as to maintain a gentle reflux, and the reaction stirred for 1 h. Aldehyde **65** (1.16 g, 5.7 mmol) in THF (5 mL) was added dropwise and the reaction stirred for 2 h at room temperature. The reaction was diluted with Et₂O (75 mL) and 5% HCl (10 mL) and washed successively with water (2 \times 25 mL) and brine (20 mL). The organic layer was dried (MgSO₄) and the solvent removed *in vacuo*. Silica gel chromatography (7% Et₂O in petroleum ether) provided the alcohol **67** (1.64 g, 90% from **65**) as a colourless oil.

¹H NMR (400 MHz, CDCl₃): δ 1.42 (br s, 1H), 1.48 (dq, J = 2.5, 13.3 Hz, 1H), 1.63 (m, 2H), 1.73 (m, 3H), 1.84 (br m, 1H), 1.97 (br m, 1H), 2.06 (m, 1H), 2.15 (m, 1H), 1.19-2.40 (m, 5H), 2.66 (dd, J = 65, 6.2 Hz, 1H), 3.54 (dt, J = 1.4, 6.1 Hz, 2H), 4.90-5.08 (m, 4H), 5.64 (s, 1H, $\underline{\text{CHOH}}$), 5.85 (m, 1H), 5.98 (m, 1H), 7.19 (m, 3H), 7.62 (m, 1H).

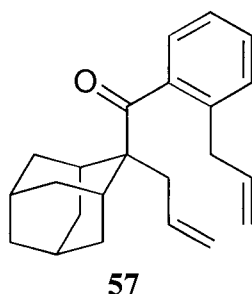
¹³C NMR (75 MHz, CDCl₃): δ 27.21, 27.85, 30.80, 31.98, 32.94, 33.15 (2 acc. eq.), 34.39, 35.40, 37.91, 39.63, 45.69, 73.36, 115.72 (2 acc. eq.), 125.78, 127.22, 129.38, 130.52, 137.01, 138.17 (2 acc. eq.), 140.97.

IR (neat): 3470 (br), 1824, 1635, 1602, 1446, 1463, 996, 910, 739 cm^{-1} .

HRMS (EI) calcd for $\text{C}_{23}\text{H}_{30}\text{O}$ 322.2297, found 322.2295.

Anal. Calcd: C, 85.66; H, 9.38. Found: C, 85.43; H, 9.41.

Dienone **57**



A mixture of Celite[®] 545 (8g) and PCC (1.0 g, 4.7 mmol) was ground in a mortar and pestle until homogeneous. This solid was suspended in a solution of alcohol **67** (1.0 g, 3.1 mmol) in anhydrous dichloromethane (80 mL) and stirred for 1.5 h at room temperature. Following the addition of anhydrous Et_2O (150 mL), the reaction mixture was filtered through a column of Celite[®] 545 on Florisil[®] and the remaining solids triturated well with anhydrous Et_2O . Solvent removal *in vacuo* was followed by silica gel chromatography (5% Et_2O in petroleum ether) to give the ketone **57** (924 mg, 93%) as a colourless oil.

^1H NMR (400 MHz, CDCl_3): δ 1.51-1.70 (br m, 8H), 1.77 (br m, 1H), 1.83 (br m, 1H), 2.10 (s, 1H), 2.13 (s, 1H), 2.34 (s, 2H), 2.80 (d, $J = 7.4$ Hz, 2H), 3.47 (d, $J = 6.8$

Hz, 2H), 5.08 (m, 4H), 5.75 (m, 1H), 6.04 (m, 1H), 7.15 (m, 1H), 7.33 (m, 2H), 7.57 (d, $J = 7.8$ Hz, 1H).

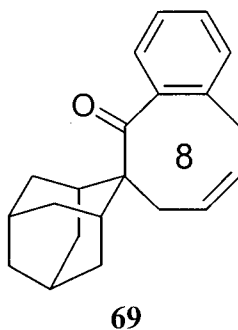
^{13}C NMR (75 MHz, CDCl_3): δ 26.63, 27.19, 32.34, 32.49, 34.90, 37.45, 38.31, 39.75, 57.25, 115.85, 117.00, 124.64, 125.16, 129.68, 131.19, 133.57, 137.62, 139.01, 139.60, 210.02.

IR (neat): 1669, 1638, 1599, 1572, 1478, 1461, 1214, 1101, 995, 912, 745 cm^{-1} .

HRMS (CI, isobutane) calcd for $\text{C}_{23}\text{H}_{29}\text{O}$ ($\text{M}+\text{H}$) $^+$ 321.2218, found 321.2217.

Anal. Calcd for $\text{C}_{23}\text{H}_{28}\text{O}$: C, 86.20; H, 8.81. Found: C, 86.34; H, 8.90.

Spiro[6*H*-benzocyclooctene-6,2'-tricyclo[3.3.1.1^{3,7}]decan]-5(10*H*)-one (69)



To a solution of ketone **57** (410 mg, 1.28 mmol) under an atmosphere of argon in degassed, anhydrous dichloromethane (100 mL) was added a solution of Grubbs catalyst¹¹⁰ (53 mg, 5 mol%) in degassed, anhydrous dichloromethane over ten minutes. A light orange colour replaced the initial purple colour, and the reaction was allowed to stir at room temperature for 2 h. Silica gel (2 g) and triethylamine (1 mL) were added and the mixture stirred for 3 h. The suspension was filtered through Celite[®] 545 and the organic layer washed successively with 5% aqueous sodium bicarbonate (3 \times 15 mL), 5% HCl (3

× 15 mL), water (3 × 20 mL), and brine (50 mL). The organic layer was dried (MgSO₄) and the solvent removed *in vacuo* to afford the enone **69** (336mg, 90%) as a pale yellow oil.

¹H NMR (400 MHz, CDCl₃): δ 1.50-1.80 (br m, 6H), 1.80-2.00 (br m, 5H), 2.10 (br m, 1H), 2.28 (br m, 2H), 2.50 (m, 2H), 3.48 (m, 2H), 5.68 (m, 1H), 5.79 (m, 1H), 7.10-7.28 (m, 4H).

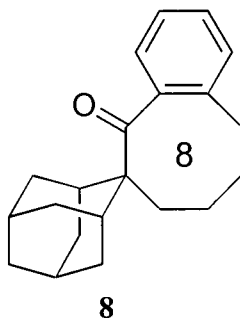
¹³C NMR (100 MHz, CDCl₃): δ 27.19, 27.63, 30.98 (br), 32.26, 32.18 (br), 32.26 (br), 33.52 (br), 34.67 (br), 35.00, 36.22 (br), 38.58, 59.76, 125.40, 126.33, 126.90, 128.39, 129.48, 129.64, 134.94, 141.39, 213.58. Slow conformational exchange at room temperature has broadened and split some of the carbon signals.

IR (neat): 1695, 1678, 1459, 1215, 1101, 947, 754 cm⁻¹.

HRMS (EI) calcd for C₂₁H₂₄O 292.1827, found 292.1828.

Anal. Calcd: C, 86.26; H, 8.27. Found: C, 86.01; H, 8.28.

9,10-Dihydrospiro[6*H*-benzocyclooctene-6,2'-tricyclo[3.3.1.1^{3,7}]decan]-5(7*H*)-one (**8**)



A suspension of 10% palladium on charcoal (100 mg) and ketone **69** (1.53 g, 5.2 mmol) in EtOAc (20 mL) was placed under an atmosphere of H₂. The mixture was stirred for 1 h and filtered through Celite[®] 545. Removal of the solvent *in vacuo* provided analytically pure ketone **8** (1.48 g, 97%) as a white solid.

mp: 118-119 °C (MeCN)

¹H NMR (400 MHz, CDCl₃): δ 1.30-1.48 (br m, 3H), 1.50-1.79 (br m, 6H), 1.80-2.10 (br m, 8H), 2.28 (br s, 2H), 2.56 (br m, 2H), 2.86 (br m, 1H), 7.07 (m, 1H), 7.13 (m, 2H), 7.22 (m, 1H).

¹³C NMR (75 MHz, DMSO-*d*₆): δ 21.28, 26.47, 27.47, 29.09, 31.24 (br), 32.10, 32.43(br), 32.54 (br), 32.92, 33.38 (br), 36.06 (br), 38.13, 36.85, 123.27, 124.99, 128.37, 129.94, 138.75, 140.12, 213.32.

IR (KBr pellet): 1681, 1477, 1441, 1211, 935, 754 cm⁻¹.

UV / VIS (1.05 × 10⁻³ M, MeCN): 266 (380), 313 (105) nm (M⁻¹cm⁻¹).

HRMS (EI) calcd for C₂₁H₂₆O 294.1984, found 294.1983.

Anal. Calcd: C, 85.67; H, 8.90. Found: C, 85.50; H, 9.00.

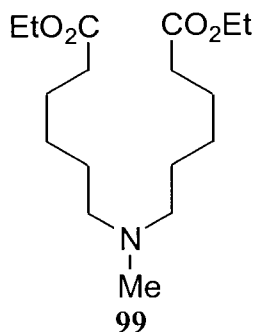
This structure was confirmed by X-ray crystallographic analysis:

Habit	colourless prisms
Space group	$Pna2_1$
a , Å	19.318(4)
b , Å	8.282(2)
c , Å	10.045(1)
α (°)	90
β (°)	90
γ (°)	90
Z	4
R	0.041

5.3 Synthesis of the Macrocyclic Aminoketones 12, 14, and 16 and Their Salts

5.3.1 Preparation of the Twelve-Membered Aminoketone 12

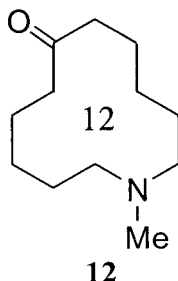
Diethyl 6,6'-Methyliminodihexanoate (99)



This aminodiester was synthesized according to a procedure modified from that of Leonard *et al.*¹¹¹ To a mixture of methylammonium chloride (9.2 g, 136 mmol), ethyl 6-bromohexanoate (64.1 g, 298 mmol), and potassium iodide (45 g, 271 mmol) in anhydrous MeCN (500 mL) was added DIPEA (70 mL, 402 mmol) over 4 h. After stirring overnight at room temperature, the reaction was heated slowly to reflux. After 40 h the reaction was cooled and diluted with water (100 mL) and saturated aqueous potassium carbonate (200 mL). The reaction was extracted with Et₂O (3 × 300 mL), and the combined organic extracts dried (MgSO₄) and concentrated *in vacuo* to yield **99** (25.4 g, 62%) as a yellow oil. This compound was of sufficient purity to use in subsequent reactions.

¹H NMR (200 MHz, CDCl₃): δ 1.19 (t, *J* = 7.1 Hz, 6H, OCH₂CH₃), 1.15-1.68 (m, 8H), 2.13 (s, 1H, N-CH₃), 2.24 (t, *J* = 7.3 Hz, 8H), 4.06 (q, *J* = 7.1 Hz, 4H, OCH₂).

¹³C NMR (50 MHz, CDCl₃): δ 14.2, 24.9, 27.0, 27.1, 34.3, 42.2, 57.6, 60.1, 173.7.

7-Methyl-7-azacyclododecanone (**12**)

A procedure modified from that of Spanka *et al.* was employed.⁴⁵ To a refluxing solution of potassium *tert*-butoxide (20.0 g, 178 mmol) in anhydrous xylenes (750 mL) was added aminodiester **99** (13.0 g, 45.3 mmol) in anhydrous xylenes (50 mL) over 40 h *via* syringe pump. Heating was continued for an additional 12 h at which time the reaction was cooled in an ice bath. Water (100 mL) and conc. HCl (200 mL) were added and the organic layer extracted successively with conc. HCl (6 × 75 mL) and 1:1 MeOH / water (200 mL). The combined aqueous extracts were refluxed for 24 h, during which time carbon dioxide was evolved. The volume was reduced to *ca.* 200 mL by distillation, and the reaction cooled. Careful addition of 50% aqueous potassium hydroxide (final pH 11) was followed by extraction into Et₂O (10 × 100 mL). The combined organic extracts were dried (MgSO₄) and concentrated *in vacuo*. Sublimation (60 °C, 3 Torr) provided ketone **12** (2.75 g, 31%) as a waxy white solid. Recrystallization of the sublimation residue from Et₂O provided aminoketone dimer **101** (1.12 g, 13%) as colourless plates.

Characterization of **12**

mp: 33 °C (lit.⁴⁵ value 33 °C)

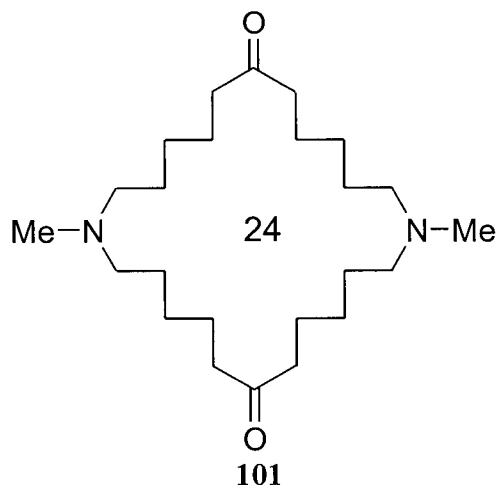
¹H NMR (200 MHz, CDCl₃): δ 1.33 (m, 8H), 1.66 (m, 4H), 2.07 (s, 3H, N-CH₃), 2.20 (m, 4H), 2.40 (m, 4H).

¹³C NMR (50 MHz, CDCl₃): δ 22.71, 23.70, 25.61, 40.52, 43.38 (-ve), 54.53, 212.82.

IR (KBr pellet): 2929, 2789, 1705, 1472, 1309, 1142, 1047, 728 cm^{-1} .

UV / VIS (2.6×10^{-3} M, *n*-pentane): 237 (320), 286 (30) nm ($\text{M}^{-1}\text{cm}^{-1}$).

7,19-Dimethyl-7,19-diazacyclotetraeicosan-1,13-dione (101)



mp: 80-81 $^{\circ}\text{C}$ (Et_2O)

^1H NMR (200 MHz, CDCl_3): δ 1.22-1.44 (m, 16H), 1.55 (quint, $J = 7.2$ Hz, 8H), 2.14 (s, 6H, CH_3), 2.24 (t, $J = 6.7$ Hz, 8H), 2.36 (t, $J = 7.2$ Hz, 8H).

^{13}C NMR (50 MHz, CDCl_3): δ 23.62, 26.67, 26.76, 45.53, 42.80, 56.75, 211.56.

IR (KBr pellet): 2935, 2777, 1701, 1459, 1420, 999, 726 cm^{-1} .

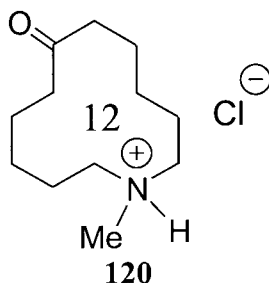
UV / VIS (2.7×10^{-3} M, *n*-pentane): 237 (930), 285 (100) nm ($\text{M}^{-1}\text{cm}^{-1}$).

HRMS (EI) calcd for $\text{C}_{24}\text{H}_{46}\text{N}_2\text{O}_2$ 394.3559, found 394.3559.

Anal. Calcd: C, 73.04; H, 11.75; N, 7.10. Found: C, 73.30; H, 11.66; N, 6.94.

5.3.2 Preparation of the Twelve-Membered Aminoketone Salts

Hydrochloride Salt (120)



Into a solution of aminoketone **12** (450 mg, 2.28 mmol) in Et₂O (25mL) was bubbled dry HCl gas for two minutes. The solvent was removed *in vacuo* to give salt **120** (490 mg, 93%) as a white powder.

mp: 182-183 °C

¹H NMR (200 MHz, CDCl₃): δ 1.37-1.93 (m, 12H), 2.36-2.65 (m, 4H), 2.68 (d, *J* = 4.7 Hz, 3H), 2.80-3.09 (m, 4H), 12.15 (br s, 1H, NH).

¹³C NMR (50 MHz, CDCl₃): δ 19.9, 21.1, 24.7, 41.2, 42.0, 51.5, 212.7.

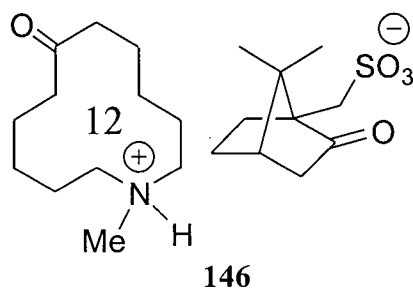
IR (KBr pellet): 2931, 2634, 2596, 2460, 1702, 1475, 1446, 1118, 1022 cm⁻¹.

Anal. Calcd for C₁₂H₂₄NOCl: C, 61.65; H, 10.35; N, 5.99. Found: C, 61.62; H, 10.21; N, 5.81.

mp: 78-80 °C (chloroform / petroleum ether)

¹³C NMR (75 MHz, CDCl₃): δ 19.80, 19.85, 19.91, 19.99, 21.15, 21.19, 24.51, 24.62, 27.01, 41.12, 41.15, 42.51, 42.61, 42.97, 47.32, 47.98, 51.78, 51.85, 58.42, 212.81, 217.10.

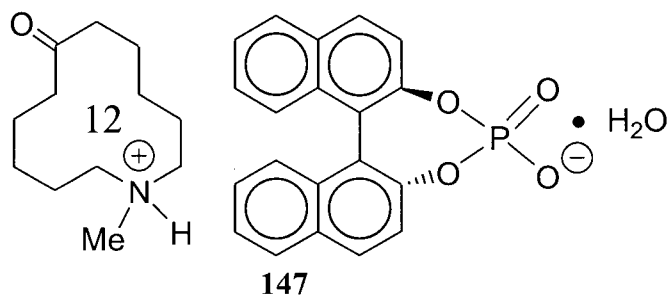
Anal. Calcd for $C_{22}H_{39}NO_5S$: C, 61.51; H, 9.15; N, 3.26. Found: C, 61.23; H, 9.39; N, 3.24.

(1*R*)-10-Camphorsulfonate Salt **146**

Aminoketone **12** (110 mg, 0.58 mmol) and (1*R*)-(+)-10-camphorsulfonic acid (125 mg, 0.54 mmol) were combined in chloroform (5 mL). Petroleum ether was added until the solution became turbid, and the reaction placed in a freezer (-20 °C). After 24 h, crystals of salt **146** (98mg, 42%) were collected.

The melting point and spectral data were identical to those reported for compound **145**.

Anal. Calcd for C₂₂H₃₉NO₅S: C, 61.51; H, 9.15; N, 3.26. Found: C, 61.30; H, 9.16; N, 3.26.

(R)-1,1'-Binaphthyl-2,2'-diyl Phosphate Salt Monohydrate 147

Aminoketone **12** (174 mg, 0.91 mmol) and (*R*)-(-)-1,1'-binaphthyl-2,2'-diyl hydrogen phosphate (300 mg, 0.86 mmol) were dissolved in separate portions of MeOH (3 mL each) and combined. Recrystallization from 2:1 MeOH / water yielded salt **147** monohydrate (280 mg, 59%) as a white solid.

mp: 154-157 °C (MeOH / water)

¹H NMR (400 MHz, CDCl₃): δ 1.12 (m, 1H), 1.18-1.39 (m, 5H), 1.40-1.61 (m, 5H), 1.68 (br s, 2H), 2.03 (br s, 2H), 2.37 (m, 4H), 2.50 (s, 3H, NCH₃), 2.59 (m, 2H), 2.84 (m, 1H), 7.22 (m, 2H), 7.37 (m, 4H), 7.55 (d, *J* = 8.8 Hz, 2H), 7.88 (d, *J* = 8.1 Hz, 2H), 7.93 (d, *J* = 8.8 Hz, 2H), 12.13 (br s, 1H, NH).

¹³C NMR (75 MHz, CD₃S(O)CD₃): δ 21.16, 21.48, 23.25, 39.58, 43.36, 52.63, 121.75, 122.69, 124.39, 126.04, 128.39, 129.68, 130.28, 131.96, 150.07, 150.20, 212.24.

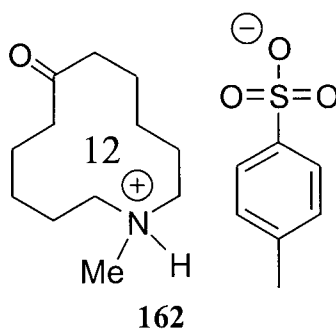
IR (KBr pellet): 3348, 1698, 1265, 1107, 964, 833 cm⁻¹.

Anal. Calcd for C₃₂H₃₈NO₆P: C, 68.19; H, 6.80; N, 2.49. Found: C, 68.26; H, 6.78; N, 2.41.

This structure was confirmed by X-ray crystallographic analysis:

Habit	colourless hexagonal prisms
Space group	$P2_12_12_1$
a , Å	6.551(1)
b , Å	12.531(1)
c , Å	35.268(3)
α (°)	90
β (°)	90
γ (°)	90
Z	4
R	0.042

4-Toluenesulfonate Salt **162**



To a solution of aminoketone **12** (80 mg, 0.42 mmol) in Et₂O (1 mL) was added 4-toluenesulfonic acid (78 mg, 0.45 mmol) in Et₂O (5 mL). Salt **162** (154 mg, 97%) precipitated as a white solid.

mp: 112-113 °C (ethanol / Et₂O)

¹H NMR (400 MHz, CDCl₃): δ 1.43 (m, 4H), 1.59 (m, 2H), 1.66-1.85 (m, 6H), 2.32 (s, 3H, ArCH₃), 2.47 (m, 4H), 2.79 (d, *J* = 4.9 Hz, 3H), 2.95 (m, 2H), 3.08 (m, 2H), 7.16 (d, *J* = 8.0 Hz, 2H), 7.74 (d, *J* = 8.0 Hz, 2H), 10.51 (br s, 1H, NH).

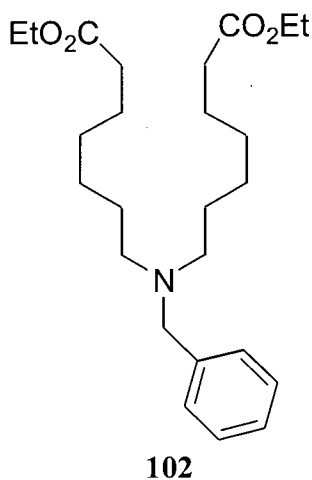
¹³C NMR (75 MHz, CDCl₃): δ 20.34, 21.21, 24.37, 40.94, 42.93, 52.25, 125.88, 128.75, 139.94, 142.17, 212.55.

IR (KBr pellet): 3536, 3047, 2958, 1704, 1479, 1192, 1124, 1036, 1011, 683, 569 cm⁻¹.

Anal. Calcd for C₁₉H₃₁NO₄S: C, 61.76; H, 8.46; N, 3.79. Found: C, 61.54; H, 8.52; N, 3.64.

5.3.3 Preparation of the Fourteen-Membered Aminoketone 14

Diethyl 7,7'-Benzyliminodiheptanoate (102)



To a solution of ethyl 7-bromoheptanoate (32.6 g, 146 mmol), benzylamine (7.9 g, 74 mmol), and suspended potassium iodide (20 g, 120 mmol) in MeCN (200 mL) was added DIPEA (28.2 mL, 162 mmol) in three portions over 3 h. The reaction was brought to reflux and stirred for 18 h after which time it was cooled and concentrated *in vacuo*. The residue was taken up in a mixture of Et₂O (100 mL) and 10% aqueous sodium carbonate (200 mL) and extracted into Et₂O (3 × 100 mL). The combined organic extracts were washed with brine (100 mL), dried (MgSO₄), and concentrated *in vacuo*. Silica gel chromatography (2% triethylamine in 2:1 hexanes / EtOAc) afforded the aminodiester **102** (23.7 g, 82%) as a pale yellow oil.

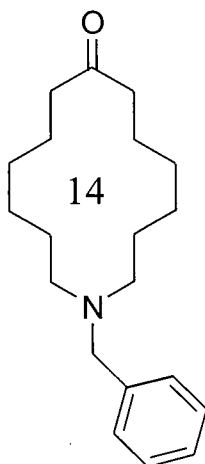
¹H NMR (200 MHz, CDCl₃): δ 1.22 (t, *J* = 7.1 Hz, 6H, CH₃), 1.25 (m, 8H), 1.42 (m, 4H), 1.57 (m, 4H), 2.24 (t, *J* = 7.6 Hz, 4H), 2.35 (t, *J* = 6.8 Hz, 4H), 3.49 (s, 2H, PhCH₂), 4.09 (q, *J* = 7.1 Hz, 4H, OCH₂), 7.26 (m, 5H).

^{13}C NMR (50 MHz, CDCl_3): δ 14.20, 24.91, 26.63, 26.99, 29.00, 34.27, 53.65, 58.59, 60.06, 126.53, 127.98, 128.71, 140.19, 173.75.

IR (neat): 2936, 1737, 1455, 1372, 1180, 1031, 737, 700 cm^{-1} .

HRMS (EI) calcd for $\text{C}_{25}\text{H}_{41}\text{NO}_4$ 419.3036, found 419.3025.

8-Benzyl-8-azacyclotetradecanone (107)



107

A 1L round bottomed flask was equipped with a Hickman still coupled to an efficient condenser. Into the flask was introduced Et_2O (750 mL) and sodium hexamethyldisilazide (100 mL of a 1.0M solution in THF, 100 mmol), and the solution brought to reflux. A solution of aminodiester **102** (10.0 g, 20.4 mmol) in THF (50 mL) was introduced to the top of the condenser over 40 h *via* syringe pump. The reaction was allowed to reflux for an additional 2 h, then cooled in an ice bath. Glacial acetic acid (100 mL) and water (100 mL) were added, followed by removal of Et_2O *in vacuo*. Water (100 mL) and conc. HCl (200 mL) were introduced, and the solution refluxed for 4 h with continuous distillation (ca. 200 mL removed) at which time evolution of carbon dioxide was observed. The reaction was cooled in an ice bath and rendered strongly alkaline with

50% aqueous potassium hydroxide. Extraction with Et₂O (5 × 150 mL) was followed by washing of the combined ethereal extracts with water (2 × 100 mL) and brine (100 mL). Drying (MgSO₄) and concentration of the organic layer *in vacuo* was followed by Kugelrohr distillation (210 °C, 0.8 Torr) to yield the macrocycle **107** (5.20 g, 85%) as a colourless oil.

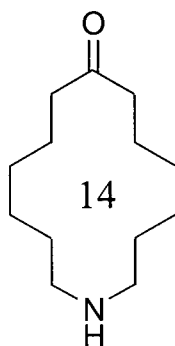
¹H NMR (400 MHz, CDCl₃): δ 1.30 (m, 8H), 1.40 (m, 4H), 1.70 (m, 4H), 2.28 (t, *J* = 5.6 Hz, 4H), 2.47 (t, *J* = 6.2 Hz, 4H), 3.43 (s, 2H, PhCH₂), 7.25 (m, 5H).

¹³C NMR (75 MHz, CDCl₃): δ 23.29, 24.85, 26.59, 26.99, 40.51, 52.04, 58.07, 126.51, 127.95, 128.86, 140.14, 212.26.

IR (neat): 3061, 1713, 1452, 1369, 976, 699 cm⁻¹.

HRMS (EI) calcd for C₂₀H₃₁NO 301.2406, found 301.2407.

Anal. Calcd: C, 79.68; H, 10.36; N, 4.65. Found: C, 79.46; H, 10.46; N, 4.66.

8-Azacyclotetradecanone (14)**14**

A suspension of 10% palladium on charcoal (50 mg) in MeOH (20 mL) containing aminoketone **107** (860 mg, 8.86 mmol) and ammonium formate (1.0 g, 15.9 mmol) was heated quickly and relaxed for eight minutes. The solution was allowed to cool for one minute, then filtered through a bed of Celite[®] 545 which was subsequently triturated with chloroform. The organic filtrate was concentrated *in vacuo*, and taken up in 30% aqueous potassium hydroxide (30 mL) and extracted with Et₂O (3 × 40 mL). The combined organic extracts were washed successively with water (2 × 10mL) and brine (10 mL), followed by drying (MgSO₄), and concentration *in vacuo*. Macrocycle **14** (601 mg, 99%) was obtained as an analytically pure white solid.

mp: 33-34 °C (*n*-pentane)

¹H NMR (300 MHz, CDCl₃): δ 0.75 (br s, 1H, NH), 1.28 (br m, 8H), 1.43 (quint, *J* = 5.7 Hz, 4H), 1.65 (quint, *J* = 6.3 Hz, 4H), 2.42 (t, *J* = 6.0 Hz, 4H), 2.52 (t, *J* = 5.4 Hz, 4H).

¹³C NMR (75 MHz, CDCl₃): δ 23.25, 24.40, 25.95, 27.61, 40.59, 46.38, 212.09.

IR (KBr pellet): 3346, 3318, 2937, 1711, 1365, 1107, 765, 731, 706 cm⁻¹.

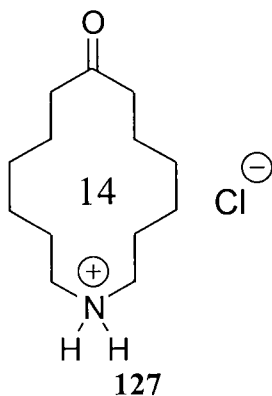
UV / VIS (*n*-hexane): 218 (370), 283 (30) nm ($M^{-1}cm^{-1}$).

HRMS (EI) calcd for $C_{13}H_{25}NO$ 211.1937, found 211.1932.

Anal. Calcd: C, 73.88; H, 11.92; N, 6.63. Found: C, 73.82; H, 12.11; N, 6.78.

5.3.4 Preparation of the Fourteen-Membered Aminoketone Salts

Hydrochloride Salt 127



A stream of dry HCl gas was passed through a solution of aminoketone **14** (233 mg, 1.10 mmol) in Et₂O (10 mL). The white powder that precipitated (250 mg, 91%) was filtered, washed with Et₂O (5 mL) and *n*-pentane (2 × 10 mL) and dried *in vacuo*.

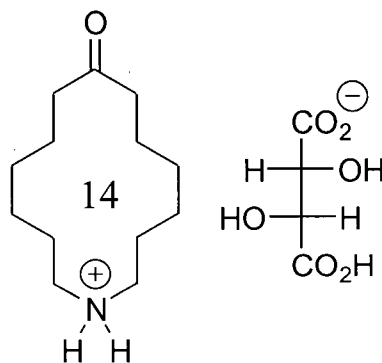
mp: 179-180 °C (Et₂O / MeOH)

¹H NMR (400 MHz, CDCl₃): δ 1.38 (m, 4H), 1.50 (m, 4H), 1.74 (m, 8H), 2.59 (t, *J* = 6.0 Hz, 4H), 2.93 (m, 4H), 9.31 (br s, 2H, NH₂).

¹³C NMR (75 MHz, CDCl₃): δ 22.04, 23.75, 24.08, 26.08, 40.16, 44.15, 212.01.

IR (KBr pellet): 3311, 2936, 1709, 1581, 1473 cm⁻¹.

Anal. Calcd for C₁₃H₂₆NOCl: C, 63.01; H, 10.58; N, 5.65. Found: C, 63.26; H, 10.53; N, 5.50.

(2R, 3R)-Tartrate Salt 148**148**

To a solution of aminoketone **14** (182 mg, 0.86 mmol) in Et₂O (2 mL) was added a solution of (2R, 3R)-tartaric acid (130 mg, 0.86 mmol) in MeOH (2 mL). The solvent was removed *in vacuo* and the resulting amorphous solid recrystallized from chloroform / petroleum ether to give salt **148** as colourless crystals (85 mg, 27%).

mp: 139-140 °C (chloroform / petroleum ether)

¹H NMR (400 MHz, CD₃OD): δ 1.39 (m, 8H), 1.76 (m, 8H), 2.52 (t, *J* = 6.4 Hz, 4H), 3.01 (t, *J* = 6.5 Hz, 4H), 3.39 (s, 2H), 4.86 (br s, exchangeable H atoms).

¹³C NMR (75 MHz, CD₃OD): δ 23.20, 24.53, 24.63, 27.29, 41.30, 45.13, 74.23, 177.08, 214.19.

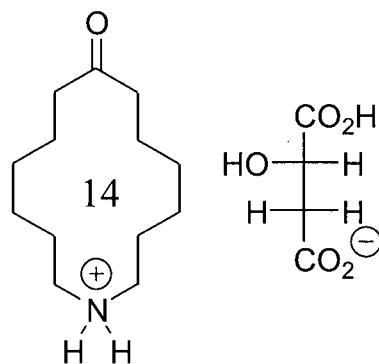
IR (KBr pellet): 3322, 2941, 1737, 1703, 1625, 1578, 1408, 1260, 1113, 1068 cm⁻¹.

Anal. Calcd for C₁₇H₃₁NO₇: C, 56.49; H, 8.65; N, 3.88. Found: C, 56.70; H, 8.78; N, 3.87.

This structure was confirmed by X-ray crystallographic analysis:

Habit	colourless plates
Space group	$P2_1$
a , Å	10.209(1)
b , Å	8.6709(8)
c , Å	10.972(1)
α (°)	90
β (°)	104.675(9)
γ (°)	90
Z	2
R	0.038

(S)-Malate Salt 149



149

Aminoketone **14** (33 mg, 0.16 mmol) and (*S*)-malic acid (21 mg, 0.16 mmol) were dissolved in refluxing Et₂O (5 mL). The salt appeared as a white precipitate on cooling and was filtered and dried (45 mg, 83%).

mp: 117-120 °C (chloroform / petroleum ether)

¹H NMR (400 MHz, CD₃OD): δ 1.38 (m, 8H), 1.72 (m, 8H), 2.51 (dd, *J* = 15.9, 7.6 Hz, 1H), 2.53 (t, *J* = 6.4 Hz, 4H), 2.78 (dd, *J* = 15.9, 5.1 Hz, 1H), 3.00 (t, *J* = 6.4 Hz, 4H), 4.27 (dd, *J* = 5.2, 7.6 Hz, 1H, CH(OH)), 4.88 (br s, exchangeable H atoms).

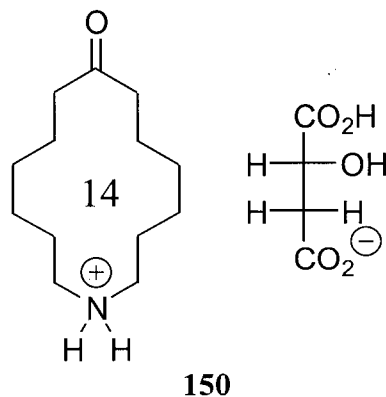
¹³C NMR (100 MHz, CD₃OD): δ 23.19, 24.52, 24.65, 27.28, 41.29, 41.90, 45.11, 69.67, 176.45, 179.59, 214.16.

IR (KBr pellet): 3389, 2941, 1708, 1561, 1093, 676 cm⁻¹.

Anal. Calcd for C₁₇H₃₁NO₆: C, 59.11; H, 9.05; N, 4.05. Found: C, 59.08; H, 9.12; N, 4.14.

This structure was confirmed by X-ray crystallographic analysis:

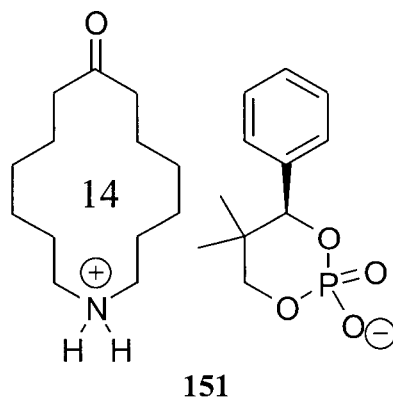
Habit	colourless plates
Space group	<i>P</i> 2 ₁
<i>a</i> , Å	7.3378(8)
<i>b</i> , Å	5.9150(4)
<i>c</i> , Å	21.041(2)
α (°)	90
β (°)	99.015(8)
γ (°)	90
<i>Z</i>	2
<i>R</i>	0.031

(R)-Malate Salt 150

A solution of aminoketone **14** (121 mg, 0.57 mmol) in chloroform (2 mL) was added to a solution of (*R*)-malic acid (76 mg, 0.57 mmol) in MeOH (1 mL). The solvent was removed *in vacuo* and the resulting solid recrystallized from chloroform / petroleum ether to afford salt **150** (160 mg, 81%).

The melting point and spectral data were identical to those reported for compound **149**.

Anal. Calcd for C₁₇H₃₁NO₆: C, 59.11; H, 9.05; N, 4.05. Found: C, 59.14; H, 8.90; N, 3.95.

(*R*)-2-Hydroxy-5,5-dimethyl-4-phenyl-1,3,2-dioxaphosphorinane-2-oxide Salt **151**

Aminoketone **14** (110 mg, 0.52 mmol) and (*R*)-2-Hydroxy-5,5-dimethyl-4-phenyl-1,3,2-dioxaphosphorinane-2-oxide (126 mg, 0.52 mmol) were dissolved in hot MeOH (5 mL). Cooling and subsequent slow evaporation of solvent led to fine white needles of salt **151** (142 mg, 60%).

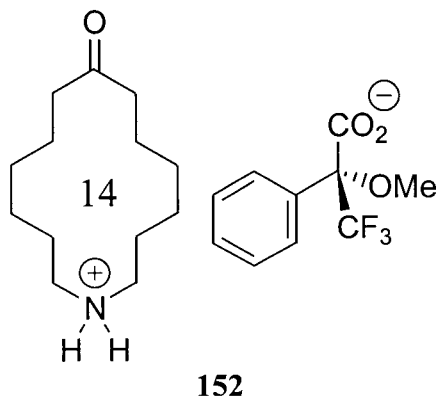
mp: 207-210 °C (MeOH)

¹H NMR (400 MHz, CDCl₃): δ 0.70 (s, 3H), 0.94 (s, 3H), 1.27 (quint, *J* = 7.1 Hz, 4H), 1.40 (quint, *J* = 7.2 Hz, 4H), 1.67 (m, 8H), 2.44 (t, *J* = 7.1 Hz, 4H), 2.86 (m, 4H), 3.64 (dd, ²*J*_{HH} = 10.2 Hz, ³*J*_{HP} = 23.7 Hz, 1H, CH₂OP), 4.22 (d, *J* = 10.2 Hz, CH₂OP, 1H), 5.18 (d, ³*J*_{HP} = 2.2 Hz, 1H, CHOP), 7.27 (br s, 5H), 9.72 (br s, 2H, NH₂).

¹³C NMR (100 MHz, CDCl₃): δ 17.45, 21.28, 22.15, 23.34, 23.42, 25.96, 29.68, 36.05, 40.31, 43.47, 85.16, 127.44, 127.55, 127.60, 138.04 (d, ³*J*_{CP} = 9.8 Hz), 212.21.

IR (KBr pellet): 3396, 2951, 1709, 1225, 1095, 1067, 791, 550 cm⁻¹.

Anal. Calcd for C₂₄H₄₀NO₅P: C, 63.56; H, 8.89; N, 3.09. Found: C, 63.71; H, 9.02; N, 3.13.

(R)- α -Methoxy- α -(trifluoromethyl)phenylacetate Salt **152**

To a solution of compound **14** (32 mg, 0.15 mmol) in Et₂O (1 mL) was added a solution of (R)- α -Methoxy- α -(trifluoromethyl)phenylacetic acid (*R*-Mosher's acid, 35 mg, 0.15 mmol) in Et₂O (2 mL). The resulting solution was concentrated *in vacuo* and the resulting white solid recrystallized from chloroform / petroleum ether to afford salt **152** (55 mg, 82%) as colourless prisms.

mp: 132 °C (sharp) (chloroform / petroleum ether)

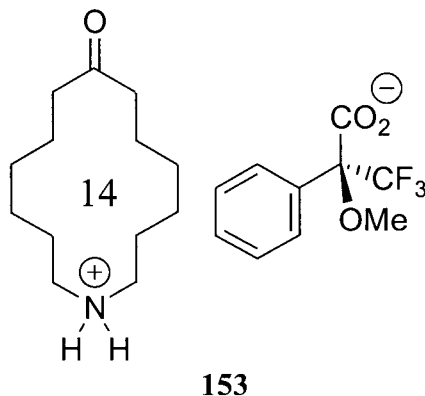
¹H NMR (400 MHz, CDCl₃): δ 1.25 (m, 8H), 1.54 (m, 8H), 2.39 (t, J = 6.1 Hz, 4H), 2.66 (m, 4H), 3.58 (s, 3H, OCH₃), 7.33 (m, 3H), 7.68 (m, 2H), 9.60 (br s, 2H, NH₂).

¹³C NMR (75 MHz, CDCl₃): δ 21.98, 23.34, 23.71, 25.94, 40.08, 43.55, 54.92, 124.86 (q, $^1J_{\text{CF}}$ = 289 Hz), 127.67, 127.75, 128.42, 136.24, 169.92, 212.25.

IR (KBr pellet): 2936, 1709, 1641, 1372, 1171, 1147, 791, 720 cm⁻¹.

Anal. Calcd for C₂₃H₃₄F₃NO₄: C, 62.01; H, 7.69; N, 3.14. Found: C, 62.15; H, 7.84; N, 3.16.

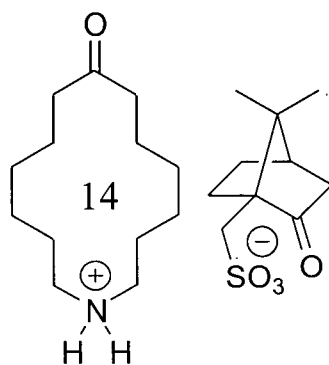
(S)- α -Methoxy- α -(trifluoromethyl)phenylacetate Salt **153**



To a solution of compound **14** (48 mg, 0.23 mmol) in Et₂O (1 mL) was added a solution of (S)- α -Methoxy- α -(trifluoromethyl)phenylacetic acid (*S*-Mosher's acid, 54 mg, 0.23 mmol) in Et₂O (2 mL). The resulting solution was concentrated *in vacuo* and the resulting white solid recrystallized from chloroform / petroleum ether to afford salt **153** (69 mg, 68%) as colourless prisms.

The melting point and spectral data were identical to those reported for compound **152**.

Anal. Calcd for C₂₃H₃₄F₃NO₄: C, 62.01; H, 7.69; N, 3.14. Found: C, 61.78; H, 7.69; N, 3.14.

(1*S*)-10-Camphorsulfonate Salt **154****154**

Solid aminoketone **14** (128 mg, 0.61 mmol) and solid (1*S*)-10-Camphorsulfonic acid (140 mg, 0.61 mmol) were combined and heated until a homogeneous melt was achieved. The liquid was cooled and recrystallized from chloroform / petroleum ether to yield salt **154** as a white solid (212 mg, 79%).

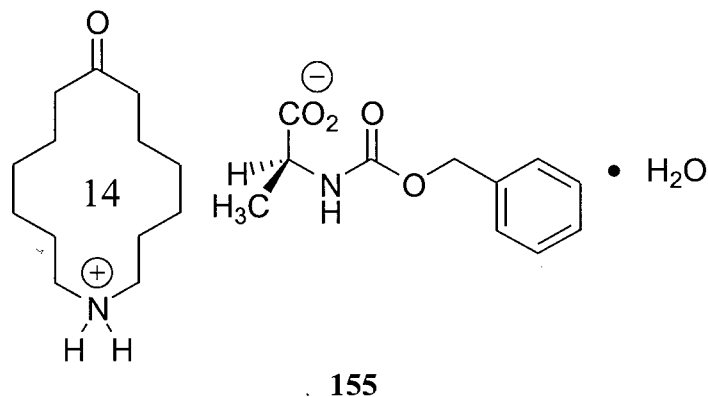
mp: 166-167 °C (chloroform / petroleum ether)

¹H NMR (400 MHz, CDCl₃): δ 0.83 (s, 3H, CH₃), 1.10 (s, 3H, CH₃), 1.38 (m, 10H), 1.72 (m, 8H), 1.87 (d, *J* = 18.2 Hz, 1H), 2.00 (m, 1H), 2.05 (t, *J* = 4.3 Hz, 1H), 2.31 (dt, *J* = 18.2, 3.3 Hz, 1H), 2.50 (t, *J* = 6.3 Hz, 4H), 2.64 (m, 1H), 2.78 (d, *J* = 14.7 Hz, 1H), 3.01 (m, 4H), 3.29 (d, *J* = 14.7 Hz, 1H), 8.29 (br s, 2H, NH₂).

¹³C NMR (100 MHz, CDCl₃): δ 19.85, 20.01, 22.18, 23.37, 23.69, 24.70, 26.07, 27.00, 40.24, 42.65, 42.90, 44.12, 47.42, 47.88, 58.47, 212.10, 216.67.

IR (KBr pellet): 3449, 2942, 1735, 1703, 1621, 1468, 1149, 1030 cm⁻¹.

Anal. Calcd for C₂₃H₄₁NO₅S: C, 62.13; H, 9.52; N, 3.15. Found: C, 62.28; H, 9.58; N, 3.19.

N-Cbz-L-Alanine Salt **155**

A solution of aminoketone **14** (110 mg, 0.52 mmol) and *N*-Cbz-L-Alanine (116 mg, 0.52 mmol) in chloroform (5 mL) was concentrated *in vacuo*. The resulting glassy solid was recrystallized from chloroform / petroleum ether to give salt **155** (150 mg, 66%) as a white powder.

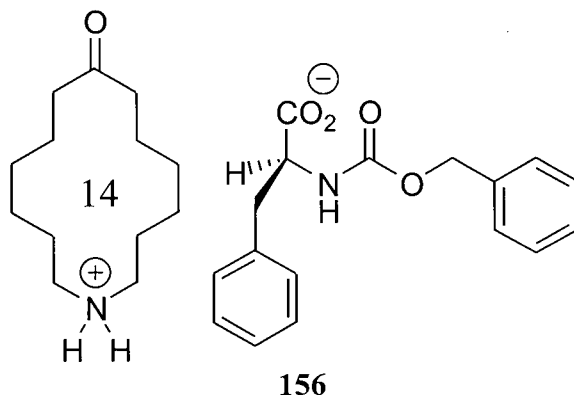
mp: 103-104 °C (chloroform / petroleum ether)

¹H NMR (400 MHz, CDCl₃): δ 1.35 (m, 13H), 1.68 (m, 8H), 2.47 (m, 4H), 2.74 (m, 4H), 4.08 (br s, 1H), 5.10 (m, 2H), 5.76 (br s, 1H), 7.35 (m, 5H), 8.5-9.1 (br s, 2H, NH₂).

¹³C NMR (75 MHz, CDCl₃): δ 19.74, 22.18, 23.50, 23.94, 26.04, 40.39, 43.89, 51.56, 66.34, 128.02, 128.46, 136.78, 155.59, 178.08, 211.90.

IR (KBr pellet): 3333, 2934, 1693, 1577, 1516, 1455, 1396, 1353, 1227, 1057, 702 cm⁻¹.

Anal. Calcd for C₂₄H₄₀N₂O₆: C, 63.69; H, 8.91; N, 6.19. Found: C, 63.30; H, 8.86; N, 6.15.

N-Cbz-L-Phenylalanine Salt **156**

A solution of aminoketone **14** (149 mg, 0.71 mmol) and *N*-Cbz-L-phenylalanine (211mg, 0.71 mmol) in chloroform (3 mL) was concentrated *in vacuo* and the remaining residue recrystallized from chloroform / petroleum ether to give salt **156** (200 mg, 56%) as a white powder.

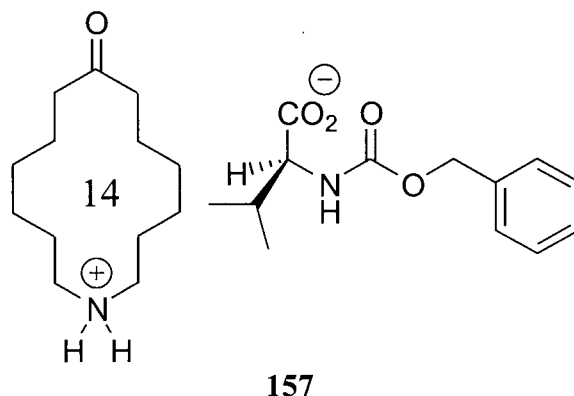
mp: 142-143 °C (chloroform / petroleum ether)

¹H NMR (400 MHz, CDCl₃): δ 1.27 (m, 8H), 1.4-1.7 (m, 8H), 2.42 (t, *J* = 6.5 Hz, 4H), 2.67 (t, *J* = 4.6 Hz, 4H), 3.16 (m, 2H, PhCH₂), 4.34 (br s, 1H), 5.10 (m, 2H), 5.53 (m, 1H), 7.18 (m, 5H), 7.29 (m, 5H), 8.4-9.2 (br s, 2H, NH₂).

¹³C NMR (75 MHz, CDCl₃): δ 22.17, 23.44, 23.82, 23.87, 38.23, 40.35, 43.62, 43.68, 56.62, 66.34, 126.23, 128.00, 128.42, 129.77, 136.80, 137.91, 155.53, 175.87, 175.90, 211.87.

IR (KBr pellet): 3030, 2938, 2863, 1712, 1529, 1396, 1232, 1045, 700 cm⁻¹.

Anal. Calcd for C₃₀H₄₂N₂O₅: C, 70.56; H, 8.29; N, 5.49. Found: C, 70.34; H, 8.31; N, 5.56.

N-Cbz-L-Valine Salt **157**

A solution of aminoketone **14** (104 mg, 0.49 mmol) and *N*-Cbz-L-valine (124 mg, 0.49 mmol) in chloroform (2 mL) was prepared and concentrated *in vacuo*. The residue recrystallized from chloroform / petroleum ether affording salt **157** (75 mg, 33%) as fine white needles.

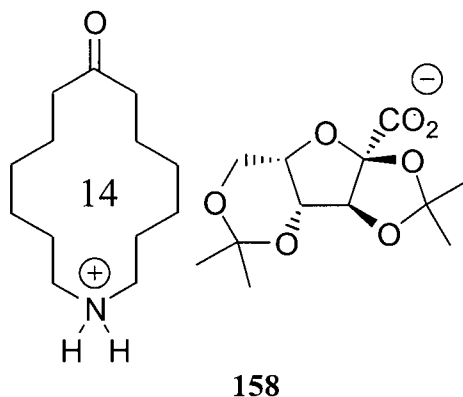
mp: 130-131 °C (chloroform / petroleum ether)

¹H NMR (400 MHz, CDCl₃): δ 0.89 (d, *J* = 6.8 Hz, 3H), 0.95 (d, *J* = 6.8 Hz, 3H), 1.32 (m, 8H), 1.66 (m, 8H), 2.18 (m, 1H), 2.47 (t, *J* = 6.2 Hz, 4H), 2.78 (t, *J* = 6.0 Hz, 4H), 4.07 (br s, 1H), 5.10 (s, 2H), 5.53 (m, 1H), 7.36 (m, 5H); ammonium protons not observed.

¹³C NMR (75 MHz, CDCl₃): δ 17.67, 19.54, 22.24, 23.55, 24.09, 26.03, 31.71, 40.42, 43.94, 60.97, 66.46, 128.02, 128.45, 136.80, 156.35, 176.90, 211.94.

IR (KBr pellet): 3282, 2938, 1713, 1543, 1403, 1236, 1091, 759 cm⁻¹.

Anal. Calcd for C₂₆H₄₂N₂O₅: C, 67.50; H, 9.15; N, 6.06. Found: C, 67.64; H, 9.24; N, 6.04.

2,3:4,6-Di-*O*-isopropylidene-2-keto-L-gulonate Salt **158**

Aminoketone **14** (35 mg, 0.17 mmol) and 2,3:4,6-di-*O*-isopropylidene-2-keto-L-gulonic acid monohydrate (48 mg, 0.17 mmol) were dissolved in chloroform (2 mL). Slow addition of petroleum ether afforded salt **158** (50 mg, 60%) as a white powder.

mp: 189-191 °C (dec.) (chloroform / petroleum ether)

¹H NMR (400 MHz, CDCl₃): δ 1.28 (s, 3H), 1.31 (m, 4H), 1.39 (s, 3H), 1.40 (m, 4H), 1.45 (s, 3H), 1.47 (s, 3H), 1.68 (m, 8H), 2.52 (t, *J* = 6.5 Hz, 4H), 2.93 (t, *J* = 6.5 Hz, 4H), 3.95-4.08 (m, 3H), 4.21 (d, *J* = 2.1 Hz, 1H), 4.86 (s, 1H), 7.7-8.8 (br s, 2H, NH₂).

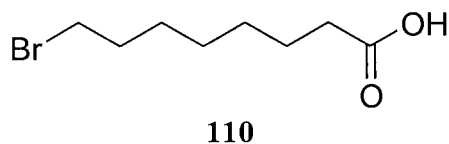
¹³C NMR (75 MHz, CDCl₃): δ 18.74, 22.25, 23.49, 23.63, 26.04, 26.08, 27.12, 28.85, 40.36, 43.49, 60.10, 72.70, 73.49, 87.02, 97.40, 112.22, 112.29, 171.15, 212.37.

IR (KBr pellet): 3444, 2935, 1710, 1611, 1374, 1188, 1133, 1110, 840 cm⁻¹.

Anal. Calcd for C₂₅H₄₃N₀O₈: C, 61.83; H, 8.92; N, 2.88. Found: C, 61.54; H, 9.12; N, 2.95.

5.3.5 Preparation of the Sixteen-Membered Aminoketone 16

8-Bromooctanoic Acid¹¹² (110)



8-Bromooctanol was first prepared according to the procedure of Kang *et al.*:¹¹³ A solution of 1,8-octanediol (30.0 g, 205 mmol) and hydrobromic acid (25 mL of a 48% solution) in benzene (400 mL) was refluxed for 24 h with continuous removal of water from a Dean-Stark trap. The reaction mixture was cooled and extracted successively with 6 M potassium hydroxide (100 mL), 10% HCl (100 mL), water (2 × 100 mL), and brine (75 mL). The organic layer was dried (MgSO₄) and concentrated *in vacuo* to yield the crude bromoalcohol as a pale brown liquid (41.9 g).

The bromoalcohol (10.0 g, 47.8 mmol) was oxidized at 0 °C in acetone (60 mL) by the slow addition of Jones' reagent (prepared from 13.4 g chromium trioxide, 40 mL water, and 11 mL of conc. H₂SO₄). After stirring for 1.5 h, water (500 mL) was added, followed by extraction into Et₂O (4 × 150 mL). After concentration *in vacuo*, the residue was taken up in 2 M potassium hydroxide (300 mL) and washed with Et₂O (2 × 50 mL). Acidification of the aqueous layer with conc. HCl produced a fine white precipitate which was extracted into Et₂O (4 × 100 mL). Drying (MgSO₄) was followed by concentration *in vacuo* to give the bromoacid **110** as a pale green solid (6.5 g, 61 % from the crude bromoalcohol). Despite the trace chromium impurity, the acid thus obtained was analytically pure and gave spectra in accord with those published previously.¹¹²

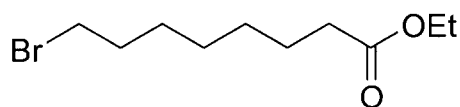
mp: 35-36 °C (lit.¹¹² value 38 °C)

^1H NMR (400 MHz, CDCl_3): δ 1.35 (m, 4H), 1.43 (m, 2H), 1.62 (quint, $J = 7.3$ Hz, 2H), 1.84 (quint, $J = 7.1$ Hz, 2H), 2.33 (t, $J = 7.3$ Hz, 2H), 3.38 (t, $J = 6.8$ Hz, 2H).

^{13}C NMR (100 MHz, CDCl_3): δ 24.49, 27.92, 28.36, 28.80, 32.66, 33.86, 33.94, 180.03.

IR (KBr pellet): 2933, 1708, 1470, 1429, 1408, 1242, 1187, 930, 644 cm^{-1} .

Ethyl 8-Bromooctanoate (**106**)



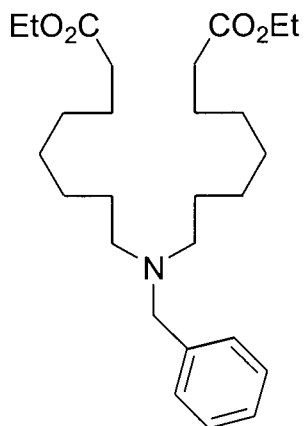
106

A solution of 8-bromooctanoic acid (**110**, 25.0 g, 111.6 mmol) and conc. H_2SO_4 (5.5 mL) in ethanol (325 mL) was refluxed for 8 h.. After cooling, water (100 mL) was added and the mixture extracted with Et_2O (3×200 mL). The combined organic extracts were washed successively with saturated sodium carbonate (2×100 mL), water (2×100 mL) and brine (100 mL), then dried (MgSO_4). Concentration of the product *in vacuo* provided the bromoester **106** (26.6 g, 95%) as a pale yellow oil. Spectral data were in accord with those previously reported.¹¹⁴

^1H NMR (400 MHz, CDCl_3): δ 1.22 (t, $J = 7.1$ Hz, 3H, CH_3), 1.31 (m, 4H), 1.39 (m, 2H), 1.60 (m, 2H), 1.83 (quint, $J = 7.0$ Hz, 2H), 2.27 (t, $J = 7.5$ Hz, 2H), 3.38 (t, $J = 7.0$ Hz, 2H), 4.10 (q, $J = 7.1$ Hz, 2H, OCH_2).

^{13}C NMR (100 MHz, CDCl_3): δ 14.21, 24.78, 27.91, 28.35, 28.86, 32.65, 33.84, 34.22, 60.14, 173.70.

IR (neat): 2934, 1736, 1183 cm^{-1} .

Diethyl 8,8'-Benzyliminodioctanoate (103)**103**

A solution of ethyl 8-bromooctanoate (**106**, 12.0 g, 47.6 mmol), benzylamine (2.55 g, 23.8 mmol) and potassium iodide (9.0 g, 54.2 mmol) in MeCN (200 mL) was stirred at room temperature for 1.5 h. DIPEA (6.75 g, 52.4 mmol) was added and the reaction heated slowly and refluxed for 24 h. The reaction mixture was concentrated *in vacuo* and the residue taken up in Et₂O (100 mL) and saturated sodium carbonate (150 mL). Extraction with Et₂O (3 × 100 mL) was followed by successive washing of the combined organic layers with water (50 mL), 5% sodium bisulfite (50 mL), water (2 × 50 mL), and brine (50 mL). A viscous yellow oil was obtained after drying (MgSO₄) and concentration *in vacuo*. Removal of a low-boiling fraction by distillation (bp 120-130 °C at 1.5 Torr) provided a residue that was chromatographed through a short column of silica (EtOAc eluent) to yield aminodiester **103** (9.1 g, 85%) as a pale yellow oil.

¹H NMR (400 MHz, CDCl₃): δ 1.20-1.31 (m, 18H), 1.43 (m, 4H), 1.59 (quint, *J* = 7.5 Hz, 4H), 2.25 (t, *J* = 7.5 Hz, 4H), 2.36 (t, *J* = 7.2 Hz, 4H), 3.50 (s, 2H, PhCH₂), 4.10 (q, *J* = 7.1 Hz, 4H, OCH₂), 7.20 (m, 1H), 7.28 (m, 4H).

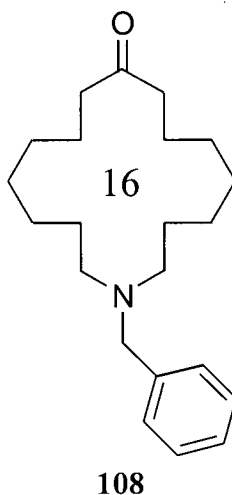
¹³C NMR (100 MHz, CDCl₃): δ 14.16, 24.83, 26.84, 27.12, 29.02, 29.06, 34.23, 53.63, 58.52, 60.00, 126.47, 127.92, 128.68, 140.11, 173.71.

IR (neat): 2932, 1737, 1180 cm^{-1} .

HRMS (EI) calcd for $\text{C}_{27}\text{H}_{45}\text{NO}_4$ 447.3349, found 447.3346.

Anal. Calcd: C, 72.44; H, 10.13; N, 3.13. Found: C, 72.62; H, 10.14; N, 3.20.

9-Aza-9-benzylcyclohexadecanone (108)



A 1L round bottomed flask was equipped with a Hickman still and coupled to an efficient condenser. Into the flask was introduced Et_2O (800 mL) and sodium hexamethyldisilazide (80 mL of a 1.0M solution in THF, 80 mmol), and the solution brought to reflux. A solution of aminodiester **103** (8.0 g, 17.8 mmol) in THF (50 mL) was introduced to the top of the condenser over 40 h *via* syringe pump. The reaction was allowed to reflux for an additional 4 h, then cooled in an ice bath. Glacial acetic acid (80 mL) and water (50 mL) were added, followed by removal of Et_2O *in vacuo*. Water (160 mL) and conc. HCl (100 mL) were introduced, and the solution refluxed for 4 h with continuous distillation (ca. 150 mL removed) at which time evolution of carbon dioxide was observed. The reaction was cooled in an ice bath and rendered strongly alkaline with 50% aqueous potassium hydroxide. Extraction with Et_2O (3×150 mL) was followed by washing of the combined ethereal extracts with water (2×50 mL) and brine (50 mL).

Drying (MgSO_4) and concentration of the organic layer *in vacuo* provided a brown oil which solidified on standing. Recrystallization from MeOH afforded aminoketone **108** (3.50 g, 60%) as a white solid.

mp: 41-42 °C (MeOH)

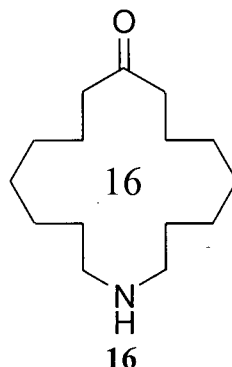
^1H NMR (400 MHz, CDCl_3): δ 1.21-1.43 (m, 16H), 1.65 (quint, $J = 6.7$ Hz, 4H), 2.33 (t, $J = 6.2$ Hz, 4H), 2.42 (t, $J = 6.7$ Hz, 4H), 3.49 (s, 2H, PhCH_2), 7.20 (m, 1H), 7.27 (m, 4H).

^{13}C NMR (100 MHz, CDCl_3): δ 23.78, 26.20, 26.77, 28.08, 28.11, 41.83, 52.84, 59.55, 126.53, 127.96, 128.79, 140.38, 212.83.

IR (thin film): 2931, 2856, 1709, 1454, 737 cm^{-1} .

HRMS (EI) calcd for $\text{C}_{22}\text{H}_{35}\text{NO}$ 329.2719, found 329.2717.

Anal. Calcd: C, 80.19; H, 10.71; N, 4.25. Found: C, 80.26; H, 10.83; N, 4.36.

8-Azacyclohexadecanone (16)

To a room temperature solution of aminoketone **108** (2.45 g, 7.45 mmol) in MeOH (70 mL) was added 96% formic acid (10 mL) and 10% palladium on charcoal (2.2 g). The mixture was stirred for 24 h then filtered through a bed of Celite[®] 545. The solids were triturated with chloroform. The organic filtrate was added to 25% KOH (35 mL), and the mixture extracted with Et₂O (3 × 75 mL). The combined organic extracts were washed with water (2 × 20 mL) followed by brine (20 mL). Drying (MgSO₄), followed by concentration *in vacuo* provided analytically pure aminoketone **16** (1.67 g, 94%) as a white solid.

mp: 50-51 °C (*n*-pentane)

¹H NMR (400 MHz, CDCl₃): δ 1.23-1.38 (m, 13H), 1.41 (quint, *J* = 6.3 Hz, 4H), 1.60 (quint, *J* = 6.9 Hz, 4H), 2.37 (t, *J* = 6.9 Hz, 4H), 2.58 (m, 4H).

¹³C NMR (100 MHz, CDCl₃): δ 23.34, 25.34, 27.22, 27.75, 27.99, 41.71, 47.20, 212.32.

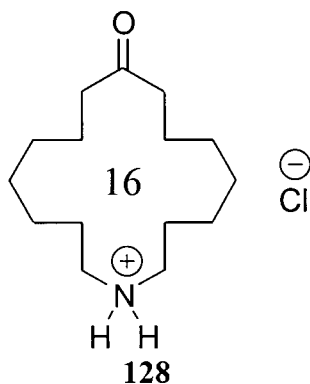
IR (KBr pellet): 3441, 2930, 1708, 1460, 1127 cm⁻¹.

HRMS (EI) calcd for C₁₅H₂₉NO 239.2249, found 239.2245.

Anal. Calcd: C, 75.26; H, 12.21; N, 5.85. Found: C, 75.18; H, 12.34; N, 5.87.

5.3.6 Preparation of the Sixteen-Membered Aminoketone Salts

Hydrochloride Salt **128**



Into a solution of aminoketone **16** (987 mg, 4.13 mmol) in Et₂O (50 mL) was introduced dry HCl gas. The white precipitate that formed was filtered, washed with *n*-pentane (20 mL) and dried *in vacuo*, affording salt **128** (990 mg, 87%) as a white powder.

mp: 200-202 °C (dec.) (MeCN)

¹H NMR (400 MHz, CDCl₃): δ 1.24 (m, 4H), 1.31 (quint, *J* = 7.0 Hz, 4H), 1.48 (quint, *J* = 6.3 Hz, 4H), 1.61 (m, 4H), 1.74 (quint, *J* = 8.0 Hz, 4H), 2.40 (t, *J* = 6.3 Hz, 4H, CH₂C=O), 2.97 (m, 4H, CH₂N), 9.42 (br s, 2H, NH₂).

¹³C NMR (100 MHz, CDCl₃): δ 22.72, 22.86, 24.55, 26.68, 27.38, 42.14, 44.10, 211.78.

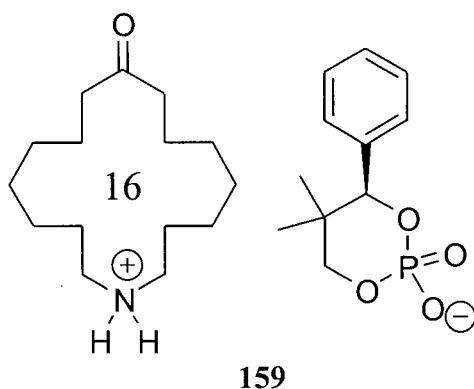
IR (KBr pellet): 3436, 2937, 1703, 1590, 1467 cm⁻¹.

Anal. Calcd for C₁₅H₃₀NOCl: C, 65.31; H, 10.96; N, 5.08. Found: C, 64.99; H, 11.02; N, 5.10.

This structure was confirmed by X-ray crystallographic analysis:

Habit	colourless prisms
Space group	$P\bar{1}$
a , Å	9.980
b , Å	12.345
c , Å	7.621
α (°)	102.88
β (°)	109.75
γ (°)	70.76
Z	2
R	0.054

(*R*)-2-Hydroxy-5,5-dimethyl-4-phenyl-1,3,2-dioxaphosphorinane-2-oxide Salt **159**



Aminoketone **16** (110 mg, 0.46 mmol) and (*R*)-2-hydroxy-5,5-dimethyl-4-phenyl-1,3,2-dioxaphosphorinane-2-oxide (111 mg, 0.46 mmol) were dissolved in hot MeOH (3 mL). The resulting solution was concentrated *in vacuo* and the residue recrystallized from chloroform / petroleum ether to give salt **159** (128 mg, 58%) as colourless needles.

mp: 235-240 °C (dec.) (chloroform / *n*-pentane)

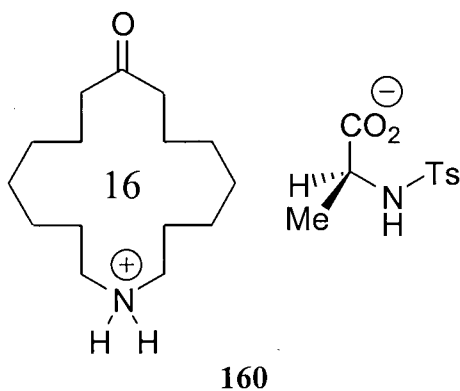
^1H NMR (400 MHz, CDCl_3): δ 0.68 (s, 3H, CH_3), 0.93 (s, 3H, CH_3), 1.23 (m, 8H), 1.32 (m, 4H), 1.55-1.69 (m, 8H), 2.36 (t, $J = 6.3$ Hz, 4H, $\text{CH}_2\text{C}=\text{O}$), 2.86 (m, 4H, CH_2N), 3.64 (dd, $^2J_{\text{HH}} = 10.9$ Hz, $^3J_{\text{HP}} = 23.7$ Hz, 1H, CH_2OP), 4.20 (d, $^2J_{\text{HH}} = 10.9$ Hz, 1H, CH_2OP), 5.12 (d, $^3J_{\text{HP}} = 2.3$ Hz, 1H, CHOP), 7.27 (m, 5H), 9.82 (br s, 2H, NH_2).

^{13}C NMR (100 MHz, CDCl_3): δ 17.43, 21.25, 22.43, 22.93, 24.57, 26.67, 27.42, 36.04 (d, $^2J_{\text{CP}} = 2.8$ Hz, CH_2OP), 42.22, 43.56, 85.11 (d, $^2J_{\text{CP}} = 2.7$ Hz, CHOP), 127.38, 127.48, 127.62, 138.04, 138.15, 211.76.

IR (KBr pellet): 3436, 2931, 1702, 1212, 1080, 1056 cm^{-1} .

Anal. Calcd for $\text{C}_{26}\text{H}_{44}\text{NO}_5\text{P}$: C, 64.84; H, 9.21; N, 2.91. Found: C, 64.62; H, 9.25; N, 2.89.

N-4-Toluenesulfonyl-L-Alanine Salt **160**



To a solution of aminoketone **16** (90 mg, 0.38 mmol) in Et_2O (2 mL) was added a solution of *N*-4-toluenesulfonyl-L-alanine (92 mg, 0.38 mmol) in Et_2O (4 mL). The white

precipitate that formed was filtered and washed with *n*-pentane to give salt **160** (121 mg, 66%) as a white powder.

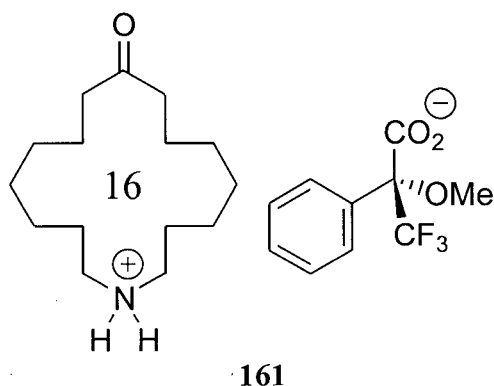
mp: 154-155 °C (chloroform / *n*-pentane)

¹H NMR (400 MHz, CDCl₃): δ 1.20-1.45 (m, 17H), 1.61 (m, 8H), 2.38 (s, 3H, *p*-CH₃), 2.42 (t, *J* = 6.0 Hz, 4H, CH₂CO), 2.83 (t, *J* = 8.0 Hz, 4H, CH₂N), 3.62 (q, *J* = 7.0 Hz, 1H, CH), 6.00 (br s, 1H, NHTs), 7.23 (AA'BB' d, *J* = 8.0 Hz, 2H), 7.74 (AA'BB' d, *J* = 8.0 Hz, 2H).

¹³C NMR (75 MHz, CDCl₃): δ 20.35, 21.51, 22.61, 23.08, 24.40, 26.60, 27.32, 42.04, 44.13, 52.89, 71.66, 127.17, 129.48, 137.55, 142.90, 212.08.

IR (KBr pellet): 3436, 3284, 2932, 1702, 1641, 1577, 1343, 1168 cm⁻¹.

Anal. Calcd for C₂₅H₄₂N₂O₅S: C, 62.21; H, 8.77; N, 5.80. Found: C, 62.31; H, 8.79; N, 5.73.

(*R*)- α -Methoxy- α -(trifluoromethyl)phenylacetate Salt **161**

To a solution of aminoketone **16** (91 mg, 0.38 mmol) in Et₂O (1 mL) was added a solution of (*R*)- α -methoxy- α -(trifluoromethyl)phenylacetic acid (*R*-Mosher's acid, 89 mg, 0.38 mmol) in Et₂O (2 mL). The white precipitate that formed was filtered and washed with *n*-pentane (5 mL) affording salt **161** (141 mg, 78%) as a white powder.

mp: 155-156 °C (chloroform / *n*-pentane)

¹H NMR (400 MHz, CDCl₃): δ 1.13-1.39 (m, 12H), 1.46-1.67 (m, 8H), 2.37 (t, J = 6.3 Hz, 4H, CH₂CO), 2.71 (t, J = 8.7 Hz, 4H, CH₂N), 3.53 (s, 3H, OCH₃), 7.33 (m, 3H), 7.65 (m, 2H), 9.62 (br s, 2H, NH₂).

¹³C NMR (75 MHz, CDCl₃): δ 22.64, 22.78, 24.55, 26.67, 27.37, 42.14, 43.82, 54.87, 125.51 (q, $^1J_{\text{CF}}$ = 288 Hz, CF₃), 127.75, 127.87, 128.52, 135.67, 170.53, 212.08.

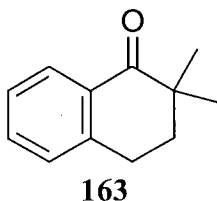
IR (KBr pellet): 3435, 2936, 2858, 1703, 1635, 1370, 1172, 1125, 721 cm⁻¹.

Anal. Calcd for C₂₅H₃₈F₃NO₄: C, 63.41; H, 8.09; N, 2.96. Found: C, 63.34; H, 7.98; N, 3.11.

5.4 Synthesis of the Linearly Conjugated Benzocyclohexadienone **52** and its Salts

5.4.1 Preparation of the Benzocyclohexadienone Carboxylic Acid **52**

3,4-Dihydro-2,2-dimethyl-1(2H)-naphthalenone (**163**)



To a cold (0 °C) suspension of potassium hydride (3.0 g, 75 mmol) and methyl iodide (19.0 g, 134 mmol) in THF (200 mL) was added α -tetralone (5.0 g, 34 mmol) in THF (20 mL) over 0.5 h. After the evolution of hydrogen ceased, the mixture was warmed to room temperature and stirred for 16 h. The reaction was quenched by the careful addition of aqueous ammonium chloride (2.0 M, 75 mL) and was followed by extraction into Et₂O (3 \times 100 mL). The combined ethereal extracts were washed with water (75 mL) and brine (75 mL) followed by concentration *in vacuo*. Vacuum distillation afforded ketone **163** as a straw-coloured liquid (5.42 g, 91%).

bp 107-100 °C (3 Torr). Lit. **bp**: 126 °C (11 Torr),¹¹⁵ 137 °C (15 Torr),¹¹⁶ 150 °C (27 Torr).¹¹⁷

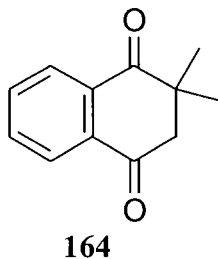
¹H NMR (400 MHz, CDCl₃): δ 1.18 (s, 6H, CH₃), 1.94 (t, J = 6.0 Hz, 2H), 2.95 (t, J = 6.0 Hz, 2H), 7.19 (d, J = 7.5 Hz, 1H), 7.27 (t, J = 5.9 Hz, 1H), 7.41 (t, J = 5.9 Hz, 1H), 8.02 (d, J = 7.5 Hz, 1H).

¹³C NMR (50 MHz, CDCl₃): δ 24.21, 25.54, 36.45, 41.43, 126.43, 127.80, 128.55, 131.28, 132.85, 143.23, 202.68.

IR (neat): 1689 cm^{-1} .

HRMS (EI) calcd for $\text{C}_{12}\text{H}_{14}\text{O}$ 174.1045, found 174.1043.

2,3-Dihydro-2,2-dimethyl-1,4-naphthalenedione (164)



To a solution of ketone **163** (5.20 g, 29.9 mmol) in dichloromethane (50 mL) was added chromium trioxide (900 mg, 9.0 mmol) and *tert*-butylhydroperoxide (80 mL of a 70% solution in water) in four equal portions, with 20 h of stirring at room temperature between each addition. The biphasic reaction mixture was worked up with aqueous sodium thiosulfate (until no longer oxidizing to starch-iodide paper), and extracted into dichloromethane (3×50 mL). The combined organic extracts were washed with water (100 mL), brine (50 mL), and subsequently dried (MgSO_4) and concentrated *in vacuo*. Silica gel chromatography (10% Et_2O in petroleum ether) afforded diketone **164** (3.87 g, 69%) as a pale yellow oil which solidified on standing.

mp: 44-45 $^{\circ}\text{C}$

^1H NMR (400 MHz, CDCl_3): δ 1.29 (s, 6H), 2.91 (s, 2H), 7.71 (m, 2H), 7.99 (m, 1H), 8.07 (m, 1H).

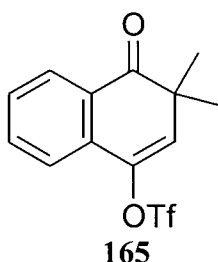
^{13}C NMR (75 MHz, CDCl_3): δ 25.73, 45.53, 51.96, 126.07, 127.51, 133.63, 133.91, 134.40, 134.86, 196.25, 201.30.

IR (KBr pellet): 2970, 1696, 1594, 1291, 760 cm^{-1} .

HRMS (EI) calcd for $\text{C}_{12}\text{H}_{12}\text{O}_2$ 188.0837, found 188.0837.

Anal. Calcd C, 76.57; H, 6.43. Found: C, 76.40; H, 6.38.

3,4-Dihydro-3,3-dimethyl-4-oxo-1-naphthalenyl Trifluoromethanesulfonate (**165**)



To a cold ($-78\text{ }^{\circ}\text{C}$) solution of LDA (10.8 mmol; formed by reaction of DIPA (1.7 mL, 11.8 mmol) and butyllithium (10.8 mmol)) in THF (120 mL) was added diketone **164** (1.85 g, 9.84 mmol) in THF (10 mL) over a period of 10 minutes. The solution was stirred in the cold for 1.5 h, followed by the addition of *N*-phenyl triflimide (4.04 g, 11.3 mmol) as a solid in one portion. The suspension was allowed to warm to room temperature and stirred for an additional 2 h. Workup with aqueous sodium bicarbonate (5% solution, 20 mL) was followed by extraction into Et_2O ($3 \times 50\text{ mL}$), washing of the combined organic extracts with water (50 mL) followed by brine (50 mL), then drying (MgSO_4) and concentration *in vacuo*. Purification by silica gel chromatography (15% Et_2O in petroleum ether) gave vinyl triflate **165** as an off-white solid (2.74 g, 87%).

mp: 39-40 $^{\circ}\text{C}$

^1H NMR (400 MHz, C_6D_6): δ 0.98 (s, 6H), 5.80 (s, 1H), 6.86 (t, $J = 7.5\text{ Hz}$, 1H), 7.00 (dt, $J = 0.9, 7.7\text{ Hz}$, 1H), 7.37 (d, $J = 7.7\text{ Hz}$, 1H), 8.09 (dd, $J = 1.1, 7.7\text{ Hz}$, 1H).

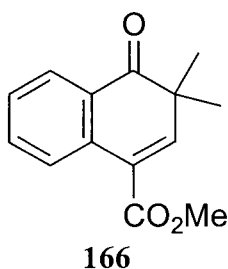
^{13}C NMR (50 MHz, C_6D_6): δ 25.51, 45.57, 119.13 (q, $^1J_{\text{CF}} = 320$ Hz), 122.01, 128.23, 129.47, 129.81, 129.89, 132.37, 134.48, 142.09, 198.78.

IR (KBr pellet): 2983, 1665, 1595, 1427, 1142, 1018, 837 cm^{-1} .

HRMS (EI) calcd for $\text{C}_{13}\text{H}_{11}\text{F}_3\text{O}_4\text{S}$ 320.0330, found 320.0327.

Anal. Calcd C, 48.75; H, 3.46. Found: C, 48.37; H, 3.76.

Methyl 3,4-Dihydro-3,3-dimethyl-4-oxo-1-naphthalenecarboxylate (**166**)



To a solution of Palladium (II) acetate (176 mg, 0.8 mmol), triphenylphosphine (444 mg, 1.7 mmol), DIPEA (4.5 mL, 26 mmol), and anhydrous MeOH (20 mL) in DMF (50 mL) was added vinyl triflate **165** (2.18 g, 6.80 mmol) under an atmosphere of carbon monoxide. The reaction was stirred at 50 °C for 9 h, during which time a steady stream of carbon monoxide gas was bubbled through the mixture. Addition of Et_2O (200 mL), followed by washing of the organic layer with brine (6×50 mL), drying (MgSO_4), and concentration *in vacuo* provided ester **166** (1.33 g, 85%) as a pale yellow liquid.

^1H NMR (400 MHz, CDCl_3): δ 1.30 (s, 6H), 3.85 (s, 3H), 7.38 (dt, $J = 1.0, 7.4$ Hz, 1H), 7.59 (dt, $J = 1.5, 7.0$ Hz, 1H), 8.06 (dt, $J = 1.4, 7.7$ Hz, 1H), 8.15 (d, $J = 7.4$ Hz, 1H).

^{13}C NMR (75 MHz, CDCl_3): δ 25.14, 44.98, 52.08, 125.18, 126.47, 127.49, 128.38, 128.79, 134.03, 134.29, 148.96, 166.43, 201.85.

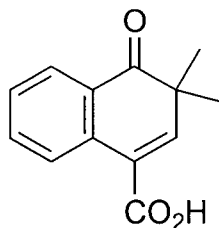
IR (neat): 2970, 1729, 1682, 1595, 1032 cm^{-1} .

UV / VIS (MeCN, 5.0×10^{-4} M): 322 (2160) nm ($\text{M}^{-1}\text{cm}^{-1}$).

HRMS (EI) calcd for $\text{C}_{14}\text{H}_{14}\text{O}_3$ 230.0943, found 230.0949.

Anal. Calcd C, 73.03; H, 6.13. Found: C, 72.77; H, 6.15.

3,4-Dihydro-3,3-dimethyl-4-oxo-1-naphthalenecarboxylic Acid (52)



52

To a room temperature solution of ester **166** (545 mg, 2.37 mmol) in THF (10 mL) was added a solution of lithium hydroxide monohydrate (1.0 g, 24 mmol) in water (5 mL). The reaction mixture was stirred for 16 h, then diluted with Et_2O (50 mL) and extracted into water (3×25 mL). The combined aqueous extracts were acidified to pH 4 with 2 M hydrochloric acid and extracted with Et_2O (3×40 mL). The combined organic extracts were washed with water (2×25 mL) and brine (50 mL), then dried (MgSO_4) and concentrated *in vacuo* to yield analytically pure acid **52** (502 mg, 98%) as a white powder.

mp: 161-162 °C

¹H NMR (400 MHz, CDCl₃): δ 1.37 (s, 6H), 7.30 (s, 1H), 7.44 (dt, *J* = 0.8, 7.5 Hz, 1H), 7.65 (dt, *J* = 1.4, 8.4 Hz, 1H), 8.11 (dd, *J* = 1.4, 7.7 Hz, 1H), 8.29 (d, *J* = 7.7 Hz, 1H). Acidic proton not observed.

¹³C NMR (100 MHz, CDCl₃): δ 25.08, 45.31, 124.31, 126.65, 127.72, 128.66, 128.92, 133.59, 134.41, 151.97, 171.46, 201.76.

IR (KBr pellet): 2976, 1695, 1673, 1251, 789 cm⁻¹.

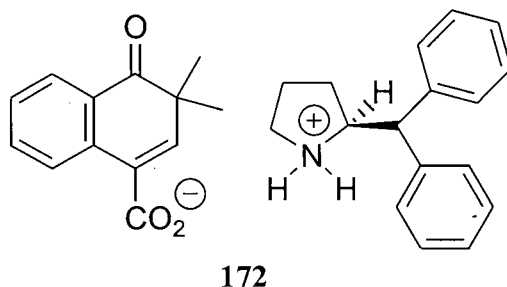
UV / VIS (MeCN, 2.2 × 10⁻³ M): 320 (13,000) nm (M⁻¹cm⁻¹).

HRMS (EI) calcd for C₁₃H₁₂O₃ 216.0786, found 216.0785.

Anal. Calcd C, 72.21; H, 5.59. Found: C, 71.95; H, 5.60.

5.4.2 Preparation of the Benzocyclohexadienone Salts

(2S)-Diphenylmethylpyrrolidine Salt (172)



Carboxylic acid **52** (120 mg, 0.56 mmol) and (2S)-Diphenylmethylpyrrolidine (133 mg, 0.56 mmol) were dissolved in hot EtOAc (4 mL). The solution was cooled and the solvent allowed to evaporate over a number of days. Crystals of salt **172** (159 mg, 63%) were collected, washed with *n*-pentane, and air-dried.

mp: 182-184 °C (EtOAc)

¹H NMR (400 MHz, CDCl₃): δ 1.36 (s, 6H), 1.57 (m, 1H), 1.85 (m, 3H), 2.90 (t, *J* = 6.4 Hz, 2H), 4.15 (m, 5H), 7.1-7.3 (m, 9H), 7.42 (m, 2H), 7.60 (dt, *J* = 1.5, 7.9 Hz, 1H), 8.09 (m, 2H).

¹³C NMR (75 MHz, CDCl₃): δ 23.84, 25.51, 25.58, 30.76, 44.91, 44.99, 54.82, 61.98, 127.19, 127.23, 127.40, 127.44, 127.62, 127.66, 127.78, 128.11, 128.91, 128.95, 129.14, 133.85, 140.70, 141.39, 144.33, 171.80, 203.30.

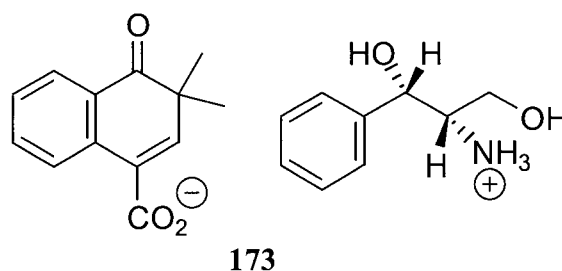
IR (KBr pellet): 3434, 1669, 1639, 1553, 1476, 707 cm⁻¹.

Anal. Calcd for C₃₀H₃₁NO₃: C, 79.44; H, 6.89; N, 3.09. Found: C, 79.48; H, 6.86; N, 3.21.

This structure was confirmed by X-ray crystallographic analysis:

Habit	colourless blocks
Space group	$P2_1$
a , Å	14.299(1)
b , Å	8.2457(6)
c , Å	21.780(2)
α (°)	90
β (°)	98.126(2)
γ (°)	90
Z	4
R	0.045

(1*S*, 2*S*)-2-Amino-1,3-dihydroxypropylbenzene Salt (**173**)



To a cold (0 °C) solution of carboxylic acid **52** (100 mg, 0.46 mmol) and (1*S*, 2*S*)-2-amino-1,3-dihydroxypropylbenzene (77 mg, 0.46 mmol) in Et₂O (3 mL) was added *n*-pentane (6 mL) over 20 minutes. The precipitate that formed was filtered, washed with petroleum ether (5 mL) and air-dried, affording salt **173** (156 mg, 88%) as off-white microcrystals.

mp: 84-88 °C (MeCN / *n*-pentane)

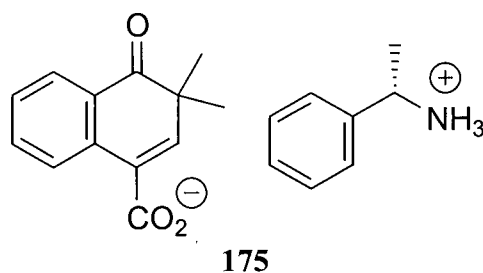
^1H NMR (400 MHz, CDCl_3): δ 0.67 (d, $J = 9.3$ Hz, 1H), 0.78 (s, 3H), 1.05 (s, 3H), 1.29 (s, 6H), 1.36 (m, 1H), 1.60-1.85 (m, 5H), 2.21 (m, 2H), 2.78 (m, 2H), 6.76 (s, 1H), 7.34 (t, $J = 6.7$ Hz, 1H), 7.51 (dt, $J = 1.6, 7.9$ Hz, 1H), 8.06 (dd, $J = 1.4, 6.9$ Hz, 1H), 8.16 (d, $J = 7.3$ Hz, 1H). Ammonium protons appear as a broad peak 6.7-7.6 ppm (3H).

^{13}C NMR (100 MHz, CDCl_3): δ 19.59, 23.07, 25.60, 27.59, 32.92, 38.37, 40.23, 40.87, 40.91, 43.83, 44.77, 45.68, 126.87, 127.58, 127.83, 129.19, 131.26, 133.87, 136.11, 143.68, 173.82, 203.06.

IR (KBr pellet): 2916, 1682, 1640, 1551, 1392, 797 cm^{-1} .

Anal. Calcd for $\text{C}_{23}\text{H}_{31}\text{NO}_3$: C, 74.76; H, 8.46; N, 3.79. Found: C, 74.96; H, 8.59; N, 3.79.

(S)-1-Phenylethylamine Salt **175**



To a solution of (*S*)-1-phenylethylamine (56 mg, 0.46 mmol) in Et_2O (1 mL) was added a solution of carboxylic acid **52** (100 mg, 0.46 mmol) in Et_2O (2 mL). The solution was cooled to -20 $^{\circ}\text{C}$ and slowly diluted with *n*-pentane (15 mL). The microcrystals that formed were filtered under argon, washed with anhydrous *n*-pentane (2 mL), and air-dried to yield salt **175** (126 mg, 81%).

mp: 96-104 °C (precipitated by *n*-pentane in Et₂O – other solvents gave rise only to oils)

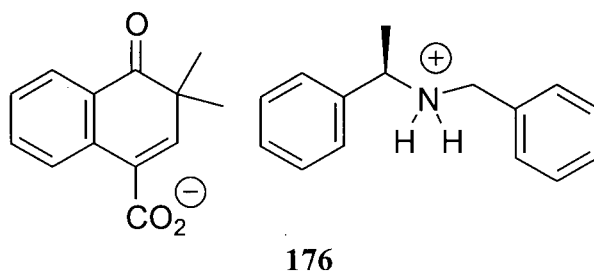
¹H NMR (400 MHz, CDCl₃): δ 1.21 (s, 6H), 1.52 (d, *J* = 6.8 Hz, 3H), 4.20 (q, *J* = 6.6 Hz, 1H), 6.63 (s, 1H), 7.19 (m, 2H), 7.28-7.65 (br m, 8H), 7.96 (d, *J* = 7.9 Hz, 1H), 8.05 (dd, *J* = 1.4, 7.7 Hz, 1H).

¹³C NMR (75 MHz, CDCl₃): δ 21.68, 25.40, 44.59, 51.03, 126.04, 126.92, 127.37, 127.62, 128.41, 128.89, 129.01, 131.23, 133.85, 135.98, 139.10, 143.54, 173.69, 203.11.

IR (KBr pellet): 3444, 2965, 1677, 1637, 1543, 1397, 699 cm⁻¹.

Anal. Calcd for C₂₁H₂₃NO: C, 74.75; H, 6.87; N, 4.15. Found: C, 74.35; H, 6.71; N, 3.94.

(*R*)-*N*-Benzyl-1-phenylethylamine Salt **176**



Solid acid **52** (100 mg, 0.46 mmol) was mixed with (*R*)-*N*-benzyl-1-phenylethylamine (98 mg, 0.46 mmol) and the resulting sticky oil taken up in MeOH (1 mL). To this was added petroleum ether (20 mL), and the resulting biphasic mixture allowed to stand open to the air. Crystallization of salt **176** as colourless prisms (152 mg, 77%) ensued.

mp: 107-109 °C (MeOH / Et₂O)

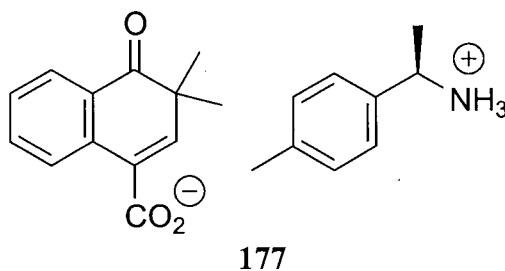
¹H NMR (200 MHz, CDCl₃): δ 1.29 (s, 3H), 1.31 (s, 3H), 1.52 (d, *J* = 6.6 Hz, 3H), 3.72 (AB quartet, *J* = 13.0 Hz, 2H), 4.02 (q, *J* = 6.6 Hz, 1H), 6.69 (s, 1H), 7.2-7.4 (br m, 11H), 7.58 (m, 1H), 8.11 (m, 2H), 9.60 (br s, 2H).

¹³C NMR (100 MHz, CDCl₃): δ 21.47, 25.50, 25.53, 44.73, 49.41, 57.39, 127.22, 127.31, 127.44, 127.68, 128.33, 128.41, 128.57, 128.95, 129.10, 129.60, 131.01, 133.82, 133.91, 136.16, 139.16, 143.39, 172.42, 203.33.

IR (KBr pellet): 2970, 1674, 1638, 1619, 1593, 1554, 1393, 705 cm⁻¹.

Anal. Calcd for C₂₈H₂₉NO₃: C, 78.66; H, 6.84; N, 3.28. Found: C, 78.73; H, 6.84; N, 3.30.

(*R*)-1-(4-Methylphenyl)ethylamine Salt **177**



Carboxylic acid **52** (100 mg, 0.46 mmol) and (*R*)-1-(4-methylphenyl)ethylamine (63 mg, 0.46 mmol) were dissolved in refluxing Et₂O (5 mL). The volume of solvent was reduced to (1 mL) *in vacuo* and the resulting solution allowed to stand at room temperature for 2 h. Colourless crystals of salt **177** deposited on the bottom of the flask and were isolated by suction filtration (145 mg, 89%).

mp: 129-138 °C (dec.) (Et₂O)

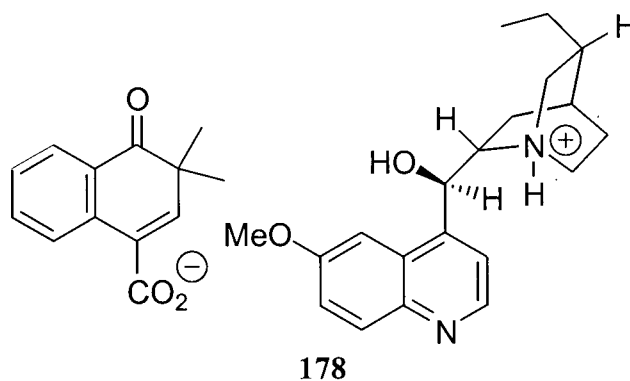
¹H NMR (200 MHz, CDCl₃): δ 1.15 (s, 6H), 1.46 (d, *J* = 6.8 Hz, 3H), 2.17 (s, 3H), 4.12 (q, *J* = 6.6 Hz, 1H), 6.42 (s, 1H), 7.04 (AA'BB' quartet, *J* = 7.9 Hz, 4H), 7.32 (m, 2H), 7.83 (m, 1H), 8.01 (m, 1H), 8.88 (br s, 3H).

¹³C NMR (75 MHz, CDCl₃): δ 21.03, 21.62, 25.33, 25.37, 44.53, 50.74, 125.98, 127.02, 127.31, 127.53, 129.00, 129.51, 129.53, 131.36, 133.73, 136.09, 137.98, 143.38, 173.70, 203.14. The methyl groups are made diastereotopic due to close ion-pairing in solution.

IR (KBr pellet): 2973, 1688, 1635, 1562, 1522, 1392, 791 cm⁻¹.

Anal. Calcd for C₂₂H₂₅NO₃: C, 75.19; H, 7.17; N, 3.99. Found: C, 75.06; H, 7.17; N, 3.97.

Hydroquinine Salt **178**



To a solution of carboxylic acid **52** (100 mg, 0.46 mmol) in Et₂O (3 mL) was added hydroquinine (151 mg, 0.46 mmol) and MeOH (250 μL). The solution was heated to reflux and allowed to cool to room temperature. A white precipitate formed over 30

minutes and was subsequently isolated by suction filtration, washed with *n*-pentane (2 mL), and air-dried, affording salt **178** (208 mg, 89%) as a white powder.

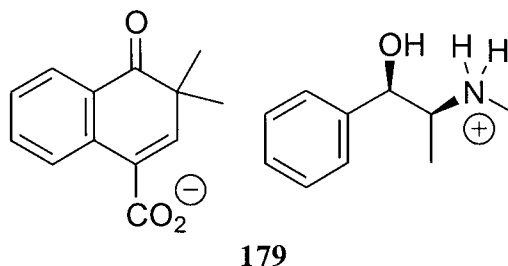
mp: 143-148 °C (MeOH / Et₂O)

¹H NMR (200 MHz, CDCl₃): δ 0.71 (t, *J* = 6.7 Hz, 3H), 1.12 (m, 3H), 1.33 (s, 3H), 1.36 (s, 3H), 1.4-2.0 (br m, 6H), 2.58 (dd, *J* = 3.3, 13.2 Hz, 1H), 2.88 (dt, *J* = 4.7, 11.3 Hz, 1H), 3.16 (t, *J* = 8.1 Hz, 1H), 3.42 (m, 1H), 3.63 (s, 3H), 4.14 (m, 1H), 6.31 (s, 1H), 6.56 (s, 1H), 6.80 (d, *J* = 2.6 Hz, 1H), 7.01 (dd, *J* = 2.4, 9.3 Hz, 1H), 7.30 (t, *J* = 7.5 Hz, 1H), 7.39 (d, *J* = 4.4 Hz, 1H), 7.52 (dt, *J* = 1.5, 7.8 Hz, 1H), 7.67 (d, *J* = 9.2 Hz, 1H), 8.04 (m, 2H), 8.46 (d, *J* = 4.5 Hz, 1H).

¹³C NMR (100 MHz, CDCl₃): δ 11.42, 17.85, 24.59, 24.95, 25.68, 26.89, 35.66, 43.21, 44.64, 55.50, 56.56, 59.89, 65.97, 99.92, 118.30, 121.33, 125.11, 127.02, 127.26, 127.50, 128.99, 131.32, 132.39, 133.81, 136.46, 141.11, 143.49, 144.85, 146.97, 157.65, 174.70, 203.54.

IR (KBr pellet): 2963, 1673, 1638, 1620, 1592, 1240, 797 cm⁻¹.

Anal. Calcd for C₃₃H₃₈N₂O₅ C, 73.04; H, 7.06; N, 5.16. Found: C, 72.96; H, 7.11; N, 5.19.

(1*R*, 2*S*)-Ephedrine Salt 179

To a solution of (1*R*, 2*S*)-ephedrine (76 mg, 0.46 mmol) in Et₂O (3 mL) was added a solution of carboxylic acid **52** (100 mg, 0.46 mmol) in Et₂O (1 mL). The white precipitate of salt **179** formed immediately and was isolated by suction filtration (155 mg, 88%).

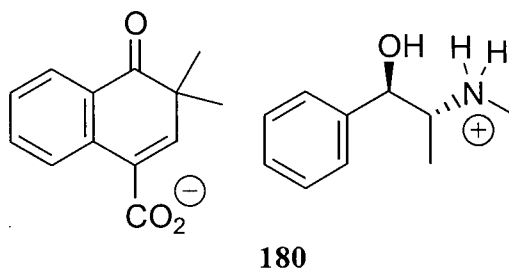
mp: 148-149 °C (EtOAc)

¹H NMR (400 MHz, CDCl₃): δ 1.04 (d, *J* = 6.7 Hz, 3H), 1.28 (s, 6H), 2.61 (s, 3H), 3.20 (m, 1H), 4.68 (d, *J* = 9.8 Hz, 1H), 6.75 (s, 1H), 7.32 (m, 6H), 7.51 (m, 1H), 8.04 (d, *J* = 6.6 Hz, 1H), 8.14 (d, *J* = 8.2 Hz, 1H), 8.4-8.8 (br s, 3H).

¹³C NMR (100 MHz, CDCl₃): δ 1.74, 25.49, 25.55, 30.16, 44.77, 60.73, 75.37, 127.06, 127.25, 127.33, 127.62, 128.47, 128.74, 129.10, 131.39, 133.96, 136.21, 140.42, 143.31, 174.42, 203.44.

IR (KBr pellet): 3311, 2965, 1681, 1638, 1576, 1390, 703 cm⁻¹.

Anal. Calcd for C₂₃H₂₇NO₄: C, 72.42; H, 7.13; N, 3.67. Found: C, 72.78; H, 7.06; N, 3.65.

(1*R*, 2*R*)-Pseudoephedrine Salt **180**

A solution of (1*R*, 2*R*)-pseudoephedrine (76 mg, 0.46 mmol) and carboxylic acid **52** (100 mg, 0.46 mmol) in EtOAc (6 mL) was concentrated *in vacuo*. The residue was taken up in MeCN (2 mL) and cooled to 0 °C. Petroleum ether (10 mL) was added dropwise with stirring. The white precipitate was isolated by suction filtration, washed with *n*-pentane (2 mL), and air-dried to give salt **180** (143 mg, 81%) as an off-white powder.

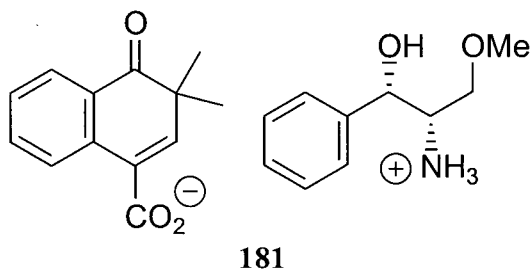
mp: 144-145 °C (MeCN / hexanes)

¹H NMR (400 MHz, CDCl₃): δ 1.03 (d, *J* = 6.6 Hz, 3H), 1.30 (s, 6H), 2.61 (s, 3H), 3.19 (m, 1H), 4.67 (d, *J* = 9.6 Hz, 1H), 6.73 (s, 1H), 7.32 (m, 6H), 7.5-7.8 (br s, 3H), 7.53 (m, 1H), 8.04 (dd, *J* = 1.3, 7.8 Hz, 1H), 8.13 (d, *J* = 7.5 Hz, 1H).

¹³C NMR (75 MHz, CDCl₃): δ 12.69, 25.48, 25.56, 30.08, 44.70, 60.55, 75.33, 127.03, 127.24, 127.27, 127.57, 128.40, 128.68, 129.05, 131.84, 133.93, 136.28, 140.50, 142.72, 174.61, 203.50. The methyl groups are made diastereotopic due to close ion-pairing in solution.

IR (KBr pellet): 3317, 1682, 1638, 1576, 1389, 703 cm⁻¹.

Anal. Calcd for C₂₃H₂₇NO₄: C, 72.42; H, 7.13; N, 3.67. Found: C, 72.32; H, 7.17; N, 3.83.

(1*S*, 2*S*)-2-Amino-3-methoxy-1-phenyl-1-propanol Salt **181**

To a solution of carboxylic acid **52** (100 mg, 0.46 mmol) in Et₂O (2 mL) was added a solution of (1*S*, 2*S*)-2-amino-3-methoxy-1-phenyl-1-propanol (84 mg, 0.46 mmol) in Et₂O (3 mL). Colourless crystals of salt **181** (131 mg, 71%) grew over the course of 24 h.

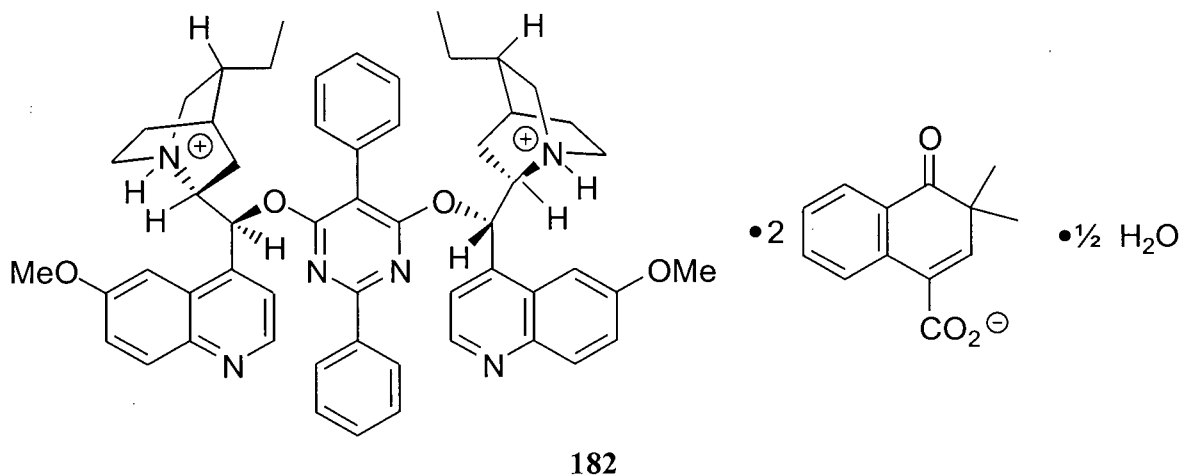
mp: 101-103 °C (Et₂O)

¹H NMR (200 MHz, CDCl₃): δ 1.22 (s, 6H), 3.10 (s, 3H, OCH₃), 3.16 (m, 2H), 3.39 (m, 1H), 4.80 (d, *J* = 9.3 Hz, 1H), 6.72 (s, 1H, C=CH), 7.32 (m, 6H), 7.46 (m, 1H), 7.62 (br s, 4H, NH₃ + OH), 8.02 (d, *J* = 7.8 Hz, 1H), 8.11 (d, *J* = 7.4 Hz, 1H).

¹³C NMR (75 MHz, CDCl₃): δ 25.41, 25.47, 44.79, 57.44, 59.01, 69.93, 72.28, 126.63, 127.19, 127.38, 127.76, 128.50, 128.77, 129.07, 130.82, 134.08, 135.96, 140.20, 143.99, 173.82, 203.25.

IR (KBr pellet): 2965, 1678, 1640, 1544, 1392, 703 cm⁻¹.

Anal. Calcd for C₂₃H₂₇NO₅: C, 69.50; H, 6.85; N, 3.52. Found: C, 69.57; H, 6.90; N, 3.59.

DHQD₂PYR Salt **182**

Carboxylic acid **52** (100 mg, 0.46 mmol) and DHQD₂PYR (204 mg, 0.23 mmol) were dissolved in hot MeOH (2 mL) and the resulting solution cooled to room temperature. Addition of Et₂O (3 mL) induced the crystallization of salt **182** (197 mg, 65%) as an off-white solid.

mp: 187-189 °C (MeOH / Et₂O)

¹H NMR (400 MHz, CDCl₃): δ 0.65(t, *J* = 6.0 Hz, 6H, CH₂CH₃), 0.81 (s, 6H, CH₃), 0.87 (s, 6H, CH₃), 1.36 (m, 2H), 1.50 (m, 2H), 1.66 (m, 4H), 1.83 (m, 2H), 2.21 (t, *J* = 11.6 Hz, 2H), 2.83 (t, *J* = 10.2 Hz, 2H), 2.98 (m, 2H), 3.21 (m, 2H), 3.42 (m, 4H), 3.81 (s, 6H, OCH₃), 6.41 (s, 2H), 6.63 (m, 4H), 6.92 (m, 4H), 7.25 (m, 2H), 7.43 (dd, *J* = 2.4, 9.2 Hz, 2H), 7.48 (d, *J* = 4.5 Hz, 2H), 7.55 (t, *J* = 7.4 Hz, 2H), 7.79 (m, 12H), 7.93 (m, 2H), 8.06 (d, *J* = 9.2 Hz, 2H), 8.79 (d, *J* = 4.4 Hz, 2H).

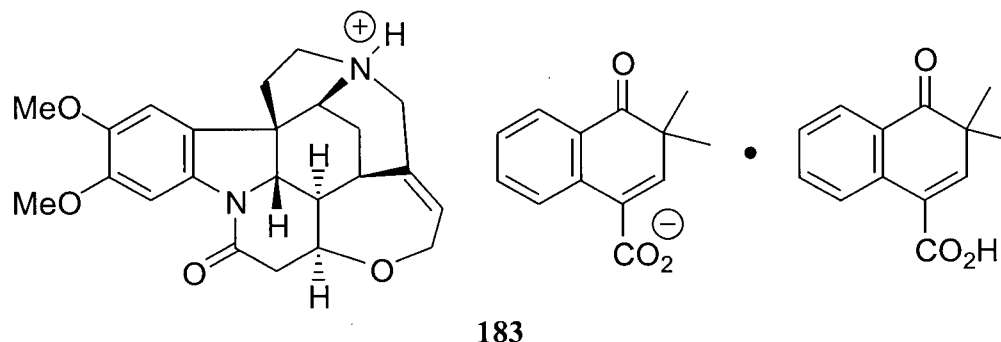
¹³C NMR (75 MHz, CDCl₃): δ 12.12, 19.44, 23.65, 24.21, 24.81, 25.17, 25.66, 35.42, 44.33, 48.34, 49.51, 56.53, 57.98, 72.62, 100.90, 104.37, 117.77, 123.17, 126.22, 126.77, 126.92, 127.00, 127.08, 127.67, 127.91, 128.36, 128.53, 129.18, 130.26,

130.46, 130.82, 131.04, 131.30, 131.89, 133.59, 135.43, 135.89, 142.23, 143.26, 144.67, 147.17, 159.18, 165.58, 173.54, 203.47.

IR (KBr pellet): 3414, 2962, 1667, 1620, 1591, 1543 cm^{-1} .

Anal. Calcd for $\text{C}_{82}\text{H}_{85}\text{N}_6\text{O}_{10.5}$: C, 74.47; H, 6.48; N, 6.35. Found: C, 74.45; H, 6.71; N, 6.10.

Brucine Complex **183**



To a solution of brucine (191 mg, 0.46 mmol) in MeOH (5 mL) was added carboxylic acid **52** (100 mg, 0.46 mmol). The resulting solution was diluted with Et₂O (5 mL) and sealed for 48 h. Colourless crystals (237 mg, 81%) of complex **183** were harvested from the mother liquor.

mp: 187-190 °C (MeOH / Et₂O)

¹H NMR (200 MHz, CDCl₃): δ 1.39-1.43 (m, 1H), 1.32 (s, 12H, CH₃), 1.71 (d, J = 15.1 Hz, 1H), 2.02 (dd, J = 5.9, 13.4 Hz, 1H), 2.25 (sextet, J = 5.9 Hz, 1H), 2.60 (dt, J = 4.0, 15.1 Hz, 1H), 2.69 (dd, J = 3.0, 17.0 Hz, 1H), 3.05-3.24 (m, 3H), 3.33 (br s, 1H), 3.85 (s, 3H, OCH₃), 3.87 (d, J = 3.9 Hz, 1H), 3.90 (s, 3H, OCH₃), 3.98 (d, J

= 10.4 Hz, 1H), 4.05-4.27 (m, 3H), 4.36 (m, 1H), 4.60 (br s, 1H), 6.27 (m, 1H), 6.91 (s, 1H), 7.02 (s, 2H), 7.38 (m, 2H), 7.58 (m, 2H), 7.80 (s, 1H), 8.08 (m, 2H), 8.23 (m, 2H).

^{13}C NMR (100 MHz, CDCl_3): δ 11.60, 15.24, 19.88, 24.67, 24.85, 25.10, 25.21, 27.19, 35.71, 42.87, 44.45, 56.33, 56.38, 57.95, 65.82, 73.04, 100.75, 104.43, 117.75, 122.93, 125.99, 126.90, 127.02, 127.22, 127.82, 127.93, 128.44, 128.64, 128.85, 130.38, 130.58, 130.90, 131.95, 133.77, 135.48, 135.95, 142.01, 144.63, 147.22, 159.13, 161.91, 165.49, 173.52, 203.49.

IR (KBr pellet): 3452, 2965, 2866, 2831, 2376, 1663, 1597, 1501, 1239, 1112, 793 cm^{-1} .

Anal. Calcd for $\text{C}_{48}\text{H}_{50}\text{N}_2\text{O}_{10}$: C, 70.75; H, 6.18; N, 3.44. Found: C, 71.14; H, 6.03; N, 3.43.

This structure was confirmed by X-ray crystallographic analysis:

Habit	colourless prisms
Space group	$P2_12_12_1$
a , Å	9.569(1)
b , Å	14.204(4)
c , Å	29.98(1)
α (°)	90
β (°)	90
γ (°)	90
Z	4
R	0.041

Chapter 6 – Photochemical Studies

6.1 General Considerations

Light Sources and Filters

Irradiations were performed using either a 450 W Hanovia medium-pressure mercury lamp in a water-cooled immersion well, or a Rayonet Photochemical Chamber Reactor (model RPR-100) fitted with 16 RPR-3500 lamps (384 W total, line emission at 350 nm). Light from the Hanovia lamp was filtered through Pyrex (transmits $\lambda \geq 290$ nm), Corning glass #9720 (transmits $\lambda \geq 232$ nm, quartz reaction vessels used), or a uranium glass filter (transmits $\lambda \geq 330$ nm).

Solution State Photolyses

HPLC grade or spectral grade (Fisher Chemical) solvents were used for all solution state photochemical reactions. Reaction solutions were purged with nitrogen for at least 15 minutes prior to irradiation, and the reactions were performed either in sealed reaction vessels or under a positive pressure of nitrogen.

Analytical Solid State Photolyses

The solid material (2-5 mg), either as ground single crystals or in polycrystalline form (powder), was sandwiched between two quartz plates and spread out to cover a surface area of approximately 10 cm². The plates were fixed to one another with tape, and the assembly heat-sealed in a poly(ethylene) bag under nitrogen. Following irradiation, the sample was quantitatively washed from the plates with an appropriate solvent, and concentrated *in vacuo*. For neutral molecules, the sample was analyzed directly by gas chromatography and/or NMR spectroscopy. Photolysates of the salts derived from aminoketones **12**, **14**, and **16** were treated with dilute aqueous sodium hydroxide prior to analysis in order to liberate the free amines. Reaction mixtures containing ketoacid **52** or its salts were derivatized with diazomethane, and subsequent analysis based on the corresponding methyl ester **166**.

Low-Temperature Studies

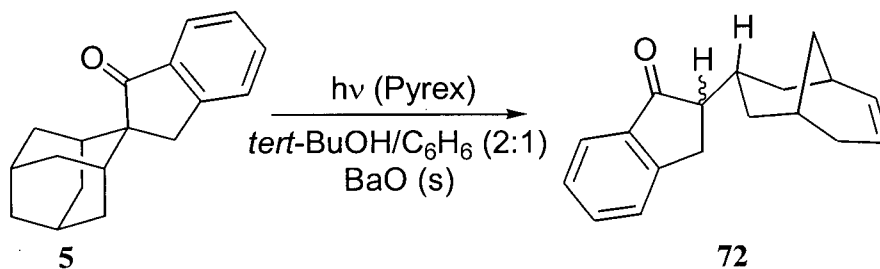
A low temperature ethanol bath contained in an unsilvered Dewar vessel (Pyrex or quartz) was maintained by a Cryocool CC-100 II Immersion Cooling System (Neslab Instrument Inc.). Samples sealed in poly(ethylene) bags were suspended in the cold liquid and irradiated through the transparent walls of the Dewar vessel.

Reaction Conversion and Yield Determinations

Yields and conversions for preparative scale photolyses were calculated based on the mass of the isolated, purified products. For analytical reactions, these values were based on the average integration of at least three GC analyses. The difference in GC detector response for a particular starting material and its reaction products was found to be negligible (all are structural isomers in most cases) and thus no corrections were applied to the integration data. The overall precision of the reported results is estimated to be $\pm 7\%$.

6.2 Photolysis of Adamantyl Spiroketones 5, 6, 7 and 8

Preparative Photolysis of Compound 5



A solution of ketone **5** (26 mg, 0.10 mmol) in 2:1 *tert*-butanol / benzene (10 mL) containing anhydrous barium oxide (10 mg) was irradiated (Pyrex filter, 450 W Hanovia lamp) for 4 h at room temperature. The solvent was removed *in vacuo* and the residue chromatographed (Chromatotron, 5% Et₂O in petroleum ether) to afford starting material **5** (9 mg, 35%) and ketone epimers (~1:1 by ¹H NMR) **72** (12 mg, 46%; 71% based on recovered starting material).

2-(1*R*^{*}, 3*R*^{*}, 5*S*^{*})-Bicyclo[3.3.1]non-6-en-3-yl-2,3-dihydro-1*H*-inden-1-one, Equal Mixture of 2*R* and 2*S* Epimers (**72**)

mp: 88-96 °C (petroleum ether)

¹H NMR (400 MHz, CDCl₃): δ 0.96 (m, 2H), 1.28-1.40 (m, 4H), 1.50-1.84 (m, 8H), 1.88-1.97 (m, 2H), 2.06-2.26 (m, 4H), 2.36 (m, 2H), 2.72 (m, 2H), 2.91 (m, 2H), 3.08 (d, *J* = 8 Hz, 1H), 3.11 (d, *J* = 8.0 Hz, 1H), 5.48 (m, 2H), 5.74 (m, 1H), 5.84 (m, 1H), 7.30 (t, *J* = 7.0 Hz, 2H), 7.43 (m, 2H), 7.55 (t, *J* = 7.4 Hz, 2H), 7.70 (d, *J* = 7.6 Hz, 2H).

¹³C NMR (100 MHz, CDCl₃): δ 24.34, 24.73, 25.61, 25.95, 27.01, 27.35, 27.61, 27.81, 29.13, 29.16, 30.71, 30.93, 31.74, 31.76, 34.69, 34.75, 51.20, 51.28, 123.51,

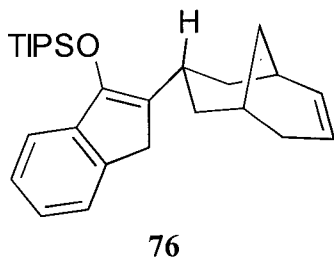
123.53, 123.93, 124.34, 126.42, 126.48, 127.15 (2 acc. eq.), 134.49 (2 acc. eq.),
135.35, 135.67, 137.59, 137.65, 154.07, 154.10, 208.99, 209.19.

IR (neat): 1709, 1609, 1464, 1435, 1325, 1280, 743 cm^{-1} .

HRMS (EI) calcd for $\text{C}_{18}\text{H}_{20}\text{O}$ 252.1514, found 252.1509.

Anal. Calcd: C, 85.67; H, 7.99. Found: C, 85.48; H, 8.08.

O-tris(2-Propyl)silyl-2-(1*R*^{*}, 3*R*^{*}, 5*S*^{*})-bicyclo[3.3.1]non-6-en-3-yl-inden-1-ol (76)



To a solution of ketone epimers **72** (13 mg, 0.052 mmol) in anhydrous benzene (1 mL) was added triisopropyl trifluoromethanesulfonate (15.2 μL , 0.057 mmol) and triethylamine (10.8 μL , 0.078 mmol). The reaction was stirred at room temperature for 3 days, then diluted with *n*-pentane (20 mL), water (5 mL) and triethylamine (1 mL). The organic layer was dried (MgSO_4) and the solvent removed *in vacuo*. Silica gel chromatography (Chromatotron, 2% Et_2O in petroleum ether) afforded silyl enol ether **76** (18.3 mg, 87%) as a colourless oil which solidified on standing.

mp: 82-84 $^{\circ}\text{C}$

^1H NMR (400 MHz, C_6D_6): δ 1.17 (d, $J = 2.2$ Hz, 9H, CH_3), 1.19 (d, $J = 2.2$ Hz, 9H, CH_3), 1.33 (m, 6H), 1.68 (m, 1H), 1.91 (m, 3H), 2.15 (m, 2H), 2.31 (br s, 1H), 2.95 (AB quartet, 2H, CH_2Ph), 3.27 (m, 1H), 5.23 (dd, $J = 4.4, 9.6$ Hz, 1H), 5.87 (t, $J = 4.4$ Hz, 1H), 7.11 (t, $J = 7.4$ Hz, 1H), 7.21 (d, $J = 7.4$ Hz, 1H), 7.28 (t, $J = 7.4$ Hz, 1H), 7.56 (d, $J = 7.4$ Hz, 1H).

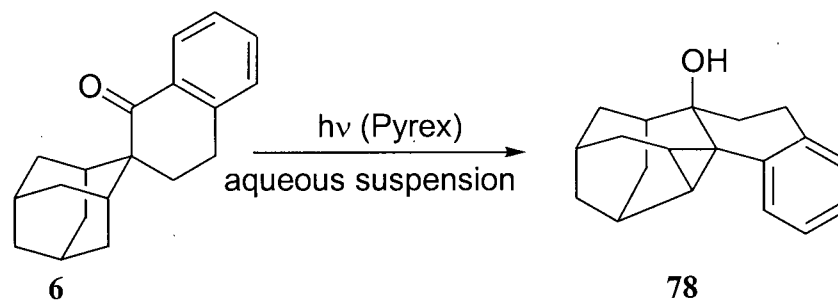
^{13}C NMR (75 MHz, CDCl_3): δ 13.71 (-ve), 18.12 (-ve), 24.70 (-ve), 25.39, 26.64 (-ve), 27.28 (-ve), 32.70, 32.77, 32.89, 34.83, 117.39 (-ve), 123.44 (-ve), 123.47 (-ve), 123.82 (-ve), 125.88 (-ve), 127.36, 136.05 (-ve), 141.08, 142.76, 147.13.

IR (thin film): 1620, 1464, 1370, 1137, 883 cm^{-1} .

HRMS (EI) calcd for $\text{C}_{27}\text{H}_{40}\text{OSi}$ 408.2849, found 408.2845.

Anal. Calcd: C, 79.35; H, 9.86. Found: C, 79.08; H, 9.97.

Preparative Solid State Photolysis of Spiroketone 6 as an Aqueous Suspension



Ketone **6** (405 mg, 1.52 mmol) was finely ground in a mortar and pestle and suspended in distilled water (400 mL) containing sodium dodecylsulfonate (30 mg) as a surfactant. The rapidly stirred suspension was irradiated in an immersion well (450 W Hanovia lamp, Pyrex filter) for 72 h under an atmosphere of nitrogen during which time the solid became fluffy in appearance. Following photolysis, the suspension was saturated

with sodium chloride and extracted with Et₂O (4 × 300 mL). The combined organic extracts were washed with brine (3 × 200 mL), dried (MgSO₄), and concentrated *in vacuo*. Silica gel chromatography (10% Et₂O and 1% triethylamine in petroleum ether) afforded recovered **6** (236 mg, 58%) and alcohol **78** (86 mg, 21%, 51% based on recovered starting material) as a white solid.

1,2,3,3a,4,5,6,7,11c,11d-Decahydro-2,5-methano-5aH-benzo[*c*]cyclopropa[*ef*]phenanthren-5a-ol (**78**)

mp: 131-132 °C (MeCN)

¹H NMR (500 MHz, C₆D₆): δ 1.02 (s, 1H, OH), 1.16 (ddd, *J* = 2.3, 3.8, 12.7 Hz, 1H), 1.20-1.25 (m, 2H), 1.29-1.44 (m, 4H), 1.47 (ddd, *J* = 2.1, 5.0, 12.9 Hz, 1H), 1.66 (br m, 1H), 1.76 (br s, 1H), 1.85-2.03 (m, 4H), 2.06 (dq, *J* = 2.4, 13.4 Hz, 1H), 2.53 (ddd, *J* = 2.1, 4.9, 16.2 Hz, 1H), 3.26 (ddd, *J* = 5.0, 13.8, 16.2 Hz, 1H), 6.46 (d, *J* = 7.9 Hz, 1H), 7.01 (m, 2H), 7.06 (m, 1H).

¹³C NMR (100 MHz, C₆D₆): δ 22.78 (-ve), 26.47 (-ve), 26.60 (-ve), 26.62, 28.35, 28.66, 31.93, 32.43, 33.25, 34.93 (-ve), 36.45, 41.17 (-ve), 73.07, 122.62 (-ve), 124.39 (-ve), 126.60 (-ve), 128.34 (-ve), 136.35, 142.77.

IR (KBr pellet): 3659 (br), 1494, 1449, 1055, 956, 739 cm⁻¹.

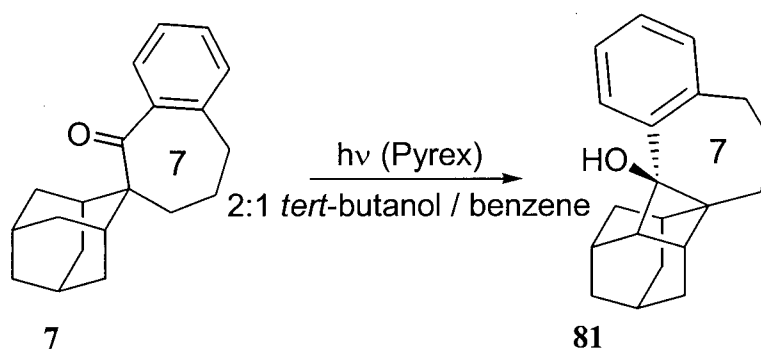
HRMS (EI) calcd for C₁₉H₂₂O 266.1671, found 266.1663.

Anal. Calcd: C, 85.67; H, 8.32. Found: C, 85.80; H, 8.33.

This structure was confirmed by X-ray crystallographic analysis:

Habit	colourless prisms
Space group	$P\bar{1}$
a , Å	19.871(3)
b , Å	24.676(4)
c , Å	12.999(2)
α (°)	99.87(1)
β (°)	101.20(1)
γ (°)	109.14(1)
Z	16
R	0.050

Preparative Photolysis of Spiroketone 7



A solution of ketone **7** (100 mg, 0.36 mmol) in 2:1 *tert*-butanol / benzene (10 mL) was purged with nitrogen for 15 minutes and irradiated (Pyrex filter, 450 W Hanovia) for 60 h. Removal of the solvent *in vacuo* was followed by silica gel chromatography (10% Et₂O in petroleum ether). Starting material **7** (25 mg, 25%) and cyclobutanol **81** (57 mg, 57%; 76% based on recovered starting material) were isolated.

(7aS*, 7bS*, 9R*, 11S*, 11aR*, 11bS*, 13R*)-6,7,7b,8,9,10,11,11a-Octahydro-9,7a,11-[1,2,3]propanetriyl-7aH-benzo[a]benzo[3,4]cyclobuta[1,2-c]cyclohepten-11b(5H)-ol (81)

mp: 130-132 °C (MeCN)

¹H NMR (500 MHz, CDCl₃): δ 0.79 (d, *J* = 11.6 Hz, 1H), 0.97 (s, 1H, OH), 1.45 (m, 1H), 1.55-1.63 (m, 6H), 1.69 (m, 1H), 1.77 (m, 2H), 1.93 (br s, 1H), 2.06 (m, 1H), 2.14 (dt, *J* = 4.5, 12.8 Hz, 1H), 2.20 (br s, 1H), 2.48 (t, *J* = 6.0 Hz, 1H), 2.55 (ddd, *J* = 2.6, 5.8, 15.1 Hz, 1H), 3.05 (m, 1H), 3.21 (m, 1H), 7.01 (m, 4H).

¹³C NMR (125 MHz, CDCl₃): δ 23.92, 25.88, 30.18, 31.80, 32.29, 32.69, 34.01, 34.58, 35.84, 36.52, 38.77, 47.97, 51.05, 84.02, 125.84, 126.12, 126.87, 131.76, 141.78, 124.01.

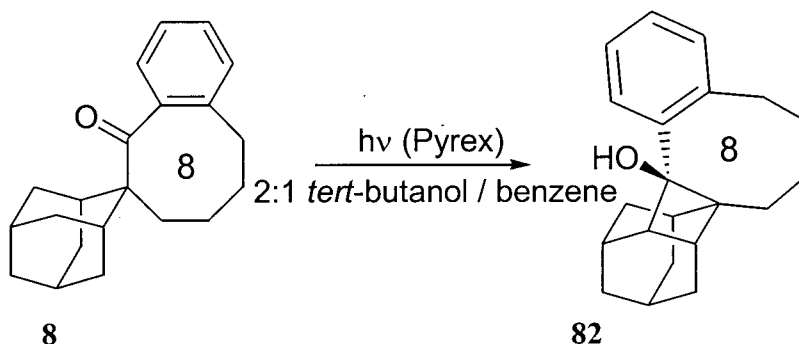
IR (KBr pellet): 3462 (br), 1484, 1448, 1396, 1337, 763, 736 cm⁻¹.

HRMS (EI) calcd for C₂₀H₂₄O 280.1827, found 280.1823.

Anal. Calcd: C, 85.67; H, 8.63. Found: C, 85.82; H, 8.64.

This structure was confirmed by X-ray crystallographic analysis:

Habit	colourless prisms
Space group	<i>P</i> 2 ₁ / <i>c</i>
<i>a</i> , Å	8.763(3)
<i>b</i> , Å	14.060(5)
<i>c</i> , Å	11.890(2)
α (°)	90
β (°)	90.51(2)
γ (°)	90
<i>Z</i>	4
<i>R</i>	0.045

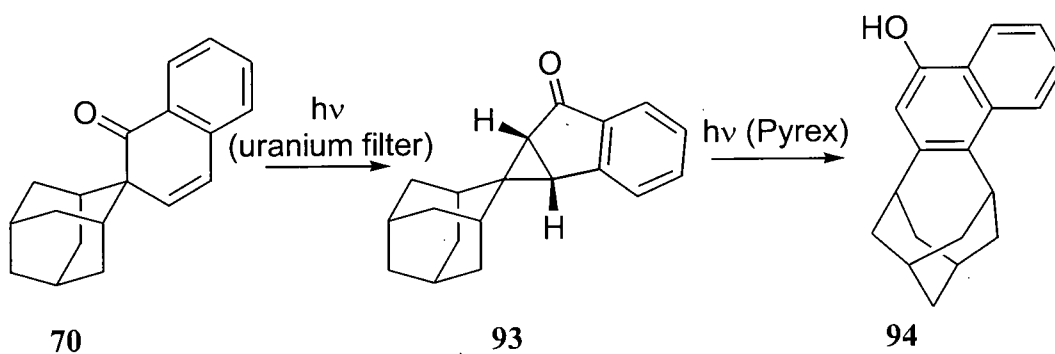
Preparative Photolysis of Spiroketone 8

Anal. Calcd: C, 85.67; H, 8.90. Found: C, 85.43; H, 9.08.

This structure was confirmed by X-ray crystallographic analysis:

Habit	colourless prisms
Space group	$P2_1/c$
a , Å	8.8308(1)
b , Å	14.646(3)
c , Å	12.0651(1)
α (°)	90
β (°)	90.954(1)
γ (°)	90
Z	4
R	0.054

Photolysis of Spiroenone **70**



Ketone **70** (132 mg, 0.5 mmol) in MeCN (20 mL) was irradiated (uranium filter, 450 W Hanovia) for 80 minutes. Removal of solvent *in vacuo* followed by silica gel chromatography (Chromatotron, 3:2 cyclohexane / dichloromethane) afforded recovered starting material (52 mg, 39%), spirocyclopropyl ketone **93** (32 mg, 24%), and naphthol **94** (17 mg, 13%).

Photolysis of Cyclopropylketone 93

Irradiation (Pyrex filter, 450 W Hanovia) of a solution of ketone **93** (45 mg, 0.2 mmol) in MeCN (5 mL) for 1 h. afforded naphthol **94** (39 mg, 87%) following removal of solvent *in vacuo* and silica gel chromatography (1:1 Et₂O / petroleum ether).

Data for Cyclopropane 93

mp: 156-157 °C (solidified slowly from an oil)

¹H NMR (500 MHz, CDCl₃): δ 1.06 (br s, 1H), 1.23 (br s, 1H), 1.42 (m, 2H), 1.60 (m, 1H); 1.66 (m, 1H), 1.72 (m, 3H), 1.80(m, 1H), 1.90 (m, 4H), 2.28 (d, *J* = 4.6 Hz, 1H), 2.87 (d, *J* = 4.6 Hz, 1H), 7.25 (dt, *J* = 1.1, 7.5 Hz, 1H), 7.40 (d, *J* = 7.5 Hz, 1H), 7.45 (dt, *J* = 1.2, 7.5 Hz, 1H), 7.53 (d, *J* = 7.5 Hz, 1H).

¹³C NMR (100 MHz, CDCl₃): δ 27.18 (-ve), 27.47 (-ve), 27.52 (-ve), 35.58, 35.81 (-ve), 35.87, 36.08, 36.86, 36.96, 40.01 (-ve), 41.08 (-ve), 60.74, 122.88 (-ve), 125.67 (-ve), 126.73 (-ve), 133.56 (-ve), 137.87, 150.19, 201.42.

IR (KBr pellet): 1695, 1605, 1468, 1445, 1271, 1102, 761, 712 cm⁻¹.

UV / VIS (MeCN): 301 (310) nm (M⁻¹cm⁻¹).

HRMS (EI) calcd for C₁₉H₂₀O 264.1514, found 264.1516.

Anal. Calcd: C, 86.32; H, 7.63. Found: C, 86.09; H, 7.66.

Data for α -Naphthol **94**

mp: 144-145 °C (Et₂O)

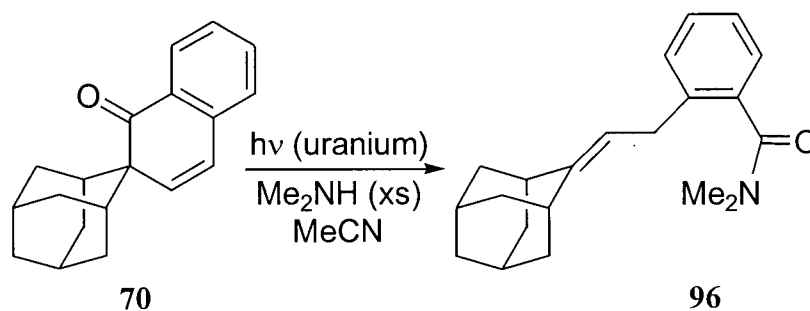
¹H NMR (400 MHz, CDCl₃): δ 1.54 (s, 1H, OH), 1.77(s, 1H), 1.80 (s, 1H), 1.88 (br m, 3H), 1.91 (s, 1H), 2.02 (m, 2H), 2.12 (m, 3H), 2.90 (t, J = 5.7 Hz, 1H), 3.93 (t, J = 5.7 Hz, 1H), 4.94 (s, 1H), 6.63 (s, 1H), 7.37 (t, J = 6.9 Hz, 1H), 7.46 (t, J = 6.9 Hz, 1H), 8.07 (d, J = 8.8 Hz, 1H), 8.15 (d, J = 8.0 Hz, 1H).

¹³C NMR (125 MHz, CDCl₃): δ 28.51 (-ve), 30.85 (-ve), 34.82, 35.08, 36.23, 42.37 (-ve), 111.40 (-ve), 121.88 (-ve), 122.95, 123.34 (-ve), 123.56 (-ve), 126.21 (-ve), 132.33, 135.81, 145.71, 148.86,

IR (KBr pellet): 3218 (br), 1626, 1601, 1576, 1441, 1396, 1067, 759 cm⁻¹.

HRMS (EI) calcd for C₁₉H₂₀O 264.1514, found 264.1514.

Anal. Calcd: C, 86.32; H, 7.63. Found: C, 86.07; H, 7.61.

Photolysis of Spiroenone **70** in the Presence of Dimethylamine

Into a solution of ketone **70** (155 mg, 0.59 mmol) in MeCN (30 mL) was bubbled dimethylamine for five minutes. The solution was irradiated (450 W Hanovia lamp, uranium filter) for 1.5 h. Following removal of the solvent *in vacuo* and silica gel chromatography (1:1 Et₂O / petroleum ether), amide **96** (148 mg, 82%) was isolated as a white solid.

Data for Amide **96**

mp: 72-74 °C (Et₂O)

¹H NMR (400 MHz, CDCl₃): δ 1.69-1.80 (br m, 4H), 1.80-1.90 (br m, 6H), 1.94 (br s, 2H), 2.34 (br s, 1H), 2.81 (s, 3H, CH₃), 2.88 (br s, 1H), 3.11 (s, 3H, CH₃), 3.30, (d, *J* = 7.4 Hz, 2H, C=CHCH₂), 5.14 (t, *J* = 7.4 Hz, 1H, C=CH), 7.12 (m, 1H), 7.17 (dt, *J* = 1.8, 6.7 Hz, 1H), 7.26 (m, 2H).

¹³C NMR (75 MHz, CDCl₃): δ 28.40, 29.65, 31.90, 34.44, 37.02, 38.63, 38.73, 39.63, 40.40, 113.64, 125.63, 125.70, 128.69, 128.11, 136.15, 138.22, 148.77, 171.36.

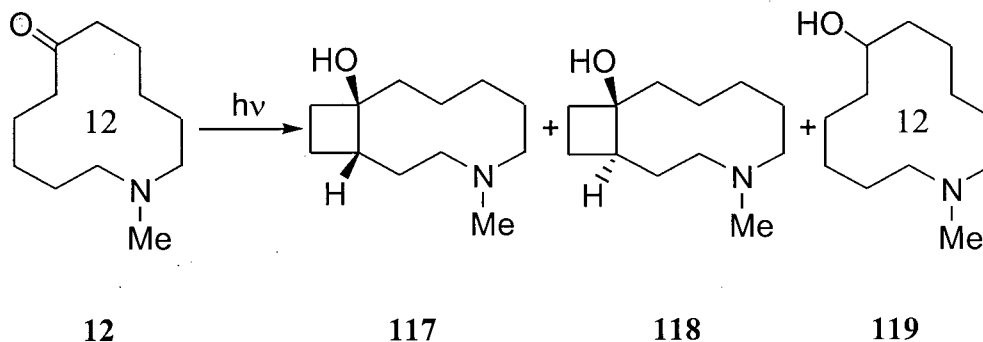
IR (thin film): 1646, 1505, 1448, 1393, 1268, 1220, 1067, 775, 755 cm⁻¹.

HRMS (EI) calcd for C₂₁H₂₇NO 309.2093, found 309.2095.

Anal. Calcd: C, 81.51; H, 8.79; N, 4.53. Found: C, 81.36; H, 8.98; N, 4.53.

6.3 Photolysis of Macrocyclic Aminoketones and Their Salts

6.3.1 Preparative Photolysis of Compound 12 in Solution



A solution of aminoketone **12** (380 mg, 1.92 mmol) in *tert*-butanol / benzene 97:3 (100 mL) was purged with nitrogen and irradiated (450 W Hanovia lamp, Pyrex filter) for 26 h. The solution was concentrated *in vacuo* and chromatographed on silica gel (10% MeOH, 1% triethylamine in petroleum ether) to give cyclobutanol **117** (oil, 62 mg, 16%), cyclobutanol **118** (oil, 40 mg, 11%), and reduced product **119** (white solid, 114 mg, 30%).

Data for (1*R*^{*}, 10*R*^{*})-4-Methyl-4-azabicyclo[8.2.0]dodecan-10-ol (**117**)

¹H NMR (400 MHz, C₆D₆): δ 1.14 (m, 1H), 1.25 (m, 1H), 1.3-1.5 (m, 4H), 1.50-1.66 (m, 3H), 1.66-1.85 (m, 4H), 1.93 (s, 3H), 1.9-2.1 (m, 4H), 2.10-2.19 (m, 2H), 2.51 (m, 1H).

¹³C NMR (75 MHz, C₆D₆): δ 19.30, 22.57, 24.82, 25.30, 28.32, 33.64, 37.48, 44.36, 51.24 (CH), 54.72, 57.39, 76.87.

IR (neat): 3381, 2932, 1456, 1105 cm⁻¹.

HRMS (DCI, isobutane) calcd for C₁₂H₂₄NO (M+H)⁺ 198.1858, found 198.1856.

Data for (1*S*^{*}, 10*R*^{*})-4-Methyl-4-azabicyclo[8.2.0]dodecan-10-ol (118)

¹H NMR (400 MHz, C₆D₆): δ 1.12-1.31 (m, 3H), 1.33-1.80 (m, 6H), 1.88 (m, 5H), 1.98 (s, 3H), 2.00 (m, 1H), 2.15 (m, 5H).

¹³C NMR (75 MHz, C₆D₆): δ 20.92, 22.43, 22.96, 26.46, 31.12, 34.12, 42.03, 43.16, 43.32 (CH), 55.74, 57.09, 76.62.

IR (neat): 3290, 2932, 1456, 1122, 1083 cm⁻¹.

HRMS (EI) calcd for C₁₂H₂₃NO 197.1780, found 197.1783.

Data for 7-Methyl-7-azacyclododecanol (119)

mp: 34 °C (*n*-pentane)

¹H NMR (400 MHz, C₆D₆): δ 0.73 (br s, 1H, OH), 1.13-1.28 (m, 6H), 1.31-1.49 (m, 6H), 1.54 (m, 2H), 1.71 (m, 2H), 1.91 (m, 2H), 2.00 (s, 3H, CH₃), 2.31 (m, 2H), 3.80 (quint, *J* = 5.6 Hz, 1H, CH(OH)).

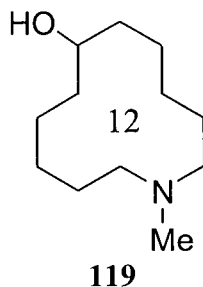
¹³C NMR (75 MHz, C₆D₆): δ 22.81, 23.18, 25.50, 34.74, 42.72, 54.86, 67.73.

IR (KBr pellet): 3349, 2927, 2856, 2781, 1467, 1006, 952, 724 cm⁻¹.

HRMS (EI) calcd for C₁₂H₂₅NO 199.1936, found 199.1936.

Anal. Calcd: C, 72.31; H, 12.64; N, 7.03. Found: C, 72.53; H, 12.65; N, 6.87.

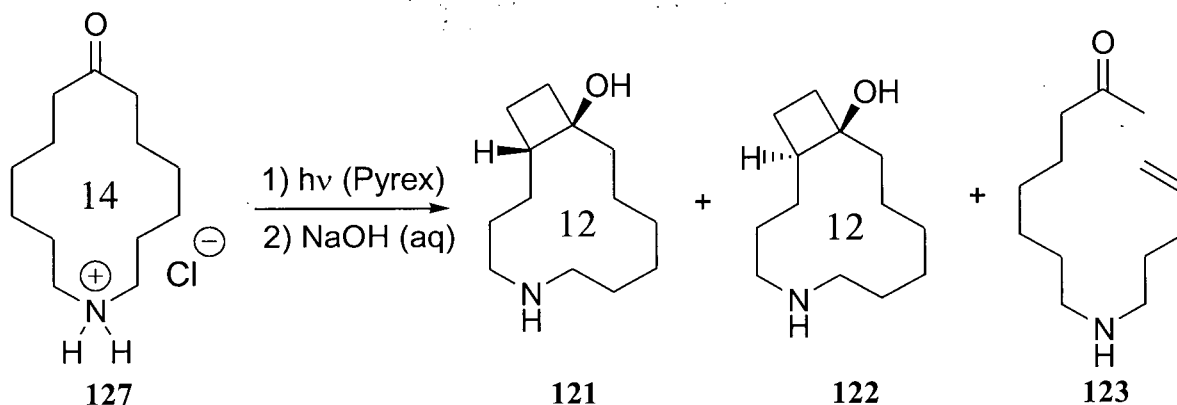
6.3.2 Independent Preparation of Alcohol Photoproduct 119



To a solution of aminoketone **12** (98 mg, 0.48 mmol) in 95% ethanol (10 mL) was added sodium borohydride (20 mg, 0.53 mmol) in one portion. The reaction was stirred overnight and quenched cautiously with 2 M HCl (3 mL). The solution was concentrated *in vacuo*, and the residue taken up in 2 M potassium hydroxide (10 mL) and extracted with Et₂O (3 × 10 mL). The combined organic extracts were dried (MgSO₄) and concentrated *in vacuo* to yield aminoalcohol **119** (94 mg, 96%). An analytically pure sample could be obtained by sublimation (60 °C, 3 Torr).

See section 6.3.1 for characterization data for compound **119**.

6.3.3 Solution Photolysis of Hydrochloride Salt 127



A solution of salt **127** (198 mg, 0.80 mmol) in MeCN (60 mL) was purged with nitrogen and irradiated (450 W Hanovia lamp, Pyrex filter) for 29 h. The photosylate was concentrated *in vacuo* and chromatographed on silica gel (Chloroform / MeOH / triethylamine 20:5:1) affording cyclobutanol **121** (oil, 59 mg, 35 %), cyclobutanol **122** (white solid, 41 mg, 24%), and cleavage product **123** (oil, 14 mg, 8%).

Data for (1*R**, 12*R**)-5-Azabicyclo[10.2.0]tetradecan-12-ol (**121**)

¹H NMR (400 MHz, C₆D₆): δ 0.80-1.40 (m, 9H), 1.40-1.59 (m, 4H), 1.71 (m, 4H), 1.80-2.07 (m, 4H), 2.32-2.55 (m, 4H).

¹³C NMR (75 MHz, C₆D₆): δ 19.52, 22.99, 24.81, 28.45, 28.57, 28.99, 29.54, 33.90, 36.10, 48.24, 48.40, 50.11 (CH), 77.34.

IR (neat): 3364, 2922, 1456, 1350, 1261, 1116 cm⁻¹.

HRMS (EI) calcd for C₁₃H₂₅NO 211.1936, found 211.1933.

Anal. Calcd: C, 73.88; H, 11.92; N, 6.63. Found: C, 73.88; H, 12.12; N, 6.69.

Data for (1*S**, 12*R**)-5-Azabicyclo[10.2.0]tetradecan-12-ol (122)

mp: 40-41 °C (Et₂O)

¹H NMR (400 MHz, C₆D₆): δ 1.14-1.72 (m, 15H), 1.88 (m, 2H), 2.08 (m, 2H), 2.23-2.48 (m, 6H).

¹³C NMR (100 MHz, C₆D₆): δ 22.70, 23.23, 25.82, 27.06, 27.27, 27.77, 29.37, 34.08, 39.80, 43.13 (CH), 48.49, 48.91, 76.73.

IR (neat): 3282, 2927, 1456, 1260, 1127 cm⁻¹.

HRMS (EI) calcd for C₁₃H₂₅NO 211.1936, found 211.1936.

Anal. Calcd: C, 73.88; H, 11.92; N, 6.63. Found: C, 73.96; H, 11.98; N, 6.69.

Data for 8-(4-Pentenylamino)-2-octanone (123)

¹H NMR (400 MHz, C₆D₆): δ 0.70 (br s, 1H), 1.10-1.28 (m, 4H), 1.35 (quint, *J* = 7.3 Hz, 2H), 1.46 (m, 4H), 1.67 (s, 3H), 1.94 (t, *J* = 7.5 Hz, 2H), 2.04 (q, *J* = 7.7 Hz), 2.48 (m, 2H), 5.00 (m, 2H), 5.79 (m, 1H).

¹³C NMR (75 MHz, C₆D₆): δ 24.00, 27.52, 29.31, 29.43, 29.90, 30.55, 31.95, 43.29, 49.72, 50.23, 114.57, 139.04, 206.31.

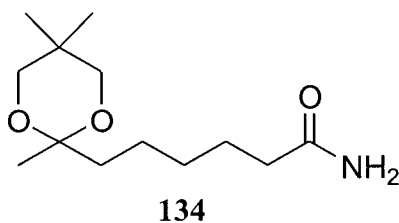
IR (neat): 2931, 1718, 1458, 1638, 1129, 911 cm⁻¹.

HRMS (EI) calcd for C₁₃H₂₅NO 211.1936, found 211.1939.

Anal. Calcd: C, 73.88; H, 11.92; N, 6.63. Found: C, 74.04; H, 12.02; N, 6.59.

6.3.4 Independent Synthesis of Fourteen-Membered Cleavage Photoproduct

6-(2,5,5-Trimethyl-[1,3]dioxan-2-yl)hexanoic Acid Amide (134)



To a room temperature solution of 7-oxooctanamide (500 mg, 3.16 mmol) and 2,2-dimethyl-1,3-propanediol (480 mg, 4.62 mmol) in benzene (50 mL) was added 4-toluenesulfonic acid (20 mg, catalyst). The solution was refluxed for 2 h with continuous removal of water *via* a Dean-Stark apparatus. The reaction was cooled and washed successively with saturated potassium carbonate (2×10 mL) and water (10 mL). The organic layer was dried (K_2CO_3) and concentrated *in vacuo*. Silica gel chromatography (5:45:1 MeOH / EtOAc / triethylamine) afforded product **134** (462 mg, 64%) as a white solid.

mp: 101-102 °C (EtOAc)

^1H NMR (400 MHz, C_6D_6): δ 0.62 (s, 3H), 0.94 (s, 3H), 1.22 (m, 2H), 1.32 (s, 3H), 1.54 (m, 4H), 1.75 (m, 4H), 3.36 (AB quartet, 4H), 4.18 (br s, 1H), 5.28 (br s, 1H).

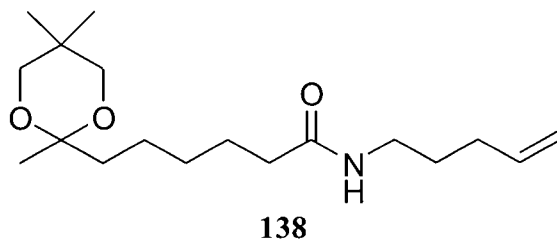
^{13}C NMR (75 MHz, C_6D_6): δ 20.09, 22.40, 22.89, 23.47, 25.70, 29.82, 29.84, 35.63, 39.03, 70.31, 99.01, 174.68.

IR (KBr pellet): 3364, 3192, 2951, 1663, 1631, 1099 cm^{-1} .

HRMS (DCI, isobutane) calcd for $\text{C}_{13}\text{H}_{26}\text{NO}_3$ ($\text{M}+\text{H}$) $^+$ 244.1913, found 244.1913.

Anal. Calcd for $C_{13}H_{25}NO_3$: C, 64.16; H, 10.35; N, 5.76. Found: C, 63.96; H, 10.37; N, 5.64.

6-(2,5,5-Trimethyl-[1,3]dioxan-2-yl)hexanoic Acid Pent-4-enylamide (138)



To a warm (50°C) suspension of potassium carbonate (280 mg, 2.1 mmol), sodium hydroxide (140 mg, 3.5 mmol), tetrabutylammonium hydrogensulfate (50 mg, 0.15 mmol) and amide **134** (200 mg, 0.82 mmol) in toluene (8 mL) was added 5-bromo-1-pentene (300 mg, 2.1 mmol) in three portions over a period of 1h. The suspension was heated to reflux for 4h, then cooled and filtered. The solids were triturated with toluene (3 × 10 mL) and the combined organic filtrates dried ($MgSO_4$) and concentrated *in vacuo*. Silica gel chromatography (EtOAc / hexanes 1:1; 1% triethylamine) provided two fractions, the more polar of which contained the desired product **138** (117 mg, 46%) as a colourless oil.

1H NMR (400 MHz, C_6D_6): δ 0.62 (s, 3H), 0.95 (s, 3H), 1.31 (m, 7H), 1.55-1.70 (m, 4H), 1.82 (m, 6H), 3.05 (q, $J = 6.8$ Hz, 2H), 3.36 (AB quartet, 4H), 4.51 (br s, 1H), 4.98 (m, 2H), 5.69 (m, 1H).

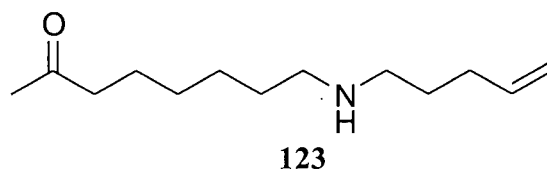
^{13}C NMR (75 MHz, C_6D_6): δ 20.05, 22.38, 22.91, 23.49, 26.00, 29.32, 29.87, 29.94, 31.33, 36.51, 38.89, 39.19, 70.32, 98.99, 114.96, 138.28, 171.62.

IR (neat): 3295, 2949, 1646, 1556, 1095, 909 cm^{-1} .

HRMS (EI) calcd for $C_{18}H_{33}NO_3$ 311.2460, found 311.2467.

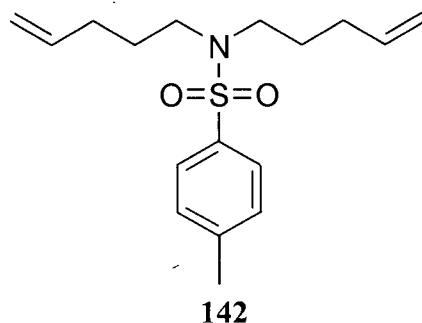
Anal. Calcd: C, 69.41; H, 10.68; N, 4.50. Found: C, 69.50; H, 10.71; N, 4.43.

8-(4-Pentenylamino)-2-octanone (**123**)



To a solution of amide **138** (180 mg, 0.58 mmol) in THF (50 mL) was added lithium aluminum hydride (200 mg, 5.2 mmol). The suspension was refluxed for 8h, then cooled in an ice-water bath and quenched carefully with 50% aqueous potassium hydroxide (1 mL). Hydrochloric acid (7 M, 5 mL) was added carefully, and the resulting mixture stirred at room temperature for 1h. The mixture was concentrated to ca. 20 mL *in vacuo* and rendered alkaline (to pH test paper) by the addition of 50% aqueous potassium hydroxide. The mixture was extracted with *n*-pentane (3 × 30 mL) and the combined organic extracts washed with water (2 × 10 mL), dried ($MgSO_4$), and concentrated *in vacuo* to give aminoketone **123** (71 mg, 58%) as a colourless oil.

See section 6.3.3 for characterization data for compound **123**.

N,N-bis(4-Pentenyl)-4-toluenesulfonamide (142)

To a solution of 4-toluenesulfonamide (480 mg, 2.8 mmol) in benzene (7 mL) was added sodium hydroxide (finely powdered, 600 mg, 15 mmol), potassium carbonate (600 mg, 6.1 mmol), and tetrabutylammonium hydrogensulfate (100 mg, 0.30 mmol). The resulting suspension was heated to 50 °C and 5-bromo-1-pentene (1.0 g, 6.7 mmol) was added over a period of 45 minutes. The reaction mixture was then refluxed for 4 h. After cooling to room temperature, the solids were filtered off and triturated with benzene (3 × 10 mL), and the combined organic filtrates washed with water (3 × 15 mL) and brine (10 mL). Drying (MgSO₄) followed by concentration *in vacuo* afforded analytically pure **142** (764 mg, 89%) as a colourless liquid.

¹H NMR (400 MHz, CDCl₃): δ 1.60 (quint, *J* = 7.5 Hz, 4H), 2.01 (q, *J* = 7.1 Hz, 4H), 2.40 (s, 3H), 3.09 (t, *J* = 7.5 Hz, 4H), 4.99 (m, 4H), 5.75 (m, 2H), 7.27 (d, *J* = 8.0 Hz, 2H), 7.67 (d, *J* = 8.0 Hz, 2H).

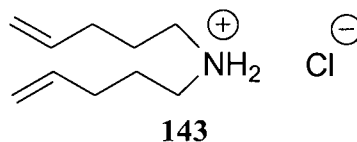
¹³C NMR (100 MHz, CDCl₃): δ 21.46, 27.92, 30.80, 47.94, 115.25, 127.12, 129.58, 136.96, 137.47, 142.99.

IR (neat): 3077, 2933, 1641, 1599, 1342, 1160, 1092, 655 cm⁻¹.

HRMS (DCI, isobutane) calcd for C₁₇H₂₆NO₂S (M+H)⁺ 308.1684, found 308.1685.

Anal. Calcd for C₁₇H₂₅NO₂S: C, 66.41; H, 8.20; N, 4.56. Found: C, 66.72; H, 8.37; N, 4.58.

bis(4-Pentenyl)amine Hydrochloride (143)



Into a 50 mL round bottomed flask containing sulfonamide **142** (820 mg, 2.67 mmol) and MeOH (500 μ L, 19.8 mmol) was condensed anhydrous ammonia (20 mL). Solid sodium was dissolved in ca. 20 mg portions until a blue colour persisted, after which MeOH was introduced until the colour disappeared. The solution was allowed to warm under a constant stream of nitrogen during which time all of the ammonia evaporated. Aqueous potassium hydroxide (20 mL of a 2 M solution) was added to the residue, and the resulting mixture extracted into *n*-pentane (3 \times 20 mL). The combined organic extracts were washed with brine (20 mL), dried over MgSO₄, and filtered. A stream of dry hydrogen chloride gas was passed through the pentane solution causing salt **143** to precipitate. The white solid (227 mg, 60%) was collected by suction filtration, washed with *n*-pentane (5 mL) and dried *in vacuo*.

mp: >275 $^{\circ}$ C (dec.)

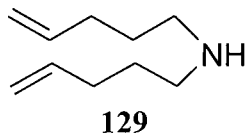
¹H NMR (400 MHz, CDCl₃): δ 2.00 (quint, J = 7.3 Hz, 4H), 2.13 (m, 4H), 2.89 (m, 4H), 5.01 (m, 4H), 5.72 (m, 2H), 9.52 (br s, 2H).

¹³C NMR (75 MHz, CDCl₃): δ 24.82, 30.74, 47.26, 116.41, 136.16.

IR (KBr pellet): 2938, 1644, 1594, 1445, 993, 913, 641 cm^{-1} .

Anal. Calcd for $\text{C}_{10}\text{H}_{20}\text{NCl}$: C, 63.31; H, 10.63; N, 7.38. Found: C, 63.24; H, 10.77; N, 7.18.

In Situ Preparation of *bis*(4-Pentenyl)amine (**129**)

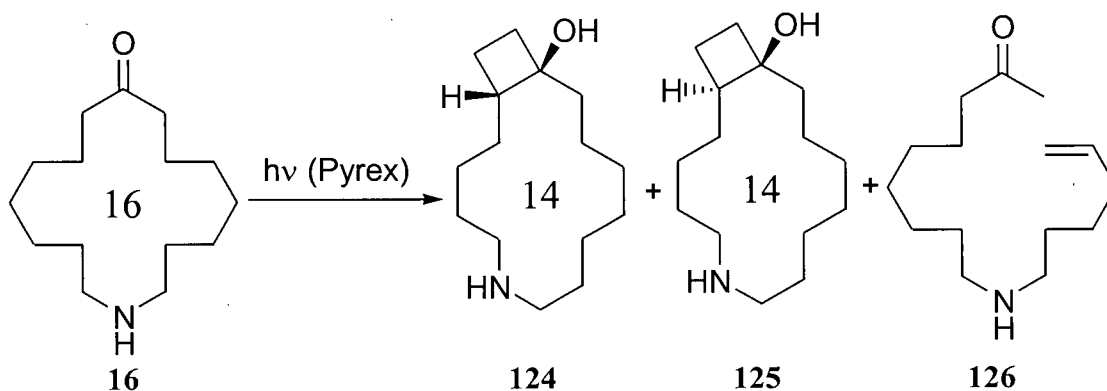


Anhydrous potassium carbonate (50 mg) and salt **143** (25 mg) were suspended in benzene- d_6 (2 mL) and stirred together for 2 h. The solids were filtered off and the solution analyzed by ^1H and ^{13}C NMR spectroscopy:

^1H NMR (200 MHz, C_6D_6): δ 0.46 (br s, 1H), 1.44 (quint, $J = 7.1$ Hz, 4H), 2.03 (q, $J = 7.1$ Hz, 4H), 2.42 (t, $J = 7.1$ Hz, 4H), 5.01 (m, 4H), 5.79 (m, 2H).

^{13}C NMR (100 MHz, C_6D_6): δ 29.87, 31.91, 49.60, 114.58, 139.03.

6.3.5 Preparative Photolysis of Aminoketone 16



A solution of aminoketone **16** (988 mg, 4.13 mmol) in MeCN (800 mL) was placed in an immersion well photoreactor and kept under an atmosphere of nitrogen. The solution was irradiated (450 W Hanovia lamp, Pyrex filter) for 21 h and subsequently concentrated *in vacuo*. Silica gel chromatography (chloroform / MeOH / triethylamine 20:5:1) afforded cyclobutanol **124** (white solid, 172 mg, 17%), cyclobutanol **125** (white solid, 81 mg, 8%) and cleavage product **126** (oil, 312 mg, 32%).

Data for (1*R*^{*}, 14*R*^{*})-6-Azabicyclo[12.2.0]hexadecan-14-ol (**124**)

mp: 95-96 °C (Et₂O)

¹H NMR (400 MHz, C₆D₆): δ 0.78 (br s, 2H), 1.00-2.09 (m, 23H), 2.48 (m, 4H).

¹³C NMR (100 MHz, C₆D₃): δ 19.25, 19.80, 22.60, 24.62, 24.73, 26.90, 28.25, 28.94, 29.47, 31.64, 34.31, 47.30, 47.52, 50.00 (CH), 76.42.

IR (KBr pellet): 3398, 2933, 1457, 1435, 1065 cm⁻¹.

HRMS (EI) calcd for C₁₅H₂₉NO 239.2249, found 239.2253.

Anal. Calcd: C, 75.26; H, 12.21; N, 5.85. Found: C, 75.38; H, 12.34; N, 5.81.

Data for (1*S**, 14*R**)-6-Azabicyclo[12.2.0]hexadecan-14-ol (125)

mp: 94-95 °C (Et₂O)

¹H NMR (400 MHz, C₆D₆): δ 1.16-1.79 (m, 20H), 1.80-2.00 (m, 4H), 2.10 (m, 1H), 2.28 (m, 2H), 2.48 (m, 1H), 2.63 (m, 1H).

¹³C NMR (100 MHz, C₆D₆): δ 20.49, 22.41, 23.34, 23.44, 25.68, 27.25, 27.44, 27.88, 28.64, 32.86, 40.52, 43.62 (CH), 47.01, 47.50, 77.63.

IR (KBr pellet): 3259, 2932, 1462, 1274, 1125, 845 cm⁻¹.

HRMS (EI) calcd for C₁₅H₂₉NO 239.2249, found 239.2252.

Anal. Calcd: C, 75.26; H, 12.21; N, 5.85. Found: C, 75.45; H, 12.22; N, 5.77.

Data for 9-(5-Hexenylamino)-2-nonanone (126)

¹H NMR (400 MHz, C₆D₆): δ 0.47 (s, 1H), 1.1-1.5 (m, 14H), 1.65 (s, 3H), 1.92 (t, *J* = 7.3 Hz, 2H), 1.99 (m, 2H), 2.50 (m, 4H), 5.00 (m, 2H), 5.78 (m, 1H).

¹³C NMR (100 MHz, C₆D₆): δ 23.99, 27.04, 27.60, 29.26, 29.48, 29.76, 30.13, 30.66, 34.07, 43.33, 50.18, 50.33, 114.57, 139.09, 206.99.

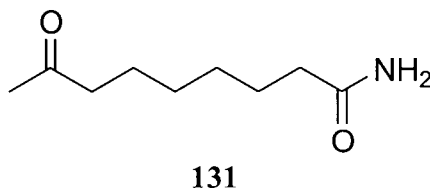
IR (neat): 2930, 1717, 1464, 1411, 1361, 910 cm⁻¹.

HRMS (EI) calcd for C₁₅H₂₉NO 239.2249, found 239.2249.

Anal. Calcd: C, 75.26; H, 12.21; N, 5.85. Found: C, 74.98; H, 12.16; N, 5.83.

6.3.6 Independent Synthesis of Sixteen-Membered Cleavage Photoproduct 126

8-Oxononanoic Acid Amide (131)



To a cold (0 °C) solution of 8-oxononanoic acid (6.0 g, 34.9 mmol) and DMF (250 μ L) in dichloromethane (100 mL) was added oxalyl chloride (19 mL of a 2.0 M solution in dichloromethane, 38.0 mmol) over 20 minutes. The reaction was stirred in the cold for 2 h, after which time a steady stream of anhydrous ammonia was bubbled through the solution. The reaction was quenched with aqueous sodium carbonate (50 mL of a 10% solution), and extracted into dichloromethane (3 \times 100 mL). The combined organic extracts were washed with brine (3 \times 60 mL), dried over MgSO_4 , and concentrated *in vacuo*. Recrystallization of the residue from water gave amide **131** (4.3 g, 72%) as white flakes.

mp: 91-92 °C (water)

^1H NMR (400 MHz, CDCl_3): δ 1.31 (m, 4H), 1.55 (quintet, $J = 7.2$ Hz, 2H), 1.62 (quintet, $J = 7.2$ Hz, 2H), 2.10 (s, 3H), 2.19 (t, $J = 7.4$ Hz, 2H), 2.40 (t, $J = 7.3$ Hz, 2H), 5.48 (br, s, 2H).

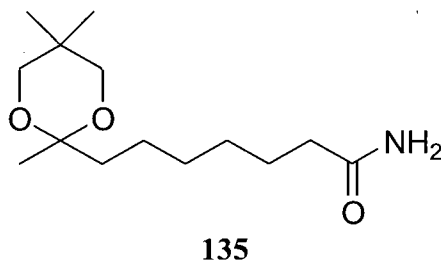
^{13}C NMR (75 MHz, CDCl_3): δ 23.50, 25.21, 28.72, 28.85, 29.89, 35.67, 43.56, 175.53, 209.27.

IR (KBr pellet): 3392, 3198, 2929, 1703, 1665, 1615, 1415 cm^{-1} .

HRMS (DCI, isobutane + NH_3) calcd for $\text{C}_9\text{H}_{18}\text{NO}_2$ ($\text{M}+\text{H}$) $^+$ 172.1338, found 172.1337.

Anal. Calcd for $C_9H_{17}NO_2$: C, 63.13; H, 10.01; N, 8.18. Found: C, 63.49; H, 9.96; N, 8.05.

7-(2,5,5-Trimethyl-[1,3]dioxan-2-yl)heptanoic Acid Amide (135)



A round bottomed flask equipped with a Hickman still and an efficient condenser was charged with a solution of amide **131** (2.03 g, 11.8 mmol), 2,2-dimethyl-1,3-propanediol (neopentyl glycol, 1.80 g, 17.8 mmol) and 4-toluenesulfonic acid monohydrate (110 mg, 0.58 mmol) in benzene (200 mL). The solution was refluxed for 6 h, with periodic removal of water from the still. The solution was cooled and extracted sequentially with aqueous sodium carbonate (50 mL of a 10% solution) and brine (3×50 mL), dried ($MgSO_4$) and concentrated *in vacuo*. Recrystallization of the residue from Et_2O afforded ketal **135** (1.8 g, 60%) as a white solid.

mp: 62-64 °C (Et_2O)

1H NMR (400 MHz, C_6D_6): δ 0.64 (s, 3H), 0.95 (s, 3H), 1.23 (m, 4H), 1.34 (s, 3H), 1.54 (m, 4H), 1.77 (m, 4H), 3.36 (AB quartet, $J = 11.3$ Hz, 4H, OCH_2), 4.41 (br s, 1H), 5.92 (br s, 1H).

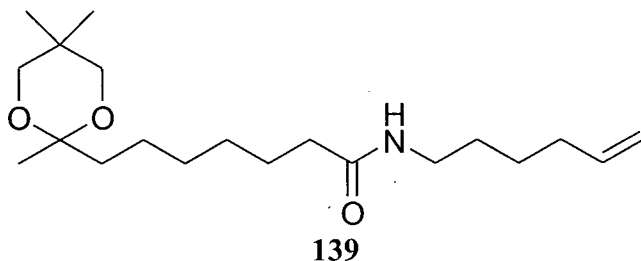
^{13}C NMR (75 MHz, C_6D_6): δ 20.11, 22.40, 22.89, 23.65, 25.72, 29.58, 29.89, 30.06, 35.83, 39.14, 70.31, 99.07, 175.40.

IR (KBr pellet): 3382, 3197, 2937, 1665, 1094 cm^{-1} .

HRMS (DCI, isobutane) calcd for $\text{C}_{14}\text{H}_{28}\text{NO}_3$ ($\text{M}+\text{H}$)⁺ 258.2069, found 258.2070.

Anal. Calcd for $\text{C}_{14}\text{H}_{27}\text{NO}_3$: C, 65.33; H, 10.57; N, 5.44. Found: C, 65.44; H, 10.50; N, 5.38.

7-(2,5,5-Trimethyl-[1,3]dioxan-2-yl)heptanoic Acid Hex-5-enylamide (**139**)



To a warm (50 °C) suspension of potassium carbonate (280 mg, 2.1 mmol), sodium hydroxide (140 mg, 3.5 mmol), tetrabutylammonium hydrogensulfate (50 mg, 0.15 mmol) and amide **135** (212 mg, 0.82 mmol) in toluene (8 mL) was added 6-bromo-1-hexene (318 mg, 2.1 mmol) in three portions over a period of 1h. The suspension was heated to reflux for 4h, then cooled and filtered. The solids were triturated with toluene (3 × 10 mL) and the combined organic filtrates dried (MgSO_4) and concentrated *in vacuo*. Silica gel chromatography (1:1 EtOAc / hexanes; 1% triethylamine) provided two fractions, the more polar of which contained the desired product **139** (168 mg, 60%) as a colourless oil.

^1H NMR (400 MHz, CDCl_3): δ 0.87 (s, 3H), 0.99 (s, 3H), 1.32 (s, 3H), 1.28-1.55 (m, 10H), 1.63 (m, 4H), 2.06 (q, $J = 7.0$ Hz, 2H), 2.12 (t, $J = 7.4$ Hz, 2H), 3.23 (q, $J = 6.8$ Hz, 2H), 3.47 (AB quartet, $J = 11.3$ Hz, 4H), 4.97 (m, 2H), 5.38 (br s, 1H), 5.78 (m, 1H).

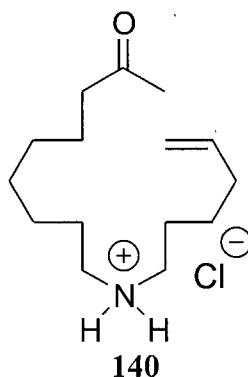
^{13}C NMR (75 MHz, CDCl_3): δ 20.22, 21.30, 22.50, 22.78, 23.25, 23.54, 25.54, 25.79, 26.11, 28.74, 28.93, 29.05, 29.28, 29.64, 29.89, 29.96, 33.30, 36.58, 36.80, 38.14, 39.37, 43.59, 70.35, 71.77, 98.98, 114.79, 138.37, 173.18. Two amide rotamers present.

IR (KBr pellet): 3296, 2936, 2861, 1551, 1457 cm^{-1} .

HRMS (EI) calcd for $\text{C}_{20}\text{H}_{37}\text{NO}_3$ 339.2773, found 339.2770.

Anal. Calcd C, 70.75; H, 10.98; N, 4.13. Found: C, 71.02; H, 10.91; N, 4.03.

9-(5-Hexenylamino)-2-nonanone Hydrochloride (140)



To a solution of amide **139** (197 mg, 0.58 mmol) in THF (50 mL) was added lithium aluminum hydride (200 mg, 5.2 mmol). The suspension was refluxed for 8h, then cooled in an ice-water bath and quenched carefully with 50% aqueous potassium hydroxide (1 mL). Hydrochloric acid (7 M, 5 mL) was added carefully, and the resulting mixture stirred at room temperature for 1h. The mixture was concentrated to ca. 20 mL *in vacuo* and rendered alkaline (to pH test paper) by the addition of 50% aqueous potassium hydroxide. The mixture was extracted with *n*-pentane (3 \times 30 mL) and the combined organic extracts washed with water (2 \times 10 mL), and dried (MgSO_4). A stream of dry hydrogen chloride was passed through the solution and the precipitate isolated by suction filtration, affording salt **140** (127 mg, 78%) as a white powder.

mp: 178-181 °C (dec.)

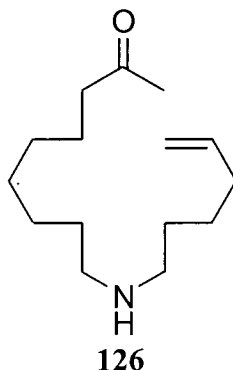
^1H NMR (400 MHz, CDCl_3): δ 1.2-1.6 (m, 10H), 1.87 (m, 4H), 2.06 (m, 2H), 2.11 (s, 3H), 2.40 (t, $J = 7.3$ Hz, 2H), 2.89 (m, 4H), 4.99 (m, 2H), 5.75 (M, 1H), 9.51 (br s, 2H).

^{13}C NMR (100 MHz, CDCl_3): δ 23.54, 25.21, 25.72, 26.09, 26.65, 28.81, 28.89, 29.89, 33.01, 43.55, 47.40, 47.49, 115.34, 137.62, 208.98.

IR (KBr pellet): 3410, 2928, 1712, 1641, 1461, 1377, 1169, 911 cm^{-1} .

Anal. Calcd for $\text{C}_{15}\text{H}_{30}\text{NOCl}$: C, 65.31; H, 10.96; N, 5.08. Found: C, 65.19; H, 10.98; N, 4.92.

9-(5-Hexenylamino)-2-nonanone (126)

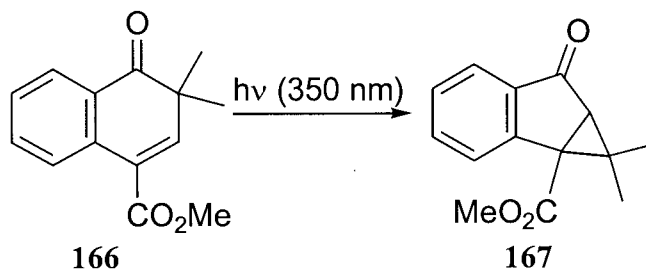


A suspension of finely ground salt **140** (56 mg, 0.20 mmol) and anhydrous potassium carbonate (200 mg) *n*-hexane (10 mL) was stirred for 6 h. The solids were filtered off and the filtrate concentrated *in vacuo* to yield aminoketone **126** (43 mg, 89%) as a colourless oil.

See section 6.3.4 for characterization data for compound **126**.

6.4 Photolysis of Benzocyclohexadienone Derivatives

Preparative Photolysis of Ketoester 166



A solution of ketoester **166** (206 mg, 0.90 mmol) in MeCN (10 mL) was purged with nitrogen and irradiated (Rayonet, 350 nm) for 3 h. The photosylate was concentrated *in vacuo* and the residue chromatographed (Chromatotron, 15% Et₂O in petroleum ether) to give ketoester **167** (168 mg, 82%) as a colourless oil which solidified on standing.

Data for Methyl 6,6a-dihydro-1,1-dimethyl-6-oxo-cycloprop[*a*]indene-1a(1*H*)-carboxylate (**167**)

mp: 52-53 °C

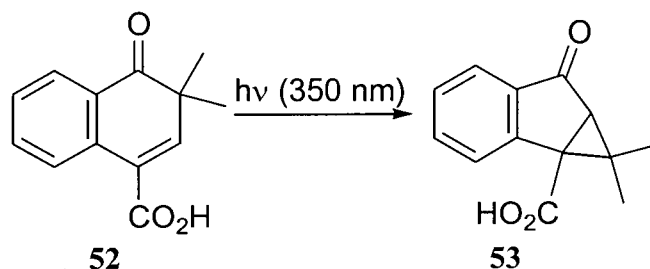
¹H NMR (200 MHz, CDCl₃): δ 0.84 (s, 3H), 1.40 (s, 3H), 2.80 (s, 1H), 3.83 (s, 3H), 7.36 (m, 1H), 7.58 (m, 2H), 7.92 (d, *J* = 7.7 Hz, 1H).

¹³C NMR (100 MHz, CDCl₃): δ 16.73, 23.20, 44.76, 45.28, 50.12, 52.03, 123.10, 126.74, 127.73, 134.03, 136.82, 148.20, 168.78, 198.58.

IR (KBr pellet): 1732, 1714, 1605, 1232, 1210, 766 cm⁻¹.

HRMS (EI) calcd for C₁₄H₁₄O₃ 230.0943, found 230.0943.

Anal. Calcd C, 73.03; H, 6.13. Found: C, 72.99; H, 6.10.

Preparative Photolysis of Ketoacid **52**

A solution of ketoacid **52** (282 mg, 1.31 mmol) in Et₂O (7 mL) was purged with nitrogen and irradiated (Rayonet, 350 nm) for 2.5 h. The photosylate was concentrated *in vacuo* and the residue recrystallized from EtOAc / hexanes to afford acid **53** (246 mg, 87%) as colourless prisms.

Data for 6,6a-Dihydro-1,1-dimethyl-6-oxo-cycloprop[a]indene-1a(1H)-carboxylic acid (**53**)

mp: 136-137 °C (EtOAc / hexanes)

¹H NMR (200 MHz, CDCl₃): δ 0.95 (s, 3H), 1.51 (s, 3H), 2.85 (s, 1H), 7.38 (m, 1H), 7.60 (m, 2H), 7.97 (d, *J* = 7.6 Hz, 1H). Acidic proton not observed.

¹³C NMR (100 MHz, CDCl₃): δ 17.13, 23.29, 44.84, 45.61, 51.62, 123.45, 127.17, 128.07, 134.41, 136.87, 147.86, 174.54, 198.64.

IR (KBr pellet): 2883, 1681, 1605, 1467, 1425, 1289, 1253, 1213 cm⁻¹.

HRMS (EI) calcd for C₁₃H₁₂O₃ 216.0786, found 216.0787.

Anal. Calcd C, 72.21; H, 5.59. Found: C, 72.29; H, 5.69.

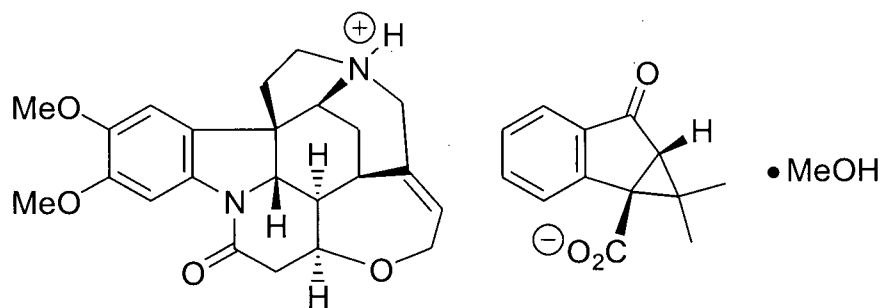
This structure was confirmed by X-ray crystallographic analysis:

Habit	irregular colourless crystals
Space group	$P2_1/c$
a , Å	10.874(2)
b , Å	9.182(1)
c , Å	11.247(2)
α (°)	90
β (°)	95.72(1)
γ (°)	90
Z	4
R	0.044

6.5 Resolution of Acid **53** with Brucine

Brucine (194 mg, 0.50 mmol) and ketoacid **53** (108 mg, 0.50 mmol) were dissolved in hot MeOH (10 mL). The solution was slowly cooled to room temperature and left for 2 h. Crystals of optically pure (as determined by chiral GC and HPLC of the methyl ester **166** produced after diazomethane workup) salt **171** (91 mg, 30%) were recovered.

Data for Brucinium (1a*S*, 6a*R*)-6,6a-Dihydro-1,1-dimethyl-6-oxo-cycloprop[*a*]indene-1a(1*H*)-carboxylate•Methanol (**171**)



mp: 172-174 °C (MeOH)

¹H NMR (400 MHz, CD₃OD): δ 0.85 (s, 3H), 1.43 (s, 3H), 1.69 (d, *J* = 15.2 Hz, 1H), 1.98-2.10 (m, 2H), 2.52 (dt, *J* = 4.2, 15.2 Hz, 1H), 2.70 (dd, *J* = 3.0, 17.5 Hz, 1H), 3.05 (dd, *J* = 8.4, 17.5 Hz, 1H), 3.17-3.40 (m, 5H), 3.64 (m, 1H), 3.81 (s, 6H, OCH₃), 4.09 (m, 2H), 4.18 (m, 2H), 4.31 (br s, 1H), 4.38 (m, 1H), 6.28 (m, 1H), 6.98 (s, 1H), 7.35 (m, 1H), 7.57 (m, 2H), 7.76 (s, 1H), 8.00 (d, *J* = 7.7 Hz, 1H).

¹³C NMR (100 MHz, CD₃OD): δ 16.77, 24.70, 26.27, 31.90, 42.00, 42.75, 46.00, 51.15, 51.77, 53.21, 53.36, 56.69, 57.23, 60.89, 62.63, 65.12, 78.32, 78.37, 102.44, 107.64, 122.49, 123.80, 127.58, 128.59, 135.35, 135.41, 135.79, 137.21, 138.25, 148.36, 151.55, 152.75, 171.23, 174.71, 203.27.

Anal. Calcd for $C_{37}H_{40}N_2O_8$: C, 69.36; H, 6.29; N, 4.37. Found: C, 69.70; H, 6.59; N, 4.34.

This structure was confirmed by X-ray crystallographic analysis:

Habit	colourless prisms
Space group	$P2_12_12_1$
a , Å	9.4684(3)
b , Å	12.4100(5)
c , Å	26.978(2)
α (°)	90
β (°)	90
γ (°)	90
Z	4
R	0.039

6.6 Quantum Yield Determinations

Quantum yields for compound **14** were determined at 313 nm. This wavelength was isolated from light produced by a 450 W Hanovia medium-pressure mercury lamp using a combination of Corning 7-54 glass plates and a 0.002 M potassium chromate solution containing 5% potassium carbonate. Irradiations were carried out in a merry-go-round¹¹⁸ apparatus. The temperature was maintained at 21 ± 2 °C using a thermostat.

Photochemical production of acetophenone from valerophenone was used as the actinometer. The quantum yield for this reaction is known to be 0.33 at 313 nm for an opaque solution of valerophenone (ca. 0.1 M) in benzene.¹¹⁹ All substrate and actinometer solutions were degassed by subjecting them to three freeze-pump-thaw cycles, and subsequently flame-sealing them under vacuum. Valerophenone, benzene, and *tert*-butanol were dried and distilled before use according to literature procedures.¹²⁰ Stern-Volmer quenching experiments were conducted using 2,5-dimethyl-2,4-hexadiene that was distilled from lithium aluminum hydride prior to use.

All quantitative photoproduct measurements were made using standard gas chromatographic techniques. GC response factors were calculated relative to linear alkane internal standards (C₁₀ to C₁₈). GC data were based on the average of three chromatographic runs, and quantum yield data were calculated based on the average of two parallel irradiations each of the actinometer and substrate solutions. Quantum yields reported are based on a plot of quantum yield versus photoproduct concentration and were extrapolated back to 0% conversion. Singlet quantum yields are based on the portion of the Stern-Volmer plot where the value of ϕ_0/ϕ remains constant and the slope is 0, indicating complete quenching of the triplet excited state. Quantum yields are reported \pm the estimated standard deviation and are presented in Table 3.4.

References

- 1 Corey, E. J.; Cheng, X.-M. *The Logic of Chemical Synthesis*; John Wiley & Sons: New York. 1995.
- 2 For an example see: Cheung, E.; Kang, T.; Scheffer, J. R.; Trotter, J. *J. Chem. Soc., Chem. Commun.*, in press.
- 3.(a) *Organic Solid State Chemistry*; Desiraju, G. R. Ed., Elsevier: Amsterdam, 1987. (b) *Photochemistry in Organized and Constrained Media*; Ramamurthy, V. Ed.; VCH: New York, 1991. (c) Ito, Y. *Synthesis* **1998**, 1.
- 4 Schmidt, G. M. J. *Pure Appl. Chem.* **1971**, 27, 647.
- 5 Desiraju, G. R. *Crystal Engineering: The Design of Organic Solids*; Elsevier: Amsterdam. 1989.
- 6 Etter, M. C. *Acc. Chem. Res.* **1989**, 23, 120. See also: Coe, S.; Kane, J. J.; Nguyen, T. L.; Toledo, L. M.; Wininger, E.; Fowler, F. W.; Lauher, J. W. *J. Am. Chem. Soc.* **1997**, 119, 86.
- 7 Vankatesan, K.; Ramamurthy, V. In *Photochemistry in Constrained and Organized Media*; Ramamurthy, V., Ed.; VCH Publishers: New York. 1991; Chapter 4.
- 8 Xiao, J.; Yang, M.; Lauher, J. W.; Fowler, F. W. *Angew. Chem., Int. Ed. Engl.* **2000**, 39, 2132.
- 9 Enkelmann, V. *Chem. Mater.* **1994**, 6, 1337.
- 10 Kiji, J.; Wegner, K. G.; Schulz, R. C. *Polymer* **1973**, 14, 433.
- 11 MacGillivray, L. R.; Reid, J. L.; Ripmeester, J. A. *J. Am. Chem. Soc.* **2000**, 122, 7817.
- 12 Toda, F.; Tanaka, K.; Tamashima, T.; Kato, M. *Angew. Chem., Int. Ed. Engl.* **1998**, 37, 2724.
- 13 (a) Hung, J. D.; Lahav, M.; Luwich, M.; Schmidt, G. M. J. *Isr. J. Chem.* **1972**, 10, 585. (b) Cohen, M. D.; Cohen, R.; Lahav, M.; Nie, P. L. *J. Chem. Soc., Perkin Trans.* **1973**, 2, 1095. (c) Green, B. S.; Heller, L. *J. Org. Chem.* **1974**, 39, 1960.
- 14 (a) Cohen, M. D.; Schmidt, G. M. J. *J. Chem. Soc.* **1964**, 1996. (b) Cohen, M. D.; Schmidt, G. M. J.; Sonntag, F. I. *J. Chem. Soc.* **1964**, 2000. (c) Schmidt, G. M. J. *J. Chem. Soc.* **1964**, 2014.

- 15 Cohen, M. D. *Angew. Chem., Int. Ed. Engl.* **1975**, *14*, 386.
- 16 Weiss, R. G.; Ramamurthy, V.; Hammond, G. S. *Acc. Chem. Res.* **1993**, *26*, 530.
- 17 *C. E. News*, **2000**, *78*, 40. See also: Yang, Z.; Garcia-Garibay, M. A. *Org. Lett.* **2000**, *2*, 1963.
- 18 Zimmerman, H. E.; Sebek, P.; Zhu, Z. *J. Am. Chem. Soc.* **1998**, *120*, 8549 and references therein. See also Garcia-Garibay, M. A.; Houk, K. N.; Keating, A. E.; Cheer, C. J.; Leibovitch, M.; Scheffer, J. R.; Wu, L.-C. *Org. Lett.* **1999**, *1*, 1279 and references therein.
- 19 For reviews of Type II photochemistry see: (a) Wagner, P. J. *Acc. Chem. Res.* **1971**, *4*, 168. (b) Wagner, P.; Park, B.-S. In *Organic Photochemistry*; Padwa, A., Ed.; Marcel Dekker: New York, 1991; Volume 11; Chapter 4.
- 20 Turro, N. J. *Modern Molecular Photochemistry*; Benjamin/Cummings: Menlo Park, California. 1978; Chapter 5.
- 21 Turro, N. J. *Modern Molecular Photochemistry*; Benjamin/Cummings: Menlo Park. 1978; p 364.
- 22 Weiss, R. G. In *CRC Handbook of Photochemistry and Photobiology*; CRC Press: Boca Raton. 1995; Chapter 39.
- 23 Yang, N. C.; Elliot, S. P.; Kim, B. *J. Am. Chem. Soc.* **1969**, *91*, 7551.
- 24 (a) Scaiano, J. C. *Tetrahedron*, **1982**, *38*, 879. (b) Griesbeck, A. G.; Mauder, H.; Stadtmuller, S. *Acc. Chem. Res.* **1994**, *27*, 70. (c) Turro, N. J.; Buchachenko, A. L.; Tarasov, V. F. *Acc. Chem. Res.* **1995**, *28*, 69. (d) Caldwell, R. *Pure Appl. Chem.* **1984**, *56*, 1167.
- 25 Ihmels, H.; Scheffer, J. R. *Tetrahedron* **1999**, *55*, 885 and references therein.
- 26 Wagner, P. J. In *CRC Handbook of Photochemistry and Photobiology*; CRC Press: Boca Raton. 1995; Chapter 38.
- 27 Bondi, A. *J. Phys. Chem.* **1964**, *68*, 441. See also: Edward, J. T. *J. Chem. Educ.* **1970**, *47*, 261.
- 28 Wagner, P. J. *Top. Curr. Chem.* **1976**, *66*, 1.
- 29 Dorigo, A. E.; McCarrick, M. A.; Loncharich, R. J.; Houk, K. N. *J. Am. Chem. Soc.* **1990**, *112*, 7508 and references therein.

- 30 Kasha, M. *Radiat. Res.* **1960**, *Suppl.* 2, 243. See also: Zimmerman, H. E. *Tetrahedron* **1963**, *19*, 393.
- 31 Gudmundsdottir, A. D.; Lewis, T. J.; Randall, L. H.; Scheffer, J. R.; Rettig, S. J.; Trotter, J.; Wu, C.-H. *J. Am. Chem. Soc.* **1996**, *116*, 6167.
- 32 Leibovitch, M.; Olovsson, G.; Scheffer, J. R.; Trotter, J. *J. Am. Chem. Soc.* **1998**, *120*, 12755.
- 33 Cheung, E.; Netherton, M. R.; Scheffer, J. R.; Trotter, J. *Org. Lett.* **2000**, *2*, 77.
- 34 Lutz, G.; Pinkos, R.; Murty, B. A. R. C.; Spurr, P. R.; Fessner, W.-D.; Wörth, H. F.; Knothe, L.; Prinzbach, H. *Chem. Ber.* **1992**, *125*, 1741.
- 35 Sauers, R. R.; Edberg, L. A. *J. Org. Chem.* **1994**, *59*, 7061.
- 36 (a) Quinkert, G. *Pure Appl. Chem.* **1973**, *33*, 285. (b) Turro, N. J. *Modern Molecular Photochemistry*; Benjamin/Cummings: Menlo Park. 1978; pp 512-514. (c) Griffiths, J.; Hart, H. *J. Am. Chem. Soc.* **1968**, *90*, 3297. (d) Griffiths, J.; Hart, H. *J. Am. Chem. Soc.* **1968**, *90*, 5296. (e) Hart, H.; Murray, R. K. Jr. *Org. Chem.* **1970**, *35*, 1535.
- 37 Quinkert, G. *Chimia* **1977**, *31*, 225.
- 38 (a) Caswell, L.; Garcia-Garibay, M. A.; Scheffer, J. R.; Trotter, J. *J. Chem. Ed.* **1993**, *70*, 785; (b) Feringa, B. L.; van Delden, R. A. *Angew. Chem., Int. Ed. Engl.* **1999**, *38*, 3418.
- 39 Evans, S. V.; Garcia-Garibay, M.; Omkaram, N.; Scheffer, J. R.; Trotter, J.; Wireko, F. *J. Am. Chem. Soc.* **1986**, *108*, 5648.
- 40 Sekine, A.; Hori, K.; Ohashi, Y.; Yagi, M.; Toda, F. *J. Am. Chem. Soc.* **1989**, *111*, 697. See also: Aoyama, H.; Hasegawa, T.; Omote, Y. *J. Am. Chem. Soc.* **1979**, *101*, 5343.
- 41 Cheung, E.; Netherton, M. R.; Scheffer, J. R.; Trotter, J.; Zenova, A. *Tetrahedron Lett.* **2000**, in press.
- 42 Gamlin, J. N.; Jones, R.; Leibovitch, M.; Patrick, B.; Scheffer, J. R.; Trotter, J. *Acc. Chem. Res.* **1996**, *29*, 203.
- 43 Cheung, E.; Netherton, M. R.; Scheffer, J. R.; Trotter, J. *J. Am. Chem. Soc.* **1999**, *121*, 2919.

- 44 Leibovitch, M.; Olovsson, G.; Scheffer, J. R.; Trotter, J. *J. Am. Chem. Soc.* **1998**, *120*, 12755.
- 45 Spanka, G.; Rademacher, P.; Duddeck, H. *J. Chem. Soc., Perkin Trans. 2* **1988**, 2119.
- 46 (a) Grubbs, R. H.; Chang, S. *Tetrahedron* **1998**, *54*, 4413; (b) Schuster, M.; Blechert, S. *Angew. Chem., Int. Ed. Engl.* **1997**, *36*, 2036; (c) Armstrong, S. K. *J. Chem. Soc., Perkin Trans. 1* **1998**, 371.
- 47 Maier, M. E. *Angew. Chem., Int. Ed. Engl.* **2000**, *39*, 2073.
- 48 Alberts, A. H.; Wynberg, H.; Strating, J. *Synth. Comm.* **1972**, *2*, 79.
- 49 Olah, G. A.; Narang, S. C.; Gupta, B. G. B.; Malhotra, R. *J. Org. Chem.* **1979**, *44*, 1247.
- 50 Manchand, P. S. *J. Chem. Soc., Chem. Commun.* **1971**, 667.
- 51 Corey, E. J.; Suggs, W. *Tetrahedron Lett.* **1975**, *31*, 2650.
- 52 (a) Schwab, P.; France, M. B.; Ziller, J. W.; Grubbs, R. H. *Angew. Chem., Int. Ed. Engl.* **1995**, *34*, 2039; (b) Schwab, P.; Grubbs, R. H.; Ziller, J. W. *J. Am. Chem. Soc.* **1996**, *118*, 100.
- 53 Henne, A.; Fischer, H. *Angew. Chem., Int. Ed. Engl.* **1976**, *15*, 435.
- 54 Turro, N. J. *Modern Molecular Photochemistry*; Benjamin/Cummings: Menlo Park, California. 1978; pp 386-392.
- 55 Jefferson, E. A.; Keefe, J. R.; Kresge, A. J. *J. Chem. Soc., Perkin Trans. 2* **1995**, 2041.
- 56 (a) Wagner, P. J. *J. Am. Chem. Soc.* **1967**, *89*, 5898; Wagner, P. J.; (b) Kochevar, I. E.; Kemppainen, A. E. *J. Am. Chem. Soc.* **1972**, *94*, 7489.
- 57 Günther, H. *NMR Spectroscopy, Second Edition*; John Wiley & Sons: New York. 1995; pp 82-84.
- 58 Wagner, P. J.; Kelso, P. A.; Kemppainen, A. E.; McGrath, J. M.; Schott, H. N.; Zepp, R. G. *J. Am. Chem. Soc.* **1971**, *94*, 7506.
- 59 Wagner, P. J.; Kelso, P. A.; Zepp, R. G. *J. Am. Chem. Soc.* **1972**, *94*, 7480.
- 60 Adam, W.; Grabowski, S.; Wilson, R. M. *Chem. Ber.* **1989**, *122*, 561.
- 61 Andrew, D.; Weedon, A. C. *J. Am. Chem. Soc.* **1995**, *117*, 5647.
- 62 O'Neal, H. E.; Miller, R. G.; Gunderson, E. *J. Am. Chem. Soc.* **1974**, *96*, 3351.
- 63 Scaiano, J. C. *J. Am. Chem. Soc.* **1977**, *99*, 1494.

- 64 Hu, S.; Neckers, D. C. *J. Chem. Soc., Perkin Trans. 2* **1999**, 1771.
- 65 Leibovitch, M.; Olovsson, G.; Scheffer, J. R.; Trotter, J. *J. Am. Chem. Soc.* **1998**, *120*, 12755.
- 66 Ihmels, H.; Scheffer, J. R. *Tetrahedron* **1999**, *55*, 885.
- 67 Wagner, P. J.; Kelso, P. A.; Kempainen, A. E. *J. Am. Chem. Soc.* **1968**, *90*, 5896.
- 68 Burdett, J. K. *Molecular Shapes*; Wiley-Interscience: New York. 1980; p 6.
- 69 Bondi, A. *J. Phys. Chem.* **1964**, *68*, 441.
- 70 (a) Dunkelblum, E.; Hart, H.; Suzuki, M. *J. Am. Chem. Soc.* **1977**, *99*, 5074; (b) Suzuki, M.; Hart, H.; Dunkelblum, E.; Li, W. *J. Am. Chem. Soc.* **1977**, *99*, 5083.
- 71 (a) Quinkert, G. *Pure Appl. Chem.* **1973**, *33*, 285; (b) Quinkert, G. *Angew. Chem., Int. Ed. Engl.* **1972**, *11*, 1072.
- 72 Hart, H.; Murraray, R. K. *J. Org. Chem.* **1970**, *35*, 1535.
- 73 Dolphin, D.; Wick, A. In *Tabulation of Infrared Spectral Data*; John Wiley and Sons: New York. 1977; pp 175-240.
- 74 Spanka, G.; Rademacher, P.; Duddeck, H. *J. Chem. Soc., Perkin Trans. 2* **1988**, 2119.
- 75 Leonard, M. J.; Fox, R. C.; Oki, M. *J. Am. Chem. Soc.* **1954**, *76*, 5708.
- 76 Leonard, N. J.; Oki, M.; Chiavarelli, S. *J. Am. Chem. Soc.* **1955**, *77*, 6234.
- 77 Hurd, R. N.; Shah, D. H. *J. Org. Chem.* **1973**, *38*, 390.
- 78 Ram, S.; Spicer, L. D. *Synth. Comm.* **1987**, *17*, 415.
- 79 Kang, S.-K.; Kim, W.-S.; Moon, B.-H. *Synthesis* **1985**, 1161.
- 80 Leonard, N. J.; Schimelpfenig, C. W. Jr. *J. Org. Chem.* **1958**, 1708.
- 81 (a) Schulte-Elte, K. H.; Willhalm, B.; Thomas, A. F.; Stoll, M.; Ohloff, G. *Helv. Chim. Acta* **1971**, *54*, 1759. (b) Mori, T.; Matsui, K.; Nozaki, H. *Tetrahedron Lett.* **1970**, *14*, 1175. (c) Matsui, K.; Mori, T.; Nozaki, H. *Bull. Chem. Soc. Jpn.* **1971**, *44*, 3440. (d) Burchill, P. J.; Kelso, A. G.; Power, A. J. *Aust. J. Chem.* **1976**, *29*, 2477.
- 82 Simonaitis, R.; Cowell, G. W.; Pitts, J. N. Jr. *Tetrahedron Lett.* **1967**, *11*, 3751 and references cited therein.
- 83 Lewis, F. D.; Hilliard, T. A. *J. Am. Chem. Soc.* **1970**, *92*, 6672.
- 84 Wagner, P. J. In *CRC Handbook of Photochemistry and Photobiology*; Horspool, W. M. and Song, P.-S. Eds.; CRC Press: Boca Raton, Florida. 1995, Chapter 38.

- 85 Ariel, S.; Evans, S.; Omkaram, N.; Scheffer, J. R.; Trotter, J. *J. Chem. Soc., Chem. Commun.* **1986**, 375.
- 86 Turro, N. J. *Modern Molecular Photochemistry*; Benjamin/Cummings: Menlo Park. 1978, pp 377-380.
- 87 (a) Scaiano, J. R.; Lissi, E. A.; Encina, M. V. In *Reviews of Chemical Intermediates, Volume 2*; Elsevier: New York. 1978, pp 139-196. (b) Wagner, P.; Park, B.-S. In *Organic Photochemistry, Volume 11*; Padwa, A., Ed.; 1990, Chapter 4.
- 88 Gajda, T.; Zwierzak, A. *Synthesis* **1981**, 1005.
- 89 Wagner, P. J.; Kelso, P. A.; kemppainen, A. E.; McGrath, J. M.; Schott, H. N.; Zepp, R. G. *J. Am. Chem. Soc.* **1972**, *94*, 7506.
- 90 Lewis, T. J. Ph. D. Thesis, University of British Columbia, 1993.
- 91 Gudmundsdottir, A. D.; Lewis, T. J.; Randall, L. H.; Scheffer, J. R.; Rettig, S. J.; Trotter, J.; Wu, C.-H. *J. Am. Chem. Soc.* **1996**, *116*, 6167.
- 92 Sauers, R. R.; Edberg, L. A. *J. Org. Chem.* **1994**, *59*, 7061.
- 93 (a) Hoffmann, R.; Swenson, J. R. *J. Phys. Chem.* **1970**, *74*, 415. (b) Wagner, P. J.; May, M.; Haug, A. *Chem. Phys. Lett.* **1972**, *13*, 545. (c) Birge, R. R.; Pringle, W. C.; Leermakers, P. A. *J. Am. Chem. Soc.* **1971**, *93*, 6715. (d) Birge, R. R.; Leermakers, P. A. *J. Am. Chem. Soc.* **1971**, *93*, 6726.
- 94 Ihmels, H.; Scheffer, J. R. *Tetrahedron* **1999**, *55*, 885.
- 95 Jacques, J.; Fouquey, C. *Tetrahedron Lett.* **1971**, *48*, 4620.
- 96 Moore, W. M.; Ketchum, M. *J. Am. Chem. Soc.* **1962**, *84*, 1369.
- 97 Gamma radiolysis experiments were graciously performed by Professor Masahiro Irie at Kyushu University, Japan. In his expert opinion, failure of the salt to react after exposure to 30 Mrad of radiation indicates that the substance is inert to gamma-radiolysis.
- 98 Muzart, J. *Tetrahedron Lett.* **1987**, *28*, 2132.
- 99 Cacchi, S.; Morera, E.; Ortar, G. *Tetrahedron Lett.* **1985**, *26*, 1109.
- 100 Quinkert, G. *Pure Appl. Chem.* **1973**, *33*, 285.
- 101 Turro, N. J. *Modern Molecular Photochemistry*; Benjamin Cummings: Menlo Park. 1978, p 107.

- 102 Griffiths, J.; Hart, H. *J. Am. Chem. Soc.* **1968**, *90*, 5296.
- 103 Jacques, J.; Collet, A.; Wilen, S. H. *Enantiomers, Racemates, and Resolutions*; Wiley-Interscience: New York. 1981, Chapter 5.
- 104 (a) Parker, D. *Chem. Rev.* **1991**, *91*, 1441. (b) Fulwood, R.; Parker, D. *J. Chem. Soc., Perkin Trans. 2* **1994**, 57.
- 105 Ladd, M. F. C.; Palmer, R. A. *Structure Determination by X-ray Crystallography*; Plenum Press: New York. 1993; p 81.
- 106 (a) Zimmerman, H. E.; Sebek, P.; Zhu, Z. *J. Am. Chem. Soc.* **1998**, *120*, 8549 and references cited therein. (b) Garcia-Garibay, M. A.; Houk, K. N.; Keating, A. E.; Cheer, C. J.; Leibovitch, M.; Scheffer, J. R.; Wu, L.-C. *Org Lett.* **1999**, *1*, 1279.
- 107 Alberts, A. H.; Wynberg, H.; Strating, J. *Synth. Comm.* **1972**, *2*, 79.
- 108 Shultz, D. A.; Boal, A. K.; Farmer, G. T. *J. Am. Chem. Soc.* **1997**, *119*, 3846.
- 109 Boymond, L.; Rottländer, M.; Cahiez, G.; Knochel, P. *Angew. Chem., Int. Ed. Engl.* **1998**, *37*, 1701.
- 110 Grubbs, R. H.; Chang, S. *Tetrahedron* **1998**, *54*, 4413.
- 111 Leonard, N. J.; Fox, R.; Oki, M.; Chiavarelli, S. *J. Am. Chem. Soc.* **1954**, *76*, 5708.
- 112 Rama Rao, A. V.; Reddy, S. P.; Reddy, E. R. *J. Org. Chem.* **1986**, *51*, 4158.
- 113 Kang, S.-K.; Kim, W.-S.; Moon, B.-H. *Synthesis* **1985**, 1161.
- 114 Yu, Q.; Yao, Z.-J.; Chen, X.-G.; Wu, Y.-L. *J. Org. Chem.* **1999**, *64*, 2440.
- 115 Marvell, E. N.; Geiszler, A. O. *J. Am. Chem. Soc.* **1952**, *74*, 1259.
- 116 Clemo, G.; Dickenson, H. G. *J. Chem. Soc.* **1937**, 255.
- 117 Sengupta, S. C. *J. Prakt. Chem.* **1938**, *131*, 82.
- 118 Murov, S. L. *Handbook of Photochemistry*; Marcel Dekker: New York, 1973.
- 119 Wagner, P. J.; Kochevar, I. E.; Kempainen, A. E. *J. Am. Chem. Soc.* **1972**, *94*, 7489.
- 120 Perrin, D. D.; Armarego, W. L. F.; Perrin, D. R. *Purification of Laboratory Chemicals*; Second Edition, Pergamon Press: Oxford, 1980.